Department of Chemistry

Preparation and Properties of Self-Assembled Resorcinarene Monolayers

Jade Kristin Pettersen

This thesis is presented for the Degree of
Doctor of Philosophy
of
Curtin University of Technology

January 2010

Declaration

To the best of my knowledge and belief this thesis contains no material previously published by any other person except where due acknowledgment has been made.

This thesis contains no material which has been accepted for the award of any other degree or diploma in any university.

Signature: …….

Date: ……...

Acknowledgments

I would like to acknowledge the following people for their generous contributions to this project:

Professor Mark Ogden and Associate Professor Mauro Mocerino; for their endless optimism, patience, and advice over the course of this project. It would not have been completed without their encouragement, for which I am extremely grateful.

Dr Matthew McIldowie, who regularly dispensed immensely helpful advice, and for always being willing to act as a sounding board.

Dr Thomas Becker for his invaluable support in obtaining and interpreting my AFM and STM data, especially as he generously sacrificed his leave to help me submit on time.

Dr Andrew Ross, and Dr Peter Eadington, along with their group at CSIRO.

Peter Chapman, Joyce Wong, Robert Herman, and Allan Oliveira for their assistance, advice, and humour that went far beyond their job descriptions.

I would also like to thank Dr David Brown, Professor Bill van Bronswijk, Dr Franca Jones and Dr Matt Myers for their contributions.

Finally I would like to acknowledge the financial contributions to this project from the Commonwealth Scientific and Industrial Research Organisation (CSIRO) Wealth from Oceans Flagship, Western Australian Energy Research Alliance (WA:ERA), and Curtin University of Technology.

Abstract

Several resorcinarene and calixarene based receptors were synthesised with the overarching aim of developing selective hydrocarbon sensors for application in the petroleum exploration industry.

Thioacetyl resorcinarenes functionalised at the upper rim with methoxy, propoxy and benzyloxy groups were synthesised, along with a methylene bridged cavitand. Similar hydroxy and methoxy resorcinarenes functionalised at the lower rim with decylsulfide groups were prepared, along with a p-*tert*-butylcalix[4]arene thiol derivative.

The receptors were allowed to self-assemble on gold substrates, and the resulting surfaces were characterised by contact angle, polarised modulation infrared reflection absorption spectroscopy (PMIRRAS), and atomic force microscopy (AFM). The results indicated that all but one of the receptors form monolayers. The exception, a resorcinarene decyl sulfide, appears to form a bilayer or multilayers.

AFM force spectroscopy was used to investigate the receptor properties of the monolayers by using tips functionalised with adamantyl, cyclohexyl and benzyl molecular probes. A quantity of a deep cavitand was obtained to use as a comparison to the shallower receptors synthesised.

Specific interactions were observed between the benzyloxy and methylene cavitand monolayers and the adamantyl probes. These monolayers along with the methoxy resorcinarene monolayer also showed significant interactions with the cyclohexyl probes. These receptors present promising targets for further studies of the complexation behaviour of resorcinarene based receptors and cyclic aliphatic hydrocarbons.

All surfaces exhibited interactions with the benzyl probes. The propoxy resorcinarene and deep cavitand monolayers appear to show selectivity towards the benzyl probes with no interactions observed for the adamantyl or cyclohexyl probes.

The binding of the monolayer was found to be influenced by not only the macrocylic receptor site, but also the monolayer structure. Evidence for this was provided by the difference in binding exhibited by the methoxy resorcinarene thiol monolayer and the methoxy resorcinarene decylsulfide monolayer.

Table of Contents

1.0 Introduction

1.1 Oil Exploration

Petroleum exploration is a risky venture, with extremely high costs and a low success rate, particularly offshore. In 2005, 68 offshore exploration wells were drilled in Australian waters with a success rate of 1 in 2.4 (oil present, not necessarily commercially viable), along with 36 development wells. In addition 15 192 km of 2D and 10,832 km^2 of 3D seismic surveys were performed.[1] A total of $856.5 million was spent, 64% of this on drilling costs.[2]

Expenditure on exploration has tripled in the 5 years 2003-2008 (Figure 1.1),[2] with drilling success rates in Australia typically oscillating around 25% with no major increases in the last decade (Figure 1.2).[1] New exploration techniques are needed to complement the existing methods in order to reduce uncertainty when predicting the presence of hydrocarbons.

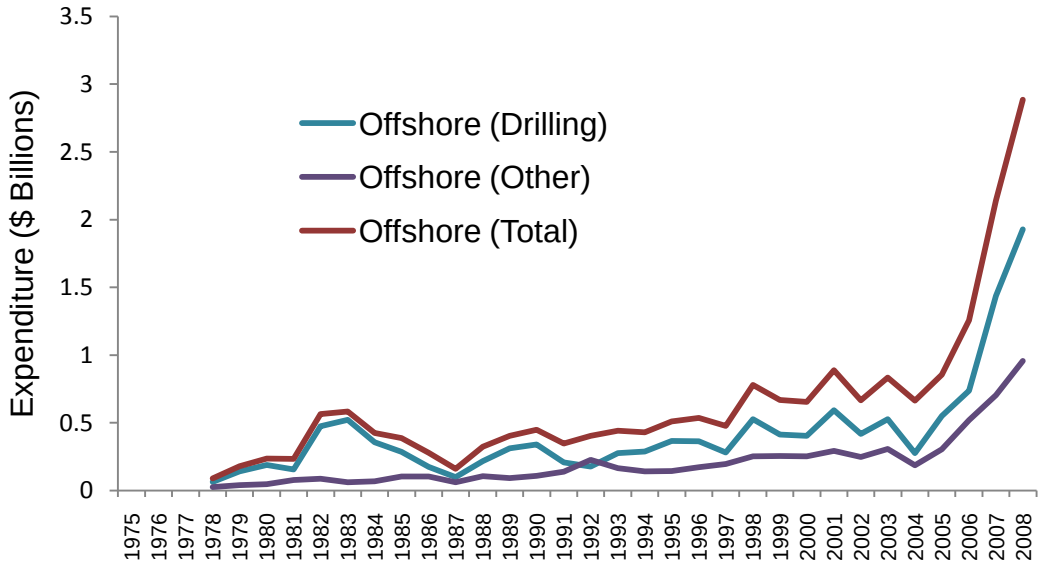

Figure 1.1 Petroleum Exploration Expenditure in Australia. Data obtained from the Australian Bureau of Statistics.[2]

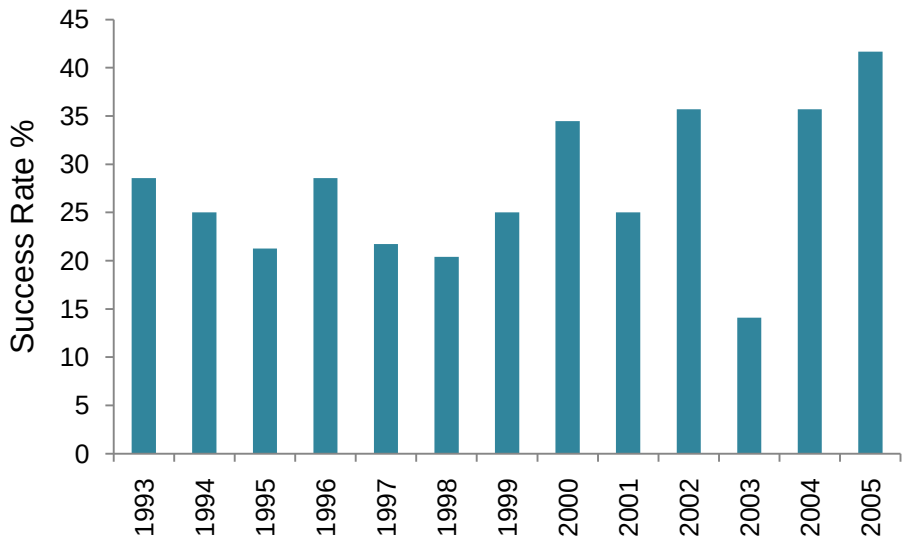

Figure 1.2 Success Rates from Australian Offshore Wells. Data obtained from Geoscience Australia.[1]

1.2 Current Exploration Techniques

Current exploration techniques combine geological techniques to find structures likely to be reservoirs,[3] with techniques to detect oil and/or gas seepage.[4-6] Seeps occur where hydrocarbons have leaked to the surface from subsurface reservoirs, and allow the direct detection of an accumulation.

1.2.1 Physical Techniques for Oil Seep Detection

Several methods are currently used to search for seep oils. These include reflectance and acoustic techniques, as well as sampling the sediment and water to directly analyse for the presence of oil. Chemosynthetic communities of bacteria, tube worms, clams and mussels are often found at significant seepage sites.[7] These can be used as indicators of petroleum seepage, along with the carbonate rocks precipitated when carbon dioxide is formed as a byproduct of bacterial oxidation.

The oil slicks on the ocean surface are generally invisible to the naked eye but can be detected from aircraft, manned space vehicles, and satellites, as the oil layer dampens the fine-scale roughness of the sea and creates

patches of increased specular reflectance.[8] The slicks appear as dark areas on synthetic aperture radar (SAR) images taken from satellites as the Bragg scattering of microwaves is dampened by the oil layers. The microwaves are not impeded by cloud cover and so 24 hour surveillance of the sea surface is possible.[9] Limitations of the method include the inability to detect slicks smaller than 125 m long, and to distinguish between organic matter with biological origins (algae, coral spawn etc) and oil slicks, and the need to include currents and seafloor topography in the analysis.[6]

Side-Scan sonar can pick up the carbonate outcroppings, gas-hydrate deposits, mud and brine flows, and pockmarks along with the oily bubble trains that often accompany seepage.[10] Acoustic profiling can also pick up these bubbles.[9]

The use of airborne laser fluorosensor (ALF) has been almost entirely discontinued.[6] The technique measures the fluorescence induced in polyaromatic hydrocarbons by a laser onboard an aircraft flying 80-100 m above sea level. The technique is very sensitive to thin films, however similar results can be observed from dissolved compounds (including natural organic matter, biota and pollution) as with a seep oil slick. These reliability concerns, combined with the relative expense of the technique, have led to the reduction in its use.

1.2.2 Oil Detection and Characterisation

The only technique currently used commercially to directly detect the presence of hydrocarbons is water and sediment sampling. This is largely done with the use of geochemical sniffers.[6] A submerged 'fish' (weighted body towed behind a vessel) continuously pumps water on board the survey vessel where it is degassed and the light hydrocarbon content (C_1-C_8) analysed by gas-chromatography (GC).[11] More comprehensive testing is undertaken on selected water samples (along with sediment samples) by extracting the entire organic content to analyse by gas-chromatography mass

spectrometry (GCMS). The sample preparation needed and the equipment used adds significantly to the cost and the delay before receiving the results. This limits the number of samples that can be analysed.

This GCMS technique is used to 'fingerprint' oil, both to determine the relationship between crude oil and source rock, and to determine the source of the seeped hydrocarbons, or anthropogenic contamination. The individual compounds can be identified in the sample,[12-15] while sensor based devices are less able to characterise the oils with respect to their chemical composition and usually detect a wide range of hydrocarbons which can be indicative of both recent organic matter and thermogenic hydrocarbons.

Quartz crystal microbalances (QCM) coated with a hydrocarbon polymer,[16] and polyethylene,[17] have been used under laboratory conditions to determine the level of petroleum products in water, by volatilizing the contaminants and analysing the absorption of the vapour by the polymer. The selectivity of the sensor is low as it discriminates based on volatility and the solubility of the compounds in the polymer. QCM devices that detect the hydrocarbons directly from the aqueous phase have also been reported.[18,19]

Fibre optic sensors operate under a similar absorption principle but use an optical detection system. Current work uses polymeric[20,21] or zeolite[22] sensing layers, and as with QCM devices, exhibit little selectivity.

An attenuated total reflectance (ATR) infrared spectroscopy technique has been developed, which combines multivariate analysis and pattern recognition to identify oil spillages and trace the source.[23] The technique has been applied to synthetic samples and residue samples from an oil spill, and various parameters were measured to monitor weathering (carbonyl index, aromaticity index etc). A similar method has been reported to detect gasoline and diesel contamination in water,[24,25] and the quantification of adamantane has been reported by Luzinova *et al*.[26]

These sensors are currently laboratory methods (with the exception of the fibre optic sensor[21]), however, it may be possible to develop portable devices. Currently, there are no real-time composition specific techniques to detect hydrocarbons in seawater.

1.3 Crude Oil Composition and Transformation

Australian oils are predominantly low sulfur, paraffinic (high in *n*-alkanes) or naphthenic-paraffinic (high in both *n*-alkanes and cycloalkanes) with input from terrestrial sources. Severe alteration of these oils by water washing and biodegradation is uncommon.[27]

1.3.1 Basic Composition

The composition of crude oil is very complex and is governed by a variety of processes. Aliphatic compounds make up the largest proportion (50-60%) of a typical producible oil, followed by aromatics (20-30%), with the remainder composed of resins and asphaltenes.[28] The aliphatic fraction is further split into paraffins (*n*-alkanes C_1-C_{40}), isoprenoids, and cyclic alkanes. The cyclic alkanes are important constituents of crude oils, with the most abundant of these being the cyclohexanes and cyclopentanes. Higher molecular weight cyclic alkanes (C>10) are still dominated by the mono and bicyclics (50-55%); tricyclics average 20% of this fraction and the abundance decreases as a function of weight. The tricyclic fraction includes compounds such as perhydrophenanthrene, as well as adamantane which is a rearrangement product of polycyclic hydrocarbons.[29,30] Adamantane (Figure 1.3) and its methyl derivatives are found to have the greatest concentrations of the diamondoids in oil (30-1880 ppm in a range of crude oils[15] with higher concentration in the lighter oils. Iraqi crude oils were found to contain 1-3ppm[31]), however higher diamondoids from tetramantanes to undecamantane also occur at trace concentrations in typical oils.[32,33] Tetra and pentacyclics also make up on average approximately 20% of the cycloalkanes C>10; and include the sterane and hopane type biomarkers.

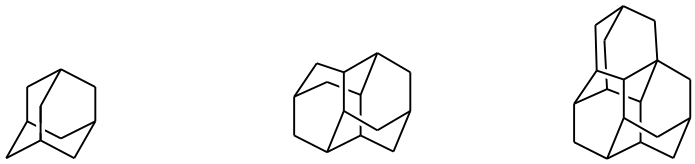

a b c

Figure 1.3 Diamondoid Structures. a) adamantane b) diamantine c) triamantane

Geochemical fossils (biomarkers) are complex hydrocarbons (see Figure 1.4) of relatively high molecular weight that are derived from biochemicals and survive with no/minor changes from their original state.[28] Ratios of various biomarkers are used to determine the source of the organic matter, to correlate various oils to the same source rock, and to determine maturity and biodegradation parameters.

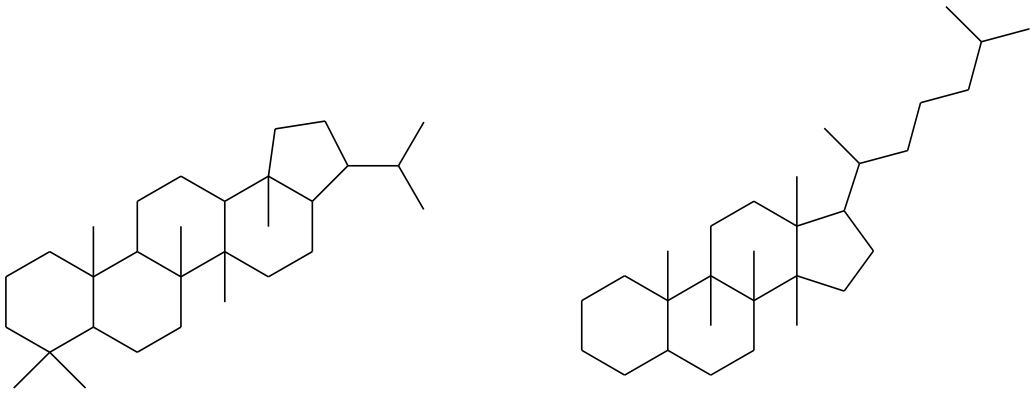

a b

Figure 1.4 Examples of Common Cyclic Biomarkers Found in Crude Oils. a) hopane b) cholestane

1.3.2 Transformation of Oil

Many mechanisms affect the oil and modify the composition. As a general rule, several mechanisms act simultaneously which complicates understanding the contribution of each.

1.3.2.1 Water Washing

Water washing is the mechanism by which relatively water soluble compounds can be removed from a crude oil. This can occur at several stages; during migration, in reservoir, and during seepage. Water washing during migration is suggested as being minimal, with the majority of the losses occurring after accumulation.[34] The presence of benzene and toluene in most crude oils indicates that water washing is not severe in the majority of cases and only becomes a significant degradation pathway during seepage.[34,35]

The effects of water washing are more pronounced at higher temperatures but are reduced by higher salinities, as is expected from general solubility trends of organic compounds in water. The solubilities of individual hydrocarbons at surface temperatures and pressures have been determined,[36,37] but it is difficult to extrapolate these to reservoir conditions and complex mixtures.

Laboratory experiments have determined general trends for the removal of compounds by water washing. For a given carbon number, the higher the degree of ring formation and unsaturation, the higher the solubility, and solubility decreases with increasing carbon number. However Lafargue and Barker[38] observed that paraffins were preferentially removed over cyclic alkanes in laboratory washing of crude oils. This phenomenon was investigated by Eganhouse and Calder[39] who found that the solubility of compounds in a mixture differs from pure compounds. Studies of biomarkers such as hopanes, show that minimal removal by water washing occurs.[40]

1.3.2.2 Biodegradation

Both anaerobic and aerobic bacteria are known to degrade oil in shallow reservoirs and seeps. The phenomenon primarily occurs in relatively cool environments (<80 °C) with low salinity (<100-150 parts per thousand) and abundant nitrate and phosphate nutrients.[34] The general order of degradation

is the removal of n-alkanes (C<25), isoprenoid alkanes, low ring cycloalkanes, and aromatics before the alteration of the more stable penta and tetracyclic biomarkers.[28,40,41] Highly biodegraded oils are lower quality and can cause problems during the production process.[42]

1.3.2.3 Photoxidation

Crude oil present at the surface is usually degraded by a combination of photoxidation and biodegradation. Photoxidation produces water soluble compounds that are more susceptible to biodegradation, and usually affects aromatics more than aliphatic compounds. For example, hopanes are relatively resistant to photoxidation.[43]

1.3.2.4 Volatility

Volatile compounds can be removed from the oil in a reservoir via evaporative fractionation from faults, which tends to enrich the residual oil in light aromatics and cycloalkanes.[35] Compounds with boiling points under 200 °C tend to be efficiently volatilized from the large surface areas of oil slicks formed from seep oils.[43]

1.4 Seep Oils

Reservoir seals are rarely perfect and so seepage will usually occur to some extent. Hydrocarbon seeps have been imaged in Australian waters,[4,5] however these generally have not been directly linked to proven reserves.[6]

The biodegradation of seep oils in sediments seems to be connected to the seepage intensity, with macroseeps showing moderate to severe biodegradation, and microseeps showing little to no evidence of biodegradation. The likely explanation is that a minimum threshold concentration of oil is needed to support a bacterial population.[44] However, microseeps are overlaid with recent organic matter, while this tends to be insignificant in macroseeps.

A comparison of a reservoired oil, and associated oil stained sediments, sea slicks and tar balls has been made in the Gulf of Mexico in order to determine the changes that they have undergone during seepage.[45] Visual observations in the region confirmed a massive amount of liquid and gas seepage. Sediment extracts showed exhaustive degradation in areas of high seepage >500 ppm (complete loss of alkanes, isoprenoids, and susceptible aromatics and biomarkers), whereas in areas with lesser oil concentrations <500 ppm, the full suite of aliphatics and isoprenoids were generally present. The sea slick and tar balls were less degraded than the sediment extract, however, they had been extensively altered (depleted in alkanes, cycloalkanes, and larger aromatics). The cyclic biomarkers were largely preserved in all samples.

1.5 Potential Interferences

1.5.1 Recent Organic Matter in Seawater

The dissolved organic matter present in seawater will overlay any crude oil present from seeps and will potentially be a major interference and potential source of false positives when trying to detect seep oil.

The levels of dissolved organic carbon (DOC) in seawater consisting of amino acids, humic acids etc range from ng/L to mg/L, and particulates range from µg/L to mg/L.[46] A large component of the DOC at the sea surface is carbohydrate based (estimates range from 15-50%), with the remainder consisting of amino acids (approx 10%),[47] aliphatics and acids; only minor portions of aromatics are present.[48,49] The composition of the organic matter is very complex, for example Dittmar and Koch[50] found more than 200 different polycyclic aromatic hydrocarbons in abyssal ocean samples, however the variety and concentration at the ocean surface was much lower.

1.5.2 Pollution

It has been estimated that the 47% of the crude oil entering the marine environment is natural seepage, while the remaining 53% results from leaks and spills during the extraction, transport, refining, or use of petroleum products.[51] Differentiating natural seepage and anthropogenic sources of hydrocarbons is very challenging.

Adamantanes and the smaller diamondoids are concentrated into the mid range distillates (up to 1200 ppm in diesels) during the refining process, while biomarkers such as the steranes and tri-pentacyclic terpanes are largely removed by the refining process.[15] This has resulted in the use of diamondoids to fingerprint these petroleum products to identify the source of environmental pollution.[13,15]

1.6 Characteristics of Ideal Target Compounds

The choice of target compounds is important as the compound has to be present at the sea surface in reasonable concentrations in order to be detected. This means that the target compounds must be present in all (or most) oils in levels such that it will be detectable at the sea-surface.

Compounds that fit this criterion are those that will be removed to some extent by weathering processes but were present in sufficient concentrations that they will still be present at the surface, or compounds that may have only been present in trace concentrations that are enriched in the residual oil as less resistant compounds are removed.

Ideal target compounds will be reasonably resistant to biodegradation, water washing and photoxidation. They will also have low volatility and not adsorb to sediments to a significant extent. Ideally they will not be present in recent organic matter or as common pollutants and will be commercially available to allow for easy testing.

The cyclic alkanes are ideal as they are relatively resistant to all weathering processes.[41] Cyclohexane is an inexpensive common laboratory solvent and is a simple model for more complicated structures, as well as being an important, if somewhat volatile component of most crude oils.[28]

The tricyclic adamantane is also a promising target compound as it is highly resistant to any chemical or bio-degradation,[33,52] leading to enrichment in seep oils, and is not naturally occurring except in crude oils. The spherical shape also provides a potential means for selective complexation. The presence of adamantanes in refined petroleum products signifies that differentiation between seep oils and oil pollutants could not occur with a single adamantane sensor, however, a sensor array including an adamantane sensor would be very useful in distinguishing between natural organic matter in seawater and oil, and widens the applicability of the sensor to environmental monitoring of anthropogenic hydrocarbon input.

The tetra and pentacyclic biomarkers also offer intriguing targets as they are very persistent,[52] and are largely absent from refined petroleum allowing for natural seeps to be distinguished from pollution. The structural similarity to recent organic matter naturally occurring in seawater and the difficulty in procuring samples may limit the viability of these targets.

1.7 Types of Sensors

There are many different sensors that can be applied to the detection of small neutral molecules in an aqueous environment. These fall broadly into several categories: mass sensors, including quartz crystal microbalance (QCM), and surface acoustic wave (SAW);[53] optical sensors including infrared (IR),[26] fibre optics,[20,22] and surface plasmon resonance (SPR); and nanoparticle sensors.[54,55]

Optical sensors especially SPR are becoming more widespread, and have been used to detect aromatic[56] and lactone[57] analytes in conjunction with a

macrocyclic sensing layer. However, the most commonly used sensor to date for the detection of small neutral molecules is the QCM.

QCMs are sensitive instruments that can be used to measure the mass of an adsorbed layer, or viscosity of a solution, by measuring the damping of the oscillation frequency of a quartz crystal.[58]

Various polymers, cyclodextrins and simple cavitands have been used as the sensing layers in QCM's in order to detect analytes in the vapour state.[59-65] These analytes include chlorinated solvents, acetone, acetonitrile, ethyl acetate, aromatic compounds, pyridine, nitromethane, alcohols and volatile amines.

A molecularly imprinted polymer allowed the detection of polycyclic aromatic hydrocarbons in water at concentrations as low as 30 ng/L.[66,67] Pollutants such as benzene, cyclohexanone, phenol and various common organic solvents have been successfully detected by calixarene, and cavitand coated QCM's at low concentrations in aqueous environments.[68-71] The common feature of these analytes is that they are all small, relatively polar molecules; few lipophilic compounds have been studied.

1.8 Supramolecular Chemistry

The selective recognition of analytes by supramolecular receptors has been a significant area of research,[72-74] much of it focused on sensing charged species, usually cations. While the complexation of neutral molecules has also attracted attention, the classes of compounds looked at tend to include polar groups, such as alcohols and amines. Hosts for the hydrocarbons found in crude oil are relatively rare, however examples such as deep cavitands (Figure 1.5) that complex with *n*-alkanes in water are known.[75,76]

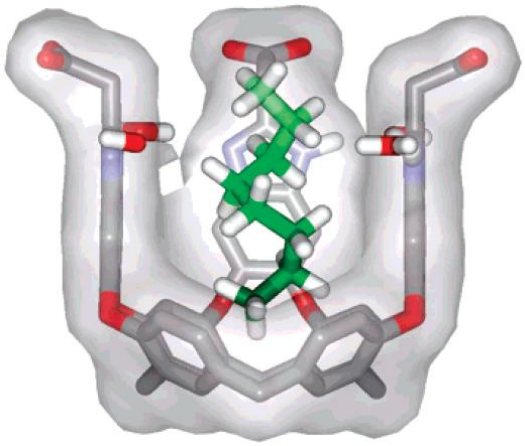

Figure 1.5 Representation of the Complex Between Octane and a Water Soluble Cavitand (hydrogens and one wall removed for clarity). Reprinted with permission from Journal of the American Chemical Society, 129(44), Hooley, Van Anda, Rebek, *Extraction of Hydrophobic Species into a Water-Soluble Synthetic Receptor*, 13464-13473. Copyright 2007, American Chemical Society.

The cyclic hydrocarbons vary only in their size and shape. They lack any functional group "handles" that are used to design a complementary host (hydrogen bonding acceptors/donors, dipoles, acidic/basic groups, pi bonds etc). Complexation of these compounds, when it occurs, is primarily driven by the hydrophobic effect.

Hydrophobic receptors will form complexes with hydrocarbons of a complementary size and shape in polar solvents. Ideally the guest will occupy approximately 55% of the cavity volume.[77]

1.8.1 Complexation of Cyclohexanes

Cyclohexane complexes are known to form with a range of receptors. Those reported to date are mostly solid state complexes formed in the absence of competing guests. Solution experiments generally do not show any association except in very polar solvents such as water and the resulting complex tends to be insoluble.

Crystal structures of the cyclohexane complex with p-*tert*-butylcalix[4]arene,[78] a simple ethylene cavitand (Figure 1.6),[72] and 'molecular tweezers'[79] have

been published. These complexes were all prepared by recrystallisation from cyclohexane with no competing guests.

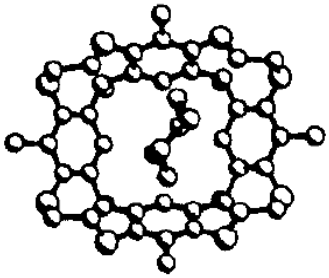

Figure 1.6 Top View of Cavitand Complex with Cyclohexane. Reprinted with permission from Journal of the American Chemical Society, 110(7), Cram, Karbach, Kim, Knobler, Maverick, Ericson, Helgeson*, Host-guest complexation. 46. Cavitands as open molecular vessels form solvates*, 2229–2237. Copyright 1988, American Chemical Society.

The vapour sorption isotherms for various solvent vapours including cyclohexane with solid p-*tert*-butylcalix[4]arene have been measured. The most favourable interaction was found to be with benzene, and cyclohexane was found to exhibit a relatively weak interaction.[80,81] A similar study with an *p*-adamantylcalix[4]arene (Figure 1.7) indicated the same trends between the guests studied. The Gibbs energy for formation of the inclusion compounds was highest for toluene, then benzene, followed by cyclohexane, and carbon tetrachloride exhibited the weakest interaction.[82]

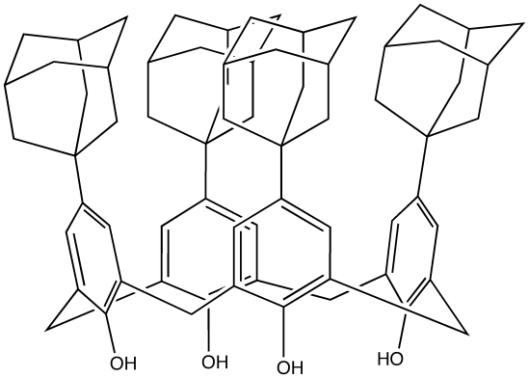

Figure 1.7 Structure of Adamantylcalix[4]arene.[82]

A number of papers have documented the interaction of substituted cyclohexanes with self-folding cavitands,[83-90] however the interaction with

substituted adamantanes tends to be stronger, and these receptors will be discussed in the following section.

A similar cavitand (Figure 1.8) with a restricted cavity was found to complex cycloalkanes in d_{12}-mesitylene (which is non-competitive due to its size).[91,92] In order for guest exchange to occur one quinoxaline unit must rotate outwards (kite conformation). The enthalpic barrier to this transition is high due to the rigidity of the framework, however the addition of acid drives the conformational change by protonating the weakly basic quinoxaline nitrogens, and allows subsequent guest exchange. This cavitand highlights the delicate balance between selectivity and kinetics that needs to be addressed for a receptor to be suitable for a real-time sensor.

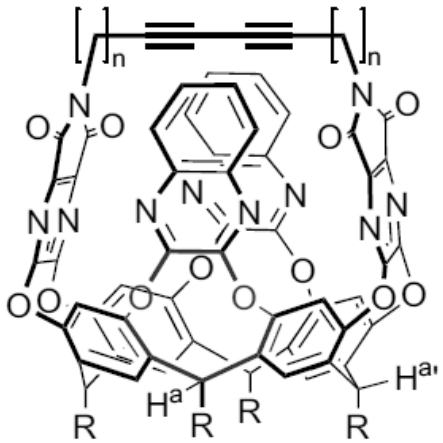

Figure 1.8 Structure of Cavitand Based Cyclohexane Receptor (n=2). Reprinted from Tetrahedron, 64(36), Gottschalk, Jarowski, Diederich, Reversibly controllable guest binding in precisely defined cavities: selectivity, induced fit, and switching in novel resorcin[4]arene-based container molecules, 8307-8317, Copyright (2008), with permission from Elsevier

1.8.2 Complexation of Adamantanes

The adamantane complex of cyclodextrin (both α and β) has been extensively studied.[93-95] The inclusion complexes have K_a constants in the order of 10^4 in water and have been used for a variety of applications including imparting aqueous solubility to both metallodendrimers,[96] and

poly(propylene imine) dendrimers,[97] the immobilisation of a modified protein to a cyclodextrin coated electrode,[98] and an adamantane terminated polymer onto cyclodextrin modified silica,[99] and as a 'stopper' for rotaxanes.[100] While the association constants for these complexes are relatively high, they can be destroyed by the addition of competitive guests, surfactants or washing with organic solvents.[98,101]

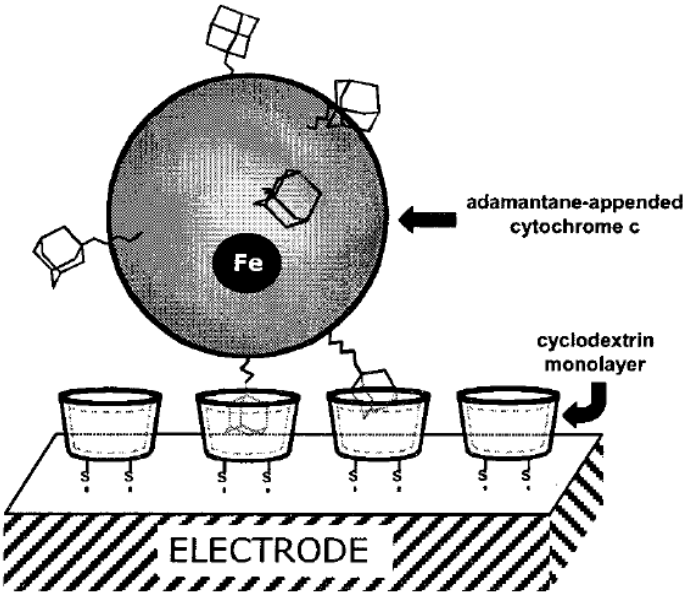

Figure1.9 Adamantane Modified Cyctochrome *c* Immobilised onto a Cyclodextrin Modified Electrode. Reprinted with permission from Langmuir, 18(13), Fragoso, Caballero, Almirall, Villalonga, Cao, *Immobilization of Adamantane-Modified Cytochrome c at Electrode Surfaces through Supramolecular Interactions*, 5051-5054. Copyright 2002, American Chemical Society

Along with adamantane, cyclodextrins are known to form complexes with many classes of organic compounds, including hydrocarbons, amines, aliphatic alcohols and diols, amino acids, cyclohexane derivatives, sugars, phenols, aromatics (including polyaromatic hydrocarbons), azo compounds, steroids, naphthalene derivatives and many pharmaceutical compounds.[102-106] This lack of selectivity precludes their use in a hydrocarbon sensor due to their high affinity not only for many of the compounds in oil, but also the natural organic matter in seawater.

The stability of a number of hemicarceplexes has been studied.[107-113] The hemicarcerands prepared by the Cram group[111,114] (Figure 1.10) were found to form stable complexes with large guests such as adamantane, camphor, and ferrocene, however they are unsuitable for use in a sensor as the decomplexation kinetics are slow.

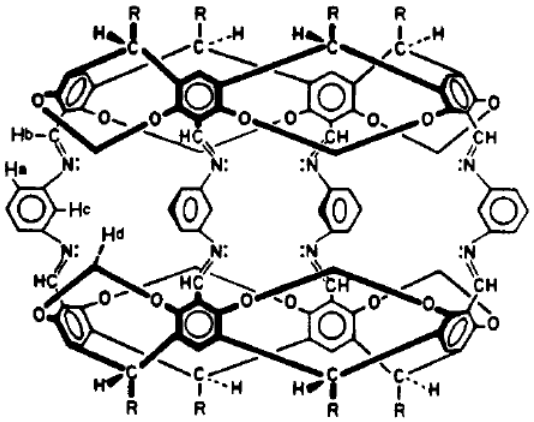

1, R = $CH_2CH_2C_6H_5$

Figure 1.10 Hemicarcerands Used to Encapsulate Large Guests. Reprinted with permission from Journal of the American Chemical Society, 113(7), Quan, Cram, *Constrictive binding of large guests by a hemicarcerand containing four portals*, 2754-2755. Copyright 1991, American Chemical Society.

Many of the complexation studies with cavitands have been performed with functionalised adamantanes, and the same receptors generally form complexes with both adamantanes and cyclohexanes, and often a variety of other hydrophobic compounds.

A cavitand stabilised in the vase conformation (Figure 1.11) by a hydrogen bonded seam was found to form kinetically stable complexes with organic cations including amantadine hydrochloride and rimantadine hydrochloride.[115] It was found that the hydrophobic adamantane base was included into the cavity with the polar group directed towards the upper rim. It was also found that sonication of an aqueous solution of the cavitand with solid adamantane resulted in the extraction of the adamantane into solution.

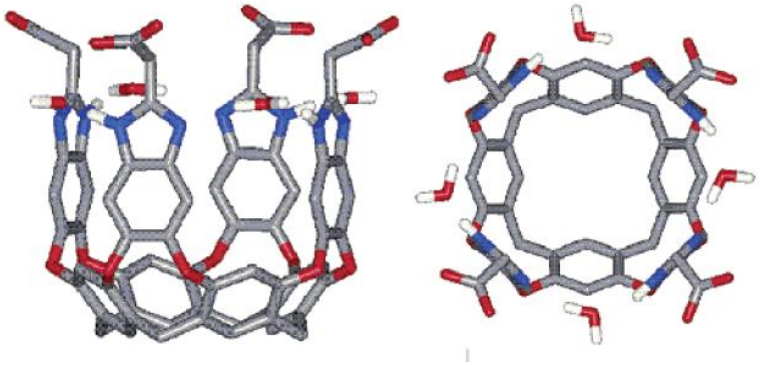

Figure 1.11 Side and Top View of a Water Soluble Cavitand for the Complexation of Organic Cations and Adamantane. Reprinted with permission from Journal of the American Chemical Society, 126(9), Biros, Ullrich, Hof, Trembleau, Rebek, *Kinetically stable complexes in water: The role of hydration and hydrophobicity*, 2870-2876. Copyright 2004, American Chemical Society.

Similar cavitands have been prepared with phosphonate groups at the upper rim[116] that form complexes with adamantane, adamantane derivatives and alkylbenzenes in deuterated chloroform. Solvents that compete for hydrogen bonds were found to destroy the complexes. Water-soluble self-folding cavitands (as mentioned in the preceding section, Figure 1.12) were found to dimerise in the kite conformation in aqueous solution in order to minimise the exposure of the hydrophobic areas to the solvent. Upon addition of a suitable guest, the hydrogen bonded seam was reformed and the complexes were in the vase conformation.[90]

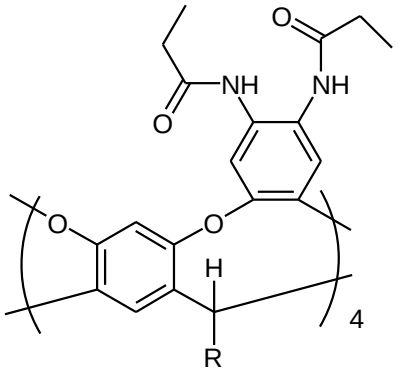

Figure 1.12 Simplified Structure of the Water-Soluble Self-Folding Cavitand.[90]

Similar organic-soluble self-folding cavitands also complex adamantanes, cyclohexanes and lactams[75,76,86,88-90,117] in deuterated chloroform, benzene, toluene, water, and xylene. It was found that the receptor has to unfold for guest exchange to occur, and as this requires the breaking of hydrogen bonds, it is slow on the NMR timescale (Figure 1.13). As with previous examples of similar cavitands, the adamantane skeleton is buried in the cavity and the polar functional groups are directed towards the solvent (and the hydrogen bonded rim). Complexes with amide functionalised guests are particularly stable and it is thought that this is due to the amide group participating in the hydrogen bonded seam at the upper rim of the receptor.[87] These observations have been reinforced by a study looking at the encapsulated site of a bi-functional guest.[86] In the case of a guest with an adamantane and cyclohexane ends joined via an amide linker, the adamantane is preferentially encapsulated. If the linker is slightly longer and the adamantane is connected via a methylene group the amide linked cyclohexane is then encapsulated, and if an analogous di-adamantane guest is tested the amide-adamantane group is preferentially encapsulated (6:1) over the methylene-adamantane group. A study by Hooley *et al.*[117] investigating the binding between substituted adamantanes with a cavitand concluded that electronic effects of the substituent played a large role in determining the binding affinity of the complex.

The binding affinity of the functionalised adamantanes (particularly amine or amide substituents) was in all cases higher than adamantane itself with this class of self-folding cavitands. This is not expected to present a particular problem for detecting hydrocarbons as the adamantane will be competing against structurally different hydrocarbons and natural organic matter in water rather than functionalised adamantanes.

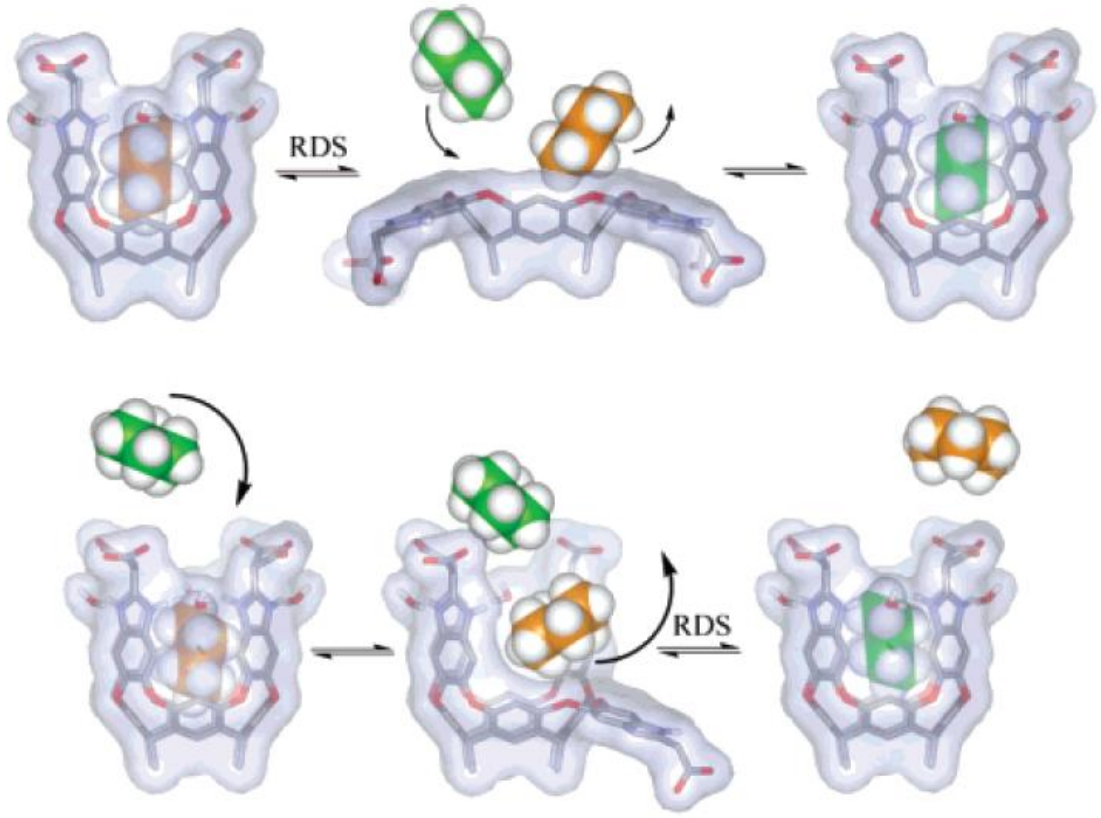

Figure 1.13 Representation of Two Proposed Mechanisms for Guest Exchange in Self-Folding Cavitands. Reprinted with permission from Journal of the American Chemical Society, 129(44), Hooley, Van Anda, Rebek, Extraction of Hydrophobic Species into a Water-Soluble Synthetic Receptor, 13464-13473. Copyright 2007, American Chemical Society.

Similar cavitands with only three 'walls' have been prepared (Figure 1.14),[118] however no binding occurred in chloroform unless the guest contained an amine/ammonium group to participate in the hydrogen bonding at the upper rim as well as a bulky aliphatic group. While adamantane exhibited no binding in the relatively hydrophobic solvent (functionalised adamantanes were bound strongly), the concept of removing structural elements may be useful in designing receptors that not only are selective but also exhibit suitable exchange kinetics for use in sensors.

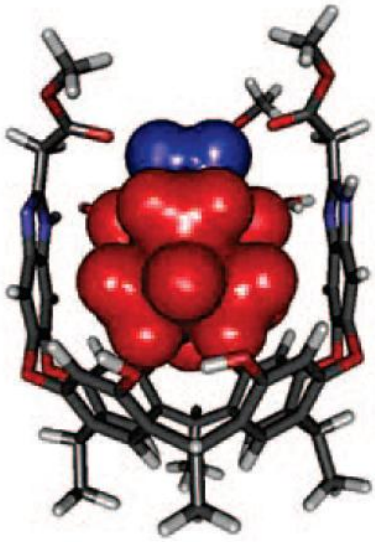

Figure 1.14 Model of the 'Three Walled' Cavitand Complexed with Amantadine. Reprinted with permission from Organic Letters, 10(17), Lledo, Hooley, Rebek, *Recognition of guests by water-stabilized cavitand hosts*, 3669-3671. Copyright 2008 American Chemical Society.

Rigid deep-cavity cavitands have been synthesised by Gibb *et al*.[119-124] The rigid cavity signifies that the host is size and shape selective as it cannot deform or partially collapse to accommodate smaller or non-spherical guests. Adamantanes are the ideal size to fill the cavity and binding studies in deuterated chloroform, toluene and dimethylsulfoxide all follow the same trend (binding constants are highest in d_6-DMSO). The highest constants were found for halogenated adamantanes as the halogen interacts with the crown of protons projecting into the cavity situated approximately two thirds of the way down into the binding pocket. While adamantane is a relatively weak binder in comparison to the halogenated derivatives, the binding constant is higher than halogenated cyclohexane and cyclopentanes and an order of magnitude higher than cyclohexane, methyl cyclohexane and iodobenzene.[124]

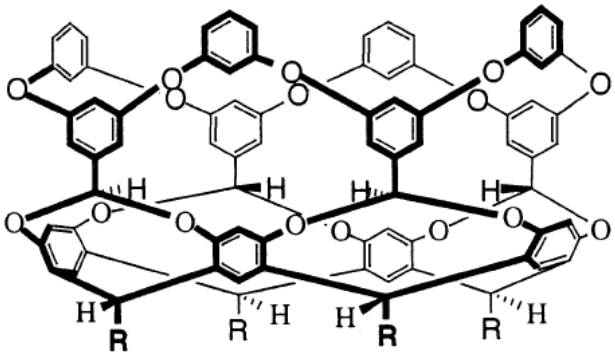

Figure 1.15 Structure of the Deep Cavity Cavitand. Reprinted with permission from Journal of the American Chemical Society, 123(24), C Gibb, Stevens, B Gibb, *C-H···X-R (X = Cl, Br, and I) Hydrogen Bonds Drive the Complexation Properties of a Nanoscale Molecular Basket* 5849-5850. Copyright 2001, American Chemical Society.

Variations of the substituents on the upper rim of the cavitand consequently alter the binding ability of the receptor. By replacing the protons at the upper rim with methyl groups, the adamantane binding ability of the receptors is greatly diminished and the preferred guests are cyclopentyls.[120] The removal of some of the aromatic rings was investigated to impart some flexibility to the structure, but this also dramatically reduced the affinity for guests.[122]

1.8.3 Complexation of Polycyclic Biomarkers

The guest properties of compounds such as steranes and hopanes are rarely studied, and so receptors known to bind steroids were examined in an effort to determine the size and shape requirements of a potential polycyclic hydrocarbon receptor. These receptors include cyclodextrins, resorcinarenes, calixarenes and cyclophanes.[125] In particular complexes of lithocholic acid (Figure 1.16) were examined as it doesn't bear any polar groups on the central rings.

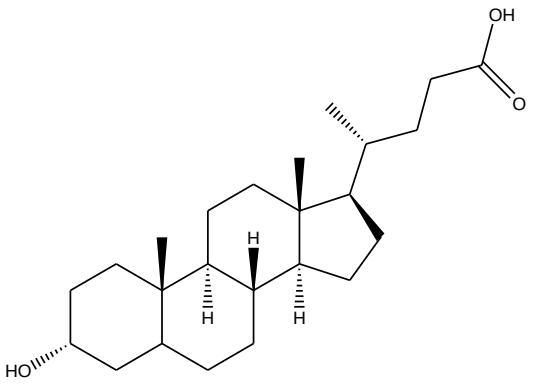

Figure 1.16 Lithocholic Acid

Lithocholic acid is known to form very strong complexes with β-cyclodextrin[126] and with a water soluble cyclophane (Figure 1.17).[127,128] The origin of the strong binding is the orientation of the guest inside the receptor such that the polar functional groups extend from the complex and are well solvated while the cycloalkane rings are 'hidden' inside the hydrophobic receptors.

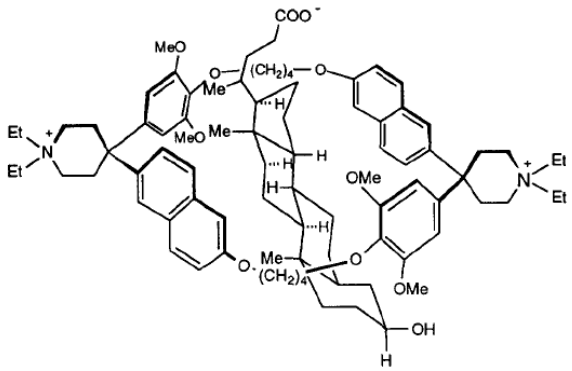

Figure 1.17 The Axial Inclusion Complex of Lithocholic Acid and a Water Soluble Cyclophane. Reprinted from Tetrahedron, 51(2), Peterson, Wallimann, Carcanague, Diederich, *Steroid complexation by cyclophane receptors in aqueous solution: Substrate selectivity, enthalpic driving force for cavity inclusion, and enthalpy-entropy compensation*, 401-421, Copyright (1995), with permission from Elsevier.

A water soluble version of the deep-cavity cavitands synthesised by Gibb[119] that strongly binds adamantane has been used to bind steroids in D_2O. It was observed that they dimerise around the steroid to form a 2:1 (host:guest) complex, and hence bulky sidegroups tend to reduce the binding affinity. Purely aliphatic guests were preferred over aromatic steroids, presumably

because the bulkier cyclohexane rings fill the cavity better than the flat aromatic rings.

A complicated 'double decker' cyclophane has been used to complex various steroids and steranes in deuterated methanol.[129,130] While cholestane exhibited the highest binding constant, other steroids had similar affinity. In general, complexes with aliphatic steroids were more stable than flat aromatic steroids, and a significant contribution to the stability appears to come from the isoprenoid side chain which is also encapsulated in the receptor.

Bridged cyclodextrins have also been used to complex a variety of steroids.[131,132] The same cyclodextrin dimers have been used to form complexes with a variety of compounds that have the appropriate length and capping groups (t-butyl, phenyl, adamantyl).[133]

In a similar vein, cyclodextrin-calixarene couples have been used as fluorescent sensors for the detection of various steroids, terpenes and adamantanes. The receptors were more sensitive to steroids (e.g. cholesterol, ethinyl-nortestosterone) than to the natural products tested (e.g. carvone, menthol, skatol), however 1-adamantylbenzoate did show a higher affinity although this was not entirely due to the adamantyl structure as 1-adamantanol had an affinity two orders of magnitude lower.[134]

Inorganic receptor materials have been used by petroleum geochemists to separate the components of crude oils. For example Dimmler *et al*.[135] used molecular sieves to selectively sorb hopanes and tricyclic terpanes from oil samples. Armanios *et al*.[136] extended this work and used an ultrastable zeolite as a chromatography phase to separate different hopanes based on shape.

1.9 Project Aims

The overarching goal of this research program is to produce a relatively inexpensive instrument to complement the existing exploration techniques and ideally improve the drilling success rate by providing additional data on the presence or absence of petroleum in proposed drilling locations. Predictions of oil quality can be made from the characterisation of the seep oils. The technology developed can immediately be applied to oil spill detection in addition to petroleum exploration, and with modification of the receptors the potential exists to develop sensors for almost any chemical. The resulting instrument could then be used in applications ranging from environmental monitoring for a range of toxins, or detection of chemical warfare agents, to online monitoring of process streams.

As a first step toward this goal receptors for the hydrocarbons found in oil must be developed and tested, and this will be the focus of this project. While the literature suggests that deep cavitand-like structures offer promise in terms of achieving selectivity, there is also evidence that deep cavitands can also form complexes with a large variety of compounds, such as the quinoxaline cavitands that form complexes with compounds ranging from ethyl acetate to substituted aromatic compounds.[137] The slow exchange kinetics are also a significant drawback in a sensor application. The complexation properties of simpler and more flexible resorcinarene structures have not been tested with hydrocarbon analytes. They cannot completely encapsulate the guest which is assumed to result in very poor binding capability; however experimental work is needed to determine whether this presumption is true. If complexes are found to form, these hosts may provide an appropriate balance between selectivity and speed.

A common feature of the sensor designs is the placement of a sensor layer over a gold electrode/surface. Although there are many ways to do this non-covalently (i.e. drop casting, spin coating, evaporative), the formation of self-assembled monolayers in the first instance allows the receptors to be

evaluated against each other with minimal complications from film processing and morphology.

The synthesis of a range of relatively simple sulfur functionalised receptors will be undertaken to test their affinity for cyclohexyl and adamantyl guests. Monolayers of the receptors will be characterised, and subsequently their complexation properties studied by atomic force microscopy (AFM) force spectroscopy, which directly measures the adhesion of a molecular probe with a monolayer. These results will be used to identify promising receptor targets for future study.

2.0 Synthesis of Receptors

2.1 Introduction

2.1.1 Resorcinarenes

Resorcinarenes are tetrameric macrocycles, formed from the acid catalysed condensation of resorcinol and an aldehyde. Numerous aldehydes have been used to generate resorcinarenes with differing substitution at the carbon bridges (see Figure 2.1, R groups). Resorcinarenes were first generated in 1872 by von Baeyer, however the tetrameric structure was not proposed until 1940 by Niederl and Vogel, and was finally proven in 1968 by Erdtman by a single crystal X-ray analysis.[138]

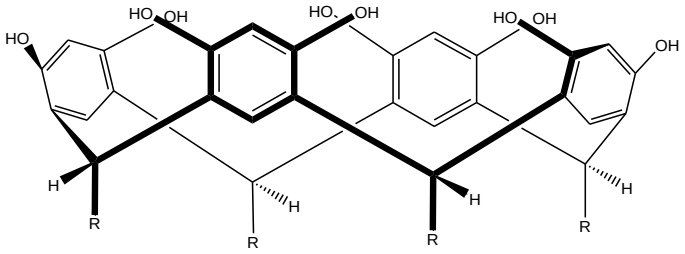

Figure 2.1 Basic Resorcinarene Structure

The traditional reaction conditions involve the use of concentrated hydrochloric acid, and an alcoholic solvent at reflux, however the use of a Lewis acid catalyst has also been reported to produce resorcinarenes from cinnamates.[139]

The basic macrocycle skeleton is identical to the calixarenes, and numerous trivial names have been suggested in the literature; such as calix[4]resorcinarenes, resorcinol derived calixarenes, octols and Högberg compounds. These have slowly been replaced by the use of “resorcinarene”.

The stereochemistry of resorcinarenes is defined as a combination of three different stereochemical elements; the conformation of the macrocyclic ring (Figure 2.2), the relative configuration of the substituents at the methylene

bridges (Figure 2.3), and the individual configuration of the substituents (axial or equatorial).

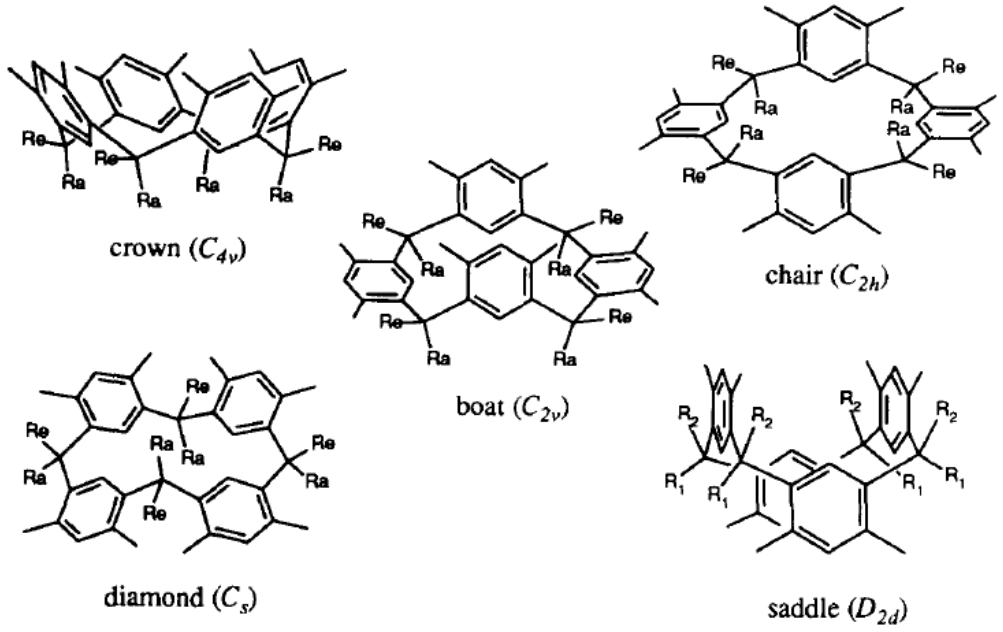

Figure 2.2 Conformations of the Macrocycle Ring. Reprinted from Tetrahedron, 52(6), Timmerman, Verboom, Reinhoudt, *Resorcinarenes*, 2663 - 2704, Copyright (1996), with permission from Elsevier.

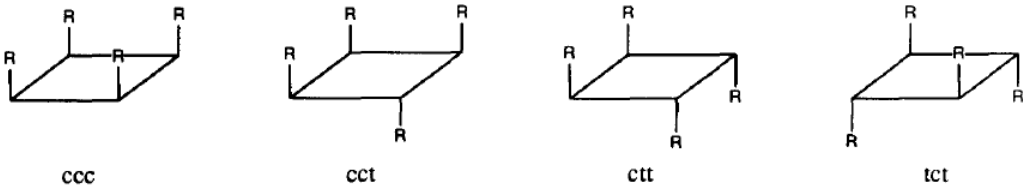

Figure 2.3 Relative Configurations of the Methylene Substituents. Reprinted from Tetrahedron, 52(6), Timmerman, Verboom, Reinhoudt, *Resorcinarenes*, 2663 - 2704, Copyright (1996), with permission from Elsevier.

Only five of the many possible isomers have been found experimentally (in the solid state): a crown conformer with an all axial, all-cis configuration; a boat conformer with an all axial, all-cis configuration; a chair conformation with an all axial ctt configuration, a diamond conformer with an all axial cct configuration, and a saddle conformer with an all-cis configuration.[140]

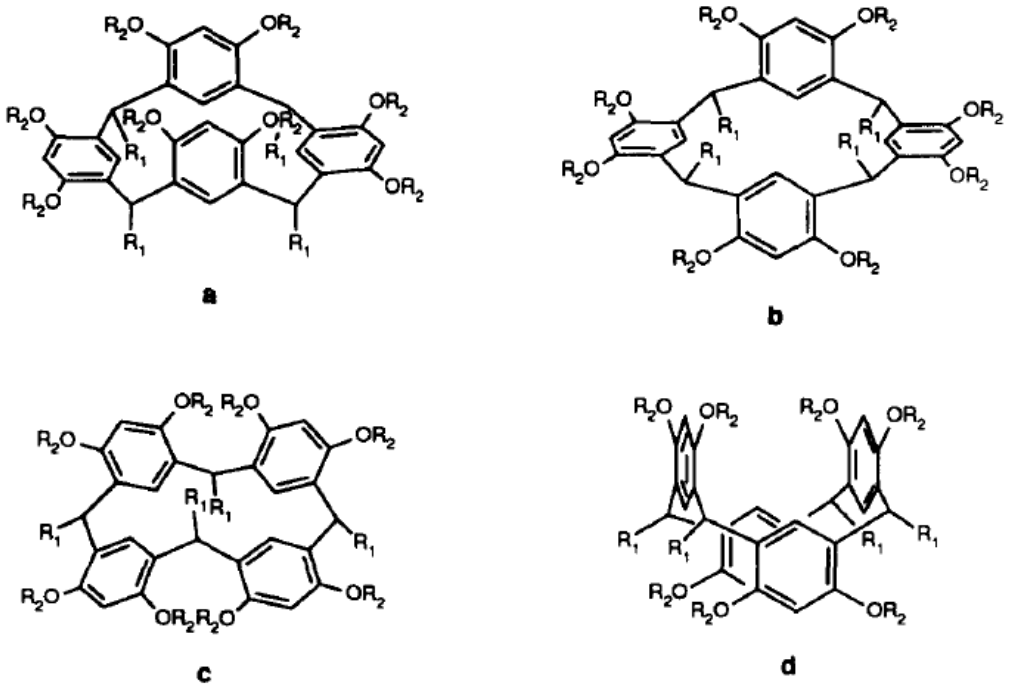

Figure 2.4 Four of the Isomers Found Experimentally a) boat (ccc) b) chair (ctt) c) diamond (ctc) and d) saddle (ccc). Reprinted from Tetrahedron, 52(6), Timmerman, Verboom, Reinhoudt, *Resorcinarenes*, 2663 - 2704, Copyright (1996), with permission from Elsevier.

Interconversion between the isomers (with the exception of the pseudorotation required for the crown ↔ boat interconversion) requires the inversion of the substituents from the lower energy axial to the higher energy equatorial.

Nuclear magnetic resonance (NMR) evidence shows that for most resorcinarene derivatives in solution at room temperature, the two boat conformers rapidly interconvert leading to an average crown structure (C_{4v} symmetry leading to two aromatic singlets). At reduced temperatures the aromatic peaks resolve into the four singlets expected from the C_{2v} symmetry of the boat conformer. NMR studies of the chair, diamond and saddle show no similar changes suggesting the barriers for interconversion are too high resulting in rigid structures.[141]

The condensation reaction is reversible, so under the typical homogeneous synthesis conditions the product mixture will reflect the thermodynamic

stability, while under heterogeneous conditions the relative solubilities determines the product ratio.

The major applications of resorcinarenes utilise their ability to act as supramolecular receptors. Complexes with cations, anions and neutral molecules have all been reported,[138] and subsequently they have been used in a wide variety of sensors.

Resorcinarenes have also been used as catalysts and as scaffolds for the synthesis of more complicated molecules such as cavitands and carcerands.[72]

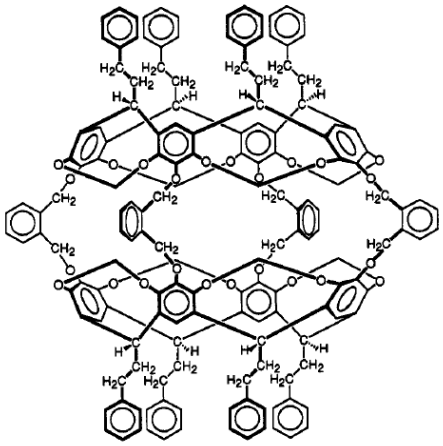

Figure 2.5 Example of a Resorcinarene Based Carcerand. Reprinted with permission from the Journal of the American Chemical Society, 116(1), Robbins, Knobler, Bellew, Cram, *A Highly Adaptive and Strongly Binding Hemicarcerand*, 111 - 122. Copyright 1994 American Chemical Society.

2.1.2 Calixarenes

Calixarenes are structurally similar to resorcinarenes (see Figure 2.6) and are formed from a base catalysed reaction between a *para* substituted phenol and formaldehyde. The *para* group needs to be a bulky substituent in order for the cyclisation to occur in high yields[142] and traditionally p-*tert*-butyl phenol is used, as the tertiary butyl groups can easily be removed from the calixarene if desired. Unlike resorcinarenes, calixarenes composed of different numbers of aryl units are common, especially calix[6]arenes and

calix[8]arenes, and are easily synthesised by controlling the amount and composition of base in the reaction.[140]

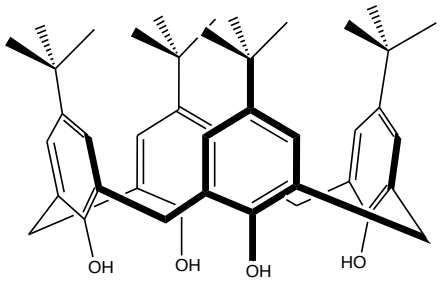

Figure 2.6 p-*tert*-butylcalix[4]arene

The methylene bridging units of the calixarenes are rotationally mobile so that interconversion between the conformations is possible. The four possible conformers of the calix[4]arene only differ with respect to the 'up down' arrangement of the aryl rings and are described as cone, partial cone, 1,3 alternate and 1,2 alternate (see Fig. 2.7). The conformation can be fixed by preventing rotation through the annulus; this is usually achieved by adding bulky groups to the lower rim. A propyl group attached to the lower rim is large enough to fix the conformation.[140]

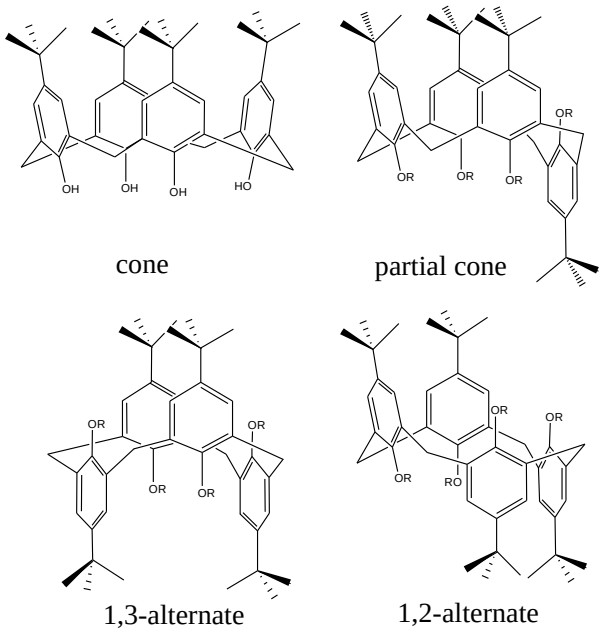

Fig. 2.7 Conformations of p-*tert*-butylcalix[4]arene

Calixarenes form inclusion complexes with a wide range of guests. These guests can be anionic, cationic or neutral depending on the functional groups present. Numerous applications for calixarenes have been developed and include antimicrobials,[143] ion exchangers, phase transfer agents, ion selective electrodes, fluorescent sensors, catalysts, and chiral additives for chromatography.[140]

2.1.3 Sulfur Compounds

Self-assembled monolayers (SAMs) form spontaneously on gold surfaces from solutions of a variety of sulfur compounds. Functional groups known to adsorb include organic thiosulfates[144] and dithiocarbamates,[145] but sulfides, disulfides and thiols are far more common.[146]

There are several examples of sulfur functionalised resorcinarenes and calixarenes in the literature which have been used to form self-assembled monolayers. Dialkylsulfide derivatives have generally been used to form physisorbed monolayers, however some examples of thiol derivatives being used to form chemisorbed monolayers have been reported.

One example is the p-*tert*-butylcalix[4]arenethiol (Figure 2.8) which was synthesised from *p-tert*-butylcalix[4]arene by reacting with dimethyl(thiocarbamoyl) chloride, thermal rearrangement to the (dimethylcarbamoyl)thio compound, then reduction to the thiol.[123]

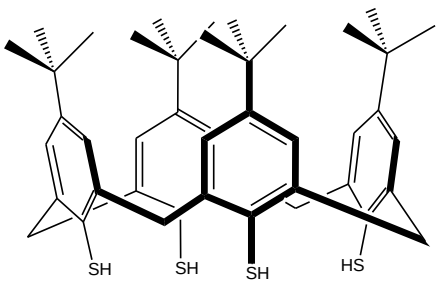

Figure 2.8 p-*tert*-butylcalix[4]arenethiol

Calixarenes functionalised with alkylsulfide groups (Figure 2.9) have been synthesised as they were expected to give more ordered monolayers.[147] Monolayers have also been formed on gold nanoparticles by similar molecules.[148]

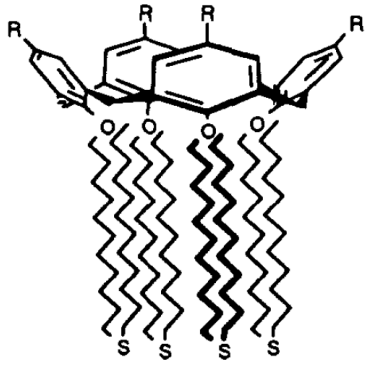

Figure 2.9 Dialkyl Sulfide Calixarene[147]. Reprinted from Tetrahedron Letters, 36(18), Huisman, van Velzen, van Veggel, Engbersen, Reinhoudt, *Self-Assembled Monolayers of Calix[4]arene Derivatives on Gold*, 3273-3276, Copyright (1995), with permission from Elsevier

Monolayers from dialkylsulfide resorcinarenes (Figure 2.10) first synthesised by van Velzen *et al.*[149] have been studied by a number of techniques such as atomic force microscopy (AFM)[150], infra-red spectroscopy, and electrochemical techniques,[151] and have also been used as the sensing layer for a surface plasmon resonance (SPR) sensor.[56]

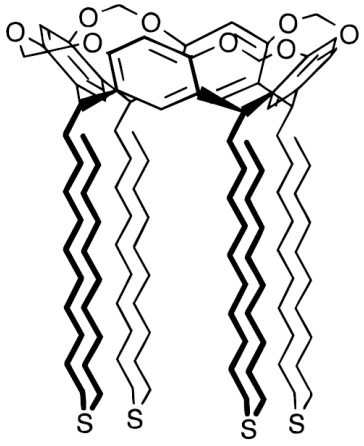

Figure 2.10 Dialkyl Sulfide Resorcinarene. Reprinted with permission from Langmuir, 13(6), Schonherr, Vancso, Huisman, van Veggel, Reinhoudt, *An atomic force microscopy study of self-assembled monolayers of calix[4]resorcinarene adsorbates on Au(111)*, 1567-1570. Copyright 1997 American Chemical Society.

Thiol functionalised resorcinarenes (Figure 2.11) have been synthesised by Davis and Stirling[152] who also investigated their receptor properties. The same resorcinarenes were used by Faull and Gupta[153] as sensing layers for SPR sensors.

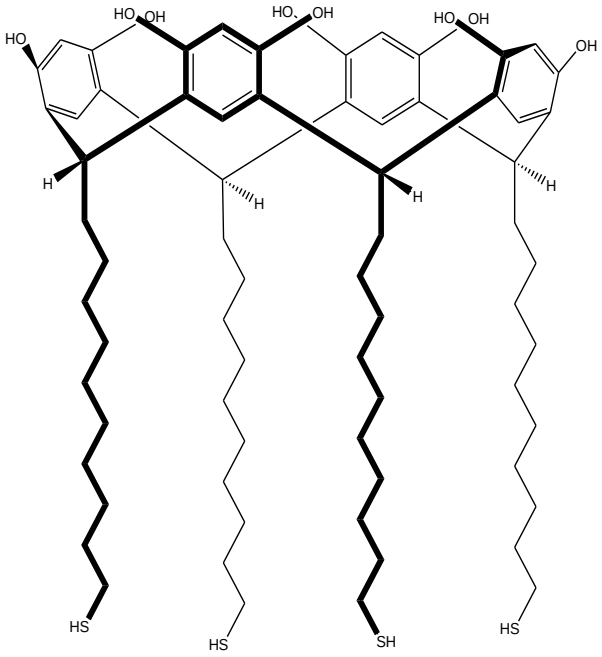

Figure 2.11 Thiol Functionalised Resorcinarene[153]

2.1.4 Nomenclature and Representations

The IUPAC naming system becomes very unwieldy when applied to calixarenes and resorcinarenes. In order to simplify identification the resorcinarenes and calixarenes used will be referred to by their substituents and compound number.

Structural representations of resorcinarenes and calixarenes throughout the literature have varied a great deal. In this work the only conformations used are the crown rccc isomer of the resorcinarenes, and the cone conformer of the calixarenes, so stereochemistry will not be specified. In order to save space, and clarify the reactions taking place only one aromatic unit is drawn (all compounds are octasubstituted at the upper rim for the resorcinarenes

and tetrasubstituted at the lower rim for both resorcinarenes and calixarenes).

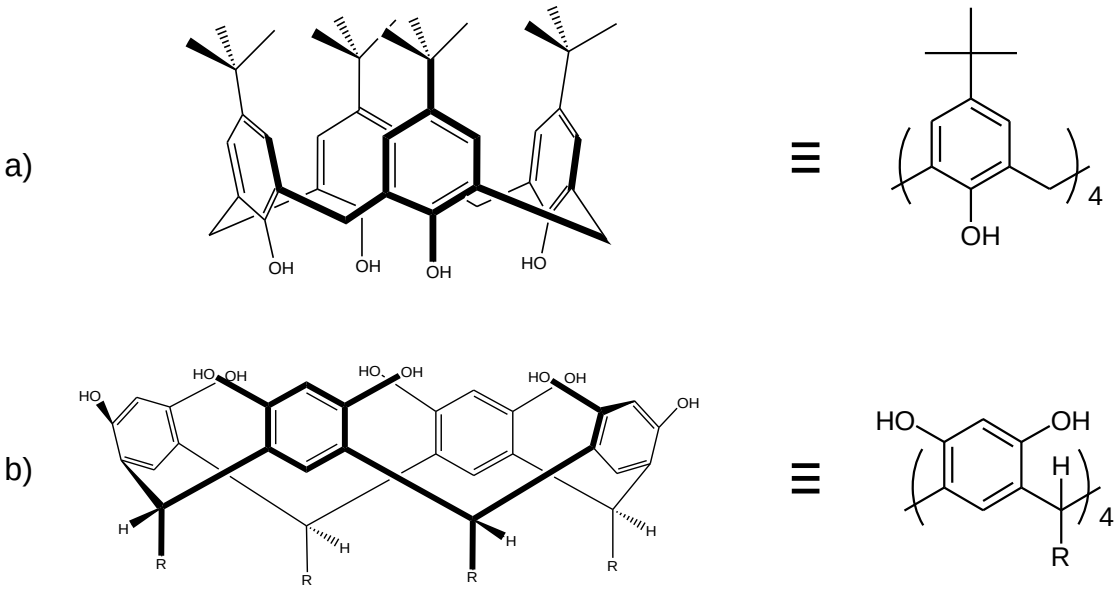

Figure 2.12 Equivalent Representations of a) Calixarenes and b) Resorcinarenes.

2.2 Discussion

Sulfur functionalised resorcinarenes were synthesised by a scheme (Scheme 1) based on those used by van Velzen *et al* [154] and Davis and Stirling.[152]

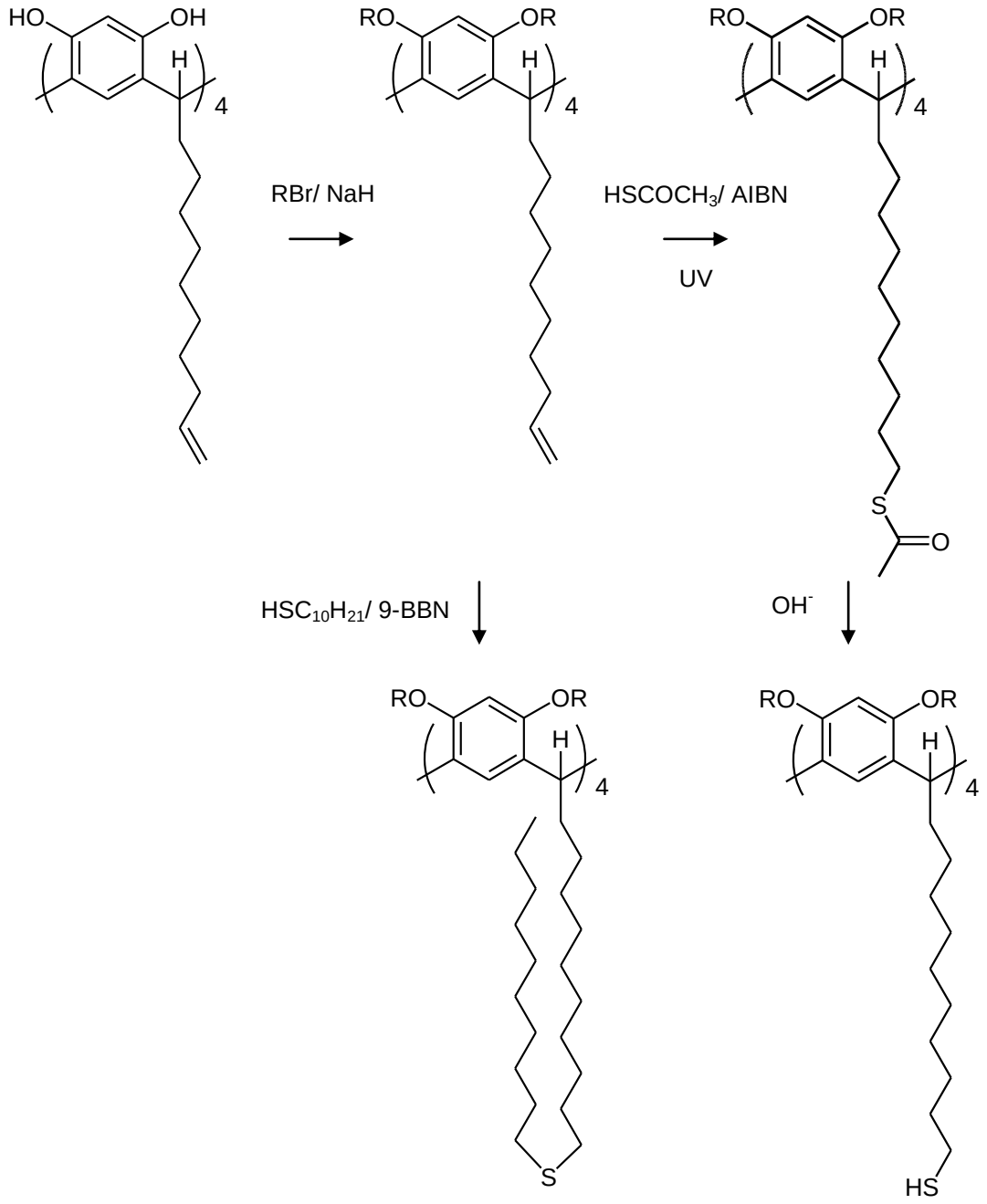

Scheme 1. Synthesis of Sulfur Functionalised Resorcinarenes

An alternative strategy had been originally proposed, based on the hydroxyl footed resorcinarene (Scheme 2) reported by Gibb *et al.*[155] The preparation

of this resorcinarene proved irreproducible, yielding either impure resorcinarene, or more often, unresolvable polymeric material. The small amount of the resorcinarene prepared proved very difficult to purify even once the phenols were functionalised, and attempts to react the alcohols to form a leaving group or to form an ester were unsuccessful. This route was abandoned due to the difficulty of preparing the starting resorcinarene.

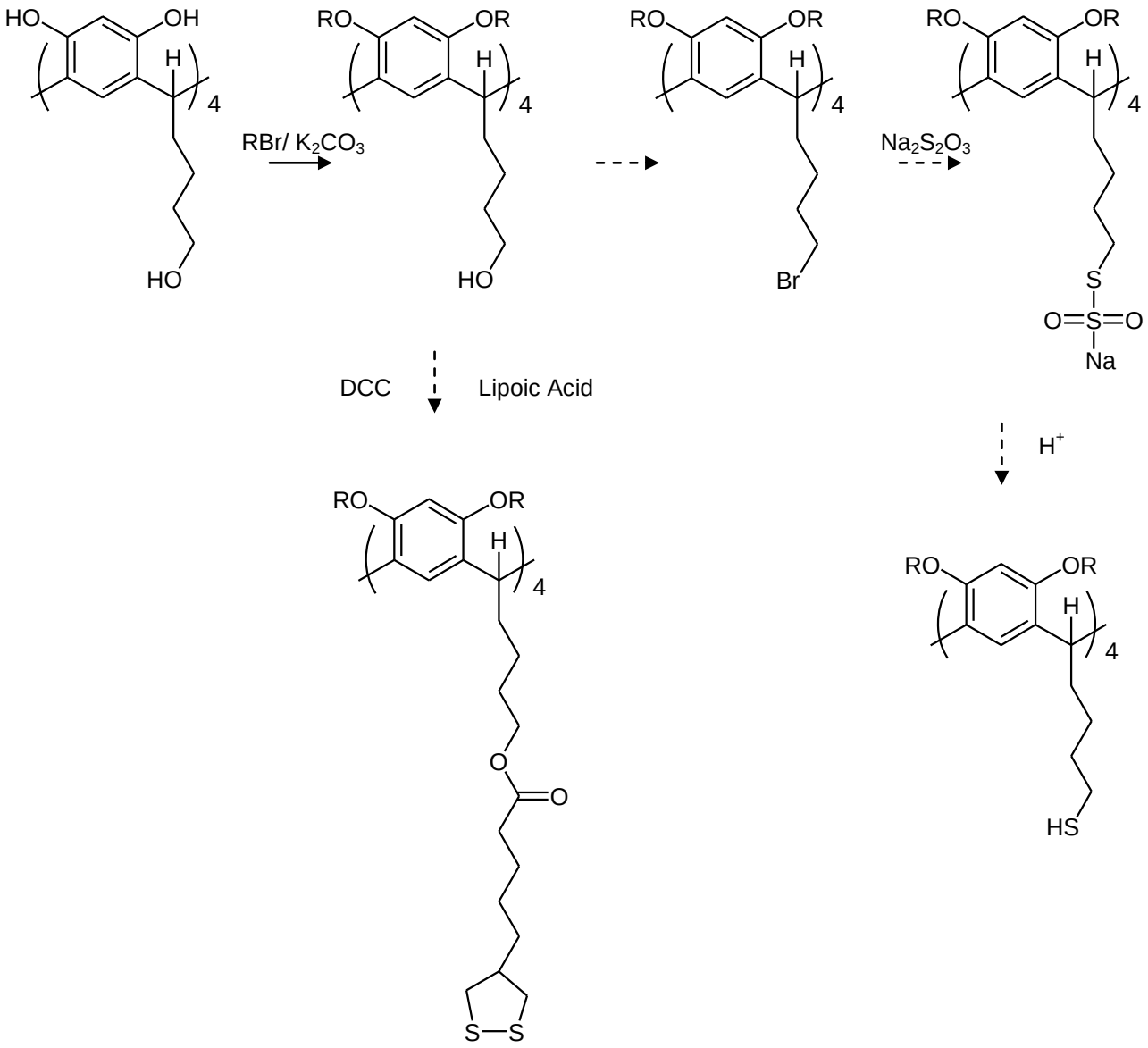

Scheme 2. Initial Scheme Based on the Hydroxyl Footed Resorcinarene.

2.2.1 Undecylenic Resorcinarene

The undecylenic resorcinarene **1** was prepared as per van Velzen *et al.*[154] (see Figure 2.13). As reported, the conditions used (70 °C, 16 hrs) resulted in the exclusive formation of the thermodynamically stable crown rccc isomer, as shown by the single resonances observed in the ^{1}H NMR for the two aromatic protons and the methine proton.[141]

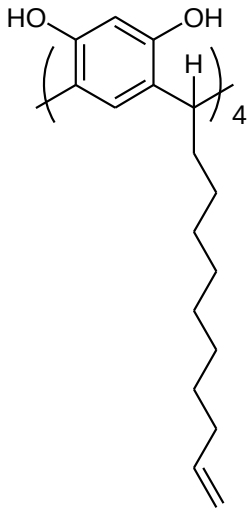

Figure 2.13 Undecylenic Resorcinarene **1**

A 63% yield was obtained, much higher than the literature yield of 22%.[154] A small amount of methanol was the only impurity visible in the ^{1}H NMR spectrum, however a ultraviolet (UV) active impurity was able to be resolved on a thin layer chromatography (TLC) plate. A small amount (<2%) impurity was reported in the literature product (a pink solid), and the authors report it was difficult to remove, however could be removed easily after functionalisation of the upper rim. The melting point measured was 290 °C (lit. 295 °C) which indicates that although the yield obtained was much higher than that reported, the material was of similar purity.

The literature procedure uses a lengthy series of recrystallisations to purify the product: three times from acetonitrile, once from cyclohexane, and twice from petroleum spirits. When later batches of the resorcinarene were prepared, this was simplified to just one recystallisation from acetonitrile.

Comparison of the analytical data obtained from this product reveals it was identical to the sample obtained from the more extensive purification procedure. The simplified procedure saved large volumes of solvent; however the yield was not significantly greater (66%).

It is likely that the impurity arises from a competing reaction or degradation product, and is structurally similar to the products, as any unreacted reagents would be visible in the NMR and/or IR spectra. No unexpected peaks were observed in any of the spectra obtained. If the assumption postulated by van Velzen *et al,*[154] that the colour of the product is due to the impurity, is correct, then it follows that the impurity is a degradation product as the colour of the material darkens over long term storage, and occurs very quickly when exposed to heat or air while in solution.

The long alkyl chains of the resorcinarene result in a product that is not crystalline, and while this increases the difficulty of handling and purification, the long chains are expected to pack more efficiently on a gold surface producing a more ordered monolayer.

2.2.2 Upper Rim Functionalisation

The Williamson ether synthesis was used to completely alkylate the phenols of the undecylenic resorcinarene **1** with methyl (**2**), propyl (**3**), and benzyl (**4**) groups (Scheme 3).

The conditions used for the synthesis of **2**[154] were adapted for the preparation of **3** and **4**. A large excess of the alkylating agent (RBr) was used along with the strong base sodium hydride, to ensure the phenols were exhaustively deprotonated, then alkylated. The reactions were performed at room temperature to minimise oxidation or decomposition of the resorcinarene. All appeared to go to completion by TLC within a few days of stirring at room temperature.

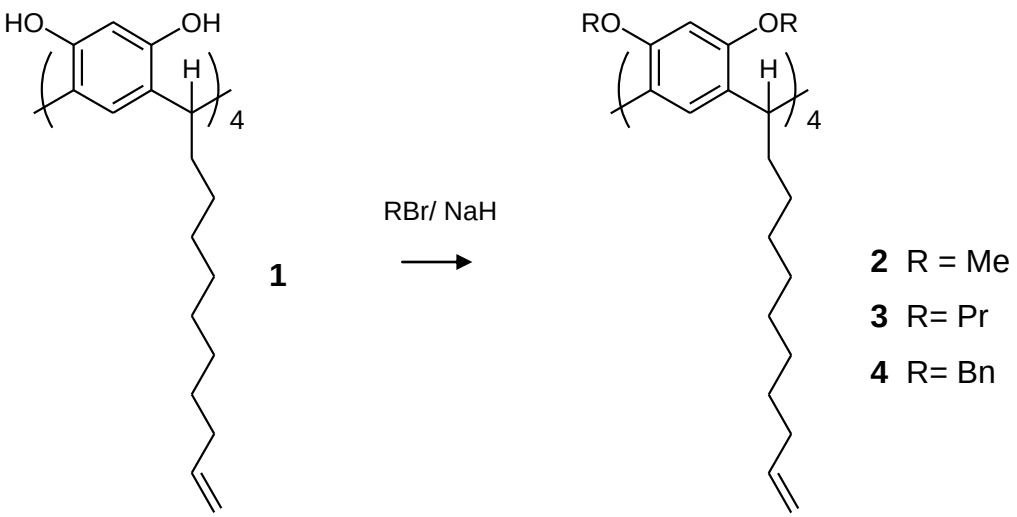

Scheme 3. Alkylation of the Upper Rim

The colour of the reaction was a fairly reliable indicator of the progression of the reaction, as the purple of the resorcinarene salt gives way to the yellowish colour of the crude product. No starting material was identified in the reaction mixture, or crude material. The small impurity peaks observed in the ^{1}H NMR spectra may be due to partially alkylated resorcinarenes or degradation products of the resorcinarene, however comparison of the integrations shows that they are a very minor component.

The compounds were not crystalline (**2** was isolated as a waxy solid, however **3** and **4** were both obtained as oils) so could not be recrystallised, and were poorly resolved by TLC, even with complete removal of any contaminating dimethylformamide. This problem was not alleviated by changing the solvent, or chromatography using an alumina phase, and it was decided that the minor impurities observed in **2** and **3** would be removed after the next step. The benzyloxy resorcinarene **4** was chromatographed to remove the majority of the impurities. The yields of these compounds were good, ranging from 50% for chromatographed compounds, to 95% for those used crude.

The NMR spectra for **2** and **4** match what was expected, with small shifts in the resorcinarene signals, and the addition of the alkyloxy signals. The aromatic signals of the propoxy resorcinarene **3** however, had an unanticipated appearance.

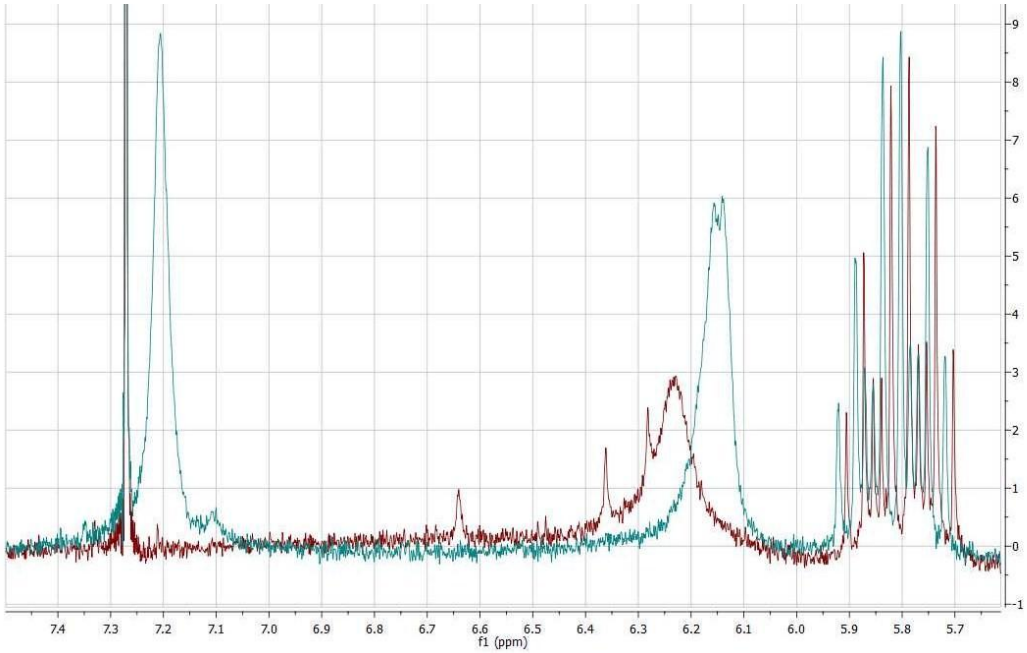

Figure 2.14 Expanded Aromatic Region in ^{1}H NMR spectra. Blue : resorcinarene **1**, Red: propoxy resorcinarene **3**.

The aromatic region of the propoxy resorcinarene **3** is overlaid with the same region from the starting material **1** (Figure 2.14). One of the aromatic singlets has broadened to the point it is invisible, while the other has broadened to a lesser degree (small sharp peaks in the shoulder are assumed to be impurities). Alternative structures were considered to explain the observed ^{1}H NMR spectrum, however the ^{13}C NMR spectrum is consistent with the proposed structure, as was the mass spectrum.

The broadening of the aromatic peaks can be attributed to a slowing of the interconversion between the two boat conformers (see Figure 2.15), so that the C_{4v} symmetry of the average structure (the crown conformer) no longer applies. This property could be investigated with variable temperature NMR, and it would be expected that at lower temperatures the broad peaks

observed would resolve into 4 aromatic singlets reflecting the C_{2v} symmetry of the boat conformer.[141]

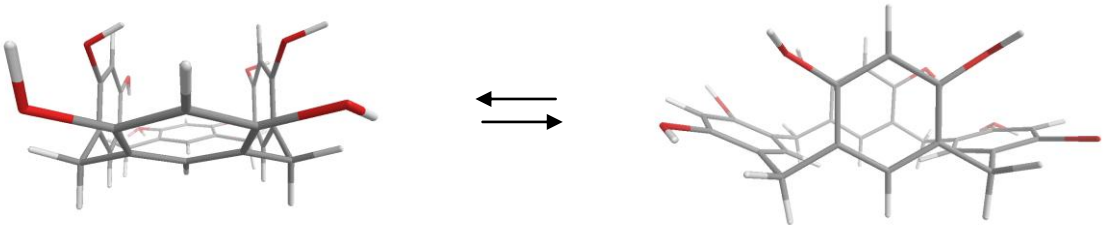

Boat Conformers

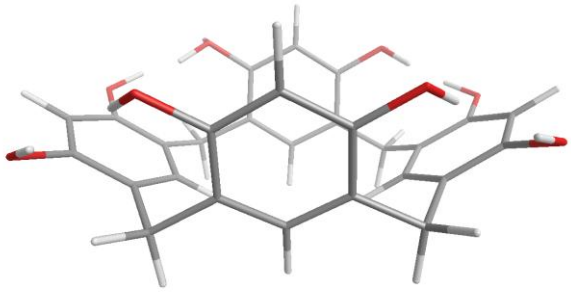

Crown Conformer (Average structure)

Figure 2.15. Conformations of Resorcinarenes in Solution (structures simplified for clarity).

2.2.2.1 Cavitands

Cavitands are resorcinarenes bridged at adjacent phenols to form a rigid enforced cavity. They are often used as receptors or as rigid scaffolds for larger molecules.

The methylene cavitand **5** was prepared following the procedure developed by van Velzen *et al.*[154] Bromochloromethane and the resorcinarene **1** were added dropwise into a suspension of sodium hydride in DMF. This pseudo-high dilution procedure is necessary to maximise the intramolecular bridging over the polymeric material obtained from the intermolecular reaction. The literature method includes a Soxhlet extraction of the crude solid with acetone, suggesting that polymeric material was still formed. This step was

omitted as the product obtained was completely soluble in a small amount of acetone, and correspondingly the yield obtained (68%, lit 55%), was higher.

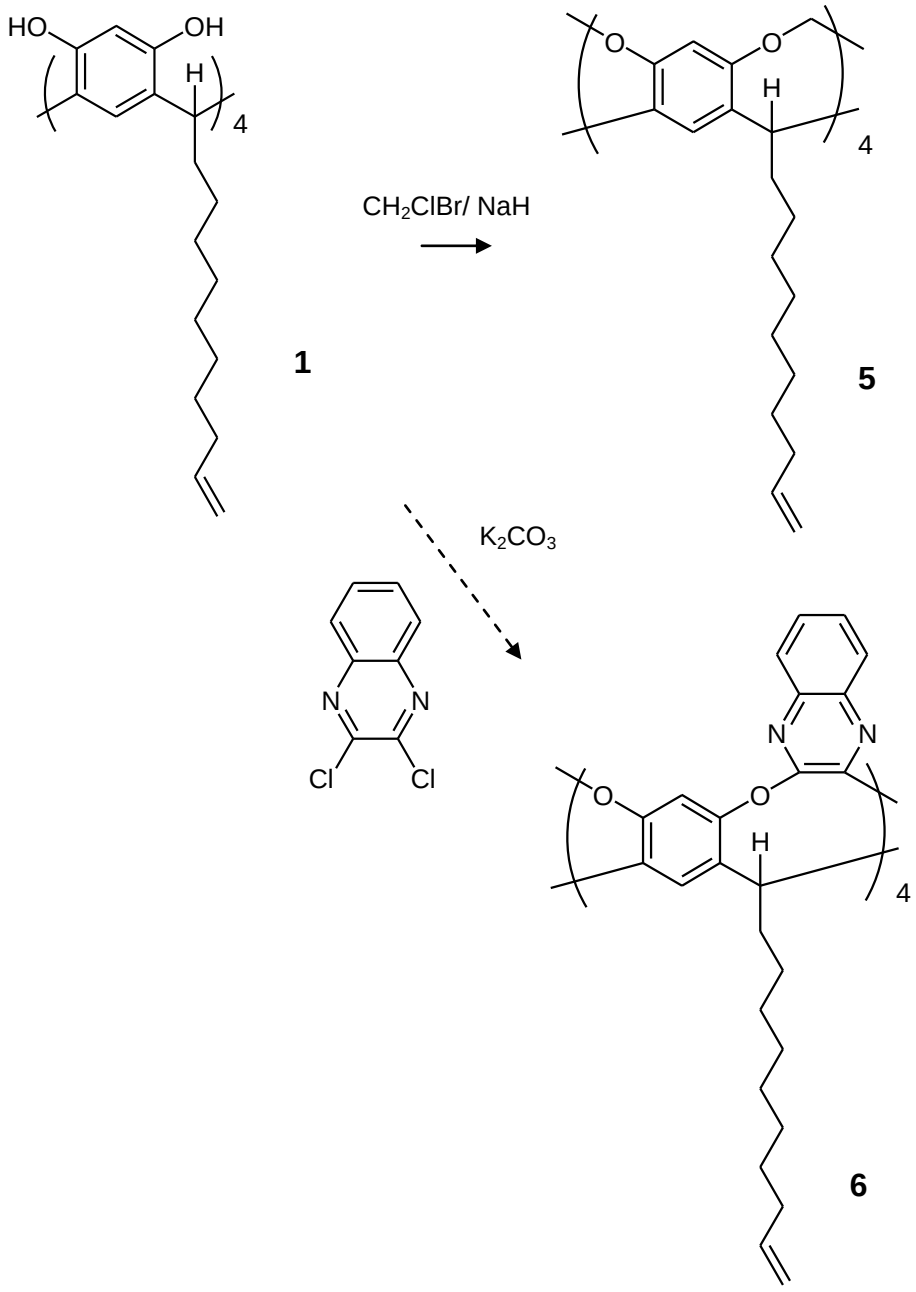

Scheme 4. Synthesis of Methylene and Quinoxaline Cavitands.

The attempted synthesis of the quinoxaline cavitand **6** was based on a series of quinoxaline cavitands prepared by the Cram group[156] to study the conformational dynamics of cavitands with extended cavities. A similar

cavitand was used to absorb organic pollutants including aromatic compounds from water samples.[137] Several attempts were made, however the product obtained exhibited very broad peaks in the NMR spectrum (see Figure 2.16) possibly indicating polymeric material. It is also possible that the desired product has been formed, but is slow moving on the NMR timescale, however this is unlikely as the structure is very similar to those prepared by Cram (the alkyl chain was saturated), which did not exhibit this behaviour.

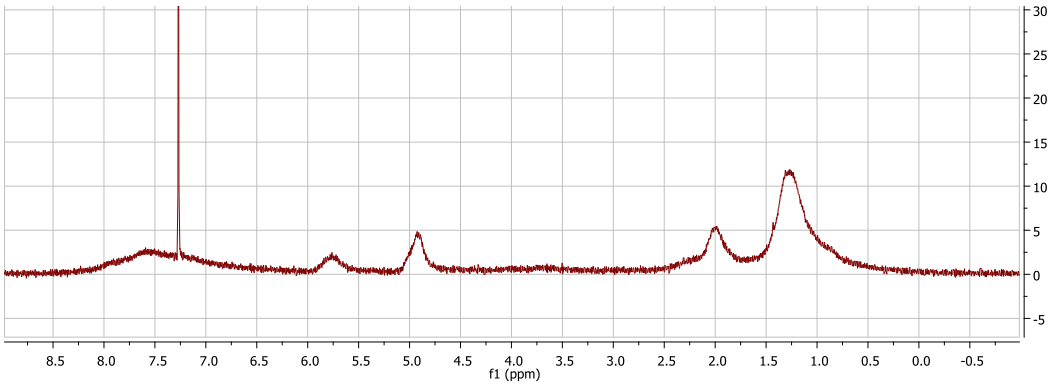

Figure 2.16 NMR of Product Obtained from Quinoxaline Cavitand Reaction.

The preparation of cavitands with deepened cavities was deemed very desirable as the receptors reported for adamantane all have this general structure, however time constraints prevented further attempts. A quantity of a similar cavitand **7** (Figure 2.17) was obtained in order to undertake the planned studies.[157]

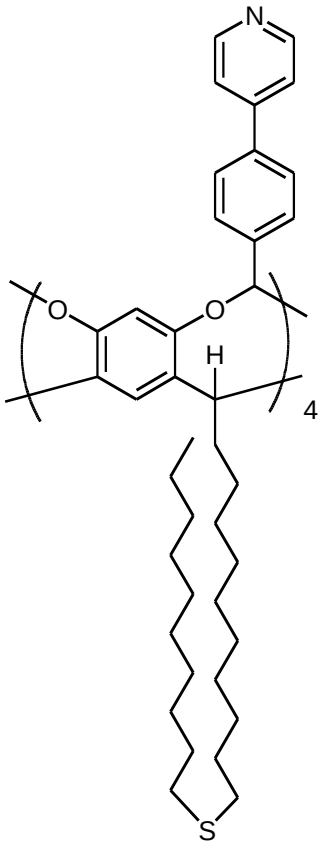

Figure 2.17 Structure of Cavitand **7**[157]

2.2.3 Alkene Functionalisation

The alkene functionalities were reacted to form thioacetyl groups via a radical addition mechanism. This allows for the anti-Markovnikov addition across the double bond (Scheme 5).

The initiator used was 2,2'-azobisisobutyronitrile (AIBN) which can be initiated with UV light, or with heat. Both methods were trialled and it was found that the UV initiation method was much faster, and the crude product was cleaner.

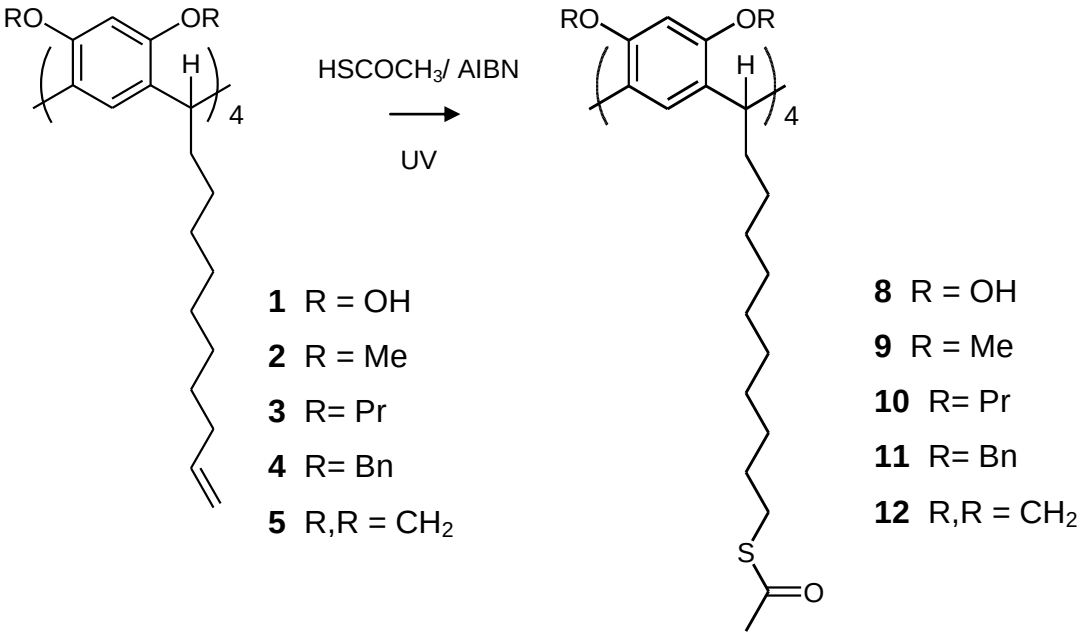

Scheme 5. Radical Addition of Thioacetic Acid Across an Alkene

The synthesis of the hydroxyl resorcinarene thioacetate **8** has been reported in the literature,[57,152,153] however the brief purification procedure described (reprecipitation from ethanol and water) was not effective. The ^{1}H NMR spectrum showed the disappearance of the alkene peaks of the starting material **1**, however the remaining peaks were broad, and the colour of the material was very dark. It was thought that the addition was occurring, however was contaminated with oxidised resorcinarene due to inadequate deoxygenation. The difficulty with this compound led to the use of a simple calixarene as a model compound to investigate the reaction conditions (described in Section 2.2.3.1) before continuing the synthesis of the remaining resorcinarenes.

The syntheses of compounds **9**-**12** were initially very successful, with complete disappearance of the alkene peaks (multiplets at ~5.8 and 4.9 ppm) in the ^{1}H NMR spectrum after four hours of UV irradiation. Column chromatography was used with difficulty to purify the compounds. On TLC the resorcinarenes tended to streak in all solvent systems tried, however with

careful solvent ramping, the thioacetates **9**-**12** were obtained with acceptable purity.

2.2.3.1 Calixarenes

Thioacetyl calixarenes were prepared as a model for the resorcinarene synthesis. The calixarene products are crystalline, hence are easier to purify, and they give simpler NMR spectra to interpret. Calixarenes are also known to form complexes with simple aromatic molecules,[140] and so they are a useful comparison to the resorcinarene based receptors for complexation studies.

The literature procedures for the p-*tert*-butylcalix[4]arene **13**[158] and the tetraallylcalix[4]arene **14**[159] are well established.

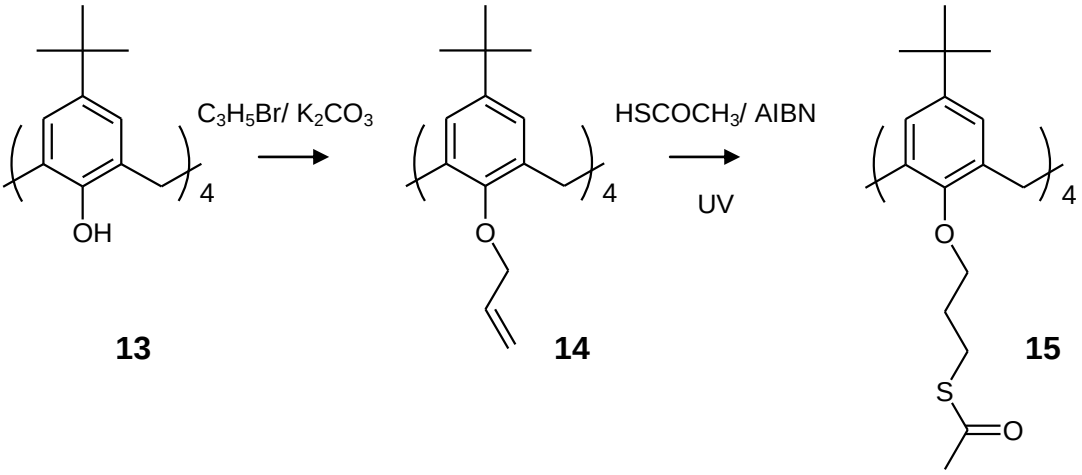

Scheme 6. Synthesis of Thioacetylcalix[4]arene.

The preparation of thioacetyl functionalised calixarenes has been reported by Arduini *et al.*[160] Calixarenes bis-substituted with hexyl thiol, or dodecyl thiol groups at the lower rim were used to functionalise gold nanoparticles. These calixarenes were synthesised by the same method except the radical addition of thioacetic acid was initiated by heat rather than irradiation with ultraviolet light.

The thioacetyl calixarene **15** was synthesised using the same conditions employed for the resorcinarenes. After four hours of irradiation no alkene signals were visible in the NMR spectrum. As expected the calixarene proved much easier to purify than the corresponding resorcinarenes, with a dichloromethane/hexanes recrystallisation yielding a pure product.

2.2.3.2 Method Failure

Reproducibility problems with the radical addition reaction became evident when the reaction was scaled up to provide more material for future studies. The initial reactions were done on a 50-200 mg scale, whereas the later reactions were attempted on an approximately 2 g scale. The methoxy and propoxy analogues (**9** and **10**) both went to completion as expected, however the benzyl and hydroxyl analogues (**11** and **8**) both failed to yield any product (starting material was recovered). This was unexpected as the reactions were undertaken within a few days of each other, and no changes had been made to the procedure.

There are several factors that can cause the reaction to fail; namely insufficient initiator present (either due to insufficient addition, or decomposition due to improper storage/age etc), inefficient removal of oxygen, insufficient irradiation with UV light (in order to initiate the reaction), and lastly impurities present in the starting material, reagents, solvent or nitrogen supply. The scaling up process was eliminated as a potential problem by repeating the reaction at the original small scale, which did not show any evidence of product formation by NMR.

It was expected that the initiator was a likely source of the difficulties, hence trials were undertaken quadrupling the amount added to 20 mg, and also substituting another bottle (that was known to work for other reactions). When these failed; benzoyl peroxide was used (at reflux to initiate the reaction); this also failed.

It was thought that problems with the reagents were unlikely as they were of the same containers as previously used, so further investigations focused on the UV light source and the deoxygenation procedure. There had not been any reason to suggest the procedure to remove oxygen used was inadequate, however the purging of nitrogen was doubled to 30 min. This did not rectify the problem. As the cylinder used was the same used throughout these reactions, it was eliminated as a potential cause of the problem.

The photoreactor appeared to be working, however when the reactions that had previously been successful were repeated (on the same scale) they also failed. Attempts with a different light source, albeit with a different wavelength were also unsuccessful (no other sources with the same wavelength were available). It was unknown as to whether the alternative lightsource with λ=330 nm would be sufficient to initiate the reaction, so the reaction was also attempted with heat used to initiate the reaction. This was also unsuccessful leading to the conclusion that the problem was due to the reagents used.

The reagents used were then investigated, FTIR, ^{1}H, and ^{13}C NMR spectra were obtained; all matching literature spectra with no impurities visible. Despite this, more trials were performed with freshly distilled toluene and thioacetic acid; again no product formation could be observed. After the continued failure of the reaction it was decided that time constraints precluded undertaking any more work on the reaction.

2.2.3.3 Hydrobromination Attempts

An alternate pathway was to hydrobrominate the alkene to yield a terminal bromide that could then be reacted with thioacetic acid under basic conditions to yield the thioacetate via a simple nucleophilic substitution. It is known that the addition of HBr to an alkene in the presence of a radical initiator will yield a terminal bromide via a radical mechanism.[161]

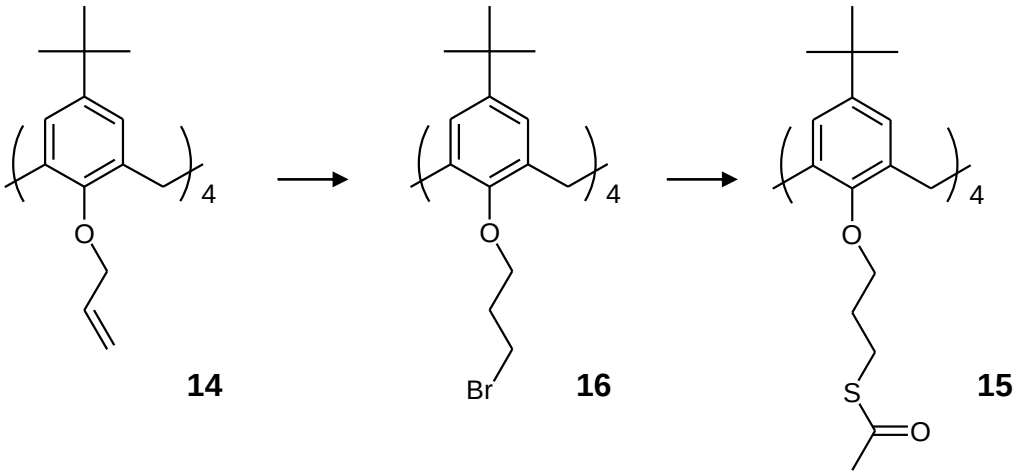

Scheme 7. Proposed Indirect Synthesis of Thioacetyl Calixarene.

This hydrobromination of the tetraallylcalixarene **14** was attempted under a number of conditions. Initially hydrobromic acid and hydrogen peroxide were used, under which conditions it appeared bromine was formed (based on the orange appearance of the reaction mixture). These conditions did result in a partial reaction however the product mixture was unresolvable via TLC. Attempts were also made with benzoyl peroxide and hydrobromic acid which also yielded an intractable mixture. The final attempt was made using dry hydrogen bromide gas (generated from the reaction of tetralin and bromine[162]) again in the presence of benzoyl chloride, yielding a similar mixture.

Time constraints prevented further work on the thioacetyl products. Sufficient quantities had been prepared in order to undertake basic monolayer formation and characterisation studies, and to investigate the receptor properties.

2.2.4 Thioacetate Hydrolysis

The hydrolysis of the impure resorcinarene thioacetates **8** was attempted following Faull's procedure[57,153] (Scheme 8) as the thiol product was found to be pure by NMR and elemental analysis even though extensive purification procedures were not undertaken.

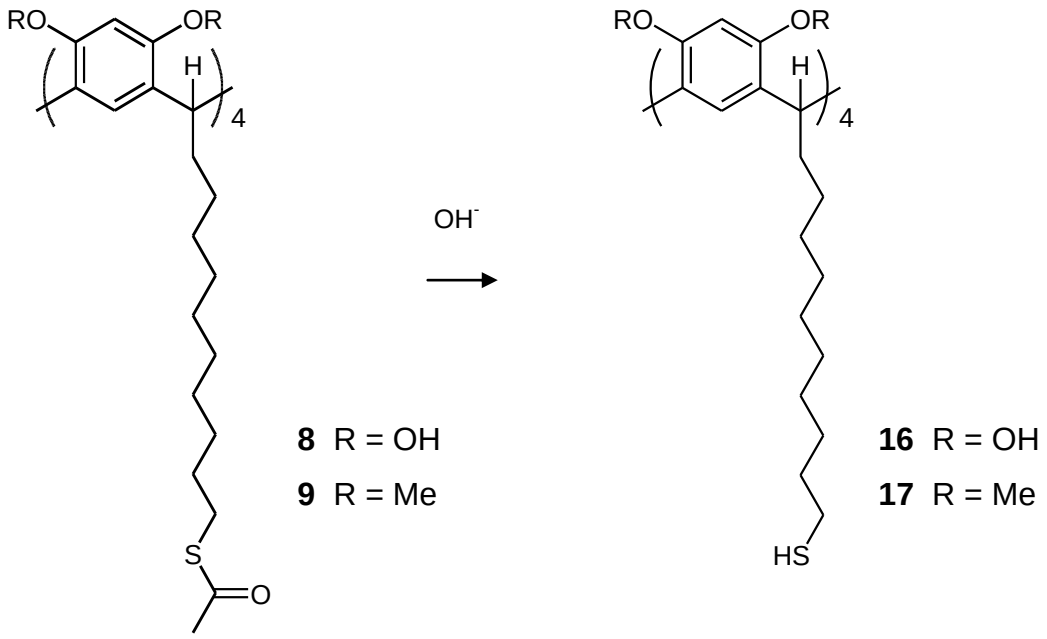

Scheme 8. Hydrolysis of the Thioacetate Groups.

The attempted synthesis of the thiol **16** resulted in a solid material that was insoluble in all solvents tested (chloroform, dimethyl sulfoxide, methanol, water, concentrated NaOH, hexanes, tetrahydrofuran, ethyl acetate, dichloromethane, toluene and glacial acetic acid). IR analysis showed the carbonyl peak of the thioacetate **8** (1690 cm^{-1}) had disappeared in the product, but no new diagnostic peaks were visible. The lack of a carbonyl signal confirms that the hydrolysis had taken place, however the structural changes that reduce the solubility of the product could not be determined.

It is known that thiols are easily oxidised to disulfides in air, and this process is catalysed by base.[163] If the thiols were reacting intermolecularly this can

result in cross-linked disulfide polymers (as there are four thiol groups on each resorcinarene) which could explain the limited solubility. Attempts to undertake the reaction in an oxygen free manner were all unsuccessful, however if the oxidation is fast enough, it is possible that the oxidation is ocurring during workup (no precipitate occurred during the reaction in methanol, however the crude material was not soluble in methanol).

The hydrolysis was attempted on the methoxy resorcinarene **9** which yielded an intractable mixture that was partially soluble in deuterated chloroform. The chloroform soluble fraction showed multiple aromatic peaks in the ^{1}H NMR spectrum (Figure 2.18). While the thiol **17** may be present in this mixture, it is likely that it is a mixture of disulfide oligomeric products.

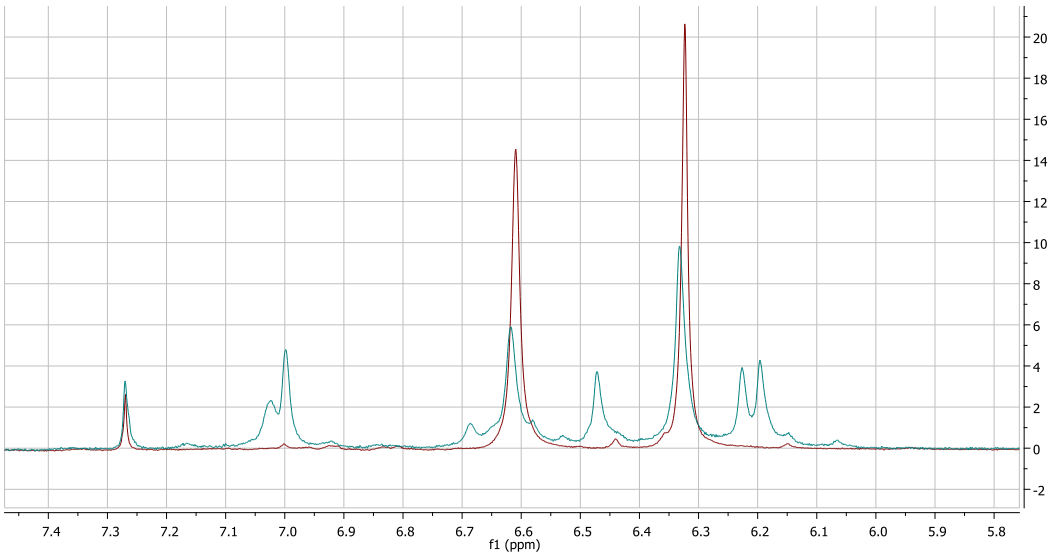

Figure 2.18 Expanded Aromatic Region of ^{1}H NMR Spectrum of the Mixture **17** (blue) Overlaid with the Same Region of the Starting Material **9** (red).

It is possible but unlikely that the product formed during the hydrolysis is a decomposition product (as the reaction is performed at room temperature, and the resorcinarenes are stable in basic conditions), however the IR spectrum and the NMR spectrum of the chloroform soluble fraction from the hydrolysis of **9** indicate that the basic resorcinarene skeleton is intact, which

further supports the hypothesis that the disulfide oxidation products are forming.

2.2.4.1 Calixarenes

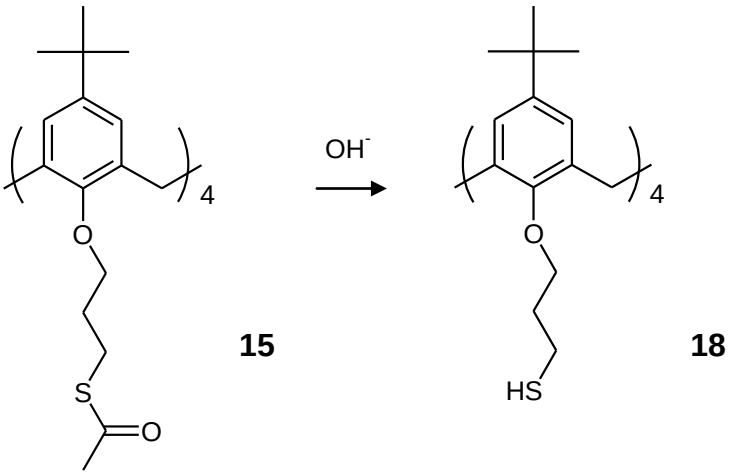

Scheme 9. Hydrolysis of the Thioacetyl Groups.

The hydrolysis of the thioacetyl calixarene **15** (Scheme 9) presented similar difficulties as with the resorcinarenes. The reaction was performed under the same basic conditions yielding a product with an unusual NMR spectrum. The ^{1}H NMR spectrum showed three aromatic and three tertiary butyl peaks (Figure 2.19), which could not be explained as no impurities were resolvable by TLC. The ^{13}C NMR spectrum also showed there were three different aromatic environments present with twelve aromatic carbon peaks visible.

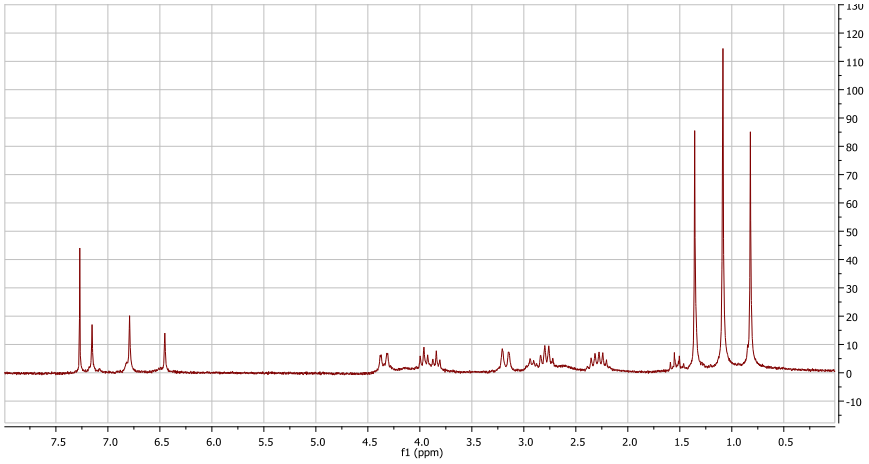

Figure 2.19 ^{1}H NMR Spectrum Obtained of the Hydrolysis Product of **15**.

The infra-red spectrum of the product shows no carbonyl signal, indicating complete hydrolysis, but no thiol SH stretch was present. A Raman spectrum was obtained which showed the thiol stretch at 2567 cm^{-1}. Based on the spectroscopic evidence it was postulated that the material was a mixture of the thiol **18** and an intramolecular disulfide **19** (Figure 2.20). Elemental analysis results also support the proposed element ratios.

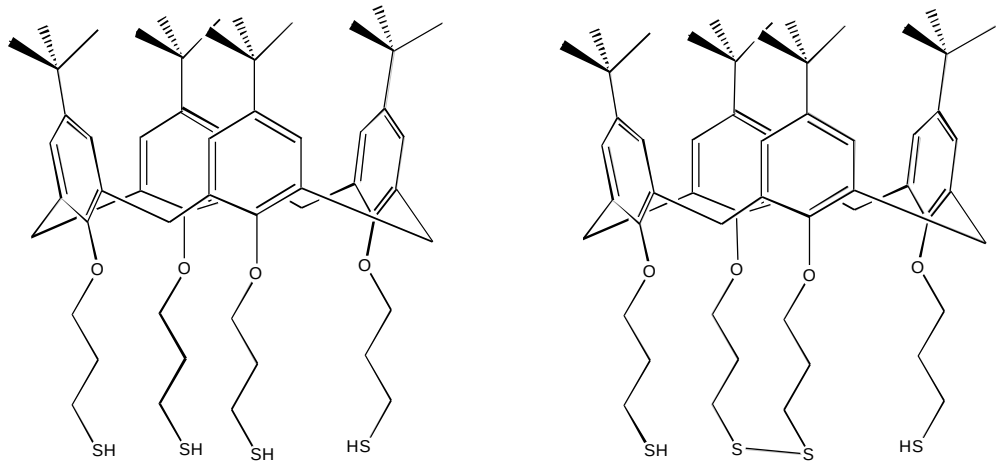

18 **19**

Figure 2.20 Proposed Structures of the Hydrolysis Products of Calixarene **15**.

A mass spectrum of the material was obtained in the hope of further supporting the proposed structures **18** and **19**. The distribution of the $M+Na^{+}$ region is shown, along with a simulated spectrum for each structure (Figure 2.21). The experimental distribution seems to match an approximately 1:1 mixture of **18** and **19** which fits with the integrations of the aromatic and tertiary butyl peaks in the ^{1}H NMR spectrum.

a)

b)

c)

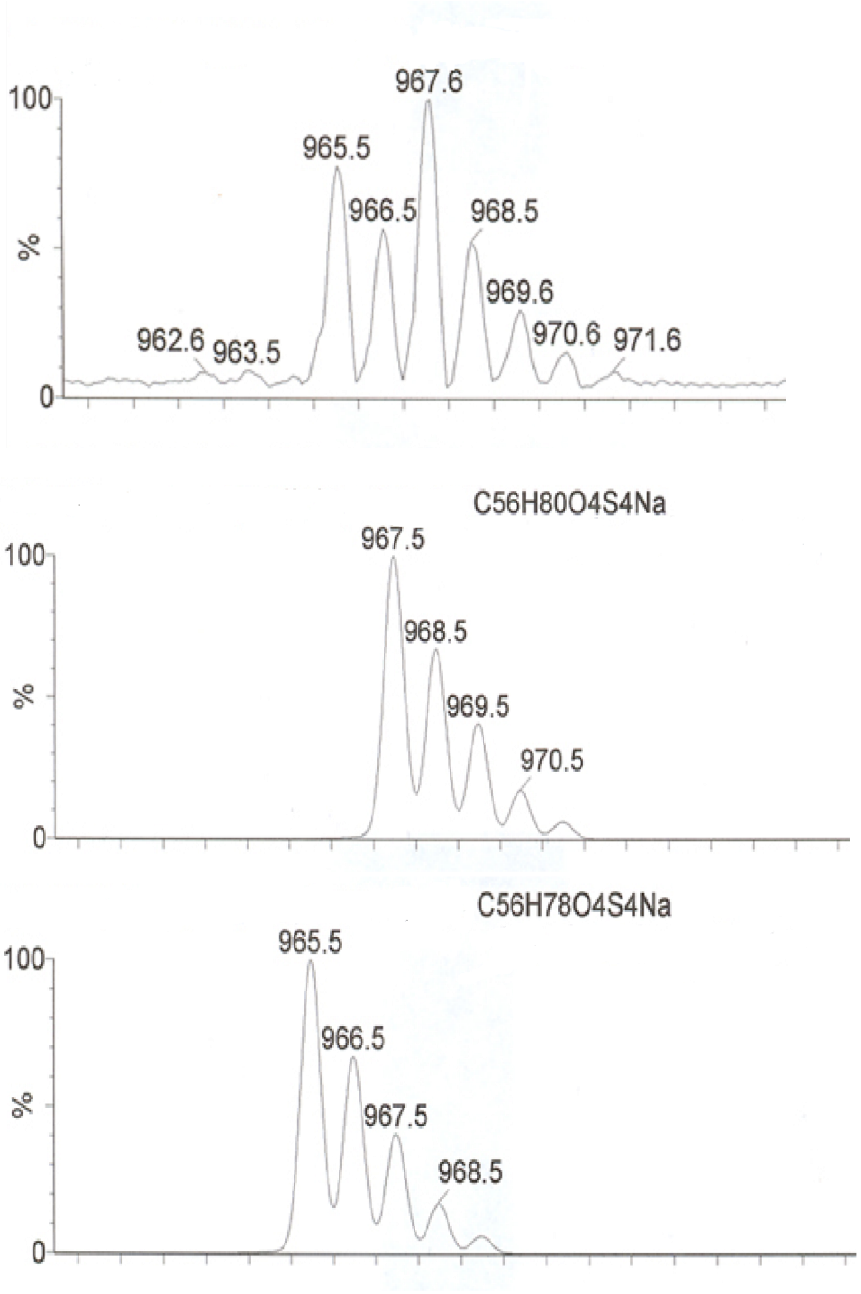

Figure 2.21 Mass Spectra a) Experimental Spectrum of the Hydrolysis Product of the Thioacetyl Calixarene **15**. b) Simulated Spectrum of Tetrathiol **18**. c) Simulated Spectrum of Disulfide **19**.

These results indicate that the hypothesised oxidation is probable, however it is still unknown whether incomplete removal of oxygen from the reaction vessel is causing this, or whether the reaction occurs during workup. As the air oxidation is base catalysed, acidic hydrolysis conditions were attempted, however the hydrolysis was very slow and the oxidation was still observed.

The product observed in all cases appeared to be a mixture of the tetrathiol **18** and the intramolecular disulfide **19**.

The two compounds could not be separated by recrystallisation or chromatography, but as the disulfide will form an identical chemisorbed monolayer on gold to the tetrathiol compound, it was decided that in this case the oxidation occurring was not detrimental to the usage of the product.

The difficulties observed with the hydrolysis of the resorcinarene thioacetates **8** and **9** is likely due to the same oxidation observed in the calixarene reaction. It is unclear why the resorcinarenes seem to give oligomeric or polymeric products, as while the calixarene **15** has the same potential, no evidence for intermolecular disulfide formation was observed.

Due to the instability observed it was decided to only form the thiol *in-situ* when adsorbing monolayers onto gold. If there was a need to isolate the thiol other procedures such as the mild conditions of 15 mol% of acetyl chloride in methanol at room temperature could be attempted as no disulfide formation was reported.[164]

2.2.5 Alternative Alkene Functionalisation

Resorcinarenes functionalised with dialkyl sulfides were prepared as an alternative to the thioacetates. They were synthesised by following the procedure described by van Velzen[154], which proceeded well (Scheme 10).

The mechanism is a radical reaction, initiated by 9-borabicyclo[3.3.1]nonane (9-BBN).[165] Under the conditions used (0 °C, dry THF) the hydroboration reaction is very slow, however if it does occur the hydroboration product can still initiate the reaction.

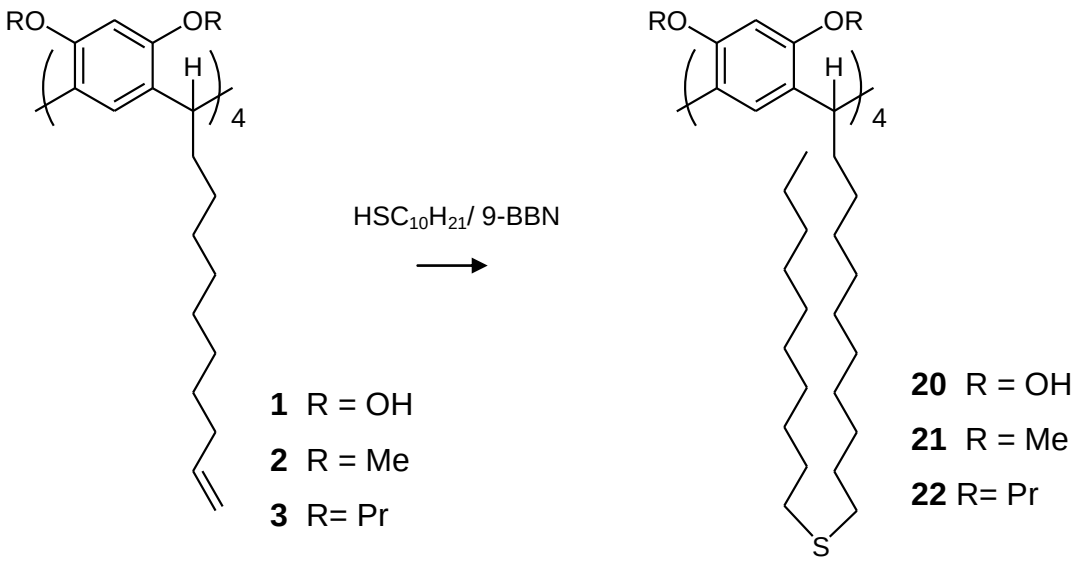

Scheme 10. Synthesis of Dialkyl Sulfides.

The ^{1}H NMR spectra of the products **20**-**22** clearly shows the disappearance of the alkenyl signals, indicating a reaction has occurred. The large number of alkyl protons makes it difficult to determine if the decyl chain has been attached, as small errors in the integrations of the aromatic peaks will vary the ratio dramatically. This is further complicated by the likely presence of decane thiol which exhibits peaks coincident with the product.

Purification of the products by chromatography was attempted and visible impurities were removed, however it is impossible to detect if any decane thiol remains. Size exclusion chromatography was attempted on the methoxy resorcinarene **21** using sephadex LH 20, swelled in ethanol for 3.5 hrs. The resorcinarene **21** was recovered in the first fraction as expected, however the decane thiol eluted in the next fraction, meaning it was impossible to be confident that no thiol remained in the sample.

*2.2.5.1 Removal of Decane Thiol from **21***

A major drawback of the formation of decane sulfides is the likely presence of decane thiol as an impurity. The thiol is known to readily form chemisorbed

monolayers on gold, and will preferentially adsorb over the resorcinarene sulfide which will form only weakly bound, physisorbed monolayers.[166,167]

The sulfide product needs to be free from even trace amounts of thiol, otherwise the composition of the resulting monolayers is ambiguous. This has been illustrated by Zhong *et al.*[167] who found that traces of thiols (concentrations of 0.1%) competitively adsorb to gold which can lead to erroneous interpretations of results, as in their earlier work.[168] This concern had been previously noted by Strong and Whitesides,[166] however the possibility has not been discussed in the literature with regards to the resorcinarene decylsulfide synthesis, even though the reaction conditions call for an excess of decanethiol.[150,154,169] Due to these concerns there is a need to detect if any thiol impurity is present in the resorcinarene products.

Detection of low levels of decane thiol is very difficult in the resorcinarene system. The decane thiol is difficult to detect by TLC as it tends to streak due to the thiol group sticking to the silica. There is no thiol (S-H) stretch visible in the IR spectrum, and the absorption in the Raman spectrum is not intense enough for trace level detection. NMR is not sensitive enough to detect impurities of less than one percent, and due to the similar alkyl signals from the product, it is difficult to detect even moderate amounts of the thiol. The thiol can be easily detected in small quantities by gas chromatography (GC), however the resorcinarene product is not volatile enough for GC, and may block the column if injected.

High performance liquid chromatography (HPLC) could be used, however only a UV detector was available at the time, and the thiol absorption is very low.

An alternative to analyzing the products for the presence of decane thiol was to develop a purification procedure using a model system that could be analysed by GC.

Thiols are weakly acidic so it was thought that washing with aqueous base may remove decane thiol from an organic solution. A solution of decane thiol and tetralin (internal standard) in ethyl acetate was washed with equivalent volumes of 3 M sodium hydroxide solution two times. Aliquots were taken of the initial solution, and after each wash. Comparison of the ratio of the decane thiol to tetralin peaks in the chromatogram revealed that minimal removal of the decane thiol occurred (see Figure 2.22). This was probably due to the lipophilic nature of the decane chain.

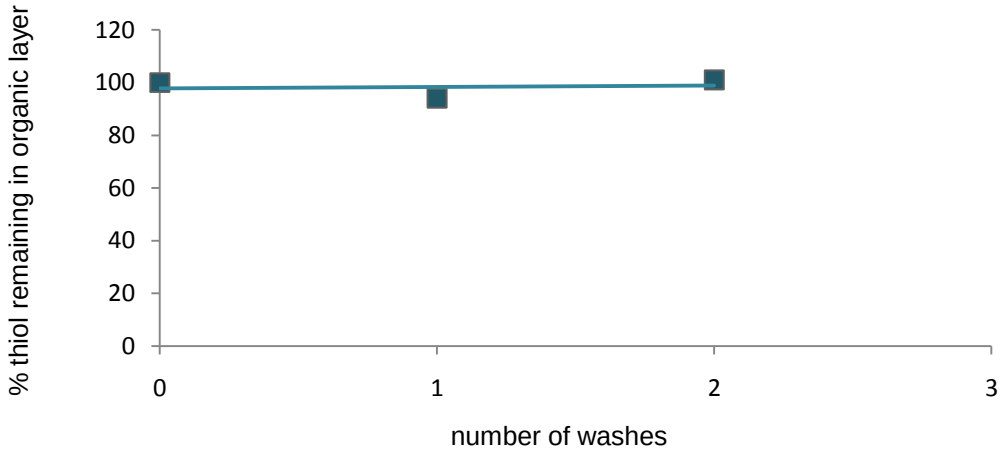

Figure 2.22 Removal of Thiol by Base Washings.

Cyclodextrins are water soluble cyclic oligosaccharides with a hydrophilic exterior and a hydrophobic cavity (see Figure 2.23). The most commonly used, β-cyclodextrin, consists of seven glucose units. Cyclodextrins are known to form complexes with alkanes[170] and it was hoped that the alkyl chain of the decane thiol would complex with the water soluble cyclodextrin allowing it to be extracted into the aqueous phase.

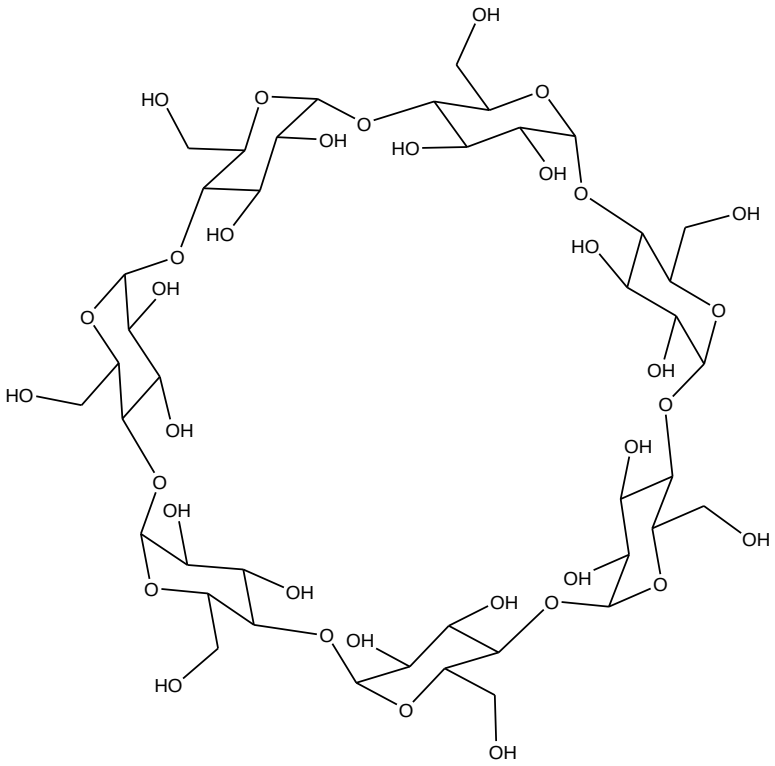

Figure 2.23 Structure of β-Cyclodextrin .

Triphenylene (see Figure 2.24) was used as the internal standard as it was expected to be too large to fit into a β-cyclodextrin cavity due to the short retention times exhibited when analysed on cyclodextrin HPLC columns.[171] Ultraviolet spectroscopy was used to substantiate this assumption, as there would have been absorption in the spectrum of the aqueous cyclodextrin washings. GC of the ethyl acetate solution initially and after each wash again revealed no significant removal of decane thiol.

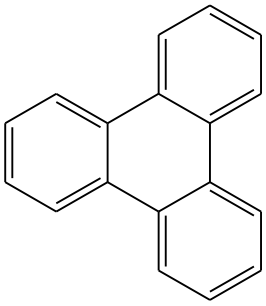

Figure 2.24 Structure of Triphenylene (used as internal standard).

After the failure to easily remove the decane thiol by extraction, it was decided that if the thiol could be methylated to form methyl decylsulfide it

may prove easier to purify as this should be easier to separate via chromatography.

Any trace amount of the sulfide remaining would be less important in respect to the monolayers formed from the compound, as the impurity would form physisorbed bonds to the gold of similar strength to the resorcinarene, and therefore would not out-compete the resorcinarene.

Methyl iodide can also react with sulfides to form a trialkylsulfonium salt (see Scheme 11). It was hoped that the rate of the methylation of the thiol would greatly exceed the rate of methylation of the sulfide, allowing it to be used on the crude reaction mixture without the competing reaction destroying a large proportion of the resorcinarene sulfide. Small percentages of the resorcinarene trialkylsulfonium salt would not affect the monolayer formation as they do not adsorb onto gold, and large excesses of the compound are used when preparing the monolayers. The rate of methylation of decane thiol was unknown, however it was known that dimethyl sulfide could be completely methylated with methyl iodide in 12 hours at room temperature.[172]

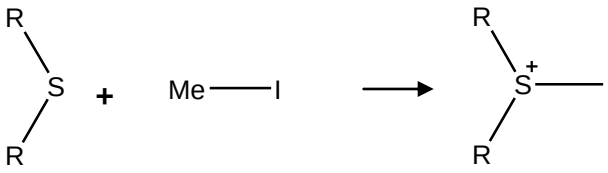

Scheme 11. Methylation of a Sulfide to Form a Trialkylsulfonium Salt.

A model system was used to investigate the relative reaction rates, in which iodomethane (3 equiv) and potassium carbonate (3 equiv) were added to a solution of previously prepared decyl propyl sulfide (as a model for the resorcinarene sulfide), decane thiol, and tetralin (internal standard), in dry acetonitrile.

Samples were periodically removed and analysed by GC to determine the progress of the competing reactions. The rate of the methylation of the thiol

could be determined by the disappearance of the decane thiol from solution (see Figure 2.25). The amount of trialkylsulfonium salt cannot be directly determined by this method as the salt will not pass through the GC, however the reaction can be indirectly monitored by the disappearance of propyl sulfide and also by the reduction in the combined amounts of decane thiol and methyl decylsulfide.

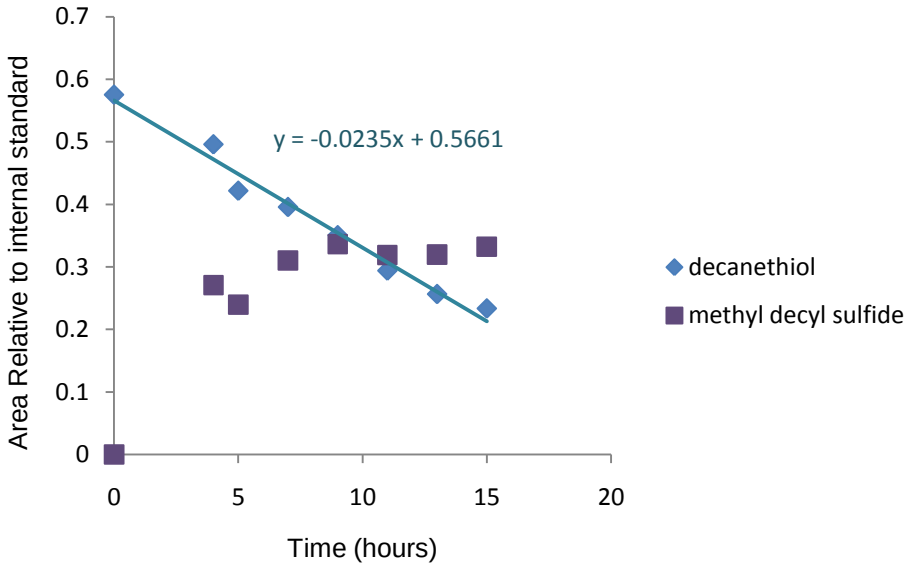

Figure 2.25 Formation of Methyl Decyl Sulfide

It is apparent from the plot of the concentrations over time (Figure 2.25) that the dimethyl decylsulfonium salt is being formed in the reaction mixture. The decane thiol shows the expected linear decrease in concentration as the methyl decyl sulfide is formed, however the methyl decyl sulfide concentration initially increases, then tapers off. The decane thiol doesn't undergo any side reactions under the conditions used, hence it is assumed that the sulfonium salt is formed, as this will not appear in the GC trace.

The slope of the decrease in the thiol concentration and the propyl sulfide concentration are similar (see Figure 2.26), and both are relatively slow with only approximately 60% of the decane thiol and 40% of the propyl sulfide having reacted after 15 hours. The rate of the methylation of decane thiol is approximately 40% faster than the methylation of propyl sulfide, however this

difference is not great enough for the reaction to be useful in removing the thiol from the resorcinarene products.

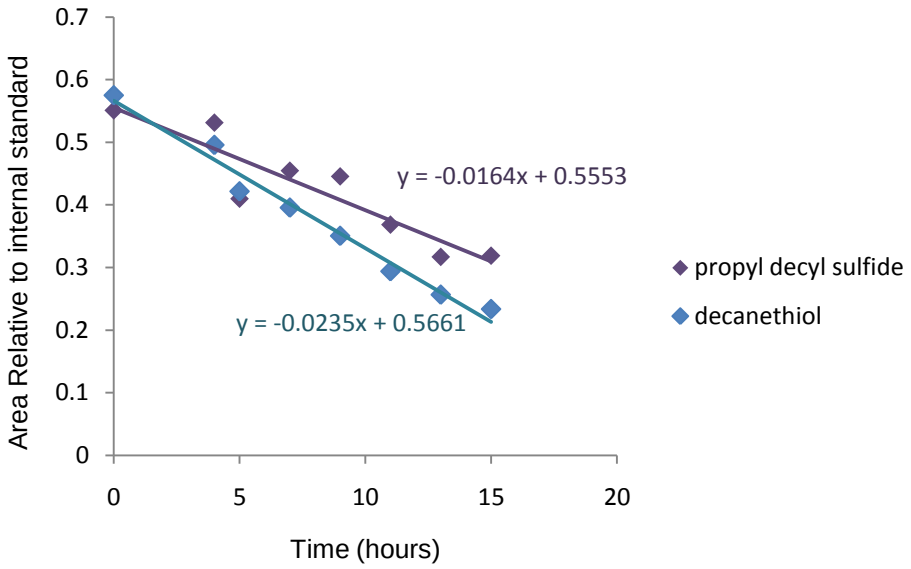

Figure 2.26 Time Resolved Decrease in Decane Thiol and Propyl Decyl Sulfide.

2.2.5.2 Acetonitrile/Hexane Partitioning

As the attempts to remove decane thiol by reaction, or washing into water failed, the converse approach was taken by attempting to wash the thiol into the non-polar solvent, hexanes.

It was more difficult to find an appropriate internal standard to investigate this system, as it was required to be entirely soluble in either the acetonitrile or hexanes. Triethylene glycol was found to remain entirely in the acetonitrile layer when extracted with hexane, and the retention time and inertness towards the solvents and the thiol meant it would be a suitable internal standard.

The model system used was equivalent volumes (0.5 mL) of decane thiol and ethylene glycol in 10 mL of acetonitrile and washed with 10 mL of hexanes. The acetonitrile layer was sampled initially and after each wash, and

analysed by GC. The results indicated that after four extractions with hexanes, the decane thiol was no longer detectible in the acetonitrile layer. Based on these results it was determined that this method was appropriate to use for the crude resorcinarene samples, although NMR analysis of the hexane washing would be needed to determine if significant amounts of the resorcinarene product was removed along with the thiol.

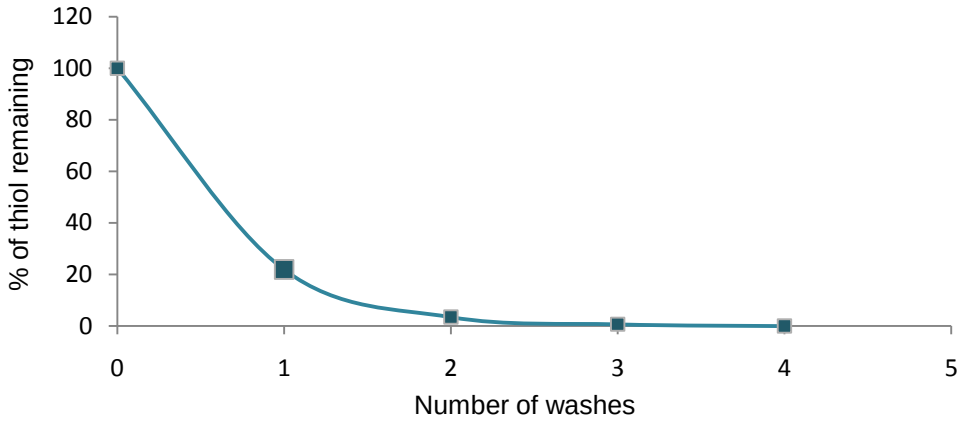

Figure 2.27 Removal of Thiol from Acetonitrile Solutions by Hexane.

This purification method was applied to the crude resorcinarene products, however large proportions of the mass was extracted into the hexane layers. NMR confirmed that the resorcinarenes were present in the hexane layer along with decane thiol.

After this treatment only a trace remained of the propoxy resorcinarene **22** and 80% of the crude weight of the hydroxyl resorcinarene **20** was lost giving a yield of just 38% of the purified product. Due to this large loss of product the method can only be applied to large masses of crude material. The mass of the methoxy resorcinarene **21** previously purified by size exclusion chromatography was too small to attempt this purification method, and was used for monolayer studies even though the presence of a decane thiol impurity could not be determined.

If this reaction was to be further investigated better analysis and purification techniques would need to be found. It is likely that with an alternative solvent, or larger column volume, that size exclusion chromatography would be an

appropriate purification technique, and could possibly also be used as an analysis method (as analytical size exclusion HPLC columns are available).

2.2.6 9-BBN Initiated Addition of Thioacetic Acid to Alkene.

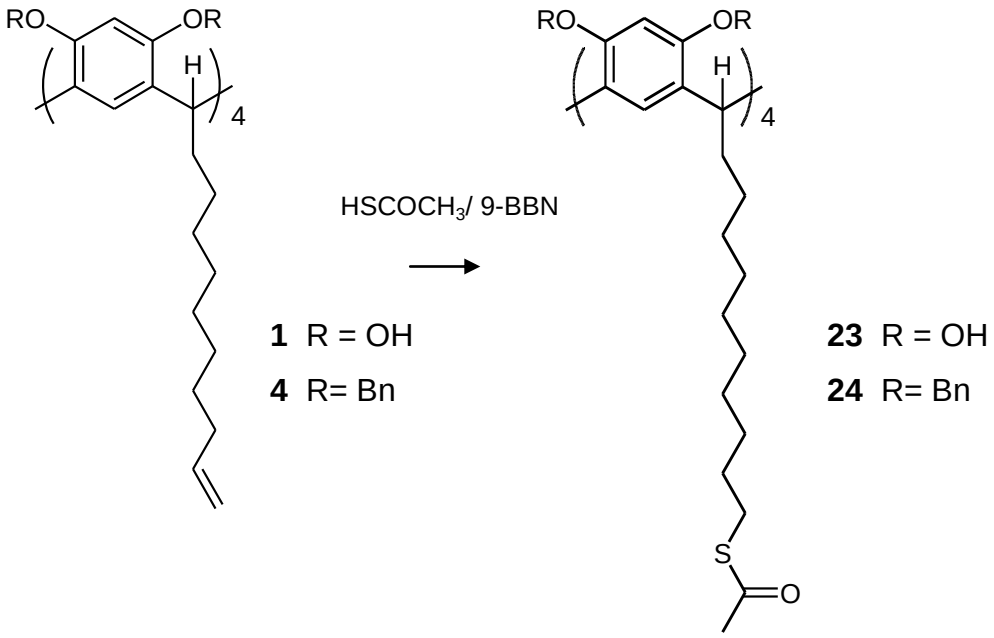

Scheme 12. Alternative Radical Addition Conditions.

The radical addition of thioacetic acid to the undecylenic resorcinarenes **1** and **4** was attempted using 9-borabicyclo[3.3.1]nonane (9-BBN) as the initiator. It was reasoned that the reaction should proceed in a similar way to the UV light/AIBN initiated procedure.

Several attempts were made varying parameters such as temperature and 9-BBN ratios, however only starting material was ever recovered.

Thioacetic acid was the only common element from the reactions that failed, other than the resorcinarenes, however the same batches were used to synthesise the dialkyl sulphides, and as this is also a radical reaction, it was assumed they could not be the source of the problem. As the solvent and initiator used are different, and no ultraviolet lamp was required, it follows that the thioacetic is likely the cause of the reaction failures. However, analysis of

the thioacetic acid revealed no impurities, all spectra matched the literature, and distillation did not improve the reaction outcome. The same thioacetic acid was successfully used in nucleophilic substitution reactions.

Time constraints prevented fresh thioacetic acid from being purchased to investigate the theory that a trace impurity not removed by distillation is hindering the radical propagation during the addition to an alkene when initiated both by AIBN and 9-BBN.

2.2.7 Conclusion

Several sulfur functionalised resorcinarenes were prepared in sufficient quantity and purity for use in the following stages of the project (see Figures 2.28-30).

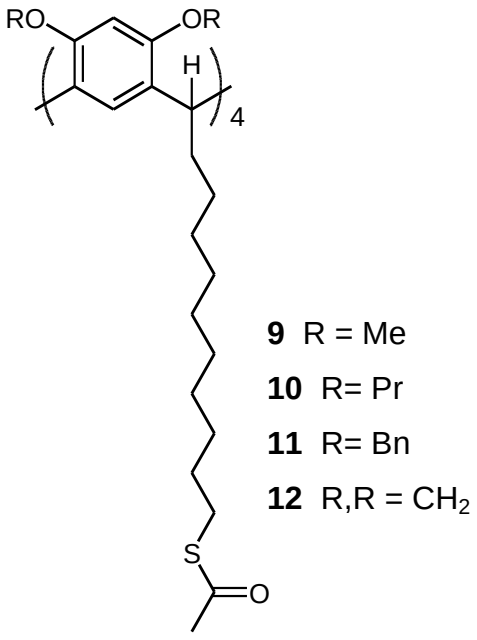

9 R = Me

10 R= Pr

11 R= Bn

12 R,R = CH_2

Figure 2.28 Thioacetyl Resorcinarenes

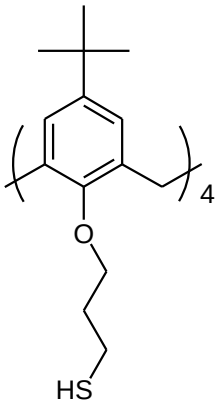

Figure 2.29 Calixarene Thiol/Disulfide Mixture **18**/**19**

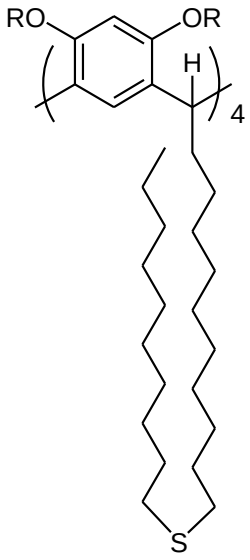

20 R = OH

21 R = Me

Figure 2.30 Decylsulfide Resorcinarenes

2.3 Experimental

Melting points were determined on an Electrothermal 9100 apparatus.

Infrared spectra were recorded on a Perkin Elmer Spectrum 100 FTIR spectrophotometer using a single bounce diamond ATR.

The UV spectrum of decane thiol was determined on a Perkin Elmer Lambda 35 UV Vis Spectrometer.

Nuclear magnetic resonance spectra were acquired at ambient temperatures on a Varian Gemini 2000 instrument at 200 MHz for proton and 50.3 MHz for carbon. The solvent used was deuterated chloroform unless otherwise stated. Carbon assignments (where given) were made with the assistance of DEPT 135 experiments. Spectra are calibrated to either tetramethylsilane or the residual solvent signal.

Gas Chromatography was carried out on a HP 5890 instrument with a DB5 column, and a flame ionisation detector.

Elemental microanalyses and high resolution mass spectrometry were carried out by the Central Science Laboratory, University of Tasmania, Australia. Mass spectrometry of the **18**/**19** mixture was performed by Dr Laura Baldini at Università di Parma.

All solvents and reagents were AR grade and used without further purification unless anhydrous solvents were specified. Dimethylformamide was dried over 3Å sieves.[173] Methanol and ethanol were dried by heating at reflux over magnesium/iodine followed by distillation under nitrogen. Anhydrous tetrahydrofuran was purchased from Sigma-Aldrich.

Chromatography was performed with Merck silica gel (0.040-0.063mm) under a positive pressure unless otherwise stated. Thin layer chromatography was on Merck silica gel 60 F_{254} aluminium backed plates.

Compounds were visualised on TLC by one or more of the following; UV light, placement in an iodine tank, or by dipping with and heating with a vanillin or palladium chloride stain.

The tetramer **13**,[158] tetraallyl calixarene **14**,[159] undecylenic resorcinarene **1**,[154] methoxy undecylenic resorcinarene **2**,[154] and the methylene cavitand **5**[154] were prepared according to literature procedures.

7[157] was provided by Professor Enrico Dalcanale of Università di Parma.

*Synthesis of tetrathioacetate calix[4]arene **15***

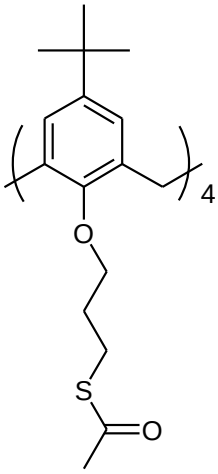

A solution of **14** (1.00 g, 1.24 mmol), thioacetic acid (2 mL, 28.10 mmol) and 2,2'-azobisisobutyronitrile (5 mg) in toluene (70 mL) was purged with nitrogen and irradiated with UV light (λ=254 nm) for 4 hours. The solvent was removed under reduced pressure and the residue recrystallised from dichloromethane/petroleum spirits to give pure **15** (653 mg, 0.59 mmol, 48%), as a white solid, m.p. 150.2-152.2 °C. ^{1}H NMR δ 1.07 (s, 36H, C(C**H**$_3$)) 2.23 (m, 8H, $CH_2C\mathbf{H}_2CH_2$) 2.37 (s, 12H, COC**H**$_3$) 3.09 (m, 12H, SC**H**$_2$, ArC**H**$_2$) 3.87 (t, 8H, J=7.3 Hz, OC**H**$_2$) 4.27 (d, 4H, J=12.1 Hz, ArC**H**$_2$) 6.76 (s, 8H, Ar**H**). ^{13}C NMR δ 26.7, 30.7, 31.3, 31.7, 32.1, 32.3, 34.5 (CH_2, CH_3, C(CH_3)), 74.4 (OCH_2), 125.8, 134.3, 145.4, 153.8 (Ar), 196.2 (C=O).

*Synthesis of tetrathiol calix[4]arene **18**, **19***

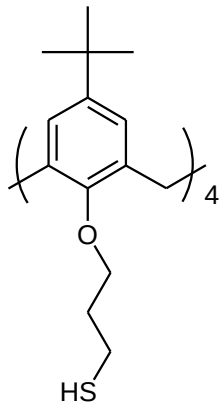

Sodium (0.10 g, 4.35 mmol) was added to a solution of **15** (350 mg, 0.31 mmol) in methanol (75 mL, anhydrous), and the solution stirred under nitrogen (3 hrs). Hydrochloric acid (1 M, 300 mL) was added to the reaction mixture, and the precipitate washed with water (50 mL), then dried to give an approximately 1:1 mixture of **18** and **19** (245 mg) as a white solid.

^{1}H NMR δ 0.82 (s, 18H, C(C**H**$_3$)) 1.09 (s,36H, C(C**H**$_3$)) 1.36 (s, 18H, C(C**H**$_3$)) 1.52 (m, 4H, C**H**$_2$) 2.28 (m, 16H, C**H**$_2$) 2.70-2.99 (m, 20H, C**H**$_2$) 3.19 (m, 8H, ArC**H**$_2$) 3.84 (t, 8H, J= 6.6 Hz, OC**H**$_2$) 3.96 (t, 8H, J=7.3 Hz, OC**H**$_2$) 4.32 (m. 8H, ArC**H**$_2$) 6.45 (s, 4H, Ar**H**) 6.79 (s, 8H, Ar**H**) 7.15 (s, 4H, Ar**H**). ^{13}C NMR δ 22.3, 22.7, 31.8, 32.1, 32.4, 35.1, 35.3 (CH_2, CH_3), 74.2, 74.3, 74.6 (OCH_2), 125.3, 125.8, 126.4, 132.3, 134.2, 136.1, 145.0, 145.5, 145.9 152.8, 153.8, 155.4 (Ar). Found: C, 69.4; H, 8.3; S, 13.2 %. $C_{56}H_{80}O_4S_4.H_2O$ (**18**) requires C, 69.8; H, 8.6; S, 13.3 %. $C_{56}H_{78}O_4S_4.H_2O$ (**19**) requires C, 69.9; H, 8.4; S, 13.3 %. MS: 965.5 (80%) 966.5 (55%) 967.6 (100%) 968.5 (50%) 969.6 (30%), 970.6 (15%) Simulated **18** ($C_{56}H_{80}O_4S_4.Na^+$) 967.5 (100%), 968.5 (65%), 969.5 (40%), 970.5 (16%), 971.5 (6%), 972.5 (2%) Simulated **19** ($C_{56}H_{78}O_4S_4.Na^+$) 965.5 (100%), 966.5 (65%), 967.5 (40%), 968.5 (16 %), 969.5 (6%), 970.5 (2%) Simulated 1:1 **18**.Na^+:**19**.Na^+ 965.5 (71%), 966.5 (46%), 967.5 (100%), 968.5 (58 %), 969.5 (33%), 970.5 (13%)

*Synthesis of Propoxy resorcinarene **3***

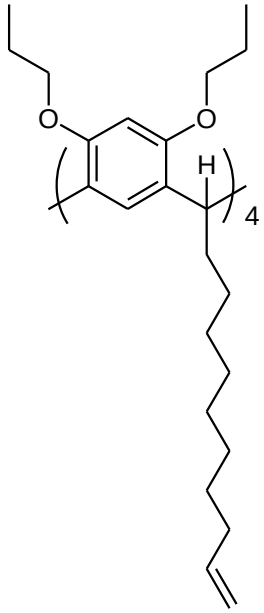

The resorcinarene **1** (2.03 g, 1.94 mmol) was added to a suspension of sodium hydride (1.38 g, 60% in oil, 36 mmol, washed with petroleum spirits) in dimethylformamide (35 mL, anhydrous) and stirred (10 min) under nitrogen. Propyl bromide (4 mL, 44.10 mmol) was added and the stirring continued for 2 days. The solvent was removed under reduced pressure and the residue dissolved in ether (80 mL) and washed with hydrochloric acid (1 M, 30 mL), water (30 mL) and brine (sat, 30 mL). The organic layer was dried over magnesium sulfate, and the solvent removed to give **3** (2.51 g, 1.82 mmol, 94%) as a beige oil. ^{1}H NMR δ 0.80-2.06 (broad, m, 120H, C**H**$_2$, C**H**$_3$) 3.20-4.00 (broad, 16H, OC**H**$_2$) 4.53 (t, J=7.1 Hz, 4H, ArC**H**) 4.95 (m, 8H, =C**H**$_2$) 5.79 (m, 4H, =C**H**) 6.20-6.40 (broad, s, 4H, Ar**H**). ^{13}C NMR δ 11.4 (CH_3), 23.6, 29.1, 29.7, 29.9, 30.3, 30.4, 30.7, 34.5, 35.3 (CH_2), 36.3 (ArCH), 70.5 (OCH_2), 98.2 (Ar), 114.7 (=CH_2), 126.7 (2 x Ar), 139.9 (=CH), 155.8 (Ar).

*Synthesis of benzyloxy resorcinarene **4***

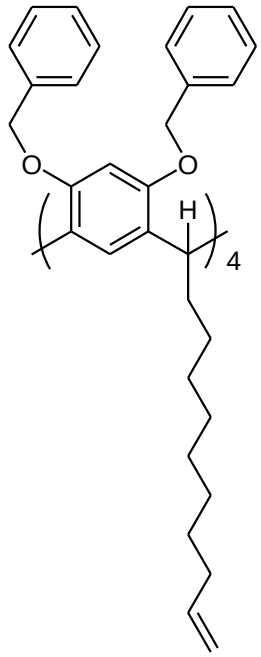

The resorcinarene **1** (482 mg, 0.46 mmol) was added to a suspension of sodium hydride (340 mg, 60% in oil, 8.50 mmol, washed with petroleum spirits) in dimethylformamide (30 mL, anhydrous) and stirred (10 min) under nitrogen. Benzyl bromide (1 mL, 7.68 mmol) was added and the stirring continued for 3 days. The solvent was removed under reduced pressure and the residue dissolved in ethyl acetate (30 mL) and washed with hydrochloric acid (1 M, 30 mL), water (30 mL) and brine (sat, 30 mL). The organic layer was dried over magnesium sulfate, and the solvent removed. The residue was then chromatographed (5-15% ethyl acetate in hexane) to give **4** (363 mg, 0.21 mmol, 46%) as an orange oil. ^{1}H NMR δ 1.20-1.50 (broad, m, 48H, C**H**$_2$) 1.8-2.1 (broad, m, 16H, C**H**$_2$) 4.50-5.05 (m, 28H, ArC**H**, =C**H**$_2$, OC**H**$_2$) 5.68 (m, 4H, =C**H**) 6.46 (s, 4H, Ar**H**) 7.08-7.38 (broad, m, 44H, Ar**H**). ^{13}C NMR δ 29.2, 29.7, 29.9, 30.3, 30.4, 30.7, 34.5, 35.3 (CH_2), 37.0 (ArCH), 71.3 (OCH_2), 99.7 (Ar), 114.7 ($=CH_2$), 127.2, 127.5, 127.8, 128.0, 128.8 (Ar), 138.3 (=CH), 139.9, 155.7 (Ar).

*Synthesis of methoxy resorcinarene thioacetate **9***

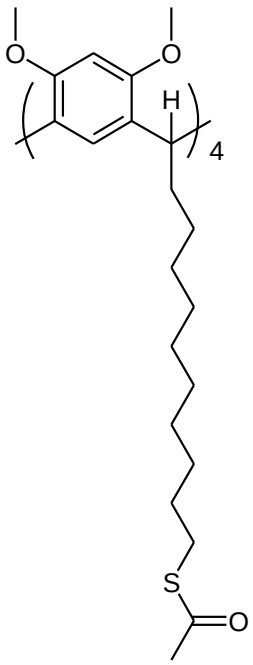

A solution of **2** (1.16 g, 1.01 mmol), thioacetic acid (1.6 mL, 22.48 mmol) and 2,2'-azobisisobutyronitrile (5 mg) in toluene (75 mL) was purged with nitrogen and irradiated with UV light (λ=254 nm) for 4.5 hours. The reaction mixture was washed with sodium carbonate (sat, 3 x 50 mL), water (50 mL) and brine (sat, 50 mL). The organic layer was dried (sodium sulfate) and the solvent removed under reduced pressure. The residue was then chromatographed using 30-50% ethyl acetate in hexanes to give **9** (555 mg, 0.38 mmol, 38%) as a waxy solid. ^{1}H NMR δ 1.20-1.90 (broad, m, 72H, C**H**$_2$) 2.32 (s, 12H, COC**H**$_3$) 2.86 (t, 8H, J=7.1 Hz, SC**H**$_2$) 3.60 (s, 24H, OC**H**$_3$) 4.45 (t, 4H, J=7.1 Hz , ArC**H**) 6.32 (s, 4H, Ar**H**) 6.61 (s, 4H, Ar**H**). ^{13}C NMR δ 28.8, 29.5, 29.79, 29.81, 30.1, 30.2, 30.3, 30.4, 30.5 (CH_2), 31.2 ($COCH_3$), 35.3 (SCH_2) , 36.0 (ArCH), 56.8 (OCH_3), 97.7, 126.7, 126.8, 156.4 (Ar), 196.6 (C=O). FTIR: 1690 cm^{-1} (C=O). HRMS *m/z* (M.NH_4^+) 1474.8627 calc for $C_{84}H_{128}O_{12}S_4.NH_4$: 1474.8627

*Synthesis of propoxy resorcinarene thioacetate **10***

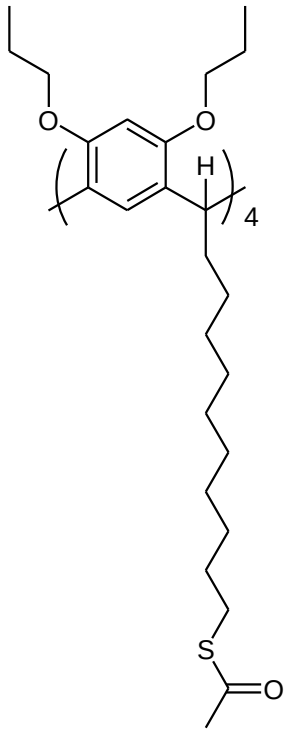

A solution of **3** (197 mg, 0.14 mmol), thioacetic acid (1 mL, 14.05 mmol) and 2,2'-azobisisobutyronitrile (5 mg) in toluene (60 mL) was purged with nitrogen and irradiated with UV light (λ=254 nm) for 4.5 hours. The reaction mixture was washed with sodium carbonate (sat, 3 x 50 mL), water (50 mL) and brine (sat, 50 mL). The organic layer was dried (sodium sulfate) and the solvent removed under reduced pressure. The residue was then chromatographed with dichloromethane to give **10** (51 mg, 0.03 mmol, 22%) as a yellow oil. ^{1}H NMR δ 0.77-1.90 (m, 112H, C**H**$_2$, C**H**$_3$) 2.33 (s, 12H, COC**H**$_3$) 2.86 (t, 8H, J=7.2 Hz, SC**H**$_2$) 3.22-4.03 (broad, m, 16H, OC**H**$_2$) 4.53 (t, 4H, J=6.9 Hz , ArC**H**) 6.09-6.35 (broad, s, 4H, Ar**H**) 6.35–7.15 (broad, s, 4H, Ar**H**). ^{13}C NMR δ 11.4, 23.6, 29.1, 29.6, 29.9, 30.1, 30.2, 30.4, 30.7, 31.3, 35.3, 36.3 (ArCH, CH_2, CH_3), 70.5 (OCH_2), 98.2, 126.8, 155.8 (Ar), 196.6 (C=O) note: co-incident signals. FTIR: 1691 cm^{-1} (C=O). HRMS *m/z* ($M.NH_4^+$) 1699.1106 calc for $C_{100}H_{160}O_{12}S_4.NH_4$: 1699.1131

*Synthesis of benzyloxy resorcinarene thioacetate **11***

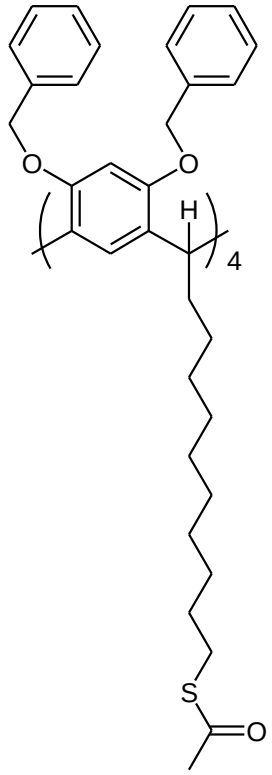

A solution of **4** (250 mg, 0.14 mmol), thioacetic acid (2 mL, 28.10 mmol) and 2,2'-azobisisobutyronitrile (5 mg) in toluene (50 mL) was purged with nitrogen and irradiated with UV light (λ=254 nm) for 4 hours. The reaction mixture was washed with sodium carbonate (sat, 3 x 50 mL), water (50 mL) and brine (sat, 50 mL). The organic layer was dried (sodium sulfate) and the solvent removed under reduced pressure. The residue was then chromatographed with (50-100% dichloromethane in hexanes) to give **11** (87 mg, 0.04 mmol, 30%) as a yellow oil. ^{1}H NMR δ 0.8-2.04 (broad, m, 72H, C**H**$_2$) 2.33 (s, 12H, COC**H**$_3$) 2.86 (t, 8H, J=7.8 Hz, SC**H**$_2$) 4.45-5.02 (m, 20H, OC**H**$_2$, ArC**H**) 6.47 (s, 4H, Ar**H**) 7.04-7.64 (m, 44H, Ar**H**). ^{13}C NMR δ 27.1, 29.2, 29.5, 29.8, 30.1, 30.2, 30.3, 30.7, 31.3, 32.9, 35.2, 39.9 (ArCH, CH_2, CH_3), 71.2 (OCH_2), 99.7, 127.1, 127.5, 127.8,127.9, 128.4, 138.3, 155.7(Ar), 196.6 (C=O). FTIR: 1689 cm^{-1} (C=O). HRMS *m/z* (M.NH_4^+) 2083.1131 calc for $C_{132}H_{160}O_{12}S_4.NH_4$: 2083.1131

*Synthesis of methylene cavitand thioacetate **12***

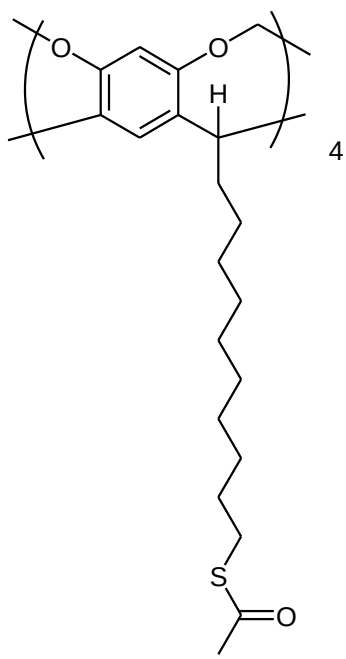

A solution of **5** (1.30 g, 1.19 mmol), thioacetic acid (2 mL, 28.10 mmol) and 2,2'-azobisisobutyronitrile (5 mg) in toluene (75 mL) was purged with nitrogen and irradiated with UV light (λ=254 nm) for 4 hours. The reaction mixture was washed with sodium carbonate (sat, 3 x 50 mL), water (50 mL) and brine (sat, 50 mL). The organic layer was dried (sodium sulfate) and the solvent removed under reduced pressure. The residue was then chromatographed (0-100% methanol in dichloromethane) to give **12** (763 mg, 0.55 mmol, 46%) as a brown oil. ^{1}H NMR δ 0.98-1.65 (m, 72H, C**H**$_2$) 2.07-2.35 (m, 20H, C**H**$_2$, COC**H**$_3$) 2.86 (t, 8H, J=7.3 Hz, SC**H**$_2$) 4.43 (d, 4H, J=6.9 Hz, OC**H**$_2$O) 4.73 (t, 4H, J=8.1 Hz , ArC**H**) 5.73 (d, 4H, J=6.9 Hz, OC**H**$_2$O) 6.49 (s, 4H, Ar**H**) 7.09 (s, 4H, Ar**H**).^{13}C NMR δ 28.4, 29.4, 29.5, 29.72, 29.74, 30.0, 30.1, 30.13, 30.3, 30.9, 34.4, 36.8 (ArCH, CH_2, CH_3), 100.1 (OCH_2O) 117.2, 121.2, 140.0, 155.4 (Ar), 196.5 (C=O). FTIR: 1687 cm^{-1} (C=O). HRMS *m/z* ($M.NH_4^+$) 1410.7375 calc for $C_{80}H_{112}O_{12}S_4.NH_4$: 1410.7375

*Synthesis of methoxy resorcinarene decylsulfide **21***

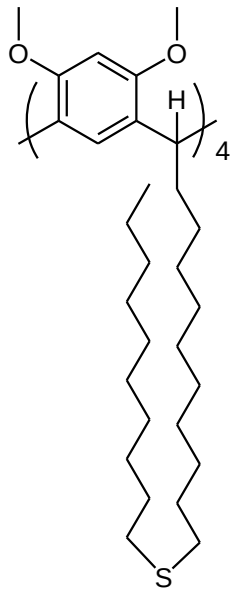

A solution of **2** (53 mg, 0.05 mmol) in tetrahydrofuran (anhydrous, 20 mL) was purged with nitrogen and cooled to 0° C. Decane thiol (100 µL, 0.47 mmol) and 9-borabicyclo[3.3.1]nonane (0.5 M in tetrahydrofuran, 0.9 mL, 0.45 mmol) were added and the solution stirred for 7 days. Hydrochloric acid (1 M, 50 mL) was added and the mixture extracted with dichloromethane (3 x 20 mL). The organic layer was dried (magnesium sulphate) and the solvent removed under reduced pressure.

The crude material was chromatographed with ethanol (Sephadex LH 20, swelled in ethanol for 3.5 hrs) to give **21** (83 mg, 0.05 mmol, 98 %) as a colourless wax. ^{1}H NMR δ 0.77-0.94 (m, 12H, C**H**$_3$) 1.03-1.93 (broad, m, 144H, C**H**$_2$) 2.68 (t, 16H, J=7.0 Hz, SC**H**$_2$) 3.61 (s, 24H, OC**H**$_3$) 4.44 (t, 4H, J=6.8 Hz , ArC**H**) 6.33 (s, 4H, Ar**H**) 6.60 (s, 4H, Ar**H**). ^{13}C NMR δ 14.7,23.3, 28.8, 29.1, 29.5, 29.6, 29.7, 29.8, 29.9, 30.0, 30.1, 30.2, 30.3, 32.5, 35.3, 36.0, 39.9 (ArCH, CH_2, CH_3), 56.9 (OCH_3), 97.9, 126.8, 126.9, 156.5 (Ar) note: co-incident signals. HRMS *m/z* ((M+1).NH_4^+) 1868.4498 calc for $C_{116}H_{200}O_8S_4.NH_4$: 1868.4464

*Synthesis of resorcinarene decylsulfide **20***

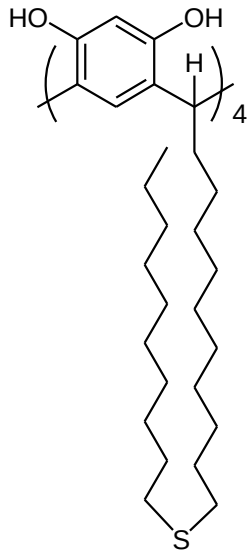

A solution of **1** (1.02 g, 0.98 mmol) in tetrahydrofuran (anhydrous, 20 mL) was purged with nitrogen and cooled to 0° C. Decane thiol (1.70 mL, 11.5 mmol) and 9-borabicyclo[3.3.1]nonane (0.5 M in tetrahydrofuran, 16.0 mL, 8.0 mmol) were added and the solution stirred for 7 days. Ethyl acetate (100 mL) was added and the solution washed with hydrochloric acid (1 M, 3 x 80 mL), water (50 mL), and brine (sat, 50 mL). The organic layer was dried (magnesium sulphate) and the solvent removed under reduced pressure. The residue was dissolved in acetonitrile (40 mL), then washed with hexanes (5 x 40 mL). The solvent was then removed from the acetonitrile layer to give **20** (0.63 g, 0.36 mmol, 37%) as a red oil. ^{1}H NMR δ 0.66-0.94 (m, 12H, C**H**$_3$) 1.02-2.62 (broad, m, 152H, C**H**$_2$) 4.33 (m, 4H, ArC**H**) 6.16 (s, 4H, Ar**H**) 7.22 (s, 4H, Ar**H**). ^{13}C NMR δ 14.5, 23.1, 25.3, 25.7, 26.1, 27.6, 27.9, 28.6, 29.4, 29.6, 29.7, 29.8, 30.0, 30.1, 30.2, 32.3, 32.4, 32.7, 35.1, 42.4 (ArCH, CH_2, CH_3), 103.6, 125.3, 151.5 (Ar). note: co-incident signals.

HRMS *m/z* ((M+1).NH_4^+) 1756.3246 calc for $C_{108}H_{184}O_8S_4.NH_4$: 1756.3212

3.0 Preparation and Characterisation of Self Assembled Monolayers

3.1 Introduction

Self-Assembled Monolayers (SAMs) are highly ordered two dimensional structures formed by the spontaneous adsorption of a compound onto a suitable substrate. Many self-assembled systems have been studied, though thiolates on gold have been the most studied SAMs, due to the strong specific interaction of sulfur with gold which allows the formation of stable monolayers.[174] A variety of sulfur species are known to adsorb onto gold, and the resulting monolayers are used for diverse applications such as selective sensing devices and nanofabrication.

3.1.1 Types of Self Assembled Monolayers

SAMs are simple to prepare, as thiols and disulfides are known to spontaneously chemisorb to gold surfaces from solution, forming highly ordered monolayers.[166,175] Physisorbed dialkyl sulfide monolayers have also been prepared[166,169] using similar methods.

Many other sulfur compounds are also known to form monolayers on gold (see Figure 3.1). These include thioacetates,[176,177] thiosulfates (Bunte salts),[144] thiophenols,[178] thioureas,[179] thioctic (lipoic) acids,[180] thiophenes,[181] cysteines,[182] dithiocarboxylic acids,[183] xanthates,[184] thiocarbaminates,[185] mercaptobenzthiazoles,[186] and imidazole-2-thiones.[187]

Some of these, such as the sulfides, xanthates and thiocarbaminates, adsorb to gold with their structure unchanged; others such as the thioacetates, thiosulfates and disulfides are adsorbed as thiolates, with the monolayers formed being indistinguishable from those formed from equivalent thiols.[144,175,188]

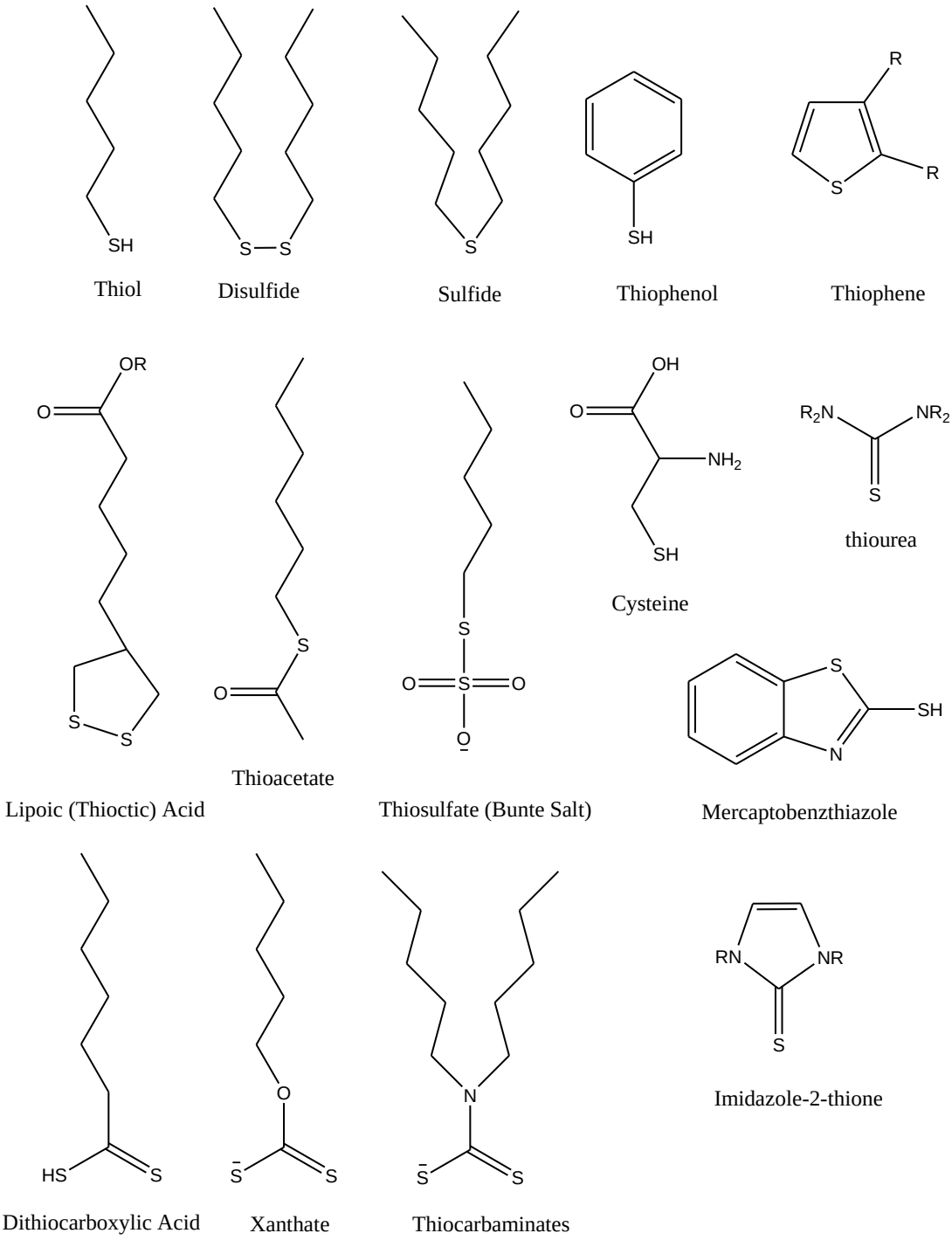

Figure 3.1. Examples of Sulfur Compounds Known to Form Self-Assembled Monolayers on Gold.

These different compounds have various advantages and applications. For example, lipoic acid monolayers are often used to immobilise biomolecules on surfaces, while thioacetates and thiosulfates are used due to their ease of synthesis and their stability (as thiols are prone to oxidation).

3.1.2 Properties of SAMs

The structural features of the monolayers are determined by the thiol-gold interaction and intermolecular interactions.

The mechanism of adsorption is a two step process. The initial adsorption is fast, and dependant on the thiol concentration in solution.[189] The monolayer is initially disordered and becomes more ordered during the second step where the molecules rearrange on the surface.[174] The initial step occurs in seconds to minutes, whereas the rearrangement can take hours to weeks to reach a steady-state dependant on the structure of the adsorbant.

The degree of order present after the system is allowed to reach equilibrium is dependent on the intermolecular forces. Alkane thiols with long chains produce higher ordered SAMs with fewer defects, than shorter chain thiols. This is explained by the greater van der Waals interaction present. The alkane chains are tilted approximately 30 degrees to the normal in order to restore the ideal crystalline packing of the chains, as the headgroup spacing is larger than the interchain distance.[174]

This crystalline packing is typical of many monolayers studied, however other structures are possible. Imidazole-2-thiones have been shown to produce monolayers with voids that can be exploited for their intercalation potential.[187]

Monolayers of alkane thiols appear to be stable indefinitely in air or in contact with liquid water or ethanol at room temperature (no observed changes over several months). Upon heating to 70° C the monolayers desorbed, this was fastest in hydrocarbon solvents, slower in ethanol and slowest in air.[190] A number of chemicals have been shown to attack the monolayers themselves, including halogens, strong oxidising agents (peroxide, ozone), ethereal solutions of borane and phosphorous pentachloride, methylene iodide, and aqueous iodide ions.[190] Hydroxyl terminated monolayers were studied by Evans *et al*,[191] and were found to be unstable over time under ambient

conditions, as determined by changing contact angles, however the majority of monolayers studied appear to be stable for long periods of time.

The terminal groups at the surface of the monolayer retain their reactivity and can be used to further functionalise the monolayer.[192,193] This is often used to attach biomolecules for sensor purposes; however a multitude of solution or gas phase reactions can be performed, providing the reagents do not destabilize the monolayer.

3.1.3 Applications of SAMs

Self assembled monolayers have found wide application in sensor technologies and material science.

They have been used as the basis of electrochemical sensors, as the monolayer can preconcentrate the analyte, prevent fouling of the electrode or enhance the selectivity of the interface.[194] Sensors for metal ions, organic molecules, biomolecules, pH, and specific DNA sequences have all been developed.[195]

Monolayers have been used in device fabrication, for example in microcontact printing,[196] photolithography,[146] and atomic force microscope (AFM) lithography[197] where patterned SAMs can be formed. These SAMs can then be used as etch resists or substrates for controlled crystal nucleation,[198] to produce well-defined and complex nanostructures (Figure 3.2). Other applications include lubricants,[199] corrosion inhibitors, and barriers to electron transport.[146,200]

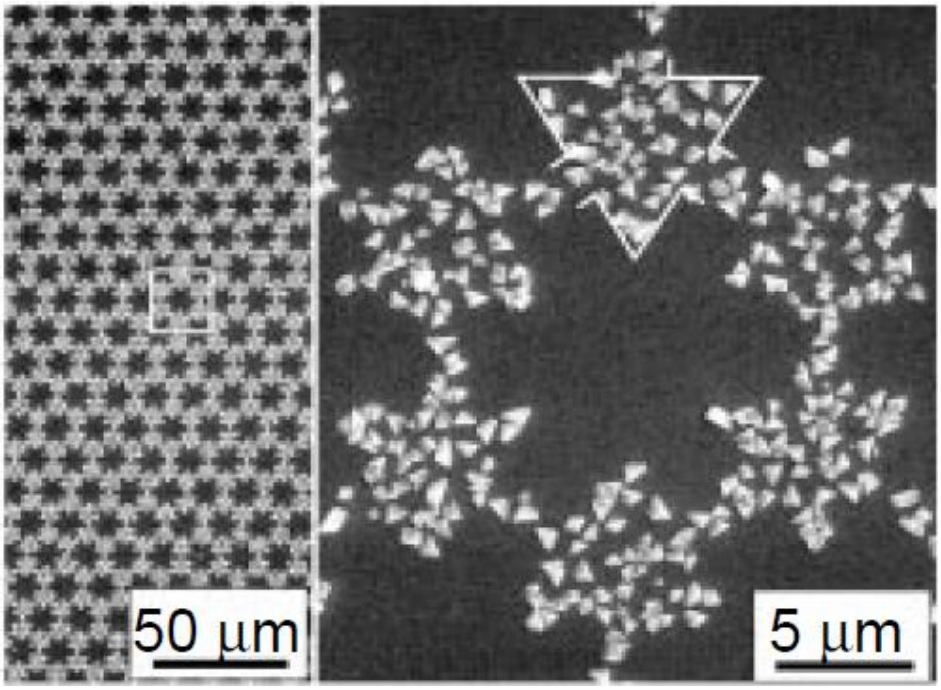

Fig 3.2 Nanostructured Surface Formed by Crystal Growth Nucleated on a SAM Patterned Surface. Reprinted by permission from Macmillan Publishers Ltd: Nature, 398(6727), Aizenberg, Black, Whitesides, *Control of crystal nucleation by patterned self-assembled monolayers*, 495-498, (copyright (1999)).

3.1.4 Characterisation of SAMs

A variety of techniques have been adapted to studying self-assembled monolayers.[201] Contact angle measurements give hydrophobicity information,[202] quartz crystal microbalance (QCM) and surface acoustic wave (SAW) measurements show changes in mass and can be used to monitor the formation of the monolayer in addition to the interaction with analytes in solution and the vapour state.

Optical techniques such as polarised grazing angle infra-red spectroscopy (PGAFTIR) can probe both the functional groups present and their orientation relative to the surface.[153,203,204] Ellipsometry and surface plasmon resonance (SPR) can give information on the monolayer thickness, and can be used to measure changes in thickness with the adsorption of analytes.[153-137,205]

High-vacuum techniques such as X-ray photoelectron spectroscopy (XPS), auger electron spectroscopy (AES), high resolution electron energy loss spectroscopy (HREELS), and mass spectrometry can provide valuable information about a monolayer.[206] AES is used to determine chemical composition, while XPS can be used to give speciation data. This technique is widely used to determine whether a monolayer is chemi- or physisorbed.[151,167,169,175] Secondary ion mass spectrometry (SIMS) or matrix assisted laser desorption/ionisation time of flight mass spectrometry (MALDI-TOF) have been used to look at the molecular weights of the adsorbate (and fragments), and is especially useful to analyse chemical reactions of a monolayer, however it is a destructive technique, limiting its use.[169,207]

Atomic force microscopy (AFM) and scanning tunnelling microscopy (STM) experiments can give molecular packing information and topography,[157,208-210] and by using a modified tip the forces between an analyte and the monolayer can be measured.[211,212]

Electrochemical methods such as cyclic voltammetry and impedance spectroscopy can give the effective thickness based on the capacitance of the monolayer, and information about the presence of defects.[151,201]

3.1.4.1 Contact Angle

The contact angle of a surface is the internal angle of an adhering drop (Figure 3.3), measured at the solid-liquid-gas interface. There are many different methods for measuring contact angles, for example the Wilhelmy plate method, and capillary rise at a vertical plate. For monolayer covered surfaces the simplest and most appropriate is the sessile drop or captive drop methods, measured with a goniometer.[213]

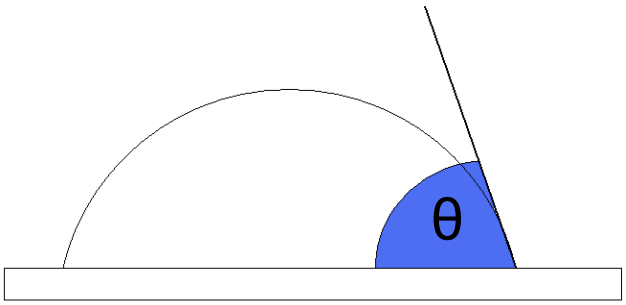

Figure 3.3 Contact Angle θ

Sessile drops from a syringe or a fine wire are attached to the surface. Detachment of the wire/needle can vibrate the drop and lead to a lower metastable contact angle than the true contact angle. Typically, if the measurement apparatus allows, the syringe is left attached to the drop and liquid added and removed in order to make several advancing and receding contact angle measurements for each drop.

Contact angle values measure the degree of wetting of a surface by a liquid. This gives an idea of how hydrophilic/phobic a surface is and the value can be used to calculate surface free energy.[213]

Contact angles are sensitive to the chemical nature of the surface,[191,214] to the roughness of the surface, and to monolayer density and orientation.

The advancing contact angles are influenced by the polarity of the interface between air and the monolayer, while the hysteresis between the advancing and receding angles is indicative of how ordered the monolayer is. A difference of ~10° is normal for well packed layers, while hysteresis values above 30° are evidence of a more disordered layer.[215]

Hysteresis can also be due to underlying substrate roughness, and Gupta *et al*.[216] have shown that it is possible to produce mixed monolayers that exhibit no contact angle hysteresis on ultra-flat gold substrates. Sorption of the liquid into the monolayer can also lead to hysteresis.[213]

3.1.4.2 Infrared Spectroscopy

Grazing angle reflectance infrared spectroscopy (GAR-IR), also known as polarised infrared external reflectance spectroscopy (PIERS), uses a configuration where the incident infrared beam is greater than 80° to the normal in order to maximize the absorbance by the monolayer.

Polarised grazing incidence reflectance infrared spectroscopy (PGAR-IR) takes advantage of the surface selection rule. For samples on metal substrates where the thickness of the layer is much smaller than the incident wavelength of radiation; significantly larger optical absorption is observed with the p-polarised beam than with a s-polarised beam.[217] The p-polarised beam is absorbed by transition dipoles perpendicular to the surface, while s-polarised light is absorbed by transition dipoles parallel to the surface (Figure 3.4). The frequencies absorbed in the PGAR-IR spectrum can be used to determine the orientation of the molecules.[203]

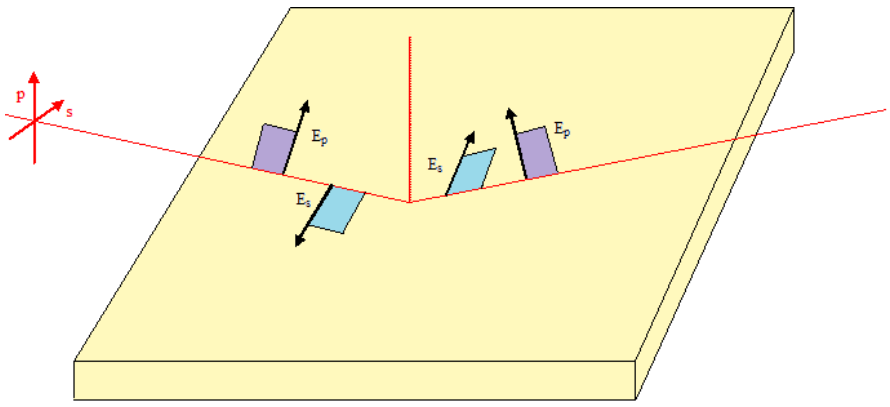

Figure 3.4 Orientation of p and s Polarised Light, Relative to a Surface.

Polarised modulation infrared reflectance absorption spectroscopy (PMIRRAS) takes advantage of the surface selection rule to eliminate the problem of carbon dioxide and water vapor in the atmosphere of the sample

chamber which often overwhelm the monolayer absorbances in PGAR spectroscopy.[217] A photoelastic modulator (PEM) is placed in the excitation beam (Figure 3.5), and the s and p polarised spectra are measured. The transmission spectrum is then calculated from Equation 3.1.

$$S = C\frac{R_p - R_s}{R_p + R_s}J_2(\phi_0)$$

Equation 3.1 Calculation of PMIRRAS Signal (S) where *C* is a constant, J_2 is the second-order Bessel function of the maximum dephasing ϕ_0 introduced by the PEM, and R_s and R_p are the s- and p-polarized reflectances of the sample, respectively.

No background needs to be recorded, eliminating the difficulty of preparing perfectly clean reference surfaces; and absorptions from atmospheric interferences are eliminated as they absorb p and s polarised light equally (R_s=R_p). This procedure results in a strongly curved spectrum due to the wavelength dependent efficiency of the photoelastic modulator. This is then baseline corrected and converted to absorbance units to yield the final spectrum. As with PGARIR, vibrations of bonds are only observed if they have a component perpendicular to the surface, however the sensitivity is greatly increased.

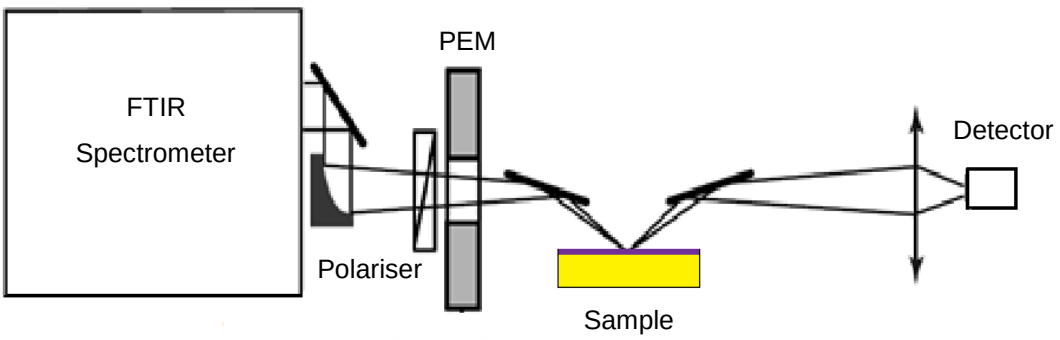

Figure 3.5 Schematic of PMIRRAS Setup.

3.1.4.3 Atomic Force Microscopy

Atomic force microscopy (AFM) is a technique where the deflection of a small tip is measured as it is scanned across a surface. Scanning tunnelling microscopy (STM) was the forerunner to this technique, and is similar except the tunnelling current between the sample and the tip is measured rather than deflection. Both techniques have been widely used to study the structure of self-assembled monolayers.

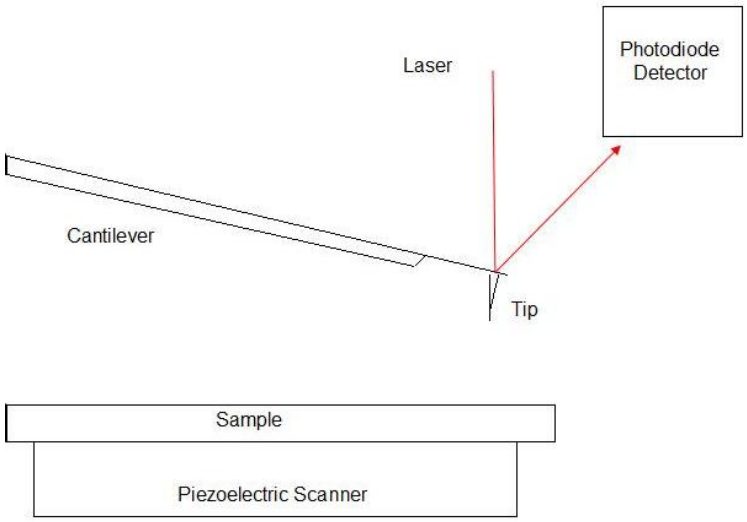

Figure 3.6 Schematic of an Atomic Force Microscope (not to scale)

In order to obtain AFM images there are three major imaging modes, contact, tapping and non-contact mode (Figure 3.7). As the name suggests, in contact mode the tip is in contact with the sample. This mode provides good resolution but can be destructive and is not suitable for soft samples. In tapping mode the tip oscillates vertically, intermittently contacting the surface which is ideal for soft samples as there are no lateral forces applied, however the resolution obtained is poor in comparison. Non-contact mode is very similar to tapping mode, however the oscillation of the tip is smaller, and it does not touch the sample preventing any possible damage or contamination. The resolution obtainable is similar to contact mode.

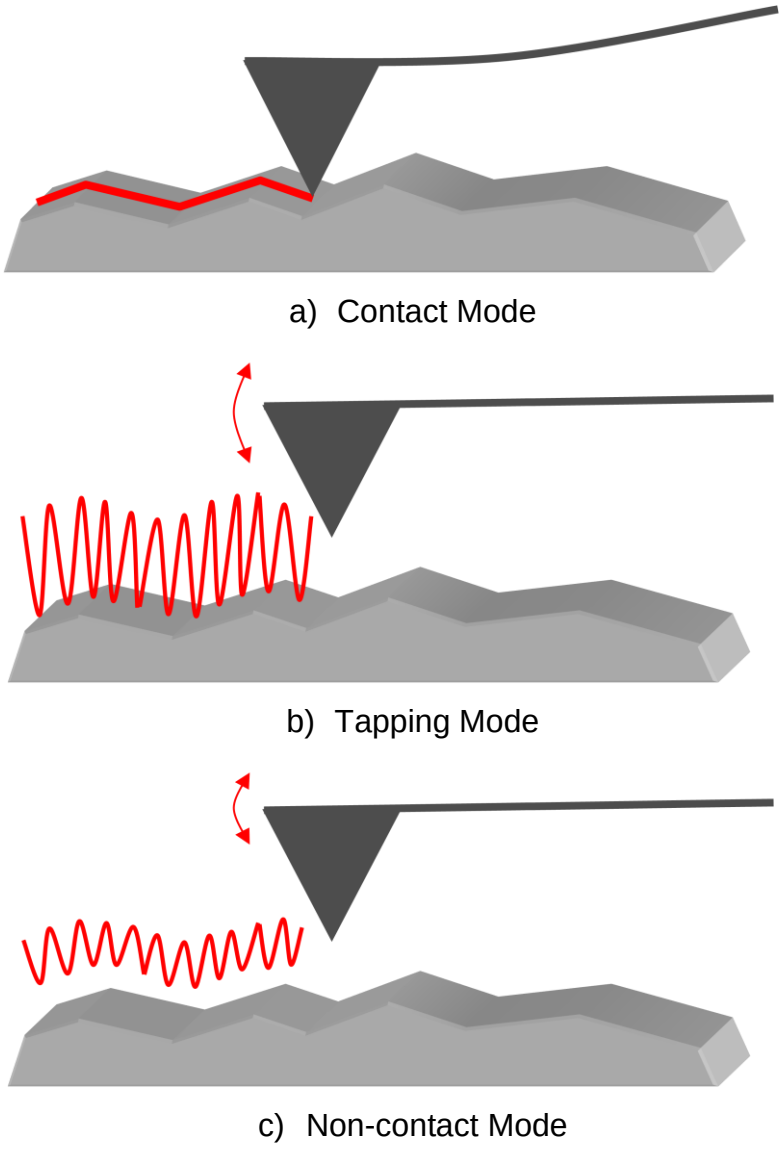

Figure 3.7 AFM Imaging Modes

AFM images surface topology (see Figure 3.8 for an image of a decane thiol monolayer), however STM images electronic structure, and requires a conductive sample. STM images are often assumed to be equivalent to the topology of the monolayers studied,[209] however there is evidence that this is not necessarily correct. Instead the perturbation of the gold substrate is measured rather than the actual monolayer.[218] This is shown by the identical lattice structure regardless of the physical size of the thiol.

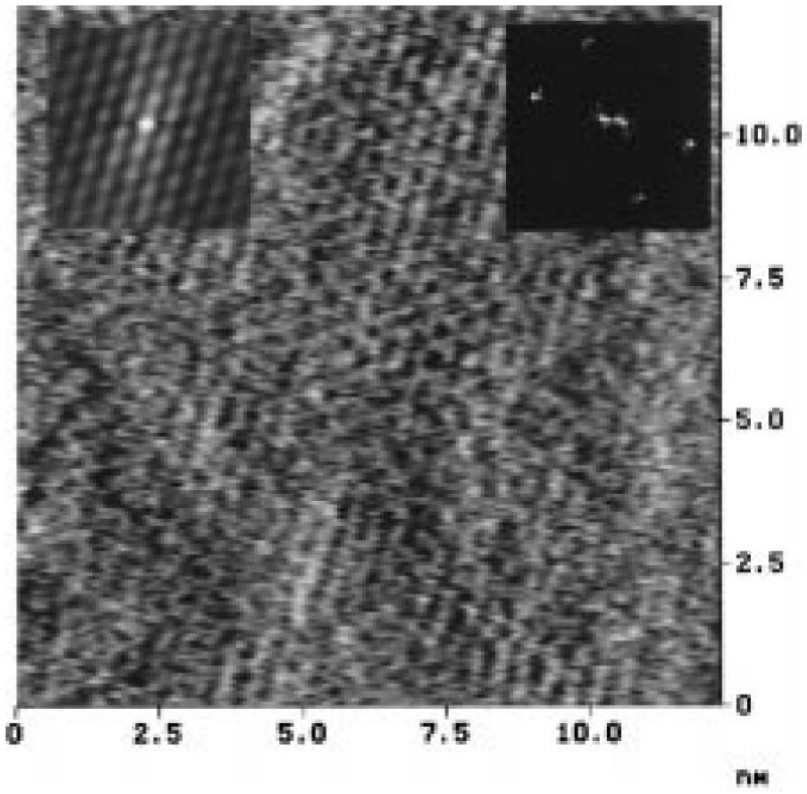

Figure 3.8 AFM Image of Dodecanethiol on Au(111) (insets: autocovariance pattern, 2-D fast fourier transform). Reprinted with permission from Langmuir, 15(17), Schonherr, Vancso, Huisman, van Veggel, Reinhoudt, *Lattice Structure of Self-Assembled Monolayers of Dialkyl Sulfides and Calix[4]arene Sulfide Adsorbates on Au(111) Revealed by Atomic Force Microscopy*, 5541- 5546. Copyright 1999, American Chemical Society.

3.2 Discussion

3.2.1 Substrate Preparation

Appropriate substrate preparation is crucial as any contamination may block the formation of, or disturb the packing of the monolayer. Preparing clean gold surfaces is a non-trivial problem as it has been shown that contamination can be detected on surfaces with as little as seven minutes exposure to a laboratory environment.[219]

Any contamination of the surface needs to be removed before exposing the surface to a thiol solution. Various methods have been used to clean gold surfaces before use, including piranha solutions (3:1 sulfuric acid: aqueous hydrogen peroxide) electrochemical polishing, plasma cleaning and UV/ozone cleaning.

The method used here to clean all substrates was UV/ozone cleaning, followed by immersion in ethanol to reduce the gold oxide formed. This method has been shown to produce clean surfaces in less than a minute.[220] Light produced by the UV lamp at 184.9 nm is absorbed by oxygen and generates ozone, while the 253.7 nm radiation is absorbed by hydrocarbons and ozone. The presence of both wavelengths means ozone is continually being formed and destroyed. An intermediate of both of these processes is atomic oxygen, which is a very strong oxidising agent. Either ozone gas or UV alone was shown to be much less effective, while UV wavelengths of greater than 300 nm were completely ineffective in cleaning the substrates.

This method is capable of removing not only general contamination, but also thiolate monolayers.[219] It was shown that treated surfaces could be used to re-form monolayers with identical parameters to those obtained prior to cleaning

The UV/ozone cleaning method requires reduction of the surface with ethanol as gold oxide is formed. It was found that a separate reduction step is still

required when using ethanol as the solvent for monolayer formation, as the oxide is encapsulated under the monolayer and is not reduced,[219] producing poor quality monolayers.[221,222]

3.2.2 Preparation of Monolayers

Monolayers were prepared from the calixarenes and resorcinarenes synthesised earlier (Figures 3.9-11).

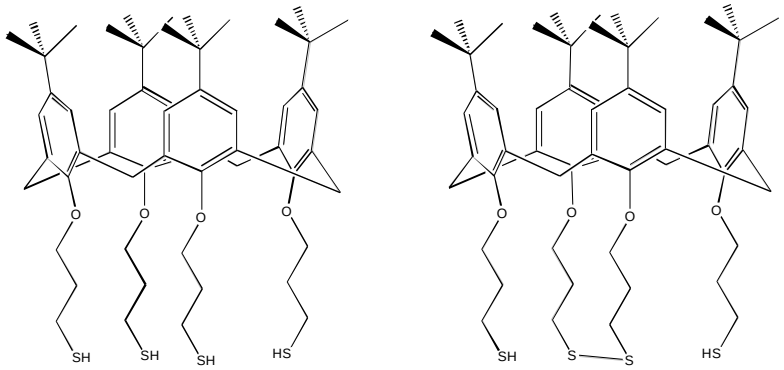

18 **19**

Figure 3.9 Calixarene Thiol/Disulfide Mixture **18**/**19**

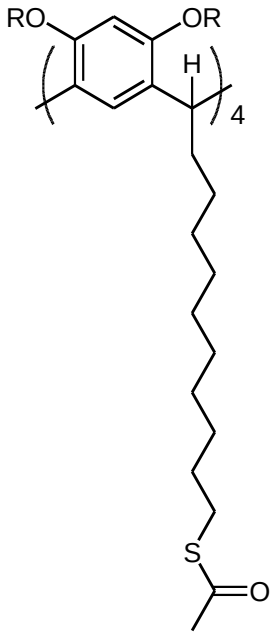

9 R = Me

10 R= Pr

11 R= Bn

12 R,R = CH_2

Figure 3.10 Thioacetyl Resorcinarenes

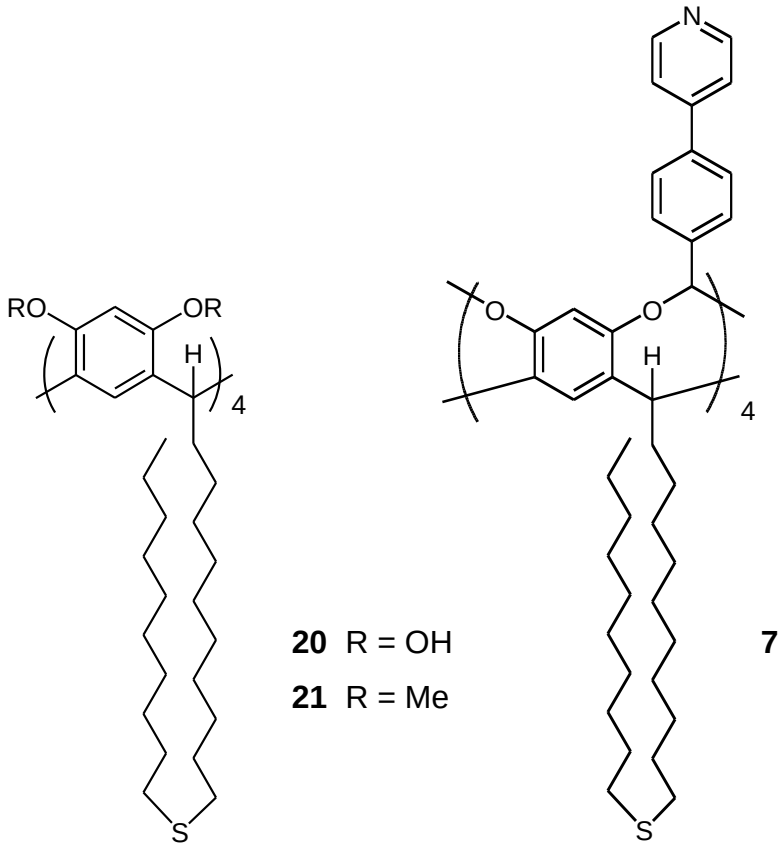

Figure 3.11 Decylsulfide Resorcinarenes

Monolayers of thiols and disulfides are easy to prepare as the compounds will spontaneously chemisorb to a clean gold substrate. Typically monolayers are prepared from ethanol solutions, however any solvent that does not react with the adsorbing compound or the substrate can be used. Monolayers of sulfides are prepared in a similar way, however they form weaker physisorbed layers.[167]

Thioacetates have been found to also spontaneously chemisorb to gold giving identical monolayers to those formed from equivalent thiols.[176,188] The kinetics of this process are slower than the adsorption of thiols, and higher concentrations are required to achieve the same rate. The acetate group is hydrolysed in this process, and the addition of mineral acids (hydrochloric[223-1199] or sulfuric[224-2909]) or base (ammonia solution[176]) to the solution was found to increase the speed of monolayer formation to rates similar to that of thiols.

Monolayers prepared for initial contact angle experiments (calixarene mixture **18**/**19** and methoxy resorcinarene **9**) were prepared from 0.5 mM solutions in ethanol with no additives. The calixarenes were soluble at this concentration, however the resorcinarene **9** was found to precipitate as the ambient temperature dropped. Tetrahydrofuran was used for all further experiments as the solubility was much higher, and the addition of acid was investigated for the thioacetyl resorcinarenes. Sulfuric acid was chosen to catalyse the *in situ* hydrolysis of the thioacetates, as it was expected to minimise the air oxidation of the thiol products (base is known to catalyse the air oxidation to disulfides[163]).

The monolayers used for the final contact angle measurements, infrared spectroscopy and atomic force microscopy were prepared from 0.5 mM tetrahydrofuran solutions of the macrocycle, with one drop of concentrated sulfuric acid added for the thioacetates. The substrates were immersed at ambient temperatures for eight days, then rinsed with copious amounts of tetrahydrofuran and dried under a stream of nitrogen.

The importance of the temperature of the adsorbing solution is unclear. The Reinhoudt group originally found that monolayers formed from resorcinarene sulfides were more organised when adsorbed from hot (60°C) solutions.[147,149,151,154] Later work from the same group[150] indicated that the monolayers formed at ambient temperatures were identical by AFM to those formed at higher temperature.

The monolayers formed from the decylsulfides **7**, **20** and **21** are expected to be more ordered than those formed from the thioacetates **9**-**12**. The cross sectional area of the eight alkyl chains is 160 $Å^2$, slightly larger than the area of the resorcinarene headgroup (140 $Å^2$).[151] This allows the molecules to pack efficiently on the surface. The resorcinarene thioacetates only have four alkyl chains for each headgroup, and the packing must compensate to fill the extra volume.

3.2.3 Contact Angles

The contact angles were measured by obtaining a digital image of a drop of MilliQ water on the surfaces, and using software to fit the curve of the drop and calculate the left and right gradients at the intersection between the vapour, solid and liquid phases. At least eighteen measurements over three substrates were measured for each sample, and the averages and standard deviations calculated. Statistical significance was calculated using the analysis of variance (ANOVA) function in Microsoft Excel using a 95% confidence level.

The contact angle of MilliQ water on monolayers formed from the calixarene **18**/**19** mixture (0.5 mM in distilled ethanol, adsorbed overnight) was found to be 99 ± 5°. The methoxy resorcinarene thioacetates **9** under the same conditions gave a monolayer with a contact angle of 76 ± 4°, which was significantly greater than the bare gold (73 ± 2°).

These results show that the surfaces were significantly more hydrophobic than clean gold, evidence that the monolayer has formed as expected, however it was unknown whether the monolayers would have reached an ordered state after eighteen hours. It has been reported that contact angles are almost at their maximum after the fast adsorption of the molecules but reach their highest value after rearrangement of the surface.[190]

There were other concerns with the results observed for the monolayer of the thioacetate **9**. The solubility of the resorcinarene in ethanol was marginal, and as the ambient temperature dropped, precipitation was observed. This complicates the interpretation of the contact angle values, as it is possible that the thioacetate has precipitated on the surface rather than forming a monolayer. Both situations would result in the observed increase in contact angle.

Adsorption experiments were then undertaken using tetrahydrofuran (as the solubility was higher) to investigate the effect of acid on the monolayer, and

to determine how long it took for the contact angle to reach a stable value. It was found that the contact angle of the monolayer formed from 1 mM solutions of resorcinarene **9** with added acid (to give a 1 mM concentration) were stable over the time period examined (Figure 3.12). The monolayer formed in twenty one hours had a contact angle of 81 ± 2°; after 46 hours, 82 ± 3°; after 71 hours, 82 ± 2°; and after 95 hours, 82 ± 2°.

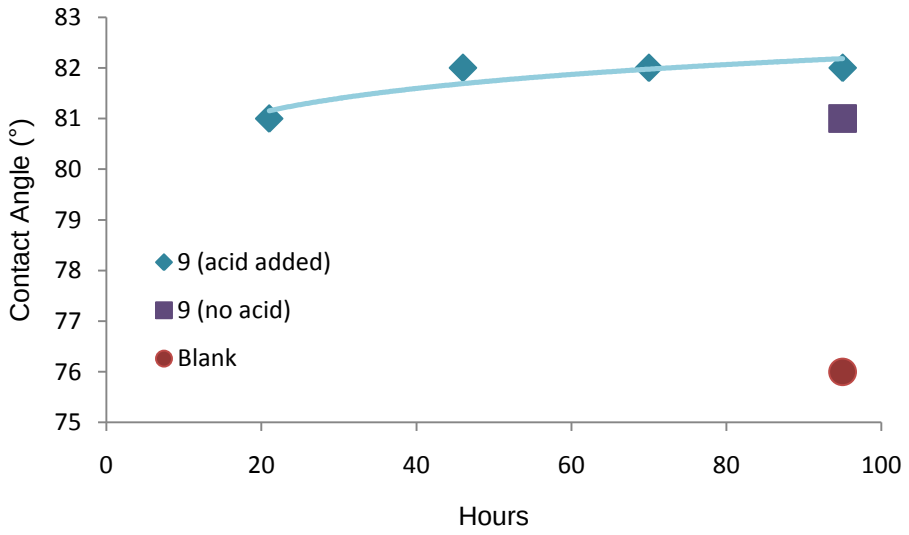

Figure 3.12 Contact Angles of Monolayers Formed from Methoxy Resorcinarene Thioacetate **9**. blue: monolayers formed with acid added. purple: monolayer formed with no additives. red: control sample (clean gold immersed in THF with no thiol added).

The values for the contact angles of resorcinarene **9** after 21, 46, 71 and 95 hours were not significantly different, however it is unknown if the results are precise enough for the small increase in contact angle associated with the monolayer becoming more ordered to be detected. All monolayers produced thereafter were allowed to adsorb for at least two days (usually ~five days to produce the most ordered monolayer possible within reasonable time constraints).

It was found that the addition of acid to the solution in order to hydrolyse the thioacetate *in situ*, does result in a monolayer that exhibits a larger contact angle. The monolayer formed from tetrahydrofuran solution after 95 hours had a contact angle of 81 ± 2°, while with acid added that value was 82 ± 2°. This difference, while small, is statistically significant.

All contact angles observed for the monolayers were greater than for the bare gold (which had been immersed in tetrahydrofuran for 95 hours to eliminate the possibility of contamination from the solvent giving erroneously high contact angles) which had a contact angle of 76 ± 4°, similar to values reported in the literature (78 ± 11°[222]). The contact angles of the bare gold samples were measured before and after the monolayer samples to determine if laboratory contamination was affecting the results due to the time taken to run the samples. The contact angle did increase from 73 ± 4° to 79 ± 2° over the ninety minutes it took to measure the values of all the samples; however it is clear that the contact angle of the surface formed from resorcinarene **9** is at least partially due to a monolayer forming and not solely due to contamination.

Static contact angles were measured for the initial experiments as the software used was not capable of measuring advancing angles. The static contact angle measured is equivalent to the advancing contact angle as long as the drop isn't perturbed by the removal of the syringe, there is evidence that this did not happen to a significant extent due to the small standard deviation in repeat measurements observed. The software problem was resolved so that advancing and receding contact angles were measured for the monolayers formed from all the compounds prepared.

The surfaces measured were prepared by adsorption from 0.5 mM solutions in tetrahydrofuran for eight days. The thioacetates had a drop of concentrated sulfuric acid added to allow *in situ* hydrolysis.

The advancing contact angle values were relatively precise with standard deviations of 1-3 ° (similar to the standard deviations observed for the static contact angles observed 2-3°). All of the values (Table 3.1) were significantly greater than the blank indicating that the surfaces are more hydrophobic due to the presence of organic material, presumably the monolayer, as it has been shown that no significant contamination is introduced in the procedure used.

Table 3.1 Advancing and Receding Contact Angles

Sample		*Advancing (°)*	*Receding (°)*	*Δθ*
Clean gold		79 ± 1	58 ± 2	21
Deep cavitand	**7**	81 ± 1	34 ± 4	47
Methoxy resorcinarene	**9**	81 ± 2	46 ± 5	35
Benzyloxy resorcinarene	**11**	85 ± 3	53 ± 5	32
Methylene cavitand	**12**	88 ± 2	50 ± 3	38
Propoxy resorcinarene	**11**	91 ± 2	49 ± 8	42
Resorcinarene decyl sulfide	**20**	98 ± 2	60 ± 4	38
Calixarenes	**18/19**	101 ± 2	56 ± 5	45
Methoxy resorcinarene decyl sulfide	**21**	102 ± 1	71 ± 3	31

The values obtained follow the pattern expected with the exception of the resorcinarene decyl sulfide **20**. The resorcinarenes with the less polar upper rims (i.e. the propoxy resorcinarene **11**) exhibit higher contact angles than those which are more polar (i.e. the methoxy resorcinarene **9**). The calixarenes with the tertiary butyl groups at the surface exhibit a contact angle of 101 ± 2°, evidence that the surface is hydrophobic.

The change of solvent and increase in adsorption times do not greatly affect the contact angle of the monolayer of the calixarene **18/19** with the monolayer formed from tetrahydrofuran solution over eight days giving a contact angle of 101 ± 2°, while a monolayer from ethanol gave a value of 99 ± 5 ° after only eighteen hours.

The decyl sulfides (cavitand **7**, hydroxyl resorcinarene **20** and methoxy resorcinarene **21**) have polar head groups which if exposed at the surface of the monolayer should exhibit a relatively small contact angle, however they are expected to pack more efficiently on the surface due to the extra alkyl

chains filling the space below the resorcinarene bowl. All exhibit significantly lower contact angles than decane thiol monolayers (advancing 108° receding 91°).[151] This provides further evidence that the resorcinarenes were not contaminated with decane thiol, as the stronger bonding between gold and the thiol would have led to decane thiol monolayers being formed instead of the resorcinarene monolayers.[167]

The large contact angle exhibited by the monolayer formed from the methoxy resorcinarene sulfide **21** (adv 102 ± 1°; rec 71 ± 3°) is very similar to the literature value (adv 102 ± 2°; rec 74 ± 2 °[149]), and can be explained by the methyl groups being exposed at the surface rather than the ether oxygen atoms.

The monolayer of the hydroxyl resorcinarene **20** exhibits a larger than expected advancing contact angle (98 ± 2°). The contact angle suggests that the hydroxyl groups are not located at the interface between the monolayer and the atmosphere. This could be due to monolayer reorganisation to avoid the high energy surface (by burying the hydroxyl's in the monolayer),[191] however it is difficult to envisage how this could happen. Another possibility is the formation of multilayers. Resorcinarene tetrathiols (Figure 3.12) were previously found to form stable multilayers when adsorbed from a hexane solvent.[152] The multilayers exhibited a contact angle of 92°, however monolayers (formed from ethanol) had a contact angle of 28°, consistent with the expected hydrophilic surface. It was hypothesised that the multilayers were formed with hydrogen bonding holding the headgroups together, and van der Waals interactions between interlocking alkyl chains (see Figure 3.14).

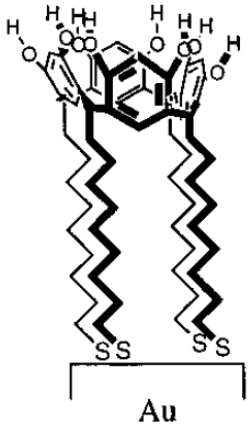

Figure 3.13 Structure of the Resorcinarene Tetrathiol. Reprinted with permission from Langmuir, 12(22), Davis and Stirling, *Calix[4]resorcinarene monolayers and multilayers: Formation, structure, and differential adsorption*, 5365-5374. Copyright 1996, American Chemical Society.

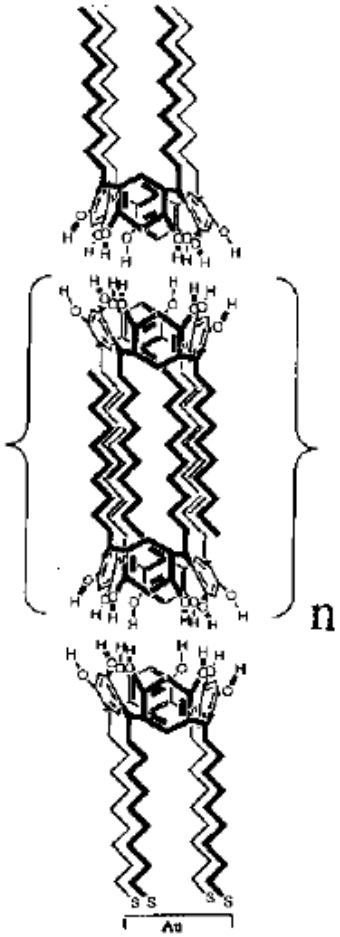

Figure 3.14 Hypothesised Structure of Multilayers. Reprinted with permission from Langmuir, 12(22), Davis and Stirling, *Calix[4]resorcinarene monolayers and multilayers: Formation, structure, and differential adsorption*, 5365-5374. Copyright 1996, American Chemical Society.

Faull and Gupta[57] formed monolayers from the same resorcinarene tetrathiol (Figure 3.13) which had a contact angle of 70-74°. Ellipsometric and surface plasmon resonance measurements were used to show that no multilayering was present, and they attributed the difference in contact angle to the technique used (sessile drop versus captive drop), and reorganisation of the surface.

van Velzen *et al*.[151] prepared monolayers of **20** and measured an advancing contact angle of 102 ± 2° and a receding contact angle of 37 ± 1°; which they attributed to a disordered bilayer. No structure was proposed, but it is likely that it may be similar to that of the resorcinarene tetrathiol. The contact angles were similar to the angles observed in this study (adv 98 ± 2°, rec 60 ± 4°) which indicates that it is likely that multilayers have been formed.

Ideal surfaces exhibit no hysteresis,[213] however differences of 30-50° were observed for all monolayers. The bare gold also exhibited a hysteresis value of 21° suggesting that the observed values for the monolayers are at least partially due to the underlying substrate, most likely roughness of the gold layer. Hysteresis can also be due to disordered packing, or the polarity of the monolayer. van Velzen *et al.*[149,151] have suggested that the receding contact angles (and hysteresis observed) reflect the flexibility of the headgroup. There doesn't seem to be any strong correlation in the observed values between the expected flexibility of the resorcinarene and the receding contact angle.

Contact angle measurements are only sensitive to the top few angstroms of the monolayer, so for many of the resorcinarenes synthesised, the values might be expected to be indicative of disordered packing as the alkoxy groups attached to the upper rim are not large enough to pack in a crystalline manner, even if the alkyl legs are packed in an ordered manner.[225]

3.2.4 Infrared Spectroscopy

Grazing incidence reflection absorption infrared spectroscopy was used to attempt to characterise the monolayers. The absorbance of the monolayers was very low, and interference from water vapour and carbon dioxide made it very difficult to identify peaks. The spectrometer was purged with nitrogen, however the concentration of water vapour and carbon dioxide was not able to be reduced to a consistent level where reliable data could be obtained.

Polarised modulation infrared reflectance absorption spectroscopy (PMIRRAS) was used to obtain spectra free from these interferences. There were no significant differences between duplicate spectra. In all cases peaks in the C-H stretching region (3000-2800 cm^{-1}) were visible, however not all samples exhibited peaks in the 1700–1000 cm^{-1} region. This could be due to the orientation of the monolayer, or the sensitivity limitations of the instrument. van Velzen *et al.*[149] reported weak headgroup related vibrations in polarised infrared external reflection spectra, due to instrumental reasons.

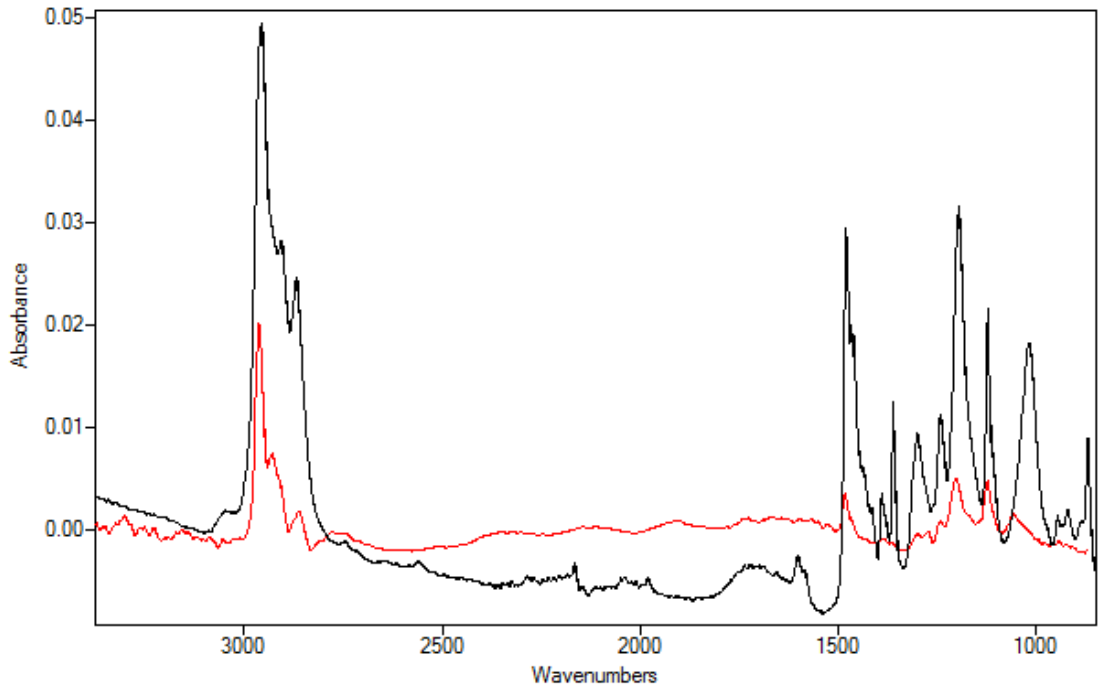

Figure 3.15 Overlaid FTIR Spectra. Red: PMIRRAS Spectrum of a Monolayer Formed From **18**/**19**. Black: FTIR Spectrum of the Bulk Material.

The PMIRRAS spectrum of the monolayer formed from the calixarenes thiol/disulfide mixture **18**/**19** (Figure 3.15) shows evidence that the monolayer has been formed as expected. The peaks from the monolayer roughly match the frequencies of the peaks in the bulk material. The ether C-O stretching peaks are visible in the PMIRRAS spectrum (aliphatic 1056 cm^{-1}, aromatic 1206 cm^{-1}), along with an aromatic peak at 1492 cm^{-1}.

The relative intensity of the C-H stretching region compared to the 1700 – 1000 cm^{-1} region has increased significantly from the bulk spectrum to the surface spectrum. This is most likely due to the orientation of the monolayer, as the bulk spectrum is obtained of a randomly oriented solid in which vibrations from all bonds contribute to the spectrum, unlike the ordered SAM in which only vibrations with a perpendicular component are visible. The C-H stretching signal will predominately come from the *t*-butyl groups and the methylene bridges, as the alkyl chains at the lower rim will be forced to be largely normal to the surface due to their short length, hence the C-H bonds will be parallel to the surface and signals from these will not appear in the PMIRRAS spectrum. If the calixarene bowl was in the crown conformation, then it would be expected that intensity of the signals due to the aromatic rings and the ethers would increase slightly relative to the C-H stretches. The opposite is observed in the spectrum recorded, suggesting that not all of the rings are normal to the surface. The observed intensities can be explained if the calixarenes are adopting a pinched cone conformation with two of the aromatic rings sitting vertically and two parallel to the surface (shown schematically in Figure 3.16) and therefore not contributing to the spectrum.

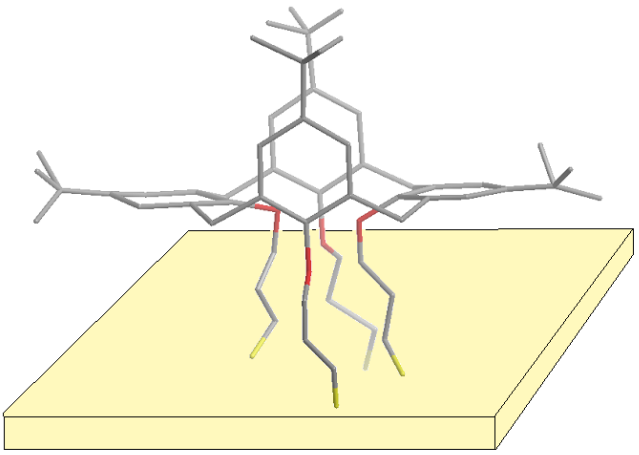

Figure 3.16 Proposed 'Pinched Cone' Conformation of **18** on the Surface (hydrogens omitted for clarity)

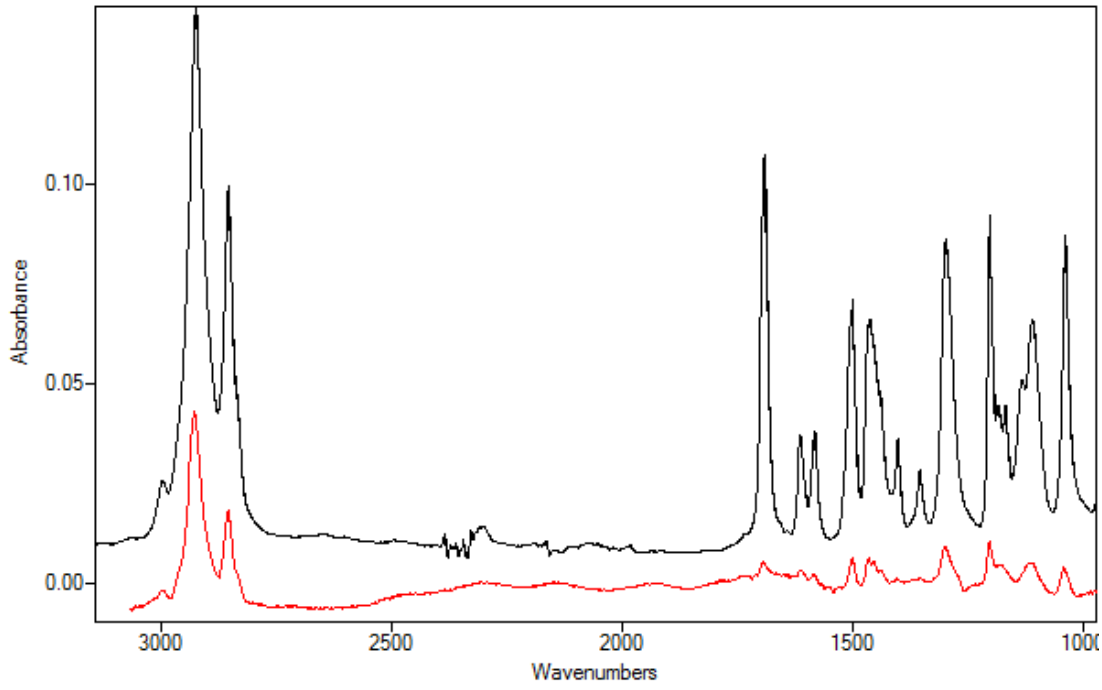

Figure 3.17 Overlaid FTIR Spectra. Red: PMIRRAS Spectrum of a Monolayer Formed From **9**. Black: FTIR Spectrum of the Bulk Material.

The PMIRRAS spectrum of the monolayer formed from the methoxy resorcinarene thioacetate **9** (Figure 3.17) also shows good evidence of the expected monolayer. In general the spectra appear to be a good match, with the exception of the carbonyl peak at 1692 cm^{-1}. The absorbance of this peak in the PMIRRAS spectrum is reduced relative to the rest of the spectrum, which is in accordance with the thioacetyl groups hydrolysing to the thiol *in situ* before adsorption to the gold surface. The small remaining peak at

1692 cm^{-1} in the PMIRRAS spectrum indicates that there is still some thioacetyl groups present, however as each resorcinarene contained four thioacetyl groups and only one is needed to hydrolyse to be bound, it is not surprising that some thioacetyl groups remain.

The intensities of the peaks in the 1700 – 1000 cm^{-1} region are again reduced relative to the C-H stretching signals. This may indicate that the resorcinarenes are tilted relative to the surface, so that the methylene legs are contributing to the observed signals at ~2800 cm^{-1}. Peaks assigned to the ether groups (1041 cm^{-1} and 1200 cm^{-1}) and the aromatic rings (1466 cm^{-1} and 1501 cm^{-1}) again are visible indicating that the resorcinarene is oriented so that aromatic rings and ethers have a component perpendicular to the surface. The inference that the ether bonds are largely perpendicular to the surface is consistent with the observed contact angles that suggest that the methyl groups are at the interface rather than the oxygen atoms.

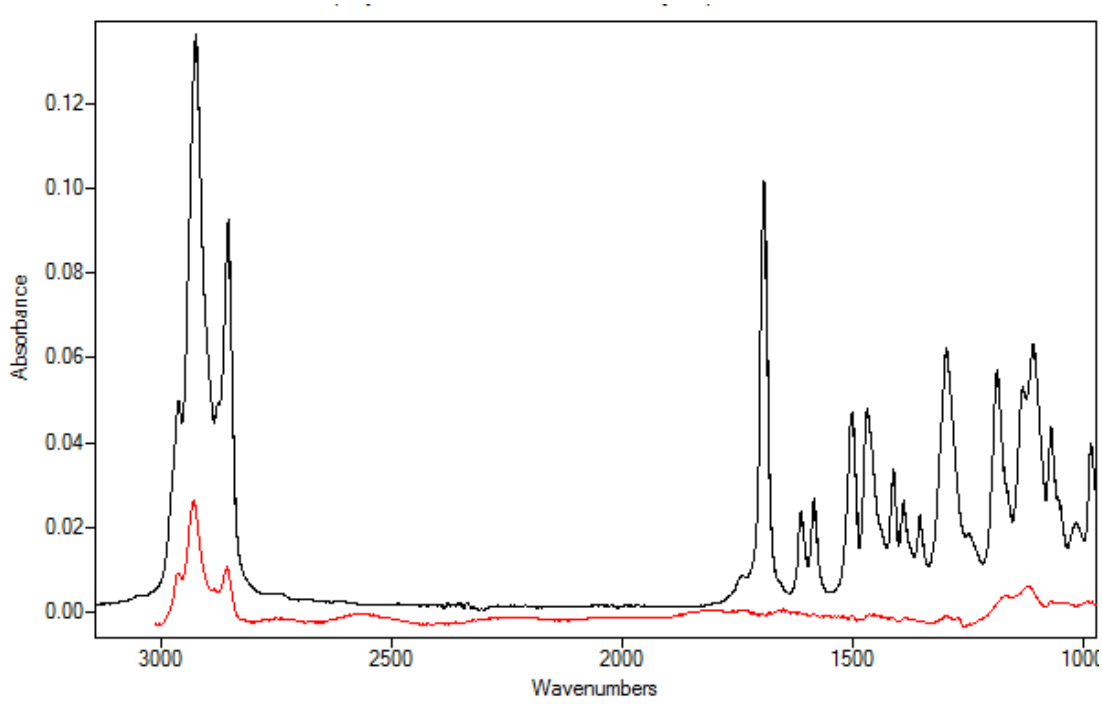

Figure 3.18 Overlaid FTIR Spectra. Red: PMIRRAS Spectrum of a Monolayer Formed From **10**. Black: FTIR Spectrum of the Bulk Material.

The PMIRRAS spectra obtained of the monolayers of the propoxy resorcinarene **10** (Figure 3.18), the benzyloxy resorcinarene **11** (Figure 3.19),

and the methylene cavitand **12** (Figure 3.20) show bands in the 3000-2800 region, however none were visible between 1700-1000 cm^{-1} (with the exception of the Si-O peaks at 1176 cm^{-1} from the underlying glass slides[226]). The C-H stretching clearly indicates that there is organic material on the substrate and the pattern matches that of the bulk material. The lack of peaks in the 1700-1000 cm^{-1} region is possibly due to the orientation of the resorcinarenes on the surface (as only bonds that have a vertical component are able to absorb infrared radiation when assembled on a metal surface), or sensitivity issues with the instrument. The absorbance values of the C-H stretching region are similar to those that did show peaks in the 1700-1000 cm^{-1} region, pointing to an orientation effect.

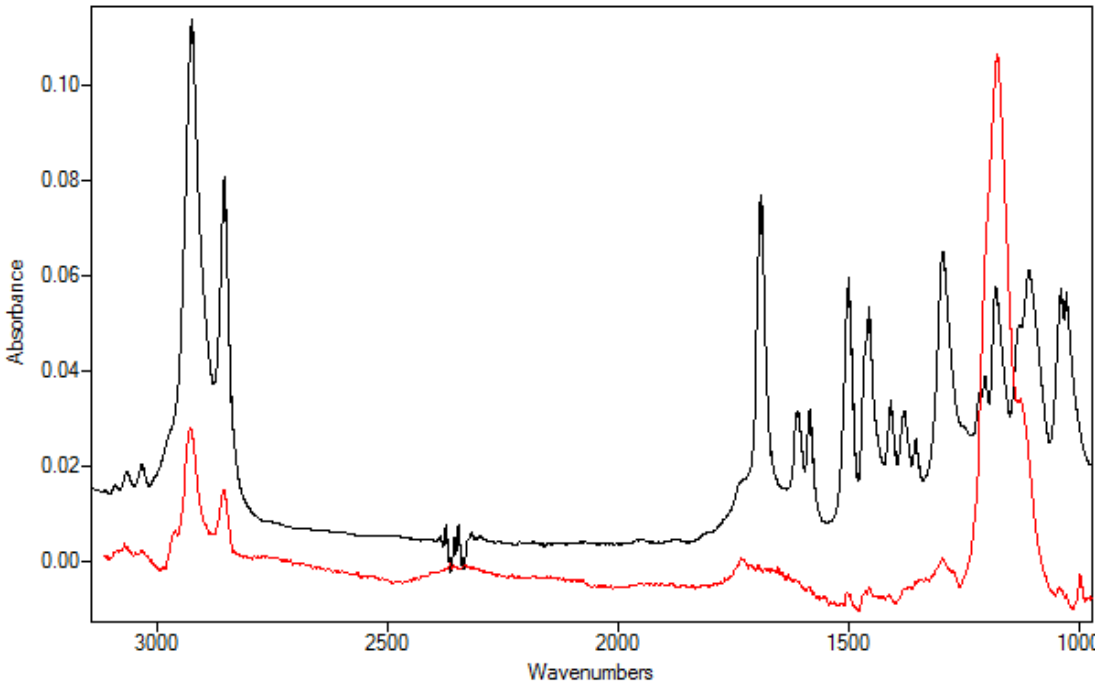

Figure 3.19 Overlaid FTIR Spectra. Red: PMIRRAS Spectrum of a Monolayer Formed From **11**. Black: FTIR Spectrum of the Bulk Material.

It is difficult to obtain any orientation information from these spectra, however, as there are no peaks assignable to the headgroup visible, it may be inferred that the component of the dipole transitions of these bonds that is normal to the surface is small enough that no peak is seen in the spectrum (i.e. the carbon-carbon bonds of the headgroup are largely parallel to the surface).

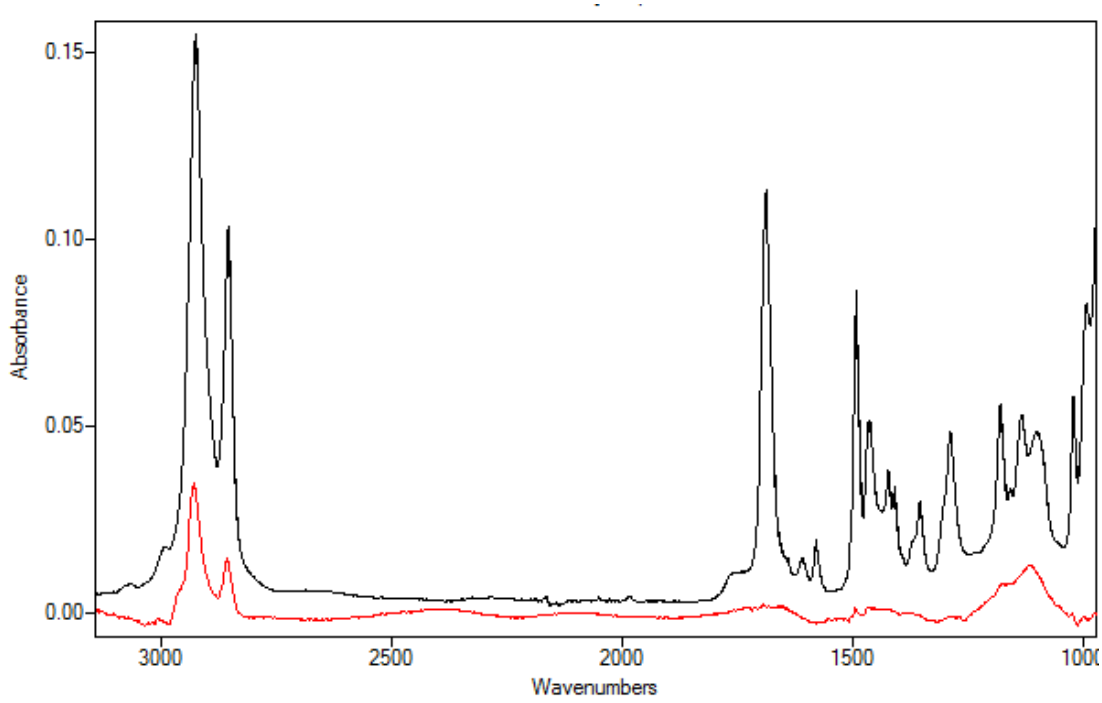

Figure 3.20 Overlaid FTIR Spectra. Red: PMIRRAS Spectrum of a Monolayer Formed From **12**. Black: FTIR Spectrum of the Bulk Material.

The PMIRRAS spectra obtained from the monolayers of the decylsulfides **20**, **21** and **7** (Figures 3.21-23) also did not show any identifiable peaks in the 1700-1000 cm^{-1} region. There are signals due to C-H stretching present in the 3000-2800 cm^{-1} region, however the pattern no longer reflects that of the bulk (Figures 3.24-26). This is likely due to the increased contribution of the methyl C-H stretches (relative to the methylene stretching) due to their orientation (as most of the methylene C-H bonds are parallel to the surface, they do not contribute to the PMIRRAS spectrum). The possibility also exists that this could be due to contamination, however this is unlikely as the samples were all prepared at the same time, but only the decyl sulfides exhibit the extra C-H stretching bands. Contamination by decane thiol (a reagent in the synthesis of these compounds) is unlikely due to the measures taken when purifying the compounds, and the contact angle data is consistent with resorcinarene monolayers/multilayers rather than an alkyl thiol monolayers.

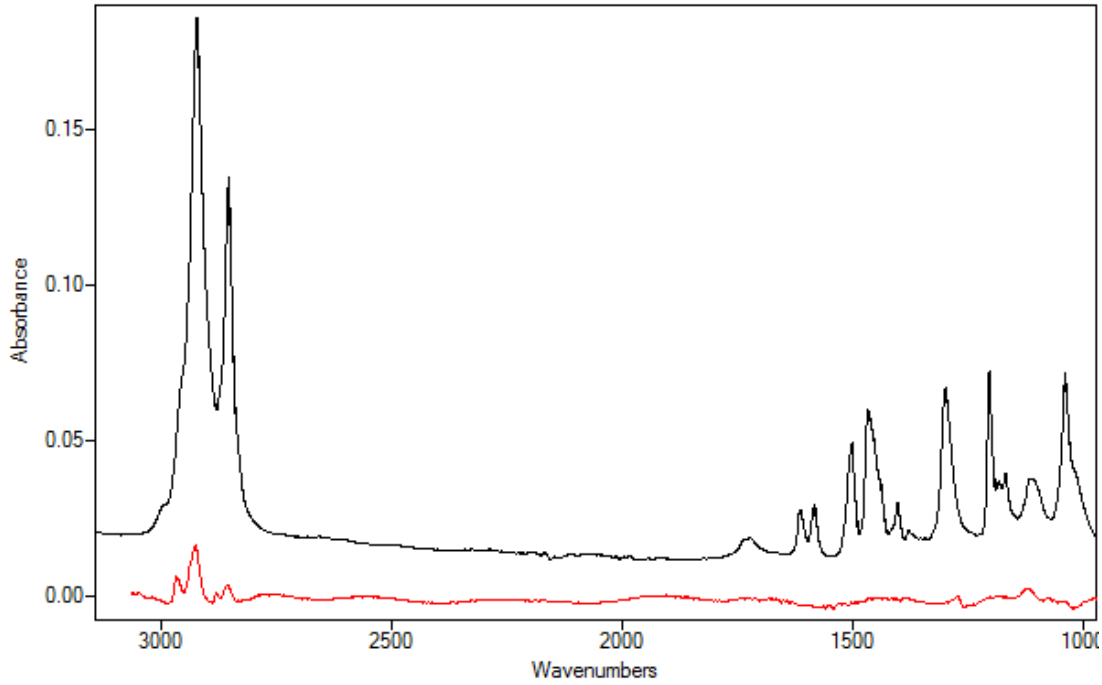

Figure 3.21 Overlaid FTIR Spectra. Red: PMIRRAS Spectrum of a Monolayer Formed From **21**. Black: FTIR Spectrum of the Bulk Material.

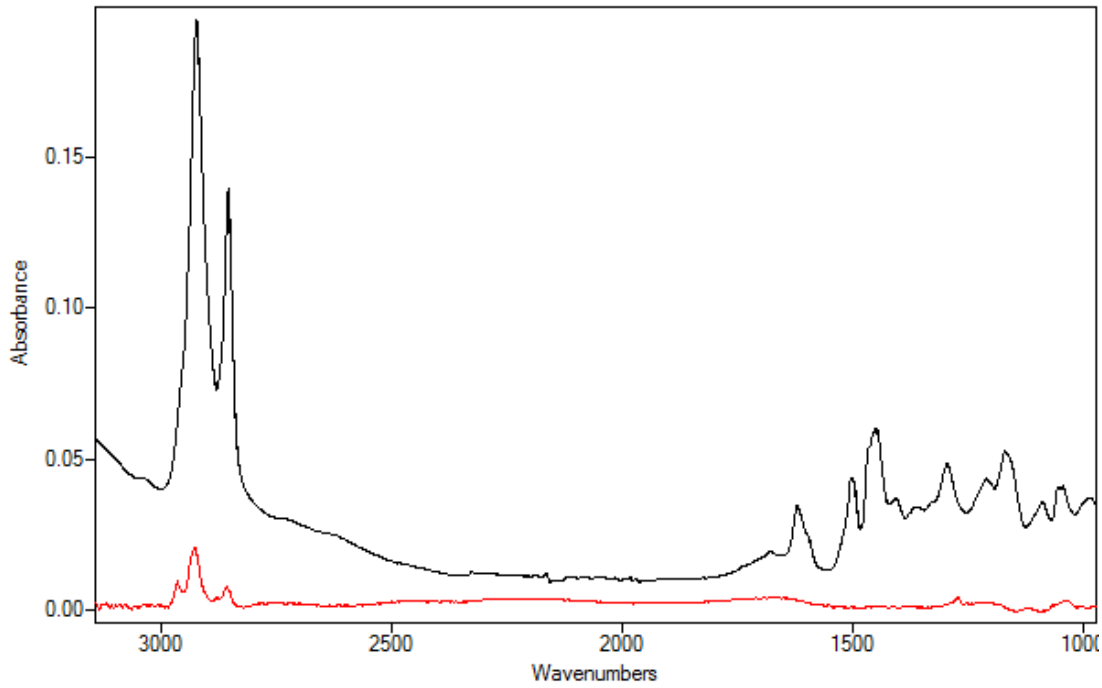

Figure 3.22 Overlaid FTIR Spectra. Red: PMIRRAS Spectrum of a Monolayer Formed From **20**. Black: FTIR Spectrum of the Bulk Material.

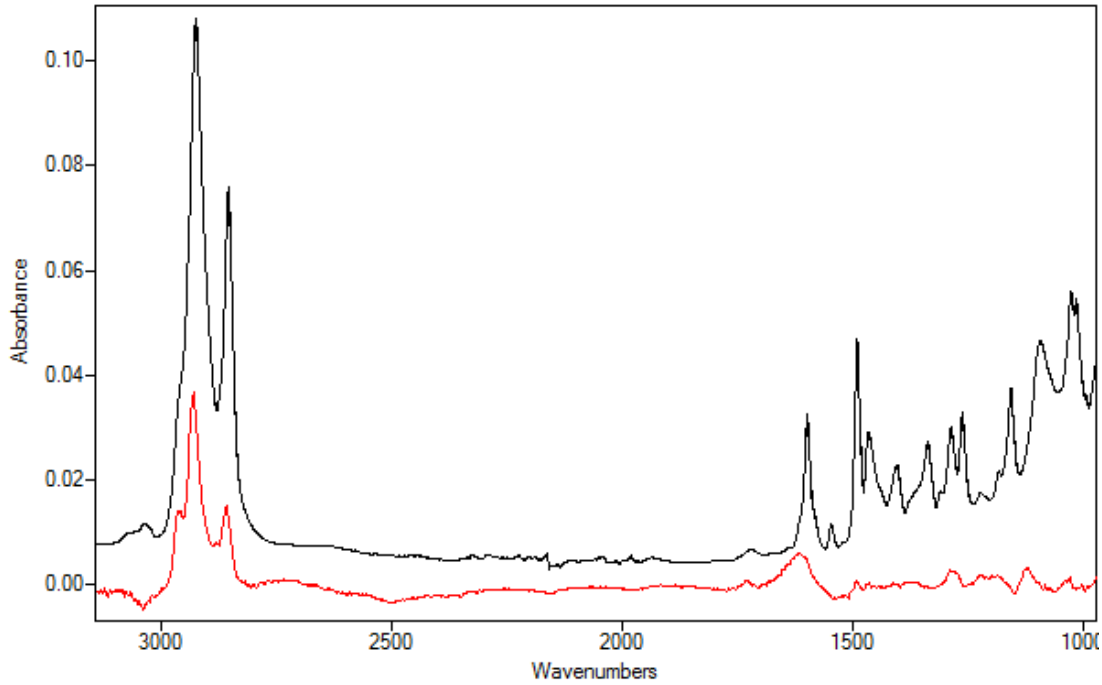

Figure 3.23 Overlaid FTIR Spectra. Red: PMIRRAS Spectrum of a Monolayer Formed From **7**. Black: FTIR Spectrum of the Bulk Material.

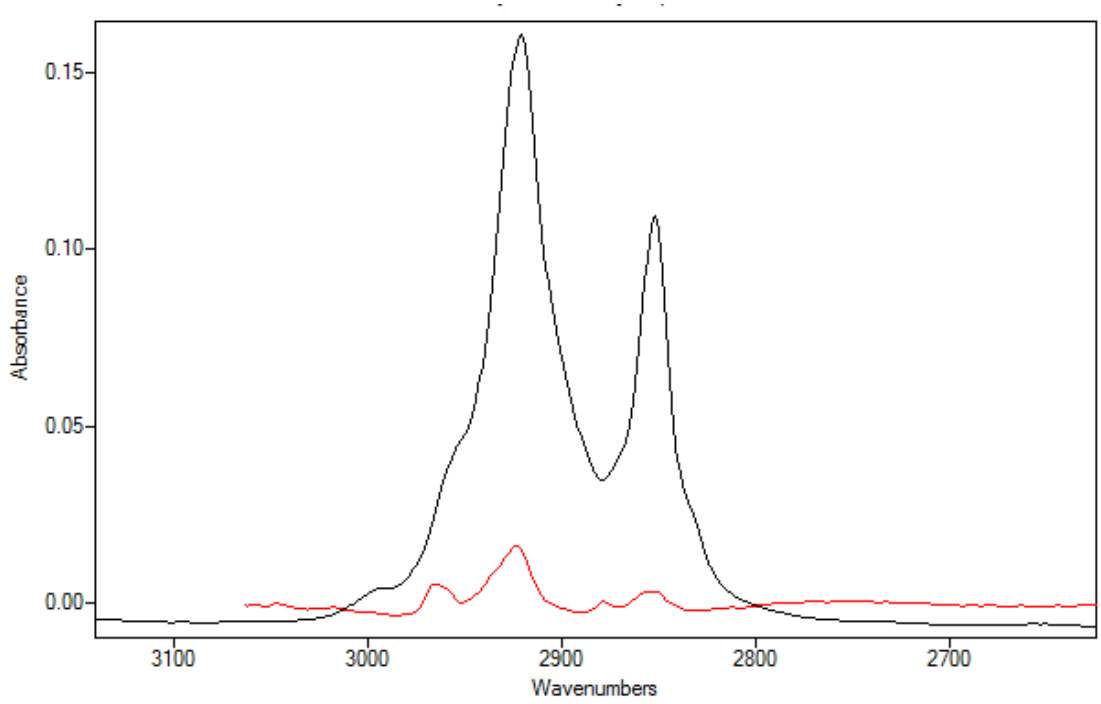

Figure 3.24 Expanded FTIR Spectra. Red: PMIRRAS Spectrum of a Monolayer Formed From **21**. Black: FTIR Spectrum of the Bulk Material.

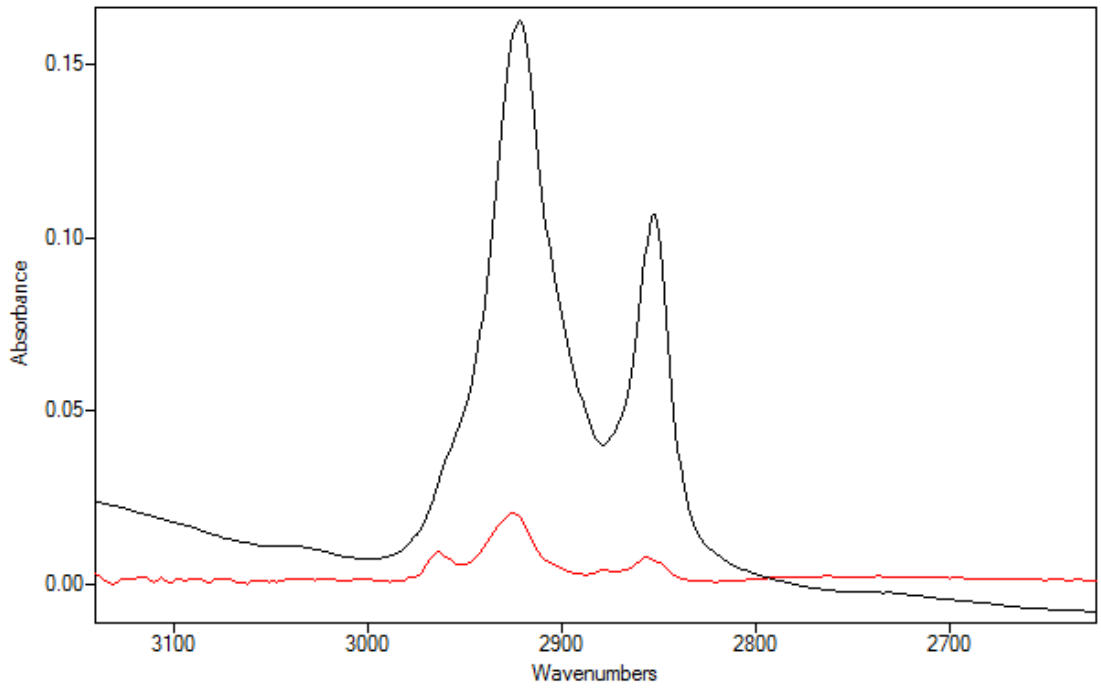

Figure 3.25 Expanded FTIR Spectra. Red: PMIRRAS Spectrum of a Monolayer Formed From **20**. Black: FTIR Spectrum of the Bulk Material.

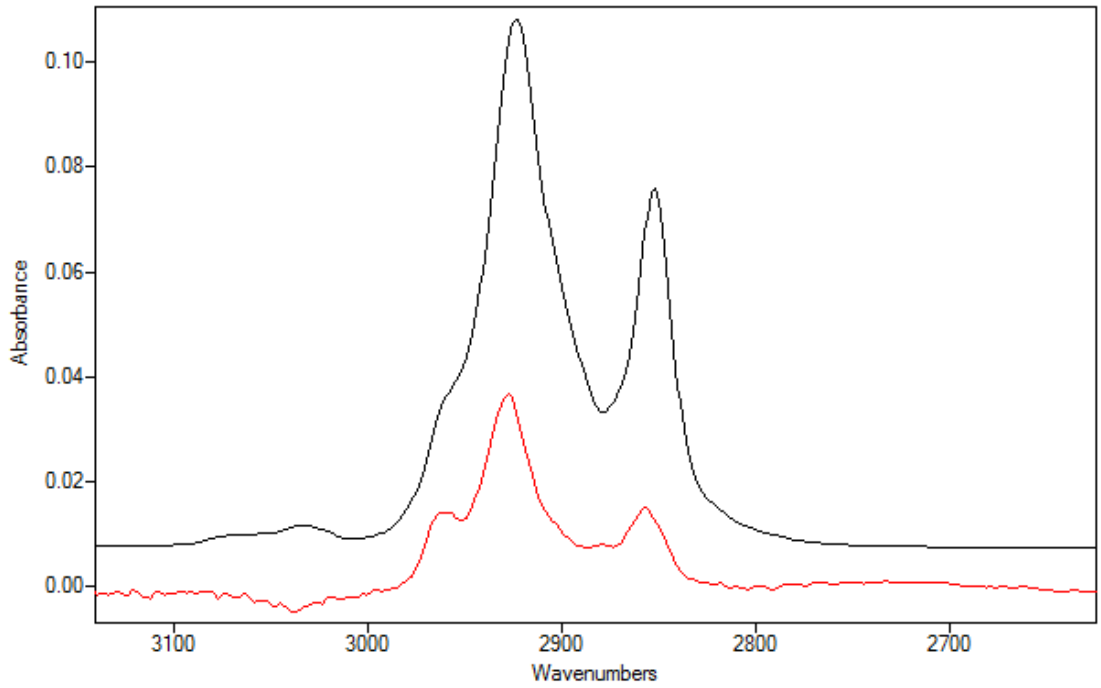

Figure 3.26 Expanded FTIR Spectra. Red: PMIRRAS Spectrum of a Monolayer Formed From **7**. Black: FTIR Spectrum of the Bulk Material.

The maximum absorbance values observed were similar for all spectra collected, suggesting that there was little variation in the density of the adsorbates on the surfaces. It is generally expected that multilayers would show increased absorbance,[152] however the monolayer of the hydroxyl resorcinarene decyl sulfide **20** exhibited the same absorbance as the other resorcinarenes. This appears to contradict the contact angle evidence for the presence of multilayers. This can be reconciled if the resorcinarene adsorbs as a bilayer or partial bilayer, as this can explain the contact angle data, yet the absorbance in the PMIRRAS spectrum would not be expected to increase drastically. This question could possibly be resolved by obtaining thickness data by ellipsometry or surface plasmon resonance if equipment access could be obtained in the future.

3.2.5 Atomic Force Microscopy Imaging

Imaging monolayers requires atomically flat substrates to ensure that any structure seen is actually due to the monolayer. Preparation of flat gold substrates is difficult and many methods have been reported in the literature, such as templating on mica with mechanical,[227] thermal,[228] and chemical stripping methods;[229] or growing single crystals from solutions of gold complexes.[230]

The preparation of substrates was attempted using several annealing and templating methods, however all were unsuccessful at producing substrates with adequate flat areas. Gold on glass substrates were purchased, and annealed using a butane flame following the manufacturer's instructions. These exhibited large flat terraces up to two micrometers in diameter (Figure 3.26), and atomic resolution images were obtained (Figure 3.27). These images were consistent with those published previously.[231]

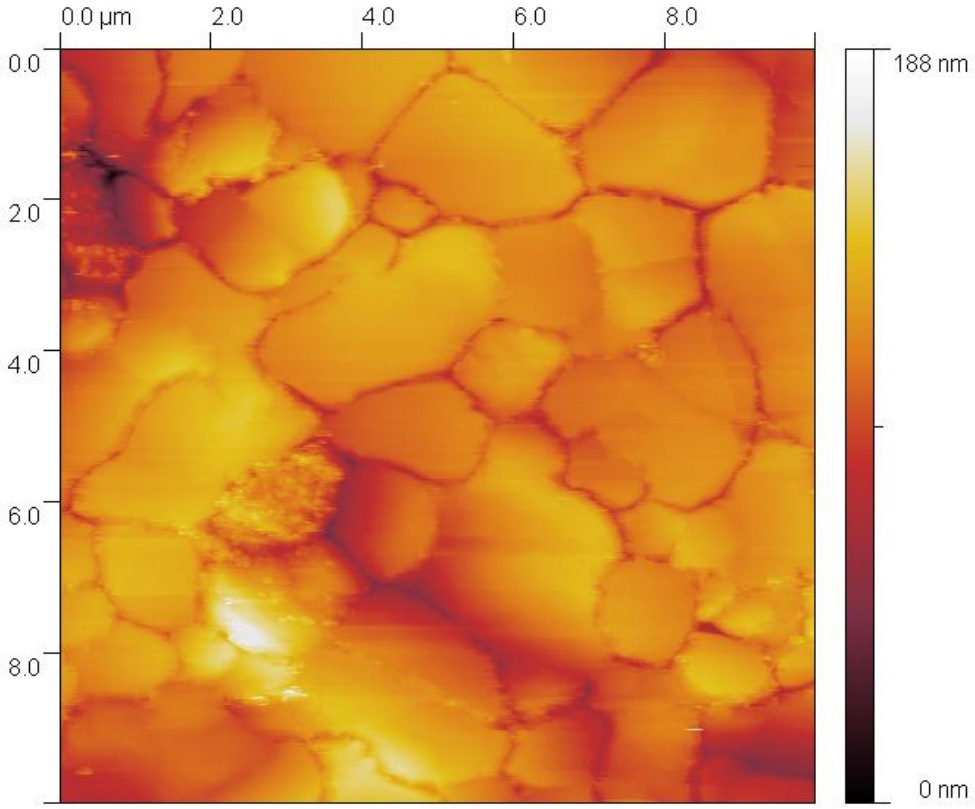

Figure 3.26 AFM Image of an Annealed Gold Substrate (10x10 µm)

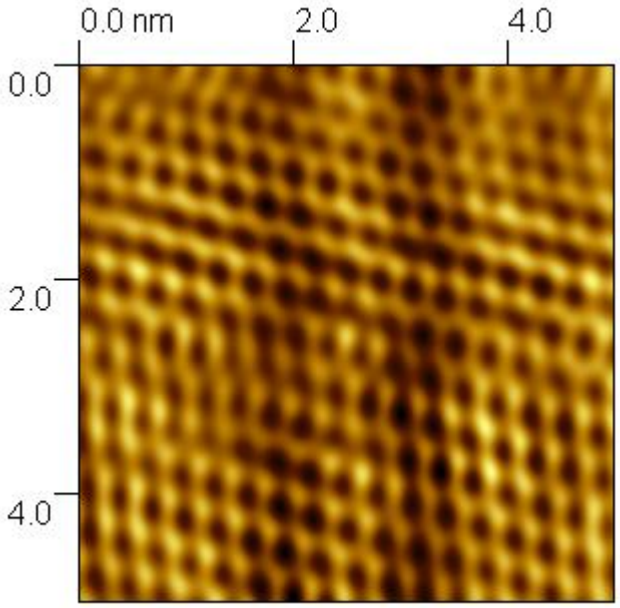

Figure 3.27 Atomic Resolution Image of the Gold Substrate (5x5 nm)

It was found by Barden *et al.*[232] that exposure to tetrahydrofuran led to the roughening of the gold surface. Although the monolayers imaged in this study were prepared using tetrahydrofuran, no similar deterioration was observed.

Scanning tunnelling microscopy (STM) has been used previously to image monolayers, however there is evidence that the perturbation of the gold is what is measured rather than the actual monolayer.[218] Atomic force microscopy (AFM) imaging is becoming common in order to ensure topographical information is measured.

STM images were obtained of monolayers of methoxy resorcinarene decylsulfide **21** by Raible *et al*.[209] Periodicies related to the size of the adsorbate were obtained (Figure 3.28). Attempts to replicate this work failed. The reason was not apparent, but may be contamination related, due to imaging in air rather than at ultra-high vacuum.

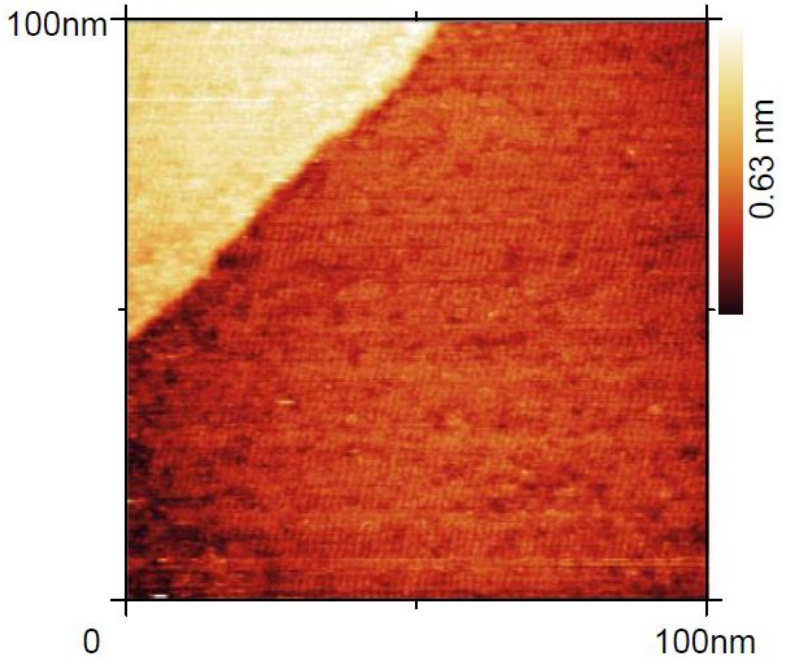

Figure 3.28 Literature STM Image of Methoxy Resorcinarene Decyl Sulfide **21**. With kind permission from Springer Science+Business Media: Applied Physics A-Materials Science & Processing, *Scanning tunneling microscopy on self-assembled calix 4 resorcinarene monolayer adsorbates on Au(111)*, 70(6), 2000, 607-611, Raible, Pfeiffer, Weiss, Clauss, Goepel, Schurig, Kern, Figure 3.

AFM imaging of the monolayers was found to be extremely difficult, due to the softness of the monolayer. Molecular resolution images were obtained of just one monolayer, the methoxy resorcinarene **9** (Figure 3.29).

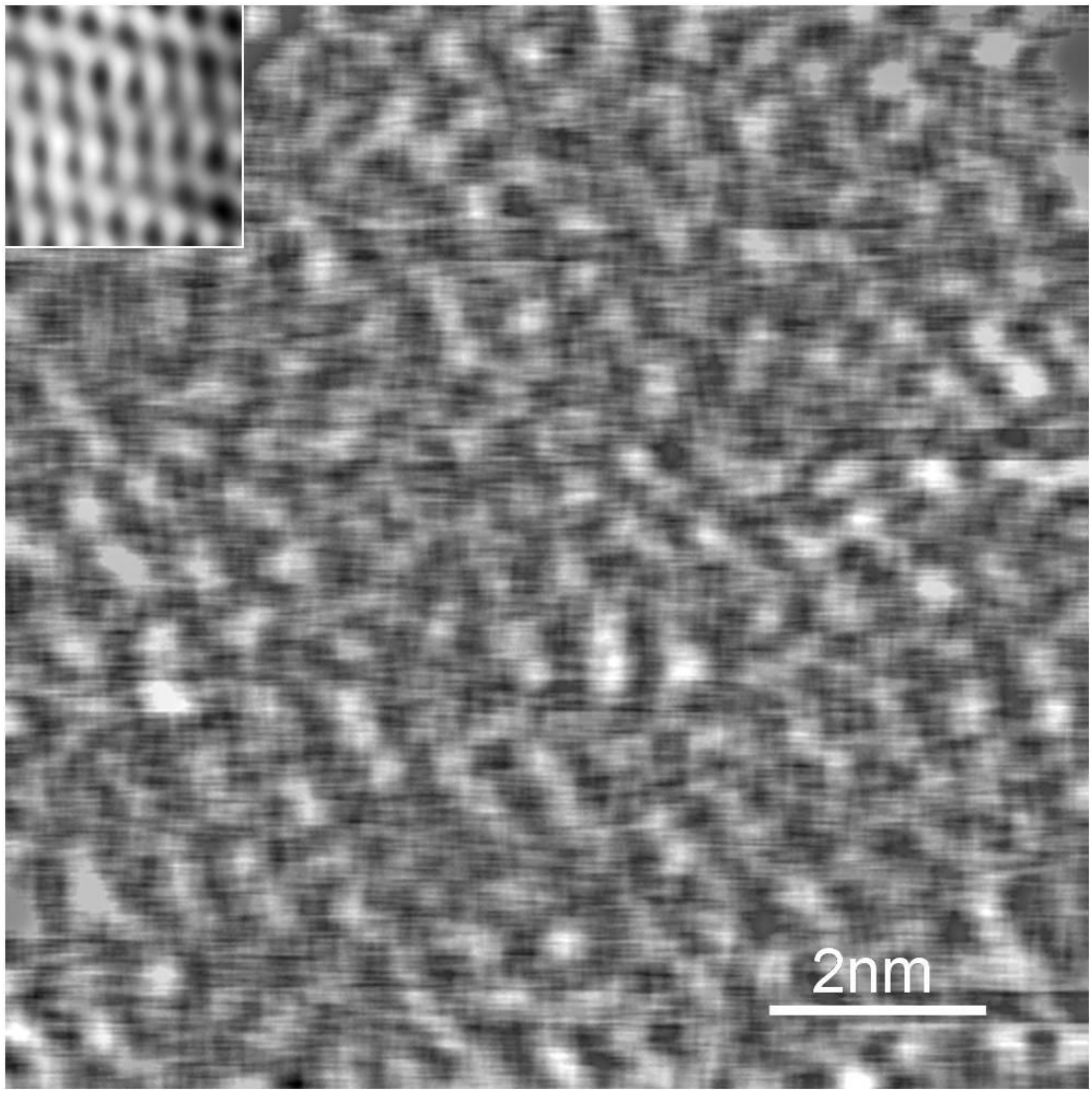

Figure 3.29 AFM Image of the Monolayer Formed From Methoxy Resorcinarene **9** (10x10 nm). Inset: AFM Image of the Gold Substrate (same scale, 2x 2 nm).

The image was obtained in non-contact mode, where the tip oscillates over the surface without contact. All attempts to image the monolayers using contact mode failed to achieve molecular resolution, most likely due to the flexibility of the monolayer.

Measuring sizes using scanning probe microscopy techniques is problematic as the tip geometry result in objects appearing larger than they are.[233] This is particularly true when imaging structures smaller than the tip radius, however peak to peak distances should not be altered (Figure 3.30).

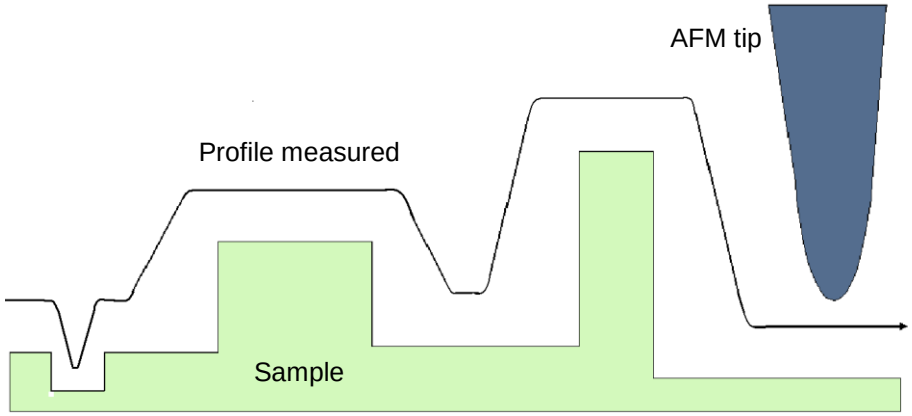

Figure 3.30 Representation of AFM Image Distortion Due to Tip Geometry.

The image of the monolayer of resorcinarene **9** is evidence that the monolayer is densely packed, however it is not ordered in a perfectly crystalline manner. The peak to peak distances observed in the image are consistent with the size of the resorcinarene headgroup in a boat conformation (0.8 nm separation between the vertical aromatic rings).

Schonherr *et al.*[150,208] were successful at imaging calixarene and methylene cavitand decyl sulfide monolayers using contact mode AFM (Figure 3.31). They observed two periodicies based on the force used for the resorcinarene monolayers. At low forces spacings corresponding to the size of the resorcinarene bowl were observed while at larger forces the packing of the alkyl chains was apparent. The alkyl chain spacing were also observed with large forces on the calixarene monolayer, however no resolved images could be obtained with low force.[208] This was attributed to the flexibility of the calixarene headgroup over the cavitand bowl, and is consistent with the difficulties encountered in this study.

The resorcinarene monolayers that have been previously studied by AFM have all contained relatively small alkoxy groups. The analogues used in this

study are larger (propyl, benzyl etc), and are likely to be disordered as they do not fill the space above the resorcinarene. This disorder may also partially explain the difficulty in obtaining images of some of the resorcinarene monolayers.

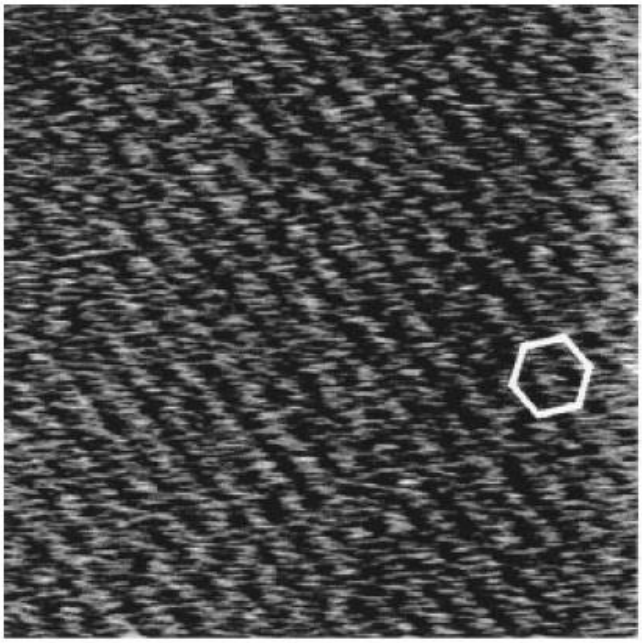

Figure 3.31 Literature AFM Image of a Methylene Cavitand Decyl Sulfide Monolayer at Low Force. Reprinted with permission from Langmuir, 13(6), Schonherr, Vancso, Huisman, van Veggel, Reinhoudt, An atomic force microscopy study of self-assembled monolayers of calix[4]resorcinarene adsorbates on Au(111), 1567-1570. Copyright 1997, American Chemical Society.

The deep cavity cavitand **7** was imaged by Menozzi *et al*.[157] in tapping mode as a mixed monolayer with alkane thiols (Figure 3.32). This study focused on forming coordination cages, and imaging the protrusions from the surrounding monolayer, but no images of single component monolayers of **7** were published.

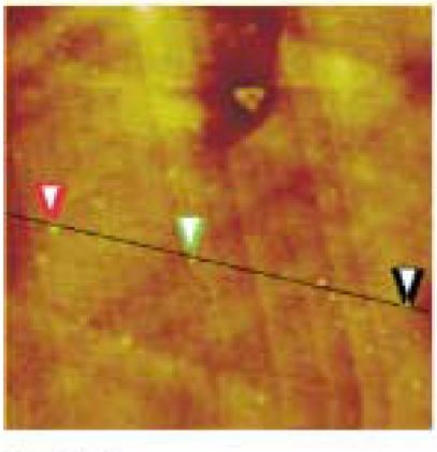

Figure 3.32 Literature Tapping Mode AFM Image of Mixed Monolayer of Cavitand **7** and 11-Mercaptoundecanol (arrows point to protruding cavitands). Menozzi, Pinalli, Speets, Ravoo, Dalcanale, Reinhoudt, *Surface-confined single molecules: Assembly and disassembly of nanosize coordination cages on gold (111)*, Chemistry – A European Journal, 10(9), 2199-2206. Copyright (2004) Wiley-VCH Verlag GmbH & Co. KGaA. Reproduced with permission.

3.2.6 Conclusion

Evidence was obtained to support the proposed structure of the resorcinarene monolayers.

The contact angle data indicate that the substrates were all more hydrophobic than clean gold, and the values were consistent with the proposed structure of the monolayers, with the exception of the hydroxyl resorcinarene **20** which appeared to have formed a multilayer.

The infrared spectra confirmed the presence of organic material, and provided orientation information for the calixarene monolayer (**18**/**19**) and the methoxy resorcinarene monolayer (**9**). The remaining monolayers only exhibited peaks in the C-H stretching region, however these were still consistent with the proposed structure.

Achieving molecular resolution of the monolayers using AFM was found to be extremely difficult, however an image of the methoxy resorcinarene monolayer (**9**) was obtained, and showed a densely packed monolayer showing some disorder.

3.3 Experimental

All glassware was annealed at 600 °C overnight, or cleaned with piranha solution (3:1 conc. sulfuric acid: 30% hydrogen peroxide) prior to use.

AR grade tetrahydrofuran was purchased from Sigma-Aldrich. AR grade ethanol was distilled in glassware cleaned with piranha solution prior to use.

3.3.1 Preparation of Substrates for Contact Angle Measurement and Infrared Spectroscopy.

Glass microscope slides were cleaned with ethanol, dried under nitrogen then cleaned in a UV/ozone cleaner for 20 min before being coated with 5 nm of chromium and 40 nm of gold at the Centre for Microscopy, Characterisation and Analysis, University of Western Australia.

3.3.2 Preparation of Substrates for Atomic Force Microscopy

Gold Arrandee substrates (gold on glass with a chromium adhesion layer, purchased from http://arrandee.com) were annealed with a butane flame prior to functionalisation.

3.3.3 Preparation of Monolayers

The gold substrates were cleaned in an UV/ozone cleaner for 20 min, and then soaked in an ethanol bath at room temperature for 30 min.

3.3.3.1 Preparation of Monolayers for Initial Contact Angle Experiments

Clean substrates were immersed in ethanol solutions (0.5 mM) of the macrocycles (**18**/**19** and **9**) at ambient temperatures for 18 hours. The substrates were rinsed with copious amounts of ethanol and dried under a stream of nitrogen.

3.3.3.2 Preparation of Monolayers for Final Contact Angle Experiments, Infrared Spectroscopy and Atomic Force Microscopy

Clean substrates were immersed in tetrahydrofuran solutions (0.5 mM) of the macrocycle at ambient temperatures for 8 days. Sulfuric acid (conc., 1 drop) was added to the thioacetate solutions immediately before immersing the substrate. The substrates were rinsed with copious amounts of tetrahydrofuran and dried under a stream of nitrogen.

3.3.4 Measurement of Contact Angles

Contact Angles were determined with a KSV CAM101 Contact Angle Goniometer. The contact angles of MilliQ water were measured. Digital images were taken of each drop and software used to fit the curve and calculate the left and right contact angles. At least 30 values were measured for each surface, with values calculated for several drops on duplicate surfaces.

3.3.5 Collection of Infrared Spectra

Grazing Incidence Reflectance Spectroscopy was performed on a Bruker IFS 66, with a liquid nitrogen cooled MCT detector. The spectrometer was purged with nitrogen gas.

Polarised modulation infrared reflection absorption spectroscopy (PMIRRAS) was performed on a Thermo Scientific Nicolet 6700 FT-IR spectrometer fitted with a Photoelastic Modulation (PEM) Module, with the help of Dr Matt Myers.

3.3.6 Atomic Force Microscopy Imaging

Atomic force microscopy images of the monolayers were obtained with a PicoPlus AFM system (Molecular Imaging/ Agilent Technologies, USA) with MikroMasch NSC 15/No Al tips, in non-contact mode.

Images of the gold substrates were obtained in contact mode using Veeco DNP-20 tips.

4.0 Host-Guest Chemistry of Self Assembled Monolayers

4.1 Introduction

Supramolecular chemistry is the study of systems with two or more components, held together by non-covalent intermolecular interactions.[106,234] The field was inspired by the highly specific biochemical interactions seen in nature, and the desire to imitate these with simpler artificial receptors.[72]

Host–guest complexes can be formed between ions or neutral molecules, and are held together by one or more of: electrostatic interactions, hydrogen bonds, π-π stacking, dispersion forces, acid/base interactions or solvophobic effects.

In order for complexation to occur, the guest must be complementary to the host in terms of size, shape and orientation of the binding sites. These parameters can be used to design appropriate receptors for guest molecules. Mecozzi and Rebek Jr[77] found that the binding affinity was greatest for guests that filled 55% of the host cavity, and the work of Gibb *et al*.[122] highlighted that the shape of the guest was important, especially for rigid hosts that cannot deform (i.e. cyclohexane is a better guest for deep cavitands than benzene as the planar structure doesn't fill the space adequately).

Pre-organisation is also an important factor in determining the affinity of a guest for a host, one example of this is the macrocyclic effect.[234,235] Less conformational change is necessary for a macrocycle to complex with a guest, compared to a linear host where the same binding sites are present, hence enhanced binding is observed.

A potential disadvantage of rigid pre-organised hosts is that they may have difficulty passing through the transition state of the complexation process,

resulting in slow binding kinetics. Conformationally mobile hosts exhibit more rapid exchange of guests.[234]

4.1.1 Techniques for Studying Complex Formation

Two aspects of the complexation phenomena are generally studied, the thermodynamic stability of the complex at equilibrium, and the kinetics of the complexation and decomplexation processes.

Nuclear magnetic resonance (NMR) studies can be used to determine association constants in solution (a measure of thermodynamic stability),[236-238] and with variable temperature capabilities, enthalpy and entropy values.[239] The kinetic stability can also be determined with NMR experiments.[111]

Other solution techniques to determine association constants include microcalorimetry,[240] isothermal titration calorimetry,[241] fluorescence titrations,[134] extraction experiments,[242] and high performance liquid chromatography.[243] The choice of technique depends on the properties of the molecules (solubility, fluorescence etc) and the magnitude of the binding.[234]

Gas phase interactions can be studied by mass spectrometry,[244] and solid state complexes can be studied by single crystal x-ray diffraction (XRD),[72] infra-red spectroscopy (IR),[245] or vapour sorption isotherms.[82]

4.1.2 Studying Complexation Phenomena in Monolayers

A significant portion of research into selective receptors is aimed at producing sensors. Often the apparatus used as the basis of the sensor can also be used to study the fundamental aspects of the complexation. Many sensor designs use monolayers or multilayers of the receptor as a sensitizing layer. Studying the receptor as a monolayer, rather than as a thin film, removes ambiguity from the data resulting from morphology differences introduced by film processing discrepancies.[246]

Techniques used to study the receptor properties of monolayers include quartz crystal microbalance (QCM),[71,247,248] surface acoustic wave (SAW),[61] surface plasmon resonance (SPR),[249] electrochemical techniques,[250] infra-red spectroscopy (IR),[152] and nanoparticle-based techniques.[148]

Studying the host properties of the receptors as a monolayer has a significant advantage in that the host does not need to be soluble in the solvent used. This can remove one of the hurdles to studying solvophobic driven complexation as the solubility of the guest in the desired solvent is often much higher than the host.

Atomic force microscopy (AFM) force spectroscopy can be used to directly probe the interaction of a guest and a surface, and is very useful in situations where the guest is not soluble to the necessary degree in the desired solvent. Although force spectroscopy is generally performed using an AFM, other techniques such as using optical or magnetic tweezers to manipulate particles/molecules have been developed, and are usually used for single molecule biophysics investigations.[251]

4.1.3 AFM Force Spectroscopy

AFM force spectroscopy is applied to investigate the interaction forces between a probe and a sample surface with pico-Newton sensitivity. Functionalised AFM tips can be used in order to study the interaction of different ‘probe’ molecules with a surface, including host-guest interactions if receptors are immobilised on the surface.[251]

A typical force curve (or force-distance curve, Figure 4.1) is measured by first approaching the surface with the tip (A). Once the tip is close enough to feel attractive forces it will ‘snap’ onto the surface (B). Further extension of the AFM z-scanner results in a linearly increasing deflection of the cantilever until, a pre-determined deflection, corresponding to a maximum load, is reached (C). During the retraction, the tip initially adheres to the sample (D),

then will ‘pull-off’ leading to a dislocation in the deflection signal, then will move away from the surface smoothly (E) unless further interactions are detected.

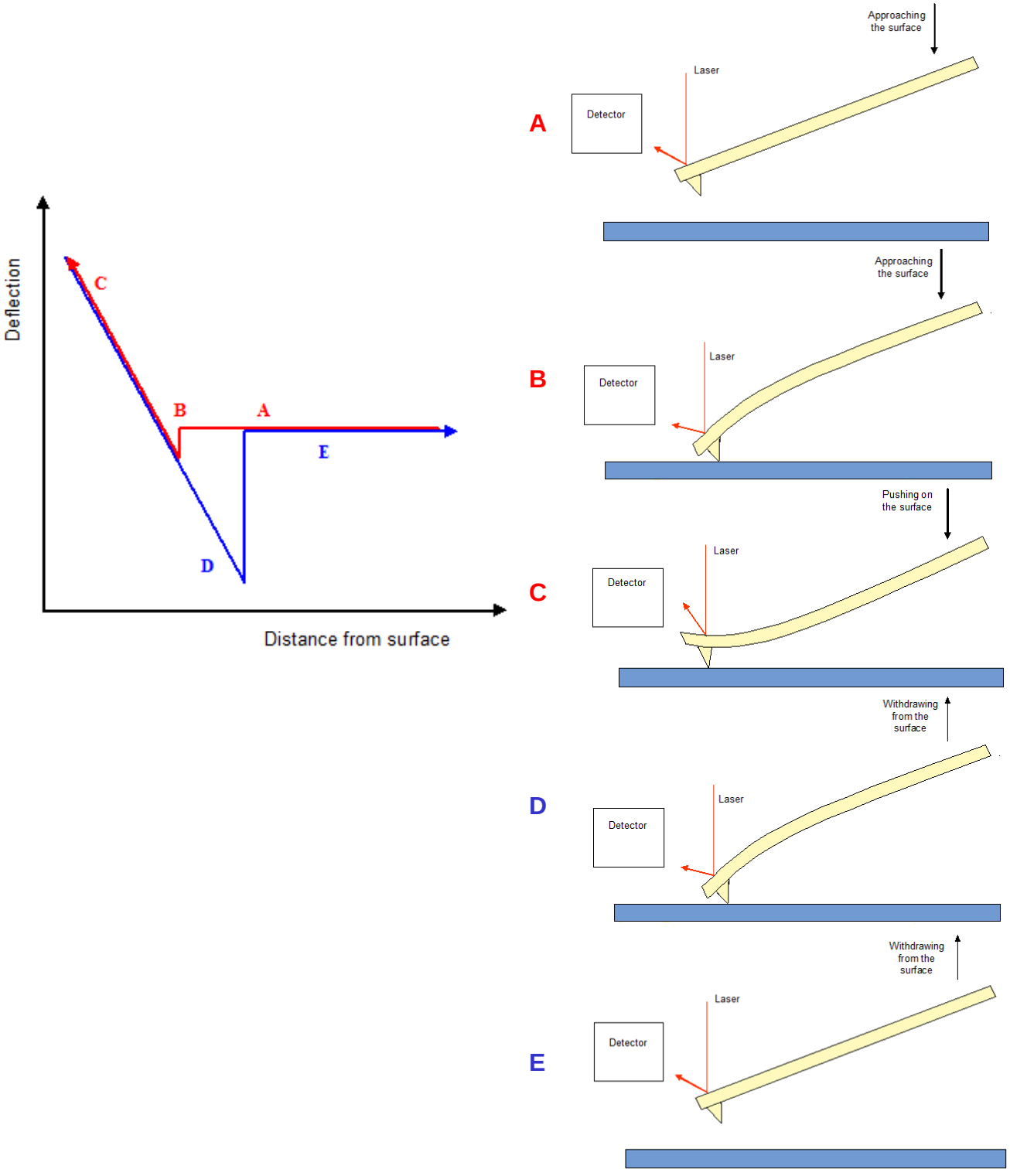

Figure 4.1 Idealised Force Curve, with a Representation of Corresponding Cantilever Positions During Measurement (not to scale). Red: Approach Curve Blue: Withdraw Curve

Force spectroscopy has been extensively applied to the study of biomolecules,[252,253] however there are only a few examples of the study of macrocycle interactions with small guests in the literature. Schonherr *et al*.[212,254,255] pioneered this area with a series of papers investigating the interaction between cyclodextrins immobilized on a gold substrate and AFM tips functionalised with ferrocene, adamantane and aromatic probes, and measured pull-off forces in the range of 40-100 pN in water. Eckel *et al*.[211] used the same technique to study the host-guest chemistry of calixarenes with ammonium ions. Longer tethers were used to attach the ions to the AFM tip, and single host-guest rupture events were observed at forces of approximately 100 pN in ethanol. This work has been followed by similar experiments with a UV switchable cavitand,[256] and a cucurbituril macrocycle.[257]

4.2 Discussion

4.2.1 Preparation of Functionalised AFM Tips

AFM tips functionalised with cyclohexyl, adamantyl and benzyl probes were prepared in order to study the affinity for these analytes with the receptor monolayers previously characterised in Chapter 3.

These probes were chosen as cyclohexane and adamantane were identified as ideal target analytes for the detection of seep oils (see Section 1.6). A benzyl analogue was also prepared in order to compare against the results obtained from the aliphatic compounds, as aromatic compounds are known to interact with resorcinarenes and calixarenes through π-π stacking and/or CH-π interactions (Figure 4.2).[68,258,259]

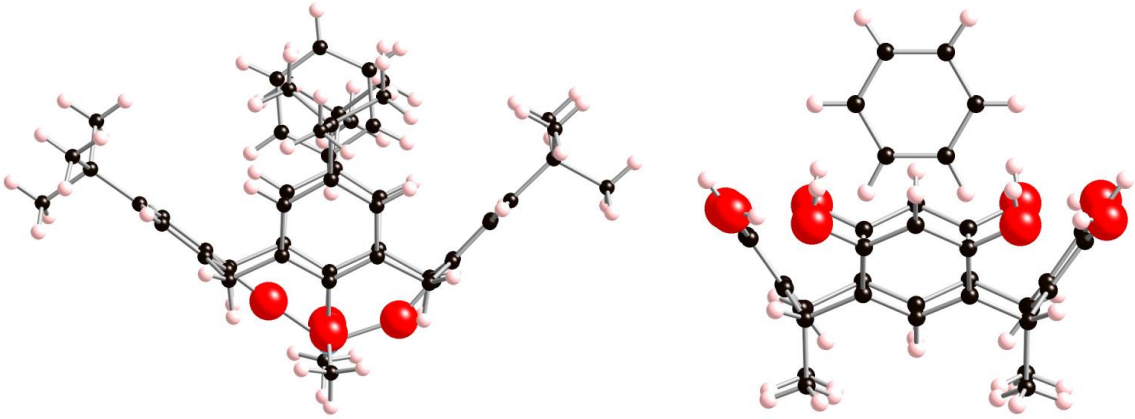

Figure 4.2 Crystal Structures of Benzene Complexes with a Calixarene Derivative (left),[260] and a Resorcinarene Derivative (right).[261]

4.2.1.1 Synthesis of Probes

The cyclohexyl **29**, benzyl **30**, and adamantyl **31** probes were prepared according to literature procedures (Scheme 13).[255,262,263] The amides **26**-**28** were formed by the reaction of bromovaleric acid with oxalyl chloride to form the acid chloride, followed by treatment with the appropriate amine. The

thioacetates **29**-**31** were prepared by reaction of the bromovaleric amides **26**-**28** with thioacetic acid in the presence of base. All compounds were adequately pure based on TLC and NMR after recrystallisation.

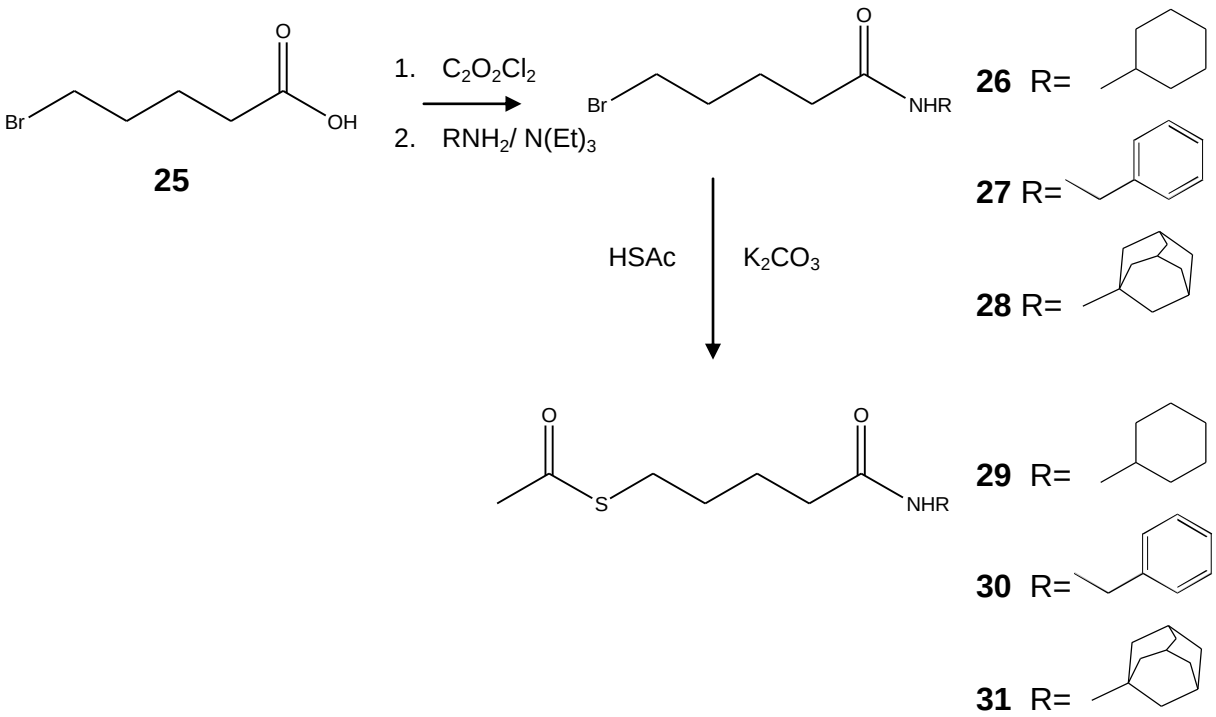

Scheme 13. Preparation of AFM Molecular Probes

4.2.1.2 Functionalisation of the AFM tips

Mixed monolayers of 2-mercaptoethanol and the probe were adsorbed onto clean gold coated AFM cantilevers.

The tips were cleaned using the same two step UV/ozone oxidation, ethanol reduction method as discussed previously (Section 3.2.1). Fujihira *et al.*[264] applied this method to AFM tips and found that tips modified after using this cleaning procedure exhibited the same tip characteristics as those modified immediately after gold deposition in the factory.

The protocol developed by Auletta *et al*.[255] was followed for the adsorption of the monolayers. Solutions with a total thiol concentration of 1 mM were prepared in ethanol. The probe to mercaptoethanol ratio was 1:99, and one drop of sulfuric acid was added to allow *in situ* hydrolysis of the thioacetate. The clean cantilevers were immersed in the solution for 24 hours before being rinsed with copious volumes of ethanol and dried in a gentle nitrogen stream.

This procedure had been found to lead to evenly distributed monolayers with no phase separation (or islands) of the two components on flat substrates.[255] It is assumed that this holds true on the AFM tips, however there are no techniques able to investigate this. This 'dilution' of the probe monolayer is necessary in order to prepare an AFM tip with a minimal number of probes at the apex (Figure 4.3).

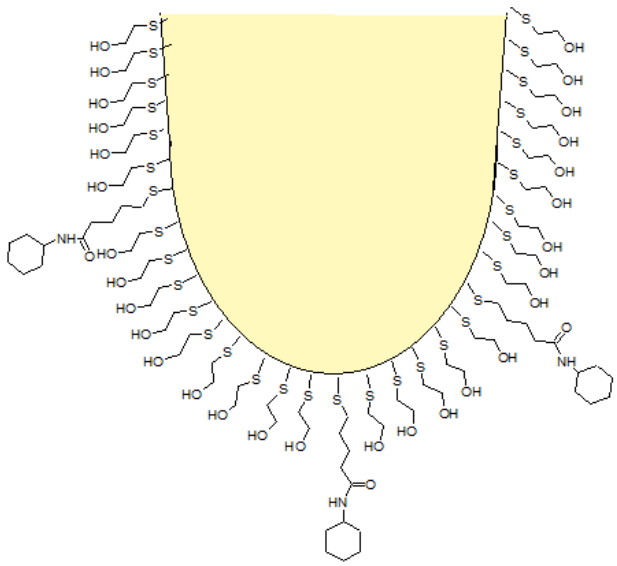

Figure 4.3 Pictorial Representation of the Mixed Cyclohexane Probe **29** Monolayer on an AFM Tip (not to scale).

4.2.2 Measuring Spring Constants

The spring constant of each cantilever is required to accurately convert the measured deflection values into forces. While values are given by the manufacturer, there is a wide range of error as it is difficult to precisely duplicate the dimensions when fabricating such a small object.

The spring constants of the cantilevers used were measured using the thermal tune method.[265] The values are estimated by measuring the cantilever fluctuations over time due to thermal noise. The software then fits a Lorentzian line shape to the frequency spectrum (Figure 4.4), and the spring constant is calculated.[265]

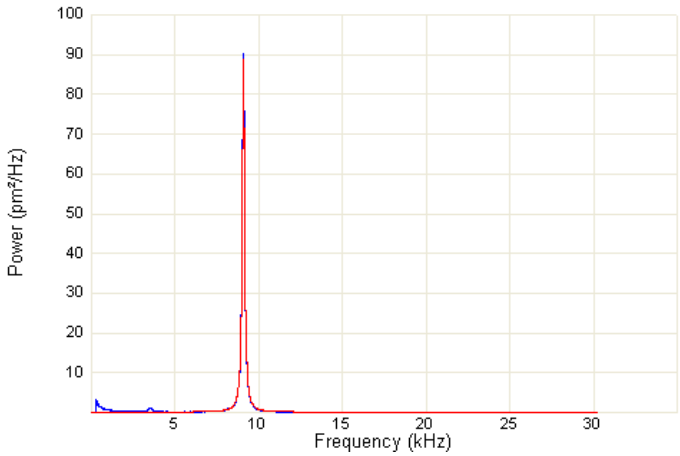

Figure 4.4 Example of the Data Obtained from a Cantilever Using the Thermal Tune Method. Blue: Experimental Data Red: Lorentzian Line Shape Fit Used to Calculate Spring Constant.

The spring constants were found to vary by up to 50% from the manufacturers specified value (0.2 N/m). Using the thermal tune method it was found that the spring constant of the cantilevers used in this work ranged from 0.10 - 0.35 N/m. However this is well within the error range specified by the manufacturer (0.07 - 0.4 N/m) and highlights the need to obtain more accurate values in order to meaningfully compare data obtained from different cantilevers.

The spring constants were measured both before and after functionalisation for three of the cantilevers used, and it was found that the values were between 1 and 13% smaller after functionalisation. The values used for all data processing were those measured after functionalisation.

4.2.3 Measuring Force Curves

Monolayers of the calixarenes **18**/**19** and the resorcinarenes **7**, **9**, **10**, **11**, **12**, **20**, and **21** (Figures 4.5-7), were prepared on flat gold substrates as previously described for AFM imaging in Sections 3.2.1 and 3.2.2.

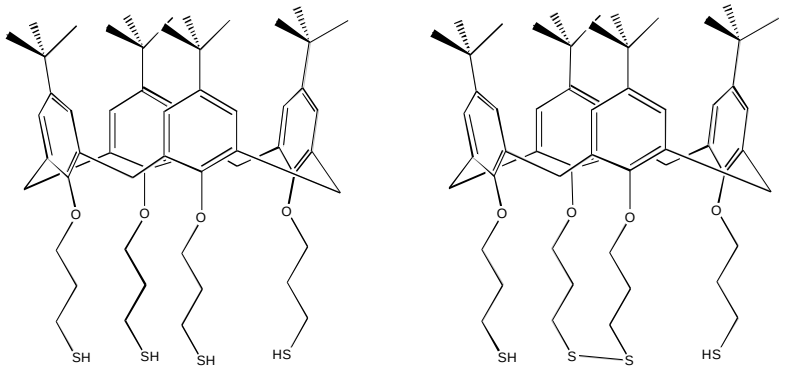

18 **19**

Figure 4.5 Calixarene Thiol/Disulfide Mixture **18**/**19**

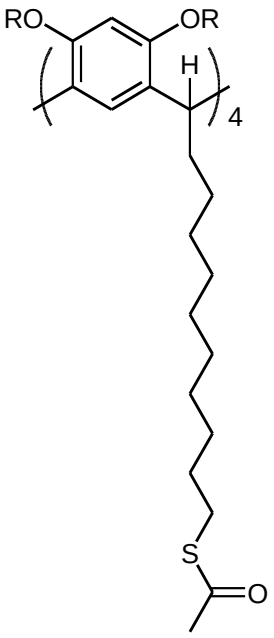

9 R = Me

10 R= Pr

11 R= Bn

12 R,R = CH_2

Figure 4.6 Thioacetyl Resorcinarenes

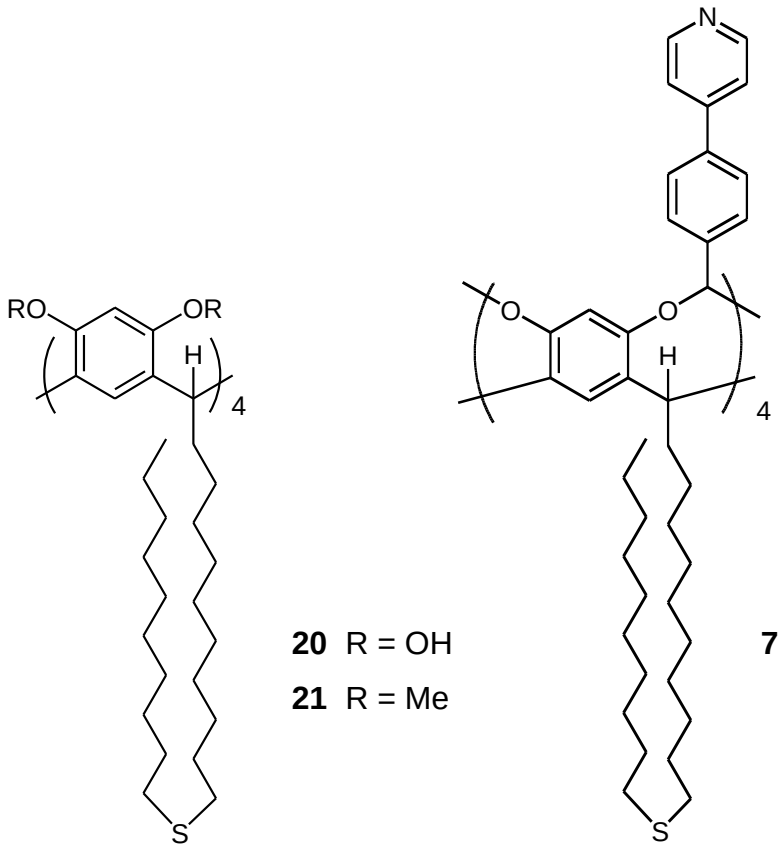

Figure 4.7 Decylsulfide Resorcinarenes

The force curves between each of the monolayers and the tips were measured in MilliQ water. This medium was used as the receptors were expected to bind the hydrocarbons of interest by a primarily hydrophobic mechanism, and the overarching goal is to develop a sensor for an aqueous environment. The *in situ* experiments also eliminate interference from capillary forces, due to water adsorbed on the tip and the sample under ambient conditions.

Duplicates of each sample surface were measured with three tips of each probe type. One thousand force curves were measured for each tip/surface combination in several locations on each surface. The raw deflection curves were converted to force distance data, and the adhesion forces extracted using a MatLab routine. An example of a processed force curve is shown in Figure 4.8.

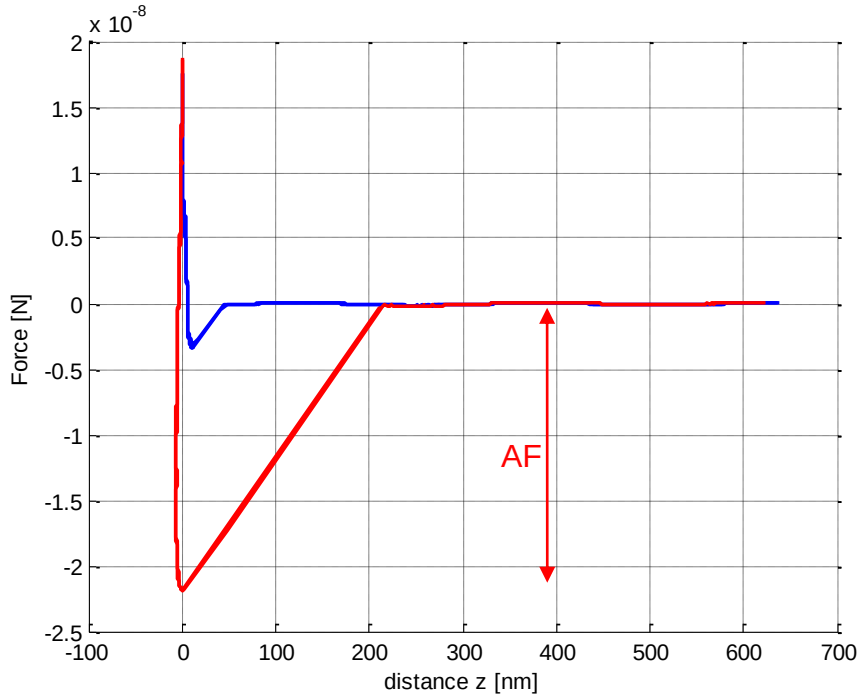

Figure 4.8 Processed Force Curve. blue: Approach Curve red: Withdraw Curve AF: Adhesion Force.

Initial experiments were undertaken to determine if the results obtained were dependant on the force applied to the surface (Figure 4.9). It was found that the adhesion force was independent of the deflection limit (proportional to the force applied to the surface).

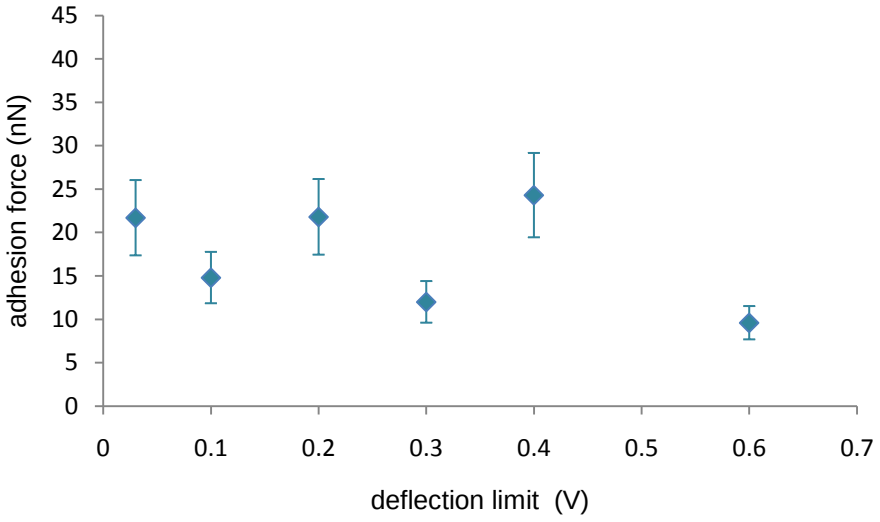

Figure 4.9 Effect of the Deflection Limit on the Adhesion Force.

A deflection limit of 0.4 V (equivalent to an applied force of approximately 2 nN depending on the spring constant of the cantilever) was used for all following experiments.

The length of the approach-withdraw cycle was also varied (Figure 4.10) in order to determine the effect of this parameter on the adhesion force measured. At very fast speeds, it initially appears that there is a trend of decreasing adhesion forces as the length of the cycle is decreased, however the differences are within the range of experimental error. A value of one second was used for all subsequent experiments.

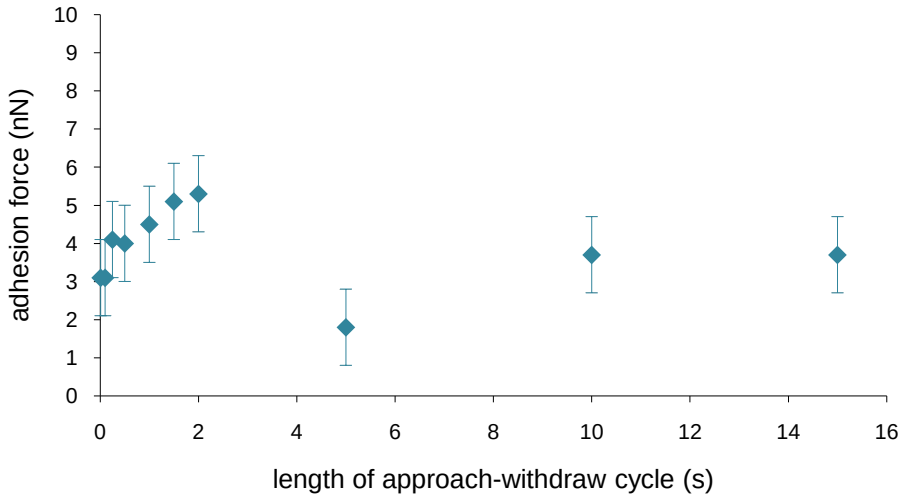

Figure 4.10 Effect of Measurement Speed on the Adhesion Force.

4.2.4 Reference Measurements

AFM tips functionalised with mercaptoethanol were prepared as a reference to compare to the probe functionalised tips. These measurements are not a true blank in the sense that the results obtained cannot be subtracted from the sample results, and it is possible for the reference adhesion forces to be larger than the forces due to the molecular probe.

The interpretation of the sample results in comparison to the reference data is not straightforward due to the different types of interactions involved. The reference tips are used to measure the adhesion force when there is no probe present. This interaction is a surface to surface adhesion as the apex

of the probe has a finite size (tip radius of <25 nm specified by the manufacturer), and the adhesion force is proportional to the area of the tip in contact with the monolayer sample surface. The interaction of the probe with the sample is a single molecule (or several molecules depending on the number present at the apex) adhering to the monolayer sample surface. Comparison of the sample values against these reference values allows the identification of data where it is likely that no probe interacted with the surface, or the interaction was very weak.

'Diluted' monolayers of the probes in mercaptoethanol are prepared to ensure that there are only small numbers of probe molecules present at the apex. As a consequence of this, it is possible that no probe may be present at the apex on some tips. Similar results are obtained if the interaction between the probe and the monolayer is smaller than the surface-surface adhesion force.

Probe-monolayer interactions will only be apparent if they are larger than the surface-surface adhesion force as both are present in each force curve measured. During each measurement the tip comes into contact with the surface. As it is withdrawn the surface-surface adhesion first needs to be overcome, before the probe-monolayer interaction is felt (as this occurs at a larger distance from the surface). If the interaction is stronger than the surface-surface interaction the cantilever will still be deflected toward the surface until a sufficient force has been applied (i.e. the cantilever has been moved far enough away) to rupture the bond. If the probe-monolayer interaction is smaller than the adhesion force this will be ruptured with the surface-surface adhesion and therefore give similar values to those observed for the reference tips.

This results in a 'detection limit' for molecular interactions using force spectroscopy. It may be possible to reduce this limit by reducing the surface-surface adhesion force, either by using sharper tips, or by using a thiol dilutant on the tip that has a lower affinity for the sample monolayer.

*4.2.5 Calixarene **18**/**19** Monolayer*

The data from the reference tips shows two peaks (Figure 4.11 a), one at approximately 2-3 nN and the other at 10-25 nN. Further examination reveals that the smaller force is exhibited by one tip, while the other two tips showed larger adhesion forces. This variation may be due to difference in the monolayer on the tip (perhaps caused by variations in the gold coating), however it is more likely that the difference is due to the area of the apex of the tip that is contacting the surface. All adhesion forces observed in the range of those obtained from the reference tips are ignored when considering the probe interactions.

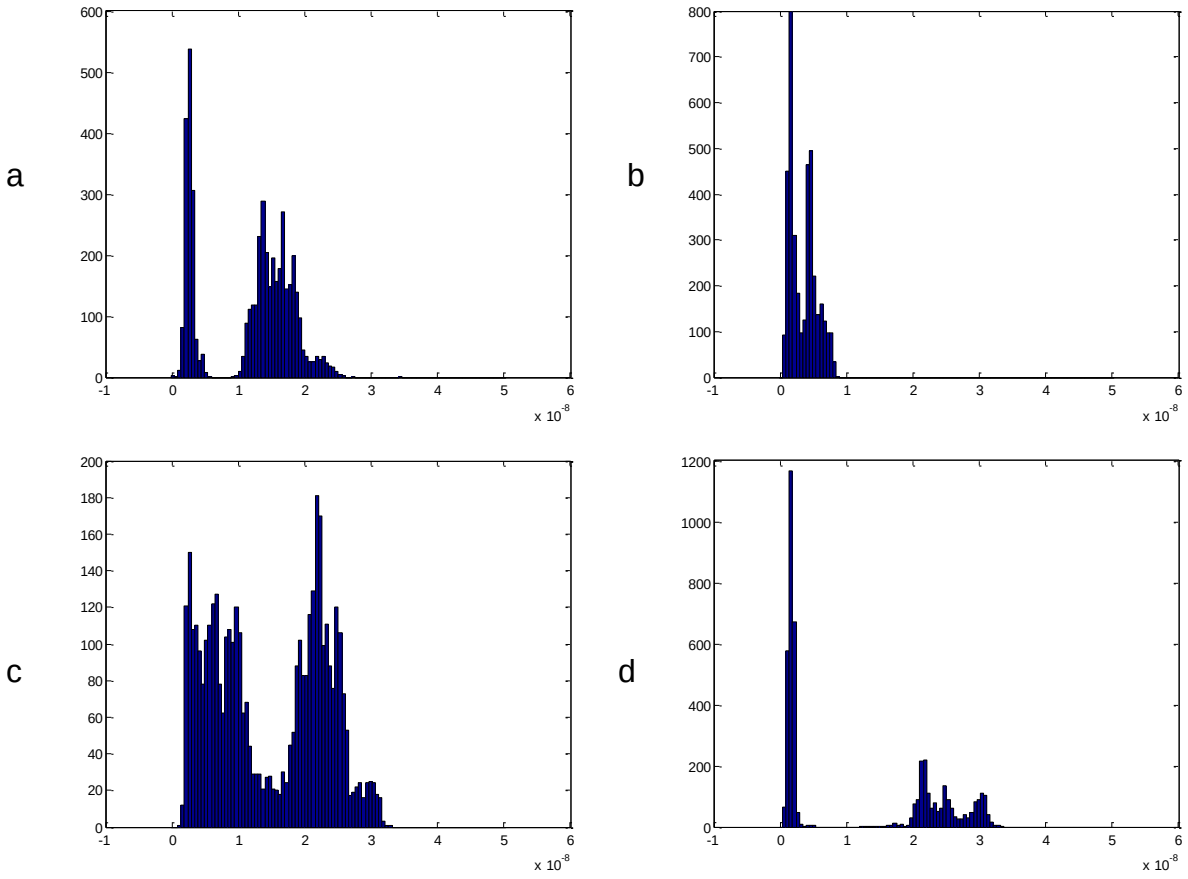

Figure 4.11 Histograms of the Pull-Off Forces Exhibited Between the Calixarene **18**/**19** Monolayers and the AFM Probes. a) Reference b) Cyclohexyl Probe c) Benzyl Probe d) Adamantyl Probe (x axis: Force ($x10^{-8}$ N))

The pull-off force between the cyclohexyl probes and the calixarene **18**/**19** monolayer was within the range of what was observed for the reference tips. Both the benzyl probes and the adamantyl probes exhibited forces larger than observed in the reference experiments with forces of 22 ± 4 nN and ~25 nN observed respectively.

The peak shape of the forces found using the benzyl probes is an approximately normal distribution, as would be expected for the forces arising from a specific interaction, such as host-guest complexation. The shape of the forces from the adamantyl probes is much more complicated and occurs in the range 15-33 nN. The shape suggests multiple overlapping peaks in this range, and may be caused by experimental noise, or a non-specific interaction with the surface. The data for this peak was obtained from one tip, and therefore the shape cannot be explained by tip variation.

*4.2.6 Methoxy Resorcinarene **9** Monolayer*

No interaction was observed with the adamantyl probes (Figure 4.12) and the methoxy resorcinarene **9** monolayer. An interaction with the cyclohexane probe was apparent at 31 ± 3 nN. Interactions with the benzyl probe were found to occur with adhesion forces of 29 ± 4 nN, 50 ± 4 nN, and 65 ± 3 nN. The interactions with the benzyl probes are roughly multiples of 16, this is consistent with multiple host guest interactions occurring as described by Auletta *et al*.[255] If this interpretation is correct than it can be inferred that the pull-off force for a single resorcinarene-benzyl probe complex is approximately 16 nN but is obscured by the surface adhesion force.

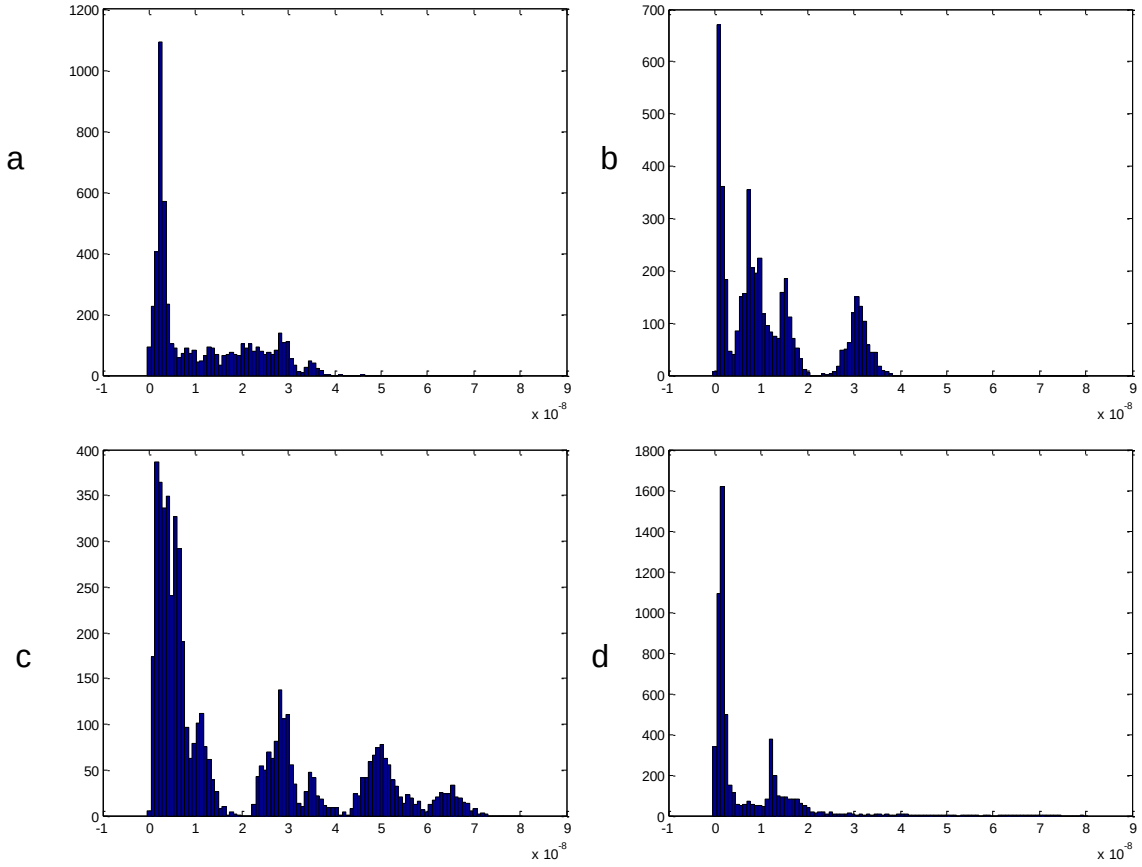

Figure 4.12 Histograms of the Pull-Off Forces Exhibited Between the Methoxy Resorcinarene **9** Monolayers and the AFM Probes. a) Reference b) Cyclohexyl Probe c) Benzyl Probe d) Adamantyl Probe (x axis: Force ($x10^{-8}$ N))

*4.2.7 Propoxy Resorcinarene **10** Monolayer*

There are two different interactions visible between the benzyl probe and the propoxy resorcinarene **10** monolayer, 26 ± 3 nN, and 37 ± 4 nN (Figure 4.13). These peaks appear to follow a normal distribution and are relatively narrow. If these correspond to multiple complexation events as previously proposed for the methoxy resorcinarene **9** monolayer (Section 4.2.6), then the single complexation event would have a rupture force of approximately 13 nN. No specific interactions were observed between the monolayer and the cyclohexyl or adamantyl probes.

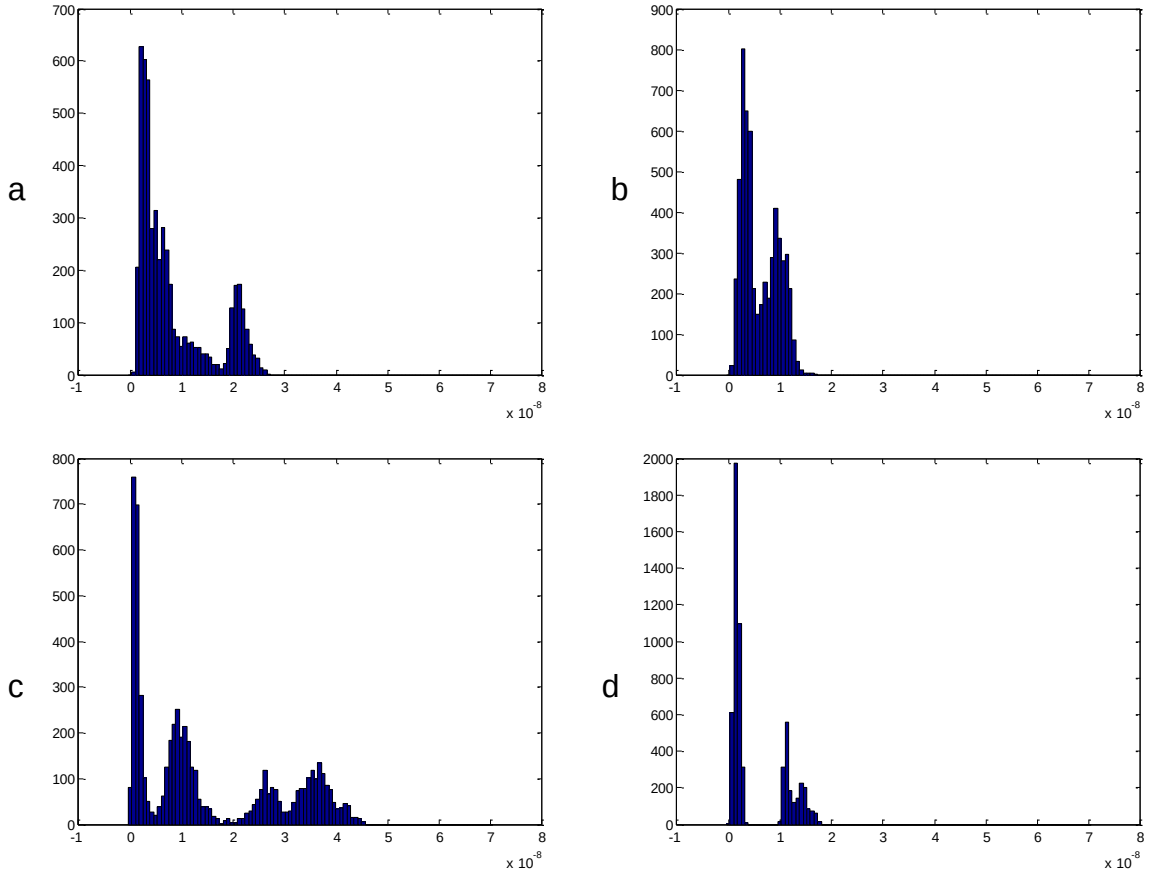

Figure 4.13 Histograms of the Pull-Off Forces Exhibited Between the Propoxy Resorcinarene **10** Monolayers and the AFM Probes. a) Reference b) Cyclohexyl Probe c) Benzyl Probe d) Adamantyl Probe (x axis: Force ($x10^{-8}$ N))

*4.2.8 Benzyloxy Resorcinarene **11** Monolayer*

Forces arising from the interaction of the benzyloxy resorcinarene **11** monolayer and the cyclohexyl, benzyl and adamantyl probes were observed at 26 ± 1 nN, 23 ± 2 nN, and 19 ± 1 nN respectively. All peaks were relatively narrow with an approximately normal distribution suggesting that they arise from specific interactions between the probes and the monolayer.

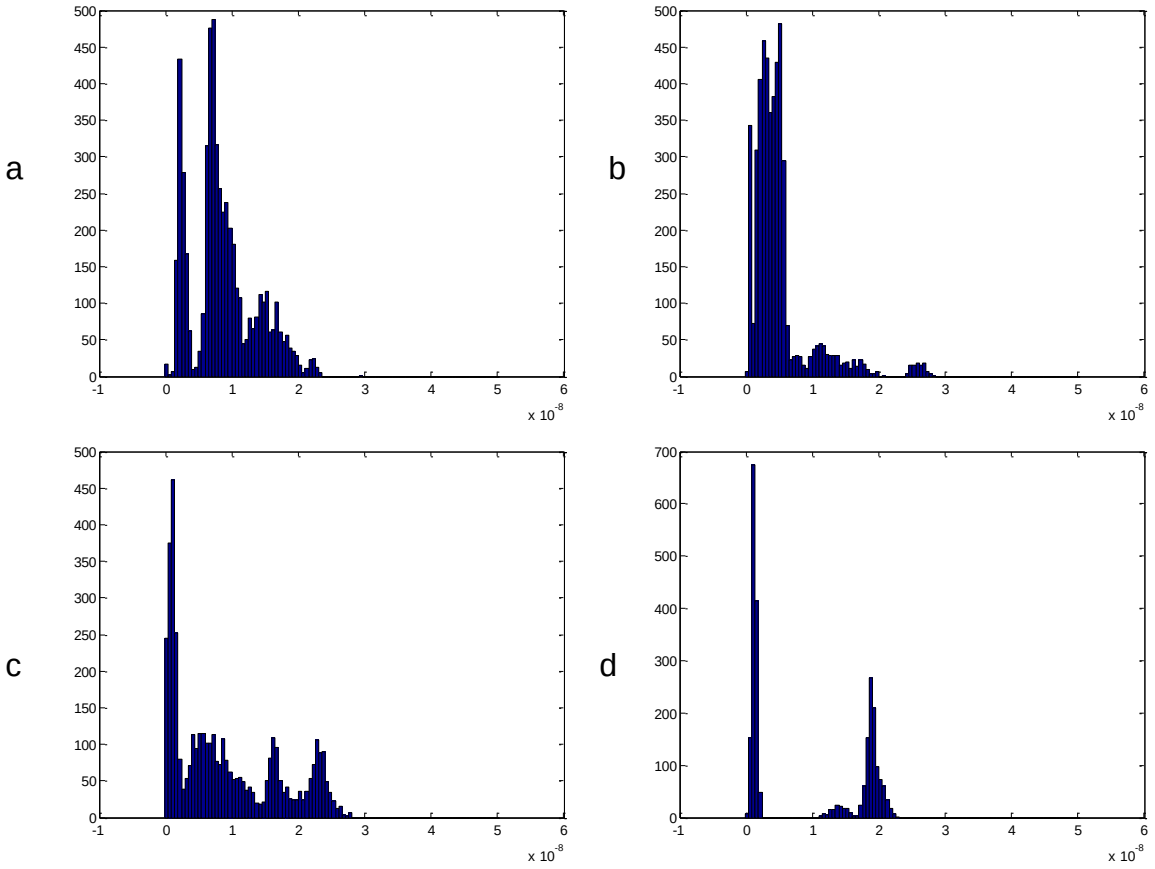

Figure 4.14 Histograms of the Pull-Off forces Exhibited Between the Benzyloxy Resorcinarene **11** Monolayers and the AFM Probes a) Reference b) Cyclohexyl Probe c) Benzyl Probe d) Adamantyl Probe (x axis: Force ($x10^{-8}$ N))

*4.2.9 Methylene Cavitand **12** Monolayer*

The largest interaction between the methylene cavitand **12** monolayer was found to be with the benzyl probe with a force of 37 ± 5 nN (Figure 4.15). This was followed by the interaction with the adamantyl probe at 23 ± 2 nN, and a possible interaction with the cyclohexyl probe at 21 ± 2 nN. All of the peaks were quite broad in comparison to those seen for other monolayers and may be indicative of non-specific interactions, which is not surprising due to the shallowness of the cavitand bowl.

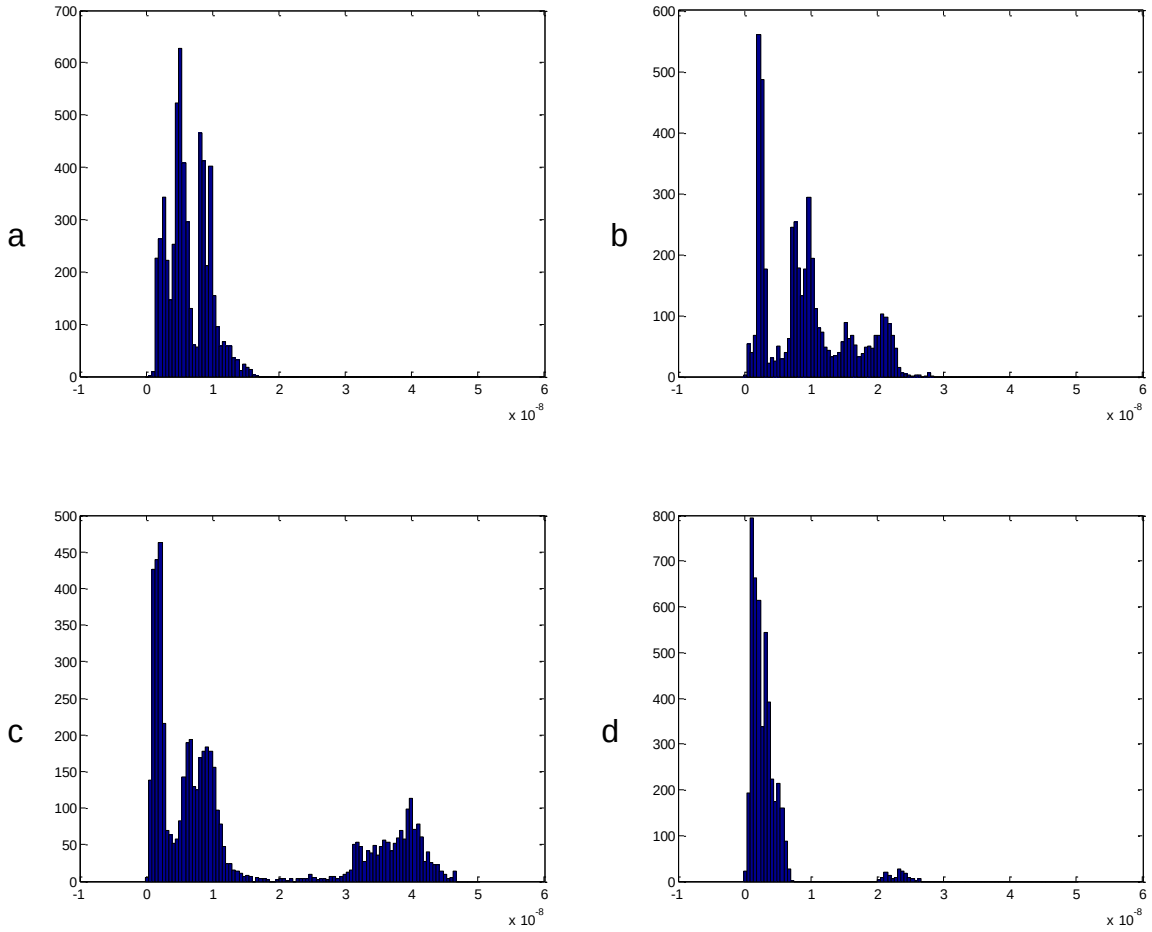

Figure 4.15 Histograms of the Pull-Off Forces Exhibited Between the Methylene Cavitand **12** Monolayers and the AFM Probes. a) Reference b) Cyclohexyl Probe c) Benzyl Probe d) Adamantyl Probe (x axis: Force ($x10^{-8}$ N))

*4.2.10 Deep Cavitand **7** Monolayer*

It was anticipated that the deep cavitand **7** may show enhanced interaction with adamantane based on its structural similarity to cavitands that form complexes with adamantyl derivatives in solution.[88,90,117] This was not observed (Figure 4.16), nor was any interaction observed with the cyclohexyl probe even though cyclohexanes are also known to form complexes with similar types of deep cavitands.[86] There was an interaction between the cavitand surface and the benzyl probe measured at 27 ± 2 nN.

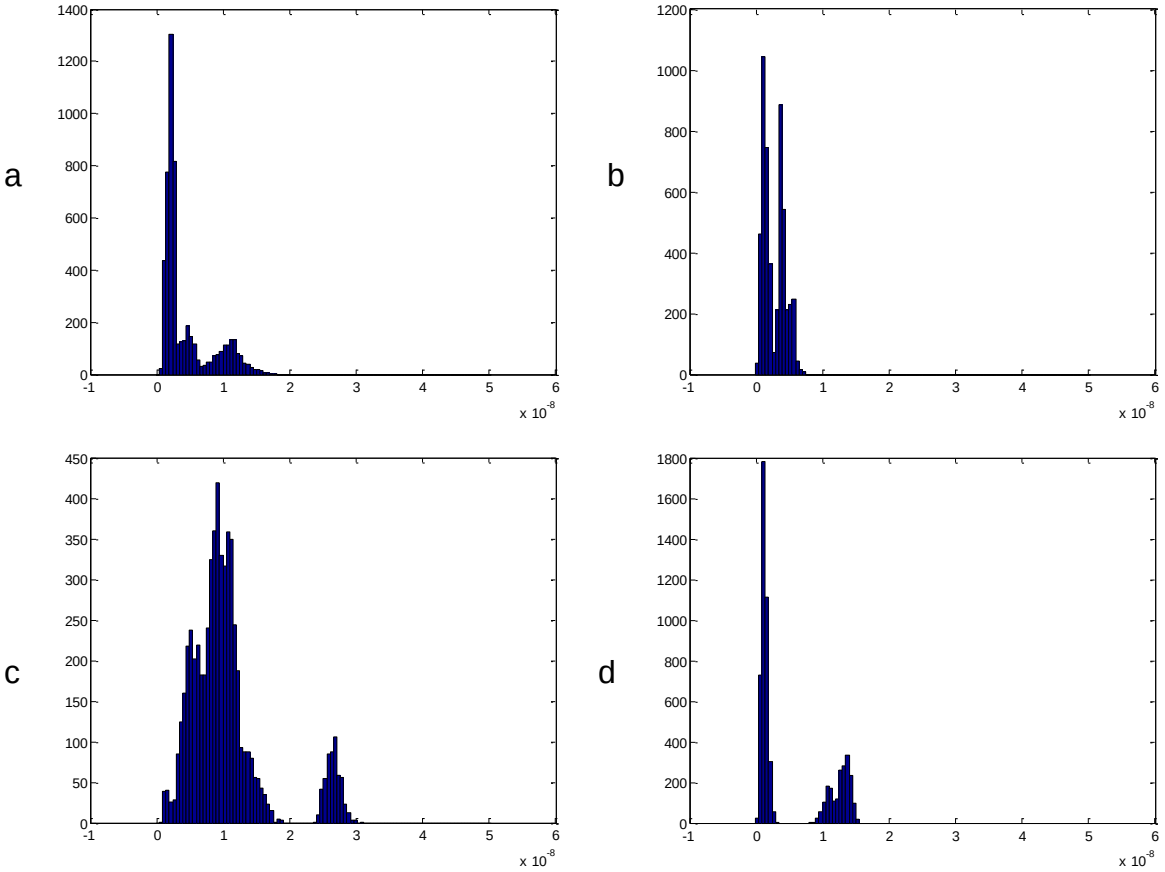

Figure 4.16 Histograms of the Pull-Off Forces Exhibited Between the Deep Cavitand **7** Monolayers and the AFM Probes. a) Reference b) Cyclohexyl Probe c) Benzyl Probe d) Adamantyl Probe (x axis: Force ($x10^{-8}$ N))

The unexpected binding behaviour of the cavitand **7** monolayer may be due to the conformation of the cavitand on the surface. The phenylpyridine groups can rotate with respect to the cavity, altering the shape and size of the binding site. No information was obtained on the orientation of the phenylpyridine bridging groups (Chapter 3), and if they are oriented perpendicular to the axis of the methine bridge, the cavity is relatively small.

*4.2.11 Resorcinarene Decylsulfide **20** Monolayer*

The interpretation of the interactions with the resorcinarene decylsulfide **20** surface is difficult, as characterisation of the surface (Chapter 3) revealed

evidence that the resorcinarene was present on the surface as a disordered bilayer or multilayer. It has been suggested in the literature that the resorcinarenes will pack 'head to head' with intermolecular hydrogen bonds between the phenol groups.[152] The contact angle data suggests that the surface is largely hydrophobic (Section 3.2.3), which is consistent with the alkyl groups lying at the surface.

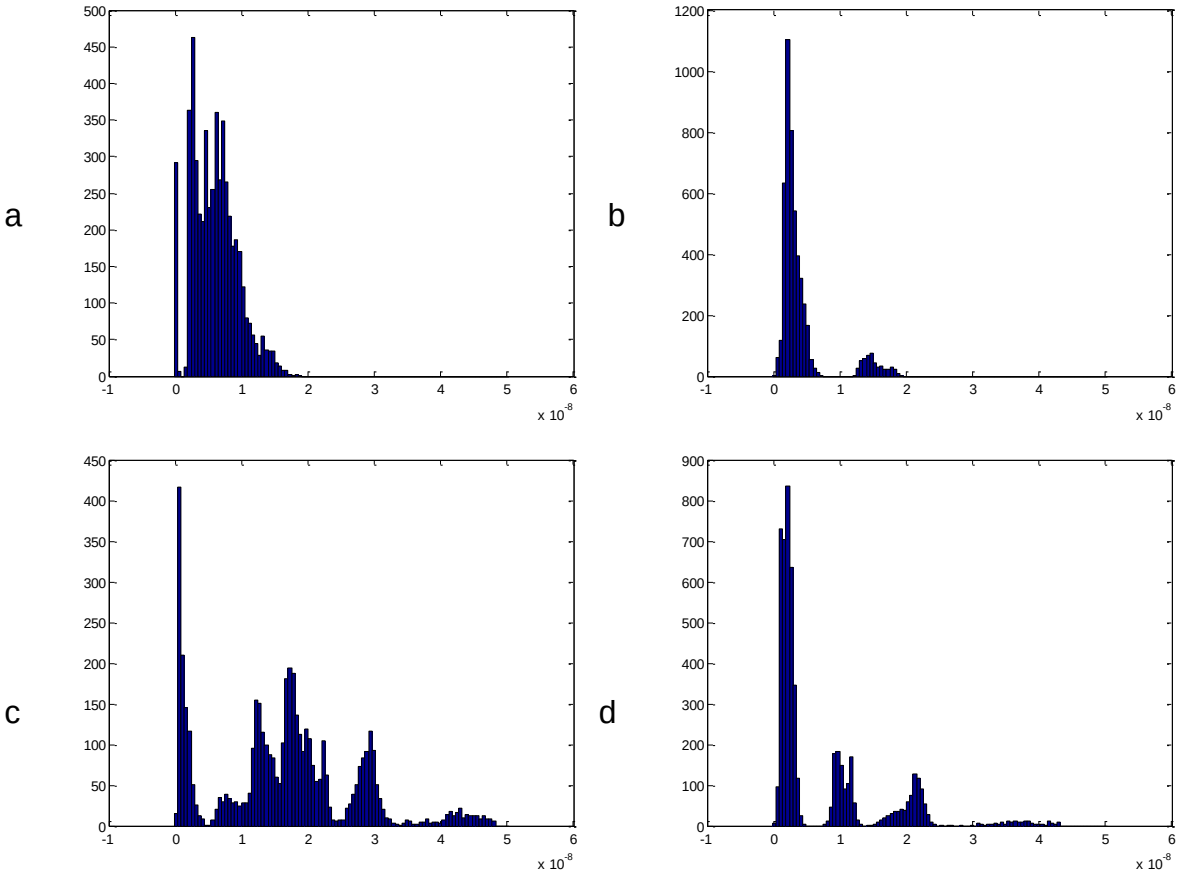

Figure 4.17 Histograms of the Pull-Off Forces Exhibited Between the Resorcinarene Decylsulfide **20** Multilayers and the AFM Probes. a) Reference b) Cyclohexyl Probe c) Benzyl Probe d) Adamantyl Probe (x axis: Force (x10^{-8} N))

This surface structure makes it unlikely that any specific complexation phenomena would be observed, and that the adhesion forces observed between the benzyl and adamantyl probes and the surface (Figure 4.17) probably arise from non-specific hydrophobic interactions. Despite this, narrow peaks are observed for the benzyl and adamantyl probes, along with the expected broad peaks. It is unknown whether immersion in water causes

the surface to rearrange, or the secondary layers to be removed, so further information is needed to draw any useful conclusions from the data.

*4.2.12 Methoxy Resorcinarene Decylsulfide **21** Monolayer*

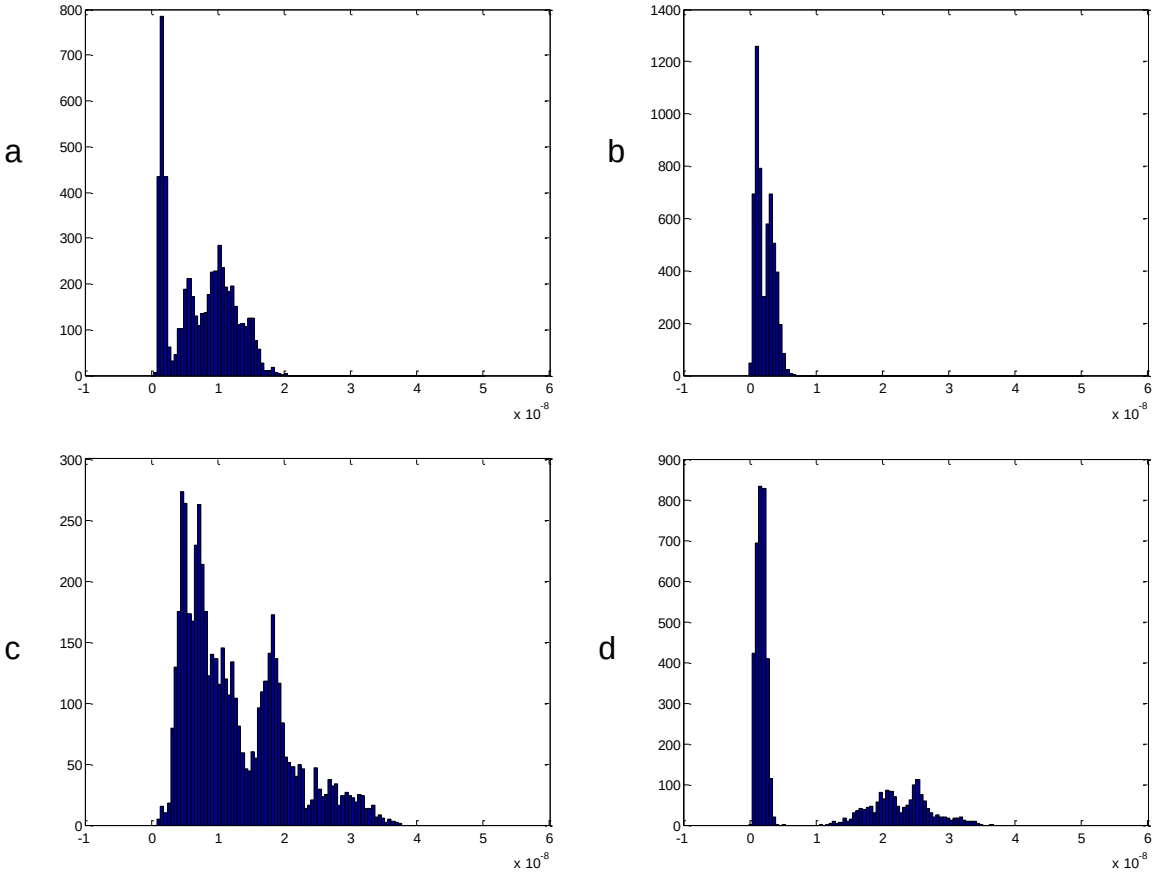

Figure 4.18 Histograms of the Pull-Off Forces Exhibited Between the Methoxy Resorcinarene Decylsulfide **21** Monolayers and the AFM Probes. a) Reference b) Cyclohexyl Probe c) Benzyl Probe d) Adamantyl Probe (x axis: Force ($x10^{-8}$ N))

An adhesion force of 23 ± 5 nN was observed between the adamantyl probe and the methoxy resorcinarene decylsulfide **21** monolayer. The benzyl probe exhibited a similarly broad peak at 28 ± 4 nN, along with a sharper peak at 18 ± 2 nN. This peak is on the borderline of the region in which the surface adhesion forces are located, however the narrow peak shape indicates that the force may be due to a specific complexation event.

The differences between the adhesion forces observed between the methoxy resorcinarene decylsulfide **21** monolayer and the methoxy resorcinarene **9** monolayer (Section 4.2.6) are pronounced, despite the identical resorcinarene headgroups. This contradicts the hypothesis that the resorcinarene cavity is the primary factor determining the binding of guests to the monolayer and suggests that the structure of the monolayer is also a contributing factor in determining binding affinities.

4.2.13 Comparison of Reference Adhesive Forces

The adhesion force of the reference tips varies significantly between the different monolayers. The maximum adhesion force ranges from 16 nN for the methylene cavitand **12** monolayer to 37 nN for the methoxy resorcinarene **9** monolayer. The number of force curves that exhibit these large forces is quite small, and the data shows the typical force for this adhesion on all samples is 3-5 nN, with some samples exhibiting another peak at 10-20 nN.

4.2.14 Comparison of Cyclohexyl Probe Interactions

Only three of the monolayer samples exhibited measurable interactions with the cyclohexyl probes. The methoxy resorcinarene **9** monolayer showed an interaction at 31 ± 3 nN, while the benzyloxy resorcinarene **11** monolayer showed an interaction at 26 ± 1 nN, and the methylene cavitand **12** monolayer showed a possible interaction at 21 ± 2 nN.

The interactions shown by these monolayers indicate that there were one or more probes present on at least one of the tips prepared, therefore the other monolayers most likely only interact very weakly with cyclohexyl groups.

There does not appear to be any discernable pattern in which monolayers interact strongly with the cyclohexyl probes. The methoxy resorcinarene **9** and the methylene cavitand **12** both have very shallow bowls, however the methoxy resorcinarene sulfide **21** has an identical cavity to **9**, and yet no similar interaction was observed. It is impossible to definitively discriminate

between forces arising from a specific complexation event, or non-specific interactions with the surface, however the narrow peak shape is suggestive of the former. The differences between the monolayers of **9** and **21** suggest that the structure of the monolayer is contributing to differences in the binding, rather than the structure of the receptor cavity alone.

4.2.15 Comparison of Benzyl Probe Interactions

Adhesion forces due to the benzyl probes were observed for all monolayers, with multiple peaks present in many cases. The adhesion forces observed range from 18 to 65 nN.

The calixarene **18**/**19** monolayer exhibited a strong interaction corresponding to a force of 22 ± 4 nN. A similar adhesion force was found with the benzyloxy resorcinarene **11** monolayer (23 ± 2 nN), and the deep cavitand **7** monolayer (27 ± 2 nN).

Broad peaks suggestive of non-specific interactions were observed for the methylene cavitand **12** monolayer (37 ± 5 nN), and the methoxy resorcinarene decyl sulfide **21** monolayer (28 ± 4 nN), however a sharper peak was also observed at 18 ± 2 nN.

The patterns of the adhesion forces measured for the methoxy and propoxy resorcinarene monolayers were the most informative. Forces of 29 ± 4 nN, 50 ± 4 nN, and 65 ± 3 nN were found to occur between the benzyl probe and the methoxy resorcinarene **9** monolayer. These are roughly multiples of 16 and if the interpretation of Auletta *et al*.[255] is correct, the data indicates that a single decomplexation event occurs with a force of approximately 16 nN. The propoxy resorcinarene **10** monolayer exhibited a similar pattern with peaks observed at 26 ± 3 nN, and 37 ± 4 nN, corresponding to a single interaction giving a rupture force of approximately 13 nN.

4.2.16 Comparison of Adamantyl Probe Interactions

The adamantyl probe interactions with the monolayer surfaces fall into two categories. Broad peaks were observed in the region of 15-33 nN with the calixarene **18**/**19** monolayer, and between 12-35 nN for the methoxy resorcinarene decylsulfide **21** monolayer. The broad peaks indicate that these forces probably arise from non-specific surface interaction of the probe with the surfaces, as this is more variable than well defined complexation events.

Sharper peaks were observed for the methylene cavitand **12** monolayer (23 ± 2 nN), and the benzyloxy resorcinarene **11** monolayer (19 ± 1 nN). These results are unexpected as the methylene cavitand **12** does not have a deep enough cavity to 'enclose' the adamantyl guest. The cavity is also of a similar size to the methoxy resorcinarene monolayers **9** and **21**, however the cavitands rigidity may account for the enhanced binding over these monolayers.

The benzyloxy resorcinarene **11** may have a deep cavity, however it is much more flexible than cavitands such as the deep cavitand **7**, and it is unknown if the benzyl groups are disordered, or oriented on the surface to provide binding sites.

4.2.17 Conclusion

The adhesion forces between the receptor monolayers and AFM tips functionalised with cyclohexyl, benzyl and adamantyl probes were measured (Table 4.1).

Table 4.1 Measured interactions between the monolayers and the functionalised AFM tips

Monolayer	Cyclohexyl Interactions	Benzyl Interactions (Single Interaction, calculated)	Adamantyl Interactions
Calixarene **18**/**19**	-	22 ± 4 nN	15-33 nN
Methoxy Resorcinarene **9**	31 ± 3 nN	29 ± 4 nN, 50 ± 4 nN, 65 ± 3 nN (16 nN)	-
Propoxy Resorcinarene **10**	-	26 ± 3 nN, 37 ± 4 nN (13 nN)	-
Benzyloxy Resorcinarene **11**	26 ± 1 nN	23 ± 2 nN	19 ± 1 nN
Methylene Cavitand **12**	21 ± 2 nN	37 ± 5 nN	23 ± 2 nN
Deep Cavitand **7**	-	27 ± 2 nN	-
Methoxy Resorcinarene Decylsulfide **21**	-	18 ± 2 nN, 28 ± 4 nN	23 ± 5 nN

A feature common to all the results obtained in this study is that the strength of the interactions observed are at least an order of magnitude greater than those reported in the literature. It is difficult to generalise given the very limited number of studies available, but it is notable that the previous work involves less hydrophobic components (cyclodextrins in the work of Schonherr *et al*,[255] for example, are water soluble) or use a less polar solvent (ethanol, in the work of Eckel *et al.*[211]). Hence the strength of the hydrophobic effect may be greater in the work presented here, than in the previous reports, leading to an overall increase in the magnitude of the interactions.

The nature of the force spectroscopy experiment means that many factors can affect the results, and due to the magnitude of the forces measured (pN to nN) it is impossible to corroborate the results using other techniques. Factors that can affect the results include temperature variations, surface roughness or defects, variable monolayer coverage, impurities in the solvent used, imperfections in the AFM tips etc. These factors were controlled as well as possible by using multiple tips and surfaces, and recording 6000 force

curves per sample. All organic contaminants were removed from glassware and substrates (prior to monolayer formation) by annealing at 600°C overnight, cleaning with piranha solution, or cleaning in a commercial UV/O_3 cleaner. The solvents used were also purified to the highest standards available, and the measurements were performed in a temperature controlled facility.

Due to the small number of groups performing these measurements and the number of systems studied to date, there is not enough evidence in the literature for there to be a consensus on the expected magnitude of the binding forces. Therefore while much more work is required in order to confirm the results, the previous literature work does not invalidate the results obtained in this study.

Some differentiation between the different probes and surfaces was achieved. As a generalisation, the adhesion between the monolayers and the benzyl probe was larger than the adamantyl which in turn was larger than the cyclohexyl. However, within the scope of this work, it is very difficult to compare the adhesion forces measured between different monolayers as in the majority of cases, it is impossible to determine the number of decomplexation events that give rise to that force.

The monolayers of the methylene cavitand **12** and the methoxy resorcinarene **9** appear to have the highest affinity for the cyclohexyl and adamantyl guests. This result was unanticipated as it was thought that the cavities of these resorcinarenes were too shallow to exhibit significant binding with guests of this size.[266]

The propoxy resorcinarene **10** monolayer and the deep cavitand **7** monolayer show selectivity for the benzyl probe. If any specific interactions occur with cyclohexyl or adamantyl probes they occur at forces low enough to be masked by the surface-surface adhesion.

The structure of the monolayer was found to be a contributing factor in determining binding affinities, at least in some cases. The hypothesis that the resorcinarene cavity is the primary factor determining the binding of guests to the monolayer was rejected due to the pronounced differences between the methoxy resorcinarene decylsulfide **21** monolayer and the methoxy resorcinarene **9** monolayer, despite the identical resorcinarene headgroups. The differences in binding in this case are presumably due to differences in packing within the monolayer, and indicate that more information is needed to understand these effects.

Significant differences were observed between tips functionalised with the same probe. This is assumed to be due to differing numbers of the probe molecules at the tip. No differences were observed between monolayer replicates.

Narrow peak shapes following a normal distribution were largely observed, and these are thought to arise from specific complexation events, whereas the broad peaks are thought to occur due to non-specific hydrophobic interactions with the surface. Time constraints prevent further investigation of this assumption, however 'blocking' experiments can be used to investigate this effect. Analogues of the probe molecule are added to the solution that the experiment is performed in. If the interaction is due to a specific host-guest complexation event it will no longer be observed, as the solution phase guests are complexed with the receptors, rather than the probe.[212] Other possibilities include using a long tether to attach the probe molecules to the AFM tip and introduce a filtering step into the data analysis to exclude any interactions that occur within a small distance from the surface (excludes surface-surface adhesion forces).[211]

4.4 Experimental

4.3.1 Synthesis of Probes

Adamantyl **31**, benzyl **30** and cyclohexyl **29** probes were prepared according to literature procedures.[255,262,263]

4.3.2 Preparation of Functionalised AFM tips

Commercial gold coated cantilevers (Budget Sensors, Cont-GB-G tips, 0.2 N/m, gold coated both sides) were cleaned in an UV/ozone cleaner (20 min), and then reduced in ethanol (30 min).

The clean cantilevers were immersed in a 0.99 mM solution of 2-mercaptoethanol, 0.01 mM of the probe, and sulfuric acid (1 drop, conc.) for 24 hours at ambient temperature. The cantilevers were rinsed in copious amounts of ethanol and dried in a gentle nitrogen stream.

Force constants were measured on Multimode PicoForce AFM (Digital Instruments, USA) using the thermal tune method after functionalisation.

4.3.3 Preparation of Monolayer Samples

Gold Arrandee substrates (gold on glass with a chromium adhesion layer) were annealed with a butane flame prior to functionalisation. The substrates were cleaned in an UV/ozone cleaner (20 min), and subsequently soaked in an ethanol bath at room temperature (30 min).

Clean substrates were immersed in tetrahydrofuran solutions (0.5 mM) of the macrocycle at ambient temperatures for 8 days. Sulfuric acid (conc., 1 drop) was added to the thioacetate solutions immediately before immersing the substrate. The substrates were rinsed with copious amounts of tetrahydrofuran and dried under a stream of nitrogen.

4.3.4 Measurement of Force Curves

Force curves were measured with a small multi-purpose scanner on a PicoPlus AFM system (Molecular Imaging/Agilent Technologies, USA) using a liquid cell filled with MilliQ water. The sweep duration used was 1 second, and the deflection limit 0.4 V.

6000 curves were measured for each monolayer/probe combination (3 tips x 2 surfaces).

Raw deflection data were converted into force data, and the adhesion force extracted using MatLab code written by Dr Thomas Becker (see Appendix 1).

5.0 Conclusion

Self-assembled monolayers of several macrocyclic receptors were prepared. The complexation properties of the monolayers were studied with the cyclic hydrocarbons, cyclohexane, adamantane, and benzene, with the aim of developing selective hydrocarbon sensors for application in petroleum exploration.

An undecylenic resorcinarene was alkylated at the upper rim with various alkyl groups. These derivatives were then thioacetylated using a radical addition procedure to yield the resorcinarenes **9**-**12** (Figure 5.1). A calixarene thiol/disulfide mixture **18**/**19** was prepared using the same procedure with a subsequent hydrolysis step (Figure 5.2). The original resorcinarene and the methylated intermediate were also alkylated at the lower rim to yield the sulfides **20** and **21** (Figure 5.1).

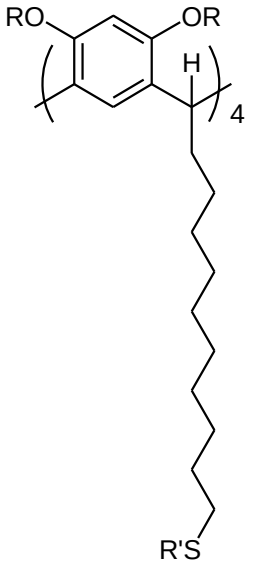

9	R=Me	R'=Ac
10	R=Pr	R'=Ac
11	R=Bn	R'=Ac
12	R,R=CH_2	R'=Ac
20	R=H	R'=$C_{10}H_{21}$
21	R=Me	R'= $C_{10}H_{21}$

Figure 5.1 Structure of the Resorcinarenes Synthesised.

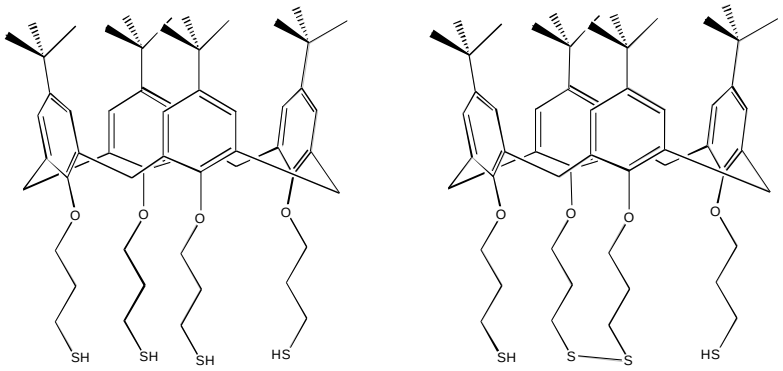

18 **19**

Figure 5.2 Structure of the Calixarenes Synthesised

Self-assembled monolayers of the receptors were prepared on gold substrates, and characterised by contact angle, polarised modulation infrared reflection absorption spectroscopy (PMIRRAS), and atomic force microscopy (AFM). All data was consistent with macrocyclic monolayers with the exception of the resorcinarene decyl sulfide **20** which appears to be a bilayer or multilayered structure.

AFM force spectroscopy was used to investigate the receptor properties of the monolayers by using tips functionalised with adamantyl, cyclohexyl and benzyl molecular probes. A quantity of a deep cavitand **7** (Figure 5.3) was obtained to use as a comparison to the shallower receptors synthesised.

All surfaces exhibited interactions with the benzyl probe. The propoxy resorcinarene **10** and deep cavitand **7** monolayers appear to show selectivity towards the benzyl probe, with no interactions observed for the adamantyl or cyclohexyl probes.

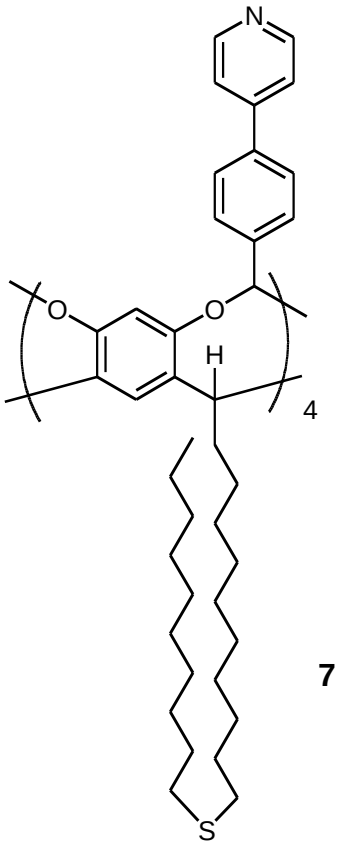

7

Figure 5.3 Structure of Deep Cavitand **7**[157]

Specific interactions were observed between the benzyloxy resorcinarene **11**, and methylene cavitand **12** monolayers with the adamantyl probes. These monolayers, along with the methoxy resorcinarene **9** monolayer also show significant interactions with the cyclohexyl probes. These receptors present promising targets for further studies of the complexation behaviour of resorcinarene based receptors and aliphatic hydrocarbons.

The monolayer structure was found to influence the binding of the molecular probes. Evidence for this was provided by the difference in binding exhibited by the methoxy resorcinarene **9** monolayer and the methoxy resorcinarene decylsulfide **21** monolayer.

This dependence of the guest binding on the underlying monolayer structure is poorly understood. More characterisation of the monolayers is needed in order to correlate the surface parameters (orientation, defects, degree of

order, density etc) to the observed binding. Further studies such as blocking experiments should also be done to obtain more conclusive evidence for the occurrence of specific complexation events over non-specific hydrophobic interaction with the monolayer.

It is assumed in the literature that more ordered monolayers give a better performing sensor (as is true for electrochemical sensors),[149-151] which is logical as an ordered monolayer is close packed with more receptors on the surface, and if the receptors are oriented appropriately the underlying alkyl chains are less accessible to the analyte/other solute reducing the non-specific interactions observed. However, an ordered monolayer may not allow enough headgroup flexibility for complexation with tightly fitting guests (where conformational changes are needed for guest exchange in solution). Future work optimising this parameter is needed.

In order to advance the goal of developing a hydrocarbon sensor, the receptors can be used as sensing layers for techniques such as surface plasmon resonance,[56] quartz crystal microbalance, or nanoparticle-based sensors,[267] and the response to the analytes in solution studied. These results can then be correlated with the force spectroscopy data in order to validate the use of the technique in determining the receptor properties of a monolayer. Competition experiments can be used to determine if co-solutes will interfere with the analysis, which is critical for the intended application. The receptor structure can also be optimised when the factors that affect the binding are better understood. In addition to macrocyclic based receptors, other options such as molecular imprinted polymers,[268,269] calixarene polymers,[270] or porous structures such as zeolites could be investigated.[271]

6.0 References

1. Geoscience Australia, **2006**, *Australian Petroleum Exploration and Development Activity, 1 October to 31 December 2005*, Retrieved 5/12/2009 from http://www.ga.gov.au.
2. Australian Bureau of Statistics, **2009**, *Mineral and Petroleum Exploration, Australia, Jun 2009* Retrieved 5/12/2009 from www.abs.gov.au.
3. Aydemir, A; Ates, A, *J. Pet. Sci. Eng.*, **2008**, *62*, 36-44.
4. O'Brien, G W; Lawrence, G M; Williams, A K; Glenn, K; Barrett, A G; Lech, M; Edwards, D S; Cowley, R; Boreham, C J; Summons, R E, *Mar. Pet. Geol.*, **2005**, *22*, 517-549.
5. Rollet, N; Logan, G A; Kennard, J M; O'Brien, P E; Jones, A T; Sexton, M, *Mar. Pet. Geol.*, **2006**, *23*, 145-164.
6. Logan, G A; Jones, A T; Kennard, J M; Ryan, G J; Rollet, N, *Mar. Pet. Geol.*, **2010**, *27*, 26-45.
7. Sassen, R; Brooks, J; Kennicutt, M; MacDonald, I; Guinasso, N, *Oil Gas J.*, **1993**, *91*, 64-69.
8. MacDonald, I; Reilly, J; Best, S; Venkataramaiah, R; Sassen, R; Guinasso, N; Amos, J, *AAPG Mem.*, **1996**, *66*, 27-37.
9. DeBeukelaer, S M; MacDonald, I R; Guinnasso, N L; Murray, J A, *Geo-Mar. Lett.*, **2003**, *23*, 177-186.
10. Pinet, N; Duchesne, M; Lavoie, D; Bolduc, A; Long, B, *Mar. Pet. Geol.*, **2008**, *25*, 271-288.
11. Sackett, W M, *J. Geochem. Explor.*, **1977**, *7*, 243-254.
12. Douglas, G S; Burns, W A; Bence, A E; Page, D S; Boehm, P, *Environ. Sci. Technol.*, **2004**, *38*, 3958-3964.
13. Stout, S A; Douglas, G S, *Environ. Forensics* **2004**, *5*, 225-235.
14. Alimi, H; Ertel, T; Schug, B, *Environ. Forensics* **2003**, *4*, 25-38.
15. Wang, Z D; Yang, C; Hollebone, B; Fingas, M, *Environ. Sci. Technol.*, **2006**, *40*, 5636-5646.
16. Ueyama, S; Hijikata, K; Hirotsuji, J, *Water Sci. Technol.*, **2002**, *45*, 175-180.

17. Ogawa, S; Sugimoto, I, *Water Sci. Technol.*, **2002**, *45*, 201-206.
18. Applebee, M; Geissler, J; Schellinger, A; Jaeger, R; Pierce, D, *Environ. Sci. Technol.*, **2004**, *38*, 234-239.
19. Pejcic, B; Barton, C; Crooke, E; Eadington, P; Jee, E; Ross, A, *Sens. Actuators, B* **2009**, *135*, 436-443.
20. McCue, R P; Walsh, J E; Walsh, F; Regan, F, *Sens. Actuators, B* **2006**, *114*, 438-444.
21. Bürck, J; Mensch, M; Krämer, K, *Field Anal. Chem. Technol.*, **1998**, *2*, 205-219.
22. Zhang, J; Dong, J, *Langmuir*, **2005**, *21*, 8609-8612.
23. Fresco-Rivera, P; Fernandez-Varela, R; Gomez-Carracedo, M P; Ramirez-Villalobos, F; Prada, D; Muniategui, S; Andrade, J M, *Talanta*, **2007**, *74*, 163-175.
24. Silva, A M S; Pimentel, M F; Raimundo Jr, I M; Almeida, Y M B, *Sens. Actuators, B* **2009**, *139*, 222-230.
25. Perez-Palacios, D; Armenta, S; Lendl, B, *Appl. Spectrosc.*, **2009**, *63*, 1015-1021.
26. Luzinova, Y; Dobbs, G T; Sassen, R; Mizaikoff, B, *Org. Geochem.*, **2009**, *40*, 1143-1150.
27. Powell, T G; McKirdy, D M, *AAPG Bull.*, **1975**, *59*, 1176-1197.
28. Tissot, B P; Welte, D H, *Petroleum Formation and Occurence*, 2nd ed., Springer-Verlag: Heidelberg, **1984**.
29. Chen, J H; Fu, J M; Sheng, G Y; Liu, D H; Zhang, J J, *Org. Geochem.*, **1996**, *25*, 179-190.
30. Petrov, A; Arefjev, O; Yakubson, Z In *Advances in Organic Geochemistry*, Tissot, B, Bienner, F, Eds., Editions Technip: Paris, **1974**, p 517-522.
31. Bender, A; Said, E; Abdulsada, A, *Analyst*, **1986**, *111*, 575-576.
32. Dahl, J; Liu, S; Carlson, R, *Science*, **2003**, *299*, 96-99.
33. Wei, Z B; Moldowan, J M; Peters, K E; Wang, Y; Xiang, W, *Org. Geochem.*, **2007**, *38*, 1910-1926.
34. Palmer, S E In *Org. Geochem.* , Engel, M H, Macko, S A, Eds., Plenium Press: New York, **1993**, p 511-532.
35. Newell, N A, *APPEA J.*, **1999**, 227-247.

36. Price, L C, *AAPG Bull.*, **1976**, *60*, 213-244.
37. McAuliffe, C D In *Physical and Chemical Constraints on Petroleum Migration*, Roberts, W H, Cordell, R J, Eds., Amer. Assoc. Petrol. Geol. : New York, **1979**, p C1-C39.
38. Lafargue, E; Barker, C, *AAPG Bull.*, **1988**, *72*, 263-276.
39. Eganhouse, R P; Calder, J A, *Geochim. Cosmochim. Acta* **1976**, *40*, 555-561.
40. Brakstad, O; Bonaunet, K; Nordtug, T; Johansen, O, *Biodegradation*, **2004**, *15*, 337-346.
41. Skaare, B B; Wilkes, H; Vieth, A; Rein, E; Barth, T, *Org. Geochem.*, **2007**, *38*, 1865-1883.
42. Wenger, L; Davis, C; Isaksen, G In *Society of Petroleum Engineers Annual Technical Conference* New Orleans, Louisiana, 2001.
43. Dutta, T K; Harayama, S, *Environ. Sci. Technol.*, **2000**, *34*, 1500-1505.
44. Wenger, L M; Isaksen, G H, *Org. Geochem.*, **2002**, *33*, 1277-1292.
45. Kennicutt, M C; Brooks, J M; Denoux, G J, *Mar. Chem.*, **1988**, *24*, 39-59.
46. Likes, S, *An Introduction to Marine Biogeochemistry*, John Wiley and Sons: New York **1992**.
47. Yamashita, Y; Tanoue, E, *Org. Geochem.*, **2004**, *35*, 679-692.
48. McCarthy, M D; Hedges, J I; Benner, R, *Chem. Geol.*, **1993**, *107*, 503-507.
49. McCarthy, M; Hedges, J; Benner, R, *Mar. Chem.*, **1996**, *55*, 281-297.
50. Dittmar, T; Koch, B P, *Mar. Chem.*, **2006**, *102*, 208-217.
51. Kvenvolden, K A; Cooper, C K, *Geo-Mar. Lett.*, **2003**, *23*, 140-146.
52. Williams, J A; Bjoroy, M; Dolcater, D L; Winters, J C, *Org. Geochem.*, **1986**, *10*, 451-461.
53. Lieberzeit, P A; Greibl, W; Stathopulos, H; Dickert, F L; Fischerauer, G; Bulst, W-E, *Sens. Actuators, B* **2006**, *113*, 677-683.
54. Guerrini, L; Garcia-Ramos, J V; Domingo, C; Sanchez-Cortes, S, *Langmuir*, **2006**, *22*, 10924-10926.
55. Liu, S; Tang, Z, *J. Mater. Chem.*, **2010**, *20*, 24-35.
56. Friggeri, A; van Veggel, F; Reinhoudt, D N; Kooyman, R P H, *Langmuir*, **1998**, *14*, 5457-5463.

57. Faull, J D; Gupta, V K, *Langmuir*, **2001**, *17*, 1470-1476.
58. Kanazawa, K; Gordon, J, *Anal. Chem.*, **1985**, *57*, 1770-1771.
59. Paolesse, R; DiNatale, C; Nardis, S; Macagnano, A; D'Amico, A; Pinalli, R; Dalcanale, E, *Chem. Eur. J.*, **2003**, *9*, 5388-5395.
60. Schierbaum, K, *Sens. Actuators, B* **1994**, *18*, 71-76.
61. Dickert, F; Baumler, U P; Stathopulos, H, *Anal. Chem.*, **1997**, *69*, 1000-1005.
62. Dickert, F L; Bruckdorfer, T; Feigl, H; Haunschild, A; Kuschow, V; Obermeier, E; Bulst, O; Knauer, U; Mages, G, *Sens. Actuators, B* **1993**, *13*, 297-301.
63. Hartmann, J; Auge, J; Lucklum, R; Rosler, S; Hauptmann, P; Adler, B; Dalcanale, E, *Sens. Actuators, B* **1996**, *34*, 305-311.
64. Nelli, P; Dalcanale, E; Faglia, G; Sberveglieri, G; Soncini, P, *Sens. Actuators, B* **1993**, *13*, 302-304.
65. Wang, C; He, X W; Chen, L X, *Talanta*, **2002**, *57*, 1181-1188.
66. Dickert, F; Sikorski, R, *Mater. Sci. Eng., C* **1999**, *10*, 39-46.
67. Dickert, F L; Achatz, P; Halikias, K, *Fresenius J. Anal. Chem.*, **2001**, *371*, 11-15.
68. Cygan, M T; Collins, G E; Dunbar, T D; Allara, D L; Gibbs, C G; Gutsche, C D, *Anal. Chem.*, **1999**, *71*, 142-148.
69. Dalcanale, E; Hartmann, J, *Sens. Actuators, B* **1995**, *24*, 39-42.
70. Lucklum, R; Rosler, S; Hartmann, J; Hauptmann, P, *Sens. Actuators, B* **1996**, *35*, 103-111.
71. Hartmann, J; Hauptmann, P; Levi, S; Dalcanale, E, *Sens. Actuators, B* **1996**, *35*, 154-157.
72. Cram, D J, *Angew. Chem. Int. Ed.*, **1988**, *27*, 1009-1020.
73. Izatt, R M; Bradshaw, J S; Pawlak, K; Bruening, R L; Tarbet, B J, *Chem. Rev.*, **1992**, *92*, 1261-1354.
74. Izatt, R M; Pawlak, K; Bradshaw, J S, *Chem. Rev.*, **1995**, *95*, 2529-2586.
75. Hooley, R J; Van Anda, H J; Rebek, J, *J. Am. Chem. Soc.*, **2006**, *128*, 3894-3895.
76. Hooley, R J; Van Anda, H J; Rebek, J, *J. Am. Chem. Soc.*, **2007**, *129*, 13464-13473.

77. Mecozzi, S; Rebek Jr, J, *Chem. Eur. J.* , **1998**, *4*, 1016-1022.
78. Brouwer, E B; Ripmeester, J A; Enright, G D, *J. Inclusion Phenom. Mol. Recognit. Chem.*, **1996**, *24*, 1-17.
79. Klarner, F G; Benkhoff, J; Boese, R; Burkert, U; Kamieth, M; Naatz, U, *Angew. Chem. Int. Ed.*, **1996**, *35*, 1130-1133.
80. Gorbatchuk, V V; Tsifarkin, A G; Antipin, I S; Solomonov, B N; Konovalov, A I, *J. Inclusion Phenom. Mol. Recognit. Chem.*, **1999**, *35*, 389-396.
81. Gorbatchuk, V V; Tsifarkin, A G; Antipin, I S; Solomonov, B N; Konovalov, A I; Seidel, J; Baitalov, F, *J. Chem. Soc., Perkin Trans. 2* **2000**, 2287-2294.
82. Gorbatchuk, V V; Savelyeva, L S; Ziganshin, M A; Antipin, I S; Sidorov, V A, *Russ. Chem. Bull.*, **2004**, *53*, 60-65.
83. Starnes, S D; Rudkevich, D M; Rebek, J, *J. Am. Chem. Soc.*, **2001**, *123*, 4659-4669.
84. Lucking, U; Tucci, F C; Rudkevich, D M; Rebek, J, *J. Am. Chem. Soc.*, **2000**, *122*, 8880-8889.
85. Tucci, F C; Renslo, A R; Tudkevich, D M; Rebek, J, *Angew. Chem. Int. Ed.*, **2000**, *39*, 1076-1079.
86. Ma, S; Rudkevich, D; Rebek, J, *Angew. Chem. Int. Ed.*, **1999**, *38*, 2600-2602.
87. Renslo, A R; Tucci, F C; Rudkevich, D M; Rebek, J, *J. Am. Chem. Soc.*, **2000**, *122*, 4573-4582.
88. Rudkevich, D M; Hilmersson, G; Rebek, J, *J. Am. Chem. Soc.*, **1997**, *119*, 9911-9912.
89. Rudkevich, D; Hilmersson, G; Rebek, J, *J. Am. Chem. Soc.*, **1998**, *120*, 12216-12225.
90. Haino, T; Rudkevich, D M; Shivanyuk, A; Rissanen, K; Rebek, J, *Chem. Eur. J.*, **2000**, *6*, 3797-3805.
91. Gottschalk, T; Jarowski, P D; Diederich, F, *Tetrahedron*, **2008**, *64*, 8307-8317.
92. Gottschalk, T; Jaun, B; Diederich, F, *Angew. Chem. Int. Ed.*, **2007**, *46*, 260-264.

93. Jaime, C; Redondo, J; Sanchez-Ferrando, R; Virgili, A, *J. Mol. Struct.*, **1991**, *248*, 317-329.
94. Bendeby, B; Kenne, L; Sandstrom, C, *J. Inclusion Phenom. Mol. Recognit. Chem.*, **2004**, *50*, 173-181.
95. Harries, D; Rau, D C; Parsegian, V A, *J. Am. Chem. Soc.*, **2005**, *127*, 2184-2190.
96. Newkome, G; Kim, H J; Choi, K H; Moorefield, C, *Macromolecules*, **2004**, *37*, 6268-6274.
97. Michels, J J; Baars, M; Meijer, E W; Huskens, J; Reinhoudt, D N, *J. Chem. Soc., Perkin Trans. 2* **2000**, 1914-1918.
98. Fragoso, A; Caballero, J; Almirall, E; Villalonga, R; Cao, R, *Langmuir*, **2002**, *18*, 5051-5054.
99. Karakasyan, C; Millot, M-C; Vidal-Madjar, C, *J. Chromatogr. B*, **2004**, *808*, 63-67.
100. Miyauchi, M; Hoshino, T; Yamaguchi, H; Kamitori, S; Harada, A, *J. Am. Chem. Soc.*, **2005**, *127*, 2034-2035.
101. David, D; Millot, M C; Sebille, B; Levy, Y, *Sens. Actuators, B* **2003**, *90*, 286-295.
102. Duchene, D In *Proceedings of the Fourth International Symposium on Cyclodextrins*, Huber, O, Szejtli, J, Eds., Kluwer Academic Publishers: Dordrecht, The Netherlands **1988**, p 265-275.
103. Schneider, H J; Hacket, F; Rudiger, V; Ikeda, H, *Chem. Rev.*, **1998**, *98*, 1755-1785.
104. Rekharsky, M V; Inoue, Y, *Chem. Rev.*, **1998**, *98*, 1875-1917.
105. Udachin, K A; Ripmeester, J A, *J. Am. Chem. Soc.*, **1998**, *120*, 1080-1081.
106. Steed, J; Turner, D; Wallace, K, *Core Concepts in Supramolecular Chemistry and Nanochemistry*, John Wiley and Sons: New York, **2007**.
107. Jasat, A; Sherman, J, *Chem. Rev.*, **1999**, *99*, 931-967.
108. Sherman, J, *Tetrahedron*, **1995**, *51*, 3395-3422.
109. Piatnitski, E; Flowers, R; Deshayes, K, *Chem. Eur. J.* , **2000**, *6*, 999-1006.

110. Cram, D J; Blanda, M T; Paek, K; Knobler, C B, *J. Am. Chem. Soc.*, **1992**, *114*, 7765-7773.
111. Cram, D J; Jaeger, R; Deshayes, K, *J. Am. Chem. Soc.*, **1993**, *115*, 10111-10116.
112. Robbins, T A; Knobler, C B; Bellew, D R; Cram, D J, *J. Am. Chem. Soc.*, **1994**, *116*, 111-122.
113. Cram, D J; Tanner, M E; Knobler, C B, *J. Am. Chem. Soc.*, **1991**, *113*, 7717-7727.
114. Quan, M L C; Cram, D J, *J. Am. Chem. Soc.*, **1991**, *113*, 2754-2755.
115. Biros, S M; Ullrich, E C; Hof, F; Trembleau, L; Rebek, J, *J. Am. Chem. Soc.*, **2004**, *126*, 2870-2876.
116. Amrhein, P; Shivanyuk, A; Johnson, D W; Rebek, J, *J. Am. Chem. Soc.*, **2002**, *124*, 10349-10358.
117. Hooley, R J; Shenoy, S R; Rebek, J, *Org. Lett.*, **2008**, *10*, 5397-5400.
118. Lledo, A; Hooley, R J; Rebek, J, *Org. Lett.*, **2008**, *10*, 3669-3671.
119. Gibb, C L D; Gibb, B C, *J. Am. Chem. Soc.*, **2004**, *126*, 11408-11409.
120. Gibb, C L D; Li, X; Gibb, B C, *Proc. Nat. Acad. Sci. U.S.A.*, **2002**, *99*, 4857-4862.
121. Gibb, C L D; Stevens, E D; Gibb, B C, *J. Am. Chem. Soc.*, **2001**, *123*, 5849-5850.
122. Gibb, C L D; Xi, H; Politzer, P A; Concha, M; Gibb, B C, *Tetrahedron*, **2002**, *58*, 673-681.
123. Gibbs, C G; Sujeeth, P K; Rogers, J S; Stanley, G G; Krawiec, M; Watson, W H; Gutsche, C D, *J. Org. Chem.*, **2002**, *60*, 8394-8402.
124. Laughrey, Z R; Gibb, C L D; Senechal, T; Gibb, B C, *Chem. Eur. J.*, **2003**, *9*, 130-139.
125. Wallimann, P; Marti, T; Furer, A; Diederich, F, *Chem. Rev.*, **1997**, *97*, 1567-1608.
126. Yang, Z W; Breslow, R, *Tetrahedron Lett.*, **1997**, *38*, 6171-6172.
127. Peterson, B R; Wallimann, P; Carcanague, D; Diederich, F, *Tetrahedron*, **1994**, *51*, 401-421.
128. Carcanague, D R; Diederich, F, *Angew. Chem. Int. Ed.*, **1990**, *29*, 769-771.

129. Furer, A; Marti, T; Diederich, F; Kunzer, H; Brehm, M, *Helv. Chim. Acta* **1999**, *82*, 1843-1859.
130. Marti, T; Peterson, B R; Furer, A; Mordasini-Denti, T; Zarske, J; Jaun, B; Diederich, F; Gramlich, V, *Helv. Chim. Acta* **1998**, *81*, 109-144.
131. Liu, Y; Yang, Y W; Yang, E C; Guan, X D, *J. Org. Chem.*, **2004**, *69*, 6590-6602.
132. Breslow, R; Zhang, B L, *J. Am. Chem. Soc.*, **1996**, *118*, 8495-8496.
133. Breslow, R; Halfon, S; Zhang, B, *Tetrahedron*, **1995**, *51*, 377.
134. Bugler, J; Engbersen, J; Reinhoudt, D, *J. Org. Chem.*, **1998**, *63*, 5339-5344.
135. Dimmler, A; Strausz, O P, *J. Chromatogr.*, **1983**, *270*, 219-225.
136. Armanios, C; Alexander, R; Ian Kagi, R, *Org. Geochem.*, **1992**, *18*, 399-406.
137. Dalcanale, E; Costantini, G; Soncini, P, *J. Inclusion Phenom. Mol. Recognit. Chem.*, **1992**, *13*, 87-92.
138. Timmerman, P; Verboom, W; Reinhoudt, D N, *Tetrahedron*, **1996**, *52*, 2663-2704.
139. Botta, B; Iacomacci, P; Digiovanni, C; Dellemonache, G; Gacsbaitz, E; Botta, M; Tafi, A; Corelli, F; Misiti, D, *J. Org. Chem.*, **1992**, *57*, 3259-3261.
140. Gutsche, C D, *Calixarenes: An Introduction*, 2nd ed., Royal Society of Chemistry: London, **2008**.
141. Abis, L; Dalcanale, E; Duvosel, A; Spera, S, *J. Org. Chem.*, **1988**, *53*, 5475-5479.
142. *Calixarenes A Versatile Class of Macrocyclic Compounds*, Vicens, J; Bohmer, V, Eds., Kluwer Academic Publishers: The Netherlands, **1991**.
143. Lamartine, R; Tsukada, M; Shirata, A, *C. R. Chim*, **2002**, *5*, 1-7.
144. Lukkari, J; Meretoja, M; Kartio, I; Laajalehto, K; Rajamaki, M; Lindstrom, M; Kankare, J, *Langmuir*, **1999**, *15*, 3529-3537.
145. Zhao, Y; Perez-Segarra, W; Shi, Q C; Wei, A, *J. Am. Chem. Soc.*, **2005**, *127*, 7328-7329.
146. Love, J C; Estroff, L A; Kriebel, J K; Nuzzo, R G; Whitesides, G M, *Chem. Rev.*, **2005**, *105*, 1103-1169.

147. Huisman, B H; van Velzen, E U T; van Veggel, F; Engbersen, J F J; Reinhoudt, D N, *Tetrahedron Lett.*, **1995**, *36*, 3273-3276.
148. Tshikhudo, T R; Demuru, D; Wang, Z X; Brust, M; Secchi, A; Arduini, A; Pochini, A, *Angew. Chem. Int. Ed.*, **2005**, *44*, 2913-2916.
149. van Velzen, E U T; Engbersen, J F J; Reinhoudt, D N, *J. Am. Chem. Soc.*, **1994**, *116*, 3597-3598.
150. Schonherr, H; Vancso, G J; Huisman, B H; van Veggel, F; Reinhoudt, D N, *Langmuir*, **1997**, *13*, 1567-1570.
151. van Velzen, E U T; Engbersen, J F J; Delange, P J; Mahy, J W G; Reinhoudt, D N, *J. Am. Chem. Soc.*, **1995**, *117*, 6853-6862.
152. Davis, F; Stirling, C J M, *Langmuir*, **1996**, *12*, 5365-5374.
153. Faull, J D; Gupta, V K, *Thin Solid Films*, **2003**, *440*, 129-137.
154. van Velzen, T E U; Engbersen, J F; Reinhoudt, D N, *Synthesis*, **1995**, 989-997.
155. Gibb, B; Chapman, R; Sherman, J, *J. Org. Chem.*, **1996**, *61*, 1505-1509.
156. Moran, J R; Ericson, J L; Dalcanale, E; Bryant, J A; Knobler, C B; Cram, D J, *J. Am. Chem. Soc.*, **1991**, *113*, 5707-5714.
157. Menozzi, E; Pinalli, R; Speets, E A; Ravoo, B J; Dalcanale, E; Reinhoudt, D N, *Chem. Eur. J.*, **2004**, *10*, 2199-2206.
158. Gutsche, C D; Iqbal, M, *Org. Synth.*, **1990**, *68*, 234-237.
159. Gutsche, C D; Dhawan, B; Levine, J A; No, K H; Bauer, L J, *Tetrahedron*, **1983**, *39*, 409-426.
160. Arduini, A; Demuru, D; Pochini, A; Secchi, A, *Chem. Commun.*, **2005**, 645-647.
161. Vaughan, W E; Rust, F F; Evans, T W, *J. Org. Chem.*, **1942**, *7*, 477-490.
162. Furniss, B; Vogel, A, *Vogel's Textbook of Practical Organic Chemistry*, 5th ed., Longman Scientific: London, **1989**.
163. March, J, *Advanced Organic Chemistry*, 4th ed., John Wiley and Sons: New York, **1992**.
164. Tewari, N; Nizar, H; Mane, A; George, V; Prasad, M, *Synth. Commun.*, **2006**, *36*, 1911-1914.

165. Masuda, Y; Hoshi, M; Nunokawa, Y; Arase, A, *Chem. Commun.*, **1991**, 1444-1445.
166. Strong, L; Whitesides, G M, *Langmuir*, **1988**, *4*, 546-558.
167. Zhong, C J; Brush, R C; Anderegg, J; Porter, M D, *Langmuir*, **1999**, *15*, 518-525.
168. Zhong, C-J; Porter, M D, *J. Am. Chem. Soc.*, **1994**, *116*, 11616-11617.
169. Beulen, M W J; Huisman, B H; vanderHeijden, P A; vanVeggel, F; Simons, M G; Biemond, E; deLange, P J; Reinhoudt, D N, *Langmuir*, **1996**, *12*, 6170-6172.
170. Szaniszlo, N, *J. Inclusion Phenom. Mol. Recognit. Chem.*, **2005**, *53*, 241-248.
171. Olsson, M; Sander, L C; Wise, S A, *J. Chromatogr. A*, **1989**, *477*, 277-290.
172. Tietze, L F; Eicher, T, *Reactions and Syntheses in the Organic Chemistry Laboratory*, University Science Books: Mill Valley, CA, **1989**.
173. Burfield, D R; Smithers, R H, *J. Org. Chem.*, **1978**, *43*, 3966-3968.
174. Ulman, A, *Chem. Rev.*, **1996**, *96*, 1533-1554.
175. Jung, C; Dannenberger, O; Xu, Y; Buck, M; Grunze, M, *Langmuir*, **1998**, *14*, 1103-1107.
176. Tour, J M; Jones, L; Pearson, D L; Lamba, J J S; Burgin, T P; Whitesides, G M; Allara, D L; Parikh, A N; Atre, S V, *J. Am. Chem. Soc.*, **1995**, *117*, 9529-9534.
177. Vaughan, O P H; Turner, M; Williams, F J; Hille, A; Sanders, J K M; Lambert, R M, *J. Am. Chem. Soc.*, **2006**, *128*, 9578-9579.
178. Sabatani, E; Cohen-Boulakia, J; Bruening, M; Rubinstein, I, *Langmuir*, **1993**, *9*, 2974-2981.
179. Holze, R; Schomaker, S, *Electrochim. Acta* **1990**, *35*, 613-620.
180. Limbut, W; Kanatharana, P; Mattiasson, B; Asawatreratanakul, P; Thavarungkul, P, *Biosens. Bioelectron.*, **2006**, *22*, 233-240.
181. Li, T T T; Liu, H Y; Weaver, M J, *J. Am. Chem. Soc.*, **1984**, *106*, 1233-1239.
182. Uvdal, K; Bodö, P; Liedberg, B, *J. Colloid Interface Sci.*, **1992**, *149*, 162-173.

183. Colorado Jr, R; Villanzana, R J; Lee, T R, *Langmuir*, **1998**, *14*, 6337-6340.
184. Ihs, A; Uvdal, K; Liedberg, B, *Langmuir*, **1993**, *9*, 733-739.
185. Arndt, T; Schupp, H; Schrepp, W, *Thin Solid Films*, **1989**, *178*, 319-326.
186. Bharathi, S; Yegnaraman, V; Rao, G P, *Langmuir*, **1993**, *9*, 1614-1617.
187. Arduengo, A J; Moran, J R; Rodriguez-Parada, J; Ward, M D, *J. Am. Chem. Soc.*, **1990**, *112*, 6153-6154.
188. Kang, Y K; Won, D J; Kim, S R; Seo, K J; Choi, H S; Lee, G H; Noh, Z S; Lee, T S; Lee, C J, *Mater. Sci. Eng., C* **2004**, *24*, 43-46.
189. Karpovich, D S; Blanchard, G J, *Langmuir*, **1994**, *10*, 3315-3322.
190. Bain, C D; Troughton, E B; Tao, Y-T; Evall, J; Whitesides, G M; Nuzzo, R G, *J. Am. Chem. Soc.*, **1989**, *111*, 321-335.
191. Evans, S D; Sharma, R; Ulman, A, *Langmuir*, **1991**, *7*, 156-161.
192. Chechik, V; Crooks, R; Stirling, C, *Adv. Mater.*, **2000**, *12*, 1161-1171.
193. Sullivan, T P; Huck, W T S, *Eur. J. Org. Chem.*, **2003**, 17-29.
194. Gooding, J; Mearns, F; Yang, W; Liu, J, *Electroanalysis*, **2003**, *15*, 81-96.
195. Flink, S; van Veggel, F; Reinhoudt, D, *Sens. Update*, **2000**, *8*, 3-19.
196. Xia, Y; Whitesides, G, *Angew. Chem. Int. Ed.*, **1998**, *37*, 550-575.
197. Barsotti, R J; O'Connel, M S; Stellacci, F, *Langmuir*, **2004**, *20*, 4795-4798.
198. Aizenberg, J; Black, A; Whitesides, G, *Nature*, **1999**, *398*, 495-498.
199. McDermott, M T; Green, J-B D; Porter, M D, *Langmuir*, **1997**, *13*, 2504-2510.
200. Witt, D; Klajn, R; Barski, P; Grzybowski, B A, *Curr. Org. Chem.*, **2004**, *8*, 1763-1797.
201. Flink, S; van Veggel, F; Reinhoudt, D N, *Adv. Mater.*, **2000**, *12*, 1315-1328.
202. Davis, F; Frary, E; Stirling, C, *Langmuir*, **2004**, *20*, 9075-9079.
203. Roy, D; Fendler, J, *Adv. Mater.*, **2004**, *16*, 479-508.
204. Faull, J D; Wissmann, P J; Gupta, V K, *Thin Solid Films*, **2004**, *457*, 292-300.

205. Karpovich, D S; Blanchard, G J, *Langmuir*, **1997**, *13*, 4031-4037.
206. Duwez, A S, *J. Electron. Spectrosc. Relat. Phenom.*, **2004**, *134*, 97-138.
207. Su, J; Mrksich, M, *Langmuir*, **2003**, *19*, 4867-4870.
208. Schonherr, H; Vancso, J; Huisman, B-H; van Veggel, F; Reinhoudt, D, *Langmuir*, **1999**, *15*, 5541-5546.
209. Raible, S; Pfeiffer, J; Weiss, T; Clauss, W; Goepel, W; Schurig, V; Kern, D P, *Appl. Phys. A* **2000**, *70*, 607-611.
210. Pan, G B; Wan, L J; Zheng, Q Y; Bai, C L, *Chem. Phys. Lett.*, **2003**, *367*, 711-716.
211. Eckel, R; Ros, R; Decker, B; Mattay, J; Anselmetti, D, *Angew. Chem. Int. Ed.*, **2005**, *44*, 484-488.
212. Schonherr, H; Beulen, M W J; Bugler, J; Huskens, J; van Veggel, F; Reinhoudt, D N; Vancso, G J, *J. Am. Chem. Soc.*, **2000**, *122*, 4963-4967.
213. Kwok, D Y; Neumann, A W, *Adv. Colloid Interface Sci.*, **1999**, *81*, 167-249.
214. Bain, C D; Whitesides, G M, *J. Am. Chem. Soc.*, **1989**, *111*, 7164-7175.
215. Ulman, A, *An Introduction to Ultrathin Organic Films*, Elsevier Science Publishers: New York, **1991**.
216. Gupta, P; Ulman, A; Fanfan, S; Korniakov, A; Loos, K, *J. Am. Chem. Soc.*, **2005**, *127*, 4-5.
217. Tolstoy, V; Chernyshova, I; Skryshevsky, V, *Handbook of Infrared Spectroscopy of Ultrathin Films*, John Wiley and Sons: New York **2003**.
218. Kim, Y T; McCarley, R L; Bard, A J, *J. Phys. Chem.*, **1992**, *96*, 7416-7421.
219. Ron, H; Matlis, S; Rubinstein, I, *Langmuir*, **1998**, *14*, 1116-1121.
220. Vig, J R, *J. Vac. Sci. Technol., A* **1985**, *3*, 1027-1034.
221. Carvalhal, R F; Freire, R S; Kubota, L T, *Electroanalysis*, **2005**, *17*, 1251-1259.
222. Tsai, M-Y; Lin, J-C, *J. Colloid Interface Sci.*, **2001**, *238*, 259-266.

223. Ell, A H; Csjernyik, G; Slagt, V F; Backvall, J E; Berner, S; Puglia, C; Ledung, G; Oscarsson, S, *Eur. J. Org. Chem.*, **2006**, 1193-1199.
224. Cai, L T; Yao, Y X; Yang, J P; Price, D W; Tour, J M, *Chem. Mater.*, **2002**, *14*, 2905-2909.
225. Huisman, B H; Rudkevich, D M; van Veggel, F; Reinhoudt, D N, *J. Am. Chem. Soc.*, **1996**, *118*, 3523-3524.
226. Nakamoto, K, *Infrared and Raman Spectra of Inorganic and Coordination Compounds*, 4th ed., John Wiley and Sons: New York, **1986**.
227. Hegner, M; Wagner, P; Semenza, G, *Surf. Sci.*, **1993**, *291*, 39-46.
228. Losic, D; Shapter, J G; Gooding, J J, *Aust. J. Chem.*, **2001**, *54*, 643-648.
229. Gupta, P; Loos, K; Korniakov, A; Spagnoli, C; Cowman, M; Ulman, A, *Angew. Chem. Int. Ed.*, **2004**, *43*, 520-523.
230. Yoshimatsu, N; Kawasaki, T; Ban, K; Kusaka, T; Ikeda, T, *E-J. Surf. Sci. Nanotech.*, **2005**, *3*, 524-526.
231. Manne, S; Butt, H; Gould, S; Hansma, P, *Appl. Phys. Lett.*, **1990**, *56*, 1758-1759.
232. Barden, W; Singh, S; Kruse, P, *Langmuir*, **2008**, *24*, 2452-2458.
233. Dongmo, S, *Appl. Phys. A* **1998**, *66*, S819-S823.
234. Steed, J W; Atwood, J L, *Supramolecular Chemistry*, John Wiley and Sons Ltd: London, **2000**.
235. Doxsee, K M; Feigel, M; Stewart, K D; Canary, J W; Knobler, C B; Cram, D J, *J. Am. Chem. Soc.*, **1987**, *109*, 3098-3107.
236. Bauer, L J; Gutsche, C D, *J. Am. Chem. Soc.*, **1985**, *107*, 6063-6069.
237. Fielding, L, *Tetrahedron*, **2000**, *56*, 6151-6170.
238. Cameron, K; Fielding, L, *J. Org. Chem.*, **2001**, *66*, 6891-6895.
239. Kunsagi-Mate, S; Csok, Z; Tuzi, A; Laszlo, K, *J. Phys. Chem. B*, **2008**, *112*, 11743-11749.
240. Liu, Y; Guo, D-S; Zhang, H-Y; Ma, Y-H; Yang, E-C, *J. Phys. Chem. B*, **2006**, *110*, 3428-3434.
241. Dai, S; Tam, K C, *J. Phys. Chem. B*, **2001**, *105*, 10759-10763.
242. Martin, B; Carsten, S; Karin, L; Holger, S; Roland, F; Siegfried , R W, *Chem. Eur. J.*, **2007**, *13*, 3724-3732.

243. Baudry, R; Kalchenko, O; Dumazet-Bonnamour, I; Vocanson, F; Lamartine, R, *J. Chromatogr. Sci.*, **2003**, *41*, 157-163.
244. Vincenti, M; Irico, A, *Int. J. Mass spectrom.*, **2002**, *214*, 23-36.
245. Dormann, J; Ruoff, A; Schatz, J; Vysotsky, M; Boehmer, V, *J. Chem. Soc., Perkin Trans. 2* **2002**, 83-87.
246. Shenoy, D; Feresenbet, E; Pinalli, R; Dalcanale, E, *Langmuir*, **2003**, *19*, 10454-10456.
247. Weiss, T; Schierbaum, K D; van Velzen, U T; Reinhoudt, D N; Gopel, W, *Sens. Actuators, B* **1995**, *26*, 203-207.
248. Stanley, S; Percival, C J; Auer, M; Braithwaite, A; Newton, M I; McHale, G; Hayes, W, *Anal. Chem.*, **2003**, *75*, 1573-1577.
249. Friggeri, A; van Veggel, F; Reinhoudt, D N, *Chem. Eur. J.*, **1999**, *5*, 3595-3602.
250. Lee, J-Y; Park, S-M, *J. Phys. Chem. B*, **1998**, *102*, 9940-9945.
251. *Handbook of Molecular Force Spectroscopy*, Noy, A, Ed., Springer: New York, **2008**.
252. Hinterdorfer, P; Dufrene, Y, *Nat. Methods* **2006**, *3*, 347-355.
253. Müller, D J; Krieg, M; Alsteens, D; Dufrêne, Y F, *Curr. Opin. Biotechnol.*, **2009**, *20*, 4-13.
254. Zapotoczny, S; Auletta, T; de Jong, M R; Schonherr, H; Huskens, J; van Veggel, F; Reinhoudt, D N; Vancso, G J, *Langmuir*, **2002**, *18*, 6988-6994.
255. Auletta, T; de Jong, M R; Mulder, A; van Veggel, F; Huskens, J; Reinhoudt, D N; Zou, S; Zapotoczny, S; Schonherr, H; Vancso, G J; Kuipers, L, *J. Am. Chem. Soc.*, **2004**, *126*, 1577-1584.
256. Anselmetti, D; Bartels, F; Becker, A; Decker, B; Eckel, R; McIntosh, M; Mattay, J; Plattner, P; Ros, R; Schafer, C; Sewald, N, *Langmuir*, **2008**, *24*, 1365-1370.
257. Kim, J; Kim, Y; Baek, K; Ko, Y H; Kim, D; Kim, K, *Tetrahedron*, **2008**, *64*, 8389-8393.
258. Andreetti, G; Ungaro, R; Pochini, A, *Chem. Commun.*, **1979**, *22*, 1005-1007.
259. Cram, D J; Karbach, S; Kim, H-E; Knobler, C; Maverick, E F; Ericson, J L; Helgeson, R C, *J. Am. Chem. Soc.*, **1988**, *110*, 2229-2237.

260. Dubberley, S R; Friedrich, A; Willman, D; P, M; Radius, U, *Chem. Eur. J.*, **2003**, *9*, 3634-3654.
261. Zhang, Y; Coppens, P, Crystal Structure Data.Private Communication to The Cambridge Structural Database, **2007**
262. Suzuki, T; Nagano, Y; Kouketsu, A; Matsuura, A; Maruyama, S; Kurotaki, M; Nakagawa, H; Miyata, N, *J. Med. Chem.*, **2005**, *48*, 1019-1032.
263. Suzuki, T; Kouketsu, A; Matsuura, A; Kohara, A; Ninomiya, S; Kohda, K; Miyata, N, *Bioorg. Med. Chem. Lett.*, **2004**, *14*, 3313-3317.
264. Fujihira, M; Okabe, Y; Tani, Y; Furugori, M; Akiba, U, *Ultramicroscopy*, **2000**, *82*, 181-191.
265. Serry, F, **2005,** *Improving the Accuracy of AFM Force Measurements: The Thermal Tune Solution to the Cantilever Spring Constant Problem*, Veeco Instruments, Retrieved 17/12/2009 from http://www.veeco.com/library/Application_Notes.aspx.
266. Feresenbet, E; Busi, M; Ugozzoli, F; Dalcanale, E; Shenoy, D, *Sens. Lett.*, **2004**, *2*, 186-193.
267. Raguse, B; Chow, E; Barton, C; Wieczorek, L, *Anal. Chem.*, **2007**, *79*, 7333-7339.
268. Percival, C J; Stanley, S; Braithwaite, A; Newton, M I; McHale, G, *The Analyst*, **2002**, *127*, 1024-1026.
269. Sellergren, E, *Angew. Chem. Int. Ed.*, **2000**, *39*, 1031-1037.
270. Yang, Y; Swager, T M, *Macromolecules*, **2006**, *39*, 2013-2015.
271. Sahner, K; Schonauer, D; Kuchinke, P; Moos, R, *Sens. Actuators, B* **2008**, *133*, 502-508.

Appendix 1: MatLab Code Used to Process Force Spectroscopy Data

ReadMI_Force_multifile_Min.m

```
FILE = input('Filename without extension and without 4-digit counter: ','s');
NOF = input('Number of files to be exported: ');
COUNTER_0 = input('Number of first file (without leading zeros): ');
COUNTER_END = COUNTER_0 + NOF;
k_CL = input('Spring constant k of cantilever in [N/m]: ');
flag = input('Export data to disk? Yes(1)  No(0): ');
SAVEPATH='F:\Pico Plus\20091022\2-29@5 (surface 1, tip 1 - cyclohexane)\';
min_Counter = 0;

for COUNTER=COUNTER_0:COUNTER_0+NOF
    min_Counter = min_Counter+1;

    a = int2str(COUNTER);
    if COUNTER < 10
        I = strcat('000', a);
    elseif COUNTER < 100
        I = strcat('00', a);
    elseif COUNTER < 1000
        I = strcat('0', a);
    else
        I = a;
    end

    FILENAME = strcat(SAVEPATH,FILE,I,'.ivs');

    F_BUFFERID = di_header_find(FILENAME,'buffer_id');
    F_DATAPOINTS = di_header_find(FILENAME,'data');

    fid = fopen(FILENAME,'r');
    fseek( fid , F_BUFFERID(1), -1 );
    line = fgets(fid);
    BUFFERID = extract_num(line);


    for j=1:1

        fseek( fid,F_DATAPOINTS(1+j), -1 );
        line = fgets(fid);
        DATAPOINTS = extract_num(line);

        for i=1:DATAPOINTS

            DATA = fscanf(fid,'%f');
```

```
    pos = ftell(fid);
    DIRECTION = fscanf(fid,'%s',1);

    if DIRECTION=='«'
        DATA_down(i,:)=DATA';
    else
        if DIRECTION=='»'
            DATA_up(i,:)=DATA';
        else
        end
    end

    fseek(fid,pos+1,-1 );
end

k=1;
for n=1:length(DATA_up(:,1))-1
    if DATA_up(n,1)==0
        s(k)=n;
        k=k+1;
    else
    end
end

f = DATA_up;
f(s,:) = [];
clear DATA_up
DATA_up = f;
x_up = rot90(DATA_up(:,1),2);
y_up = rot90(DATA_up(:,2),2);
DATA_up(:,1) = x_up;
DATA_up(:,2) = y_up;
clear f x_up y_up

FD_up = ZDefl2FD_MI(DATA_up,k_CL);
FD_down = ZDefl2FD_MI(DATA_down,k_CL);

min_force(min_Counter) = min(FD_up(:,2));

SAVENAME_up=strcat(SAVEPATH,'Ret_',FILE,I);
SAVENAME_down=strcat(SAVEPATH,'Ext_',FILE,I);
SAVENAME_Min=strcat(SAVEPATH,'MIN_',FILE);

figure(1)
hold on
grid on
plot(FD_up(:,1),FD_up(:,2),'-','LineWidth',2)
xlabel('distance z [nm]');
ylabel('Force [N]');
title('Force-Distance curve (up)')
```

```
        figure(2)
        hold on
        grid on
        plot(FD_down(:,1),FD_down(:,2),'-','LineWidth',2)
        xlabel('distance z [nm]');
        ylabel('Force [N]');
        title('Force-Distance curve (down)')

        figure(3)
        hold on
        grid on
        plot(FD_down(:,1),FD_down(:,2),'b-','LineWidth',2)
        plot(FD_up(:,1),FD_up(:,2),'r-','LineWidth',2)
        xlabel('distance z [nm]');
        ylabel('Force [N]');
        title('Force-Distance plot (approach: blue, withdraw: red)')

        if flag==1

            FD_File=fopen([SAVENAME_up,'.dat'],'w');
            header = strcat('Buffer',int2str(j),'\n');
            fprintf(FD_File,['z[nm] ', header]);
            for k=1:length(FD_up)
                w(1)=FD_up(k,1);
                w(2)=FD_up(k,2);
                fprintf(FD_File,'%f %g\n',w);
            end
            status=fclose(FD_File);

            FD_File=fopen([SAVENAME_down,'.dat'],'w');
            header = strcat('Buffer',int2str(j),'\n');
            fprintf(FD_File,['z[nm] ', header]);
            for k=1:length(FD_down)
                w(1)=FD_down(k,1);
                w(2)=FD_down(k,2);
                fprintf(FD_File,'%f %g\n',w);
            end
            status=fclose(FD_File);

        else
        end

        clear  DATA_down DATA_up FD_up FD_down

    end
        fclose(fid);

end
```

ZDefl2FD_MI.m

```
function ForceDist = ZDefl2FD_MI(ZDefl,k)

x = rot90(ZDefl(:,1),2);
y = rot90(ZDefl(:,2),2);


corr2_y = mean(y(length(y)-50:length(y)));
y_corr2 = y - corr2_y;


P = polyfit(x(1:20), y_corr2(1:20), 1);

corr_x = -P(2)/P(1);
x_corr = x-corr_x;

y_Defl = y_corr2/(-P(1));
x_Dist = x_corr + y_Defl;

y_Force = y_Defl*1e-9*k;
ForceDist(:,1)=x_Dist;
ForceDist(:,2)=y_Force;
```

Appendix 2: Copyright Licensing Agreements

Elsevier

Licensee: Jade K Pettersen
License Date: Dec 13, 2009
License Number: 2327140096817
Publication: Tetrahedron
Title: Steroid complexation by cyclophane receptors in aqueous solution: Substrate selectivity, enthalpic driving force for cavity inclusion, and enthalpy-entropy compensation
Type Of Use: Thesis / Dissertation
Total: 0.00 USD

Licensee: Jade K Pettersen
License Date: Dec 01, 2009
License Number: 2320011222201
Publication: Tetrahedron Letters
Title: Self-assembled monolayers of calix[4]arene derivatives on gold
Type Of Use: Thesis / Dissertation
Total: 0.00 USD

Licensee: Jade K Pettersen
License Date: Dec 01, 2009
License Number: 2320001092544
Publication: Tetrahedron
Title: Resorcinarenes
Type Of Use: Thesis / Dissertation
Total: 0.00 USD

INTRODUCTION

1. The publisher for this copyrighted material is Elsevier. By clicking "accept" in connection with completing this licensing transaction, you agree that the following terms and conditions apply to this transaction (along with the Billing

and Payment terms and conditions established by Copyright Clearance Center, Inc. ("CCC"), at the time that you opened your Rightslink account and that are available at any time at http://myaccount.copyright.com).

GENERAL TERMS

2. Elsevier hereby grants you permission to reproduce the aforementioned material subject to the terms and conditions indicated.

3. Acknowledgement: If any part of the material to be used (for example, figures) has appeared in our publication with credit or acknowledgement to another source, permission must also be sought from that source. If such permission is not obtained then that material may not be included in your publication/copies. Suitable acknowledgement to the source must be made, either as a footnote or in a reference list at the end of your publication, as follows:

"Reprinted from Publication title, Vol /edition number, Author(s), Title of article / title of chapter, Pages No., Copyright (Year), with permission from Elsevier [OR APPLICABLE SOCIETY COPYRIGHT OWNER]." Also Lancet special credit - "Reprinted from The Lancet, Vol. number, Author(s), Title of article, Pages No., Copyright (Year), with permission from Elsevier."

4. Reproduction of this material is confined to the purpose and/or media for which permission is hereby given.

5. Altering/Modifying Material: Not Permitted. However figures and illustrations may be altered/adapted minimally to serve your work. Any other abbreviations, additions, deletions and/or any other alterations shall be made only with prior written authorization of Elsevier Ltd. (Please contact Elsevier at permissions@elsevier.com)

6. If the permission fee for the requested use of our material is waived in this instance, please be advised that your future requests for Elsevier materials may attract a fee.

7. Reservation of Rights: Publisher reserves all rights not specifically granted in the combination of (i) the license details provided by you and accepted in the course of this licensing transaction, (ii) these terms and conditions and (iii) CCC's Billing and Payment terms and conditions.

8. License Contingent Upon Payment: While you may exercise the rights licensed immediately upon issuance of the license at the end of the licensing

process for the transaction, provided that you have disclosed complete and accurate details of your proposed use, no license is finally effective unless and until full payment is received from you (either by publisher or by CCC) as provided in CCC's Billing and Payment terms and conditions. If full payment is not received on a timely basis, then any license preliminarily granted shall be deemed automatically revoked and shall be void as if never granted. Further, in the event that you breach any of these terms and conditions or any of CCC's Billing and Payment terms and conditions, the license is automatically revoked and shall be void as if never granted. Use of materials as described in a revoked license, as well as any use of the materials beyond the scope of an unrevoked license, may constitute copyright infringement and publisher reserves the right to take any and all action to protect its copyright in the materials.

9. Warranties: Publisher makes no representations or warranties with respect to the licensed material.

10. Indemnity: You hereby indemnify and agree to hold harmless publisher and CCC, and their respective officers, directors, employees and agents, from and against any and all claims arising out of your use of the licensed material other than as specifically authorized pursuant to this license.

11. No Transfer of License: This license is personal to you and may not be sublicensed, assigned, or transferred by you to any other person without publisher's written permission.

12. No Amendment Except in Writing: This license may not be amended except in a writing signed by both parties (or, in the case of publisher, by CCC on publisher's behalf).

13. Objection to Contrary Terms: Publisher hereby objects to any terms contained in any purchase order, acknowledgment, check endorsement or other writing prepared by you, which terms are inconsistent with these terms and conditions or CCC's Billing and Payment terms and conditions. These terms and conditions, together with CCC's Billing and Payment terms and conditions (which are incorporated herein), comprise the entire agreement between you and publisher (and CCC) concerning this licensing transaction. In the event of any conflict between your obligations established by these

terms and conditions and those established by CCC's Billing and Payment terms and conditions, these terms and conditions shall control.

14. Revocation: Elsevier or Copyright Clearance Center may deny the permissions described in this License at their sole discretion, for any reason or no reason, with a full refund payable to you. Notice of such denial will be made using the contact information provided by you. Failure to receive such notice will not alter or invalidate the denial. In no event will Elsevier or Copyright Clearance Center be responsible or liable for any costs, expenses or damage incurred by you as a result of a denial of your permission request, other than a refund of the amount(s) paid by you to Elsevier and/or Copyright Clearance Center for denied permissions.

LIMITED LICENSE

The following terms and conditions apply only to specific license types:

15. **Translation**: This permission is granted for non-exclusive world **English** rights only unless your license was granted for translation rights. If you licensed translation rights you may only translate this content into the languages you requested. A professional translator must perform all translations and reproduce the content word for word preserving the integrity of the article. If this license is to re-use 1 or 2 figures then permission is granted for non-exclusive world rights in all languages.

16. **Website**: The following terms and conditions apply to electronic reserve and author websites:**Electronic reserve**: If licensed material is to be posted to website, the web site is to be password-protected and made available only to bona fide students registered on a relevant course if:
This license was made in connection with a course,
This permission is granted for 1 year only. You may obtain a license for future website posting, All content posted to the web site must maintain the copyright information line on the bottom of each image,
A hyper-text must be included to the Homepage of the journal from which you are licensing at http://www.sciencedirect.com/science/journal/xxxxx or the Elsevier homepage for books at http://www.elsevier.com , and
Central Storage: This license does not include permission for a scanned version of the material to be stored in a central repository such as that provided by Heron/XanEdu.

17. **Author website** for journals with the following additional clauses:

All content posted to the web site must maintain the copyright information line on the bottom of each image, and the permission granted is limited to the personal version of your paper. You are not allowed to download and post the published electronic version of your article (whether PDF or HTML, proof or final version), nor may you scan the printed edition to create an electronic version,

A hyper-text must be included to the Homepage of the journal from which you are licensing at http://www.sciencedirect.com/science/journal/xxxxx , As part of our normal production process, you will receive an e-mail notice when your article appears on Elsevier's online service ScienceDirect (www.sciencedirect.com). That e-mail will include the article's Digital Object Identifier (DOI). This number provides the electronic link to the published article and should be included in the posting of your personal version. We ask that you wait until you receive this e-mail and have the DOI to do any posting.

Central Storage: This license does not include permission for a scanned version of the material to be stored in a central repository such as that provided by Heron/XanEdu.

18. **Author website** for books with the following additional clauses: Authors are permitted to place a brief summary of their work online only. A hyper-text must be included to the Elsevier homepage at http://www.elsevier.com

All content posted to the web site must maintain the copyright information line on the bottom of each image You are not allowed to download and post the published electronic version of your chapter, nor may you scan the printed edition to create an electronic version. Central Storage: This license does not include permission for a scanned version of the material to be stored in a central repository such as that provided by Heron/XanEdu.

19. **Website** (regular and for author): A hyper-text must be included to the Homepage of the journal from which you are licensing at http://www.sciencedirect.com/science/journal/xxxxx. or for books to the Elsevier homepage at http://www.elsevier.com

20. **Thesis/Dissertation**: If your license is for use in a thesis/dissertation your thesis may be submitted to your institution in either print or electronic form. Should your thesis be published commercially, please reapply for permission. These requirements include permission for the Library and Archives of Canada to supply single copies, on demand, of the complete thesis and include permission for UMI to supply single copies, on demand, of the complete thesis. Should your thesis be published commercially, please reapply for permission.
21. **Other Conditions**: None

American Chemical Society

Licensee: Jade K Pettersen
License Date: Dec 13, 2009
License Number: 2327150844101
Publication: Langmuir
Title: Immobilization of Adamantane-Modified Cytochrome c at Electrode Surfaces through Supramolecular Interactions
Type Of Use: Thesis/Dissertation
Total: 0.00 USD

Licensee: Jade K Pettersen
License Date: Dec 13, 2009
License Number: 2327141096632
Publication: Journal of the American Chemical Society
Title: C-H...X?R (X = Cl, Br, and I) Hydrogen Bonds Drive the Complexation Properties of a Nanoscale Molecular Basket
Type Of Use: Thesis/Dissertation
Total: 0.00 USD

Licensee: Jade K Pettersen
License Date: Dec 13, 2009
License Number: 2327121107843
Publication: Journal of the American Chemical Society

Title: Host-guest complexation. 46. Cavitands as open molecular vessels form solvates
Type Of Use: Thesis/Dissertation
Total: 0.00 USD

Licensee: Jade K Pettersen
License Date: Dec 13, 2009
License Number: 2327111434974
Publication: Journal of the American Chemical Society
Title: Extraction of Hydrophobic Species into a Water-Soluble Synthetic Receptor
Type Of Use: Thesis/Dissertation
Total: 0.00 USD

Licensee: Jade K Pettersen
License Date: Dec 13, 2009
License Number: 2327111172884
Publication: Journal of the American Chemical Society
Title: Kinetically Stable Complexes in Water: The Role of Hydration and Hydrophobicity
Type Of Use: Thesis/Dissertation
Total: 0.00 USD

Licensee: Jade K Pettersen
License Date: Dec 13, 2009
License Number: 2327110427444
Publication: Journal of the American Chemical Society
Title: Constrictive binding of large guests by a hemicarcerand containing four portals
Type Of Use: Thesis/Dissertation
Total: 0.00 USD
Licensee: Jade K Pettersen
License Date: Dec 13, 2009
License Number: 2326910562259

Publication: Organic Letters
Title: Recognition of Guests by Water-Stabilized Cavitand Hosts
Type Of Use: Thesis/Dissertation
Total: 0.00 USD

Licensee: Jade K Pettersen
License Date: Dec 01, 2009
License Number: 2320040664123
Publication: Langmuir
Title: Calix-4-resorcinarene Monolayers and Multilayers: Formation, Structure, and Differential Adsorption1
Type Of Use: Thesis/Dissertation
Total: 0.00 USD

Licensee: Jade K Pettersen
License Date: Dec 01, 2009
License Number: 2320040237982
Publication: Langmuir
Title: Lattice Structure of Self-Assembled Monolayers of Dialkyl Sulfides and Calix[4]arene Sulfide Adsorbates on Au(111) Revealed by Atomic Force Microscopy
Type Of Use: Thesis/Dissertation
Total: 0.00 USD

Licensee: Jade K Pettersen
License Date: Dec 01, 2009
License Number: 2320030596857
Publication: Langmuir
Title: An Atomic Force Microscopy Study of Self-Assembled Monolayers of Calix[4]resorcinarene Adsorbates on Au(111)
Type Of Use: Thesis/Dissertation
Total: 0.00 USD

Licensee: Jade K Pettersen

License Date: Dec 01, 2009

License Number: 2320021471669

Publication: Journal of the American Chemical Society

Title: Host-guest complexation. 67. A highly adaptive and strongly binding hemicarcerand

Type Of Use: Thesis/Dissertation

Total: 0.00 USD

Thesis/Dissertation

ACS / RIGHTSLINK TERMS & CONDITIONS

THESIS/DISSERTATION

INTRODUCTION

The publisher for this copyrighted material is the American Chemical Society. By clicking "accept" in connection with completing this licensing transaction, you agree that the following terms and conditions apply to this transaction (along with the Billing and Payment terms and conditions established by Copyright Clearance Center, Inc. ("CCC"), at the time that you opened your Rightslink account and that are available at any time at <http://myaccount.copyright.com>).

LIMITED LICENSE

Publisher hereby grants to you a non-exclusive license to use this material. Licenses are for one-time use only with a maximum distribution equal to the number that you identified in the licensing process; any form of republication must be completed within 60 days from the date hereof (although copies prepared before then may be distributed thereafter).

GEOGRAPHIC RIGHTS: SCOPE

Licenses may be exercised anywhere in the world.

RESERVATION OF RIGHTS

Publisher reserves all rights not specifically granted in the combination of (i) the license details provided by you and accepted in the course of this licensing transaction, (ii) these terms and conditions and (iii) CCC's Billing and Payment terms and conditions.

PORTION RIGHTS STATEMENT: DISCLAIMER

If you seek to reuse a portion from an ACS publication, it is your responsibility to examine each portion as published to determine whether a credit to, or copyright notice of, a third party owner was published adjacent to the item. You may only obtain permission via Rightslink to use material owned by ACS. Permission to use any material published in an ACS publication, journal, or article which is reprinted with permission of a third party must be obtained from the third party owner. ACS disclaims any responsibility for any use you make of items owned by third parties without their permission.

REVOCATION

The American Chemical Society reserves the right to revoke a license for any reason, including but not limited to advertising and promotional uses of ACS content, third party usage, and incorrect figure source attribution.

LICENSE CONTINGENT ON PAYMENT

While you may exercise the rights licensed immediately upon issuance of the license at the end of the licensing process for the transaction, provided that you have disclosed complete and accurate details of your proposed use, no license is finally effective unless and until full payment is received from you (by CCC) as provided in CCC's Billing and Payment terms and conditions. If full payment is not received on a timely basis, then any license preliminarily granted shall be deemed automatically revoked and shall be void as if never granted. Further, in the event that you breach any of these terms and conditions or any of CCC's Billing and Payment terms and conditions, the license is automatically revoked and shall be void as if never granted. Use of materials as described in a revoked license, as well as any use of the materials beyond the scope of an unrevoked license, may constitute copyright infringement and publisher reserves the right to take any and all action to protect its copyright in the materials.

COPYRIGHT NOTICE: DISCLAIMER

You must include the following copyright and permission notice in connection with any reproduction of the licensed material: "Reprinted (“Adapted” or “in part”) with permission from REFERENCE CITATION. Copyright YEAR American Chemical Society."

WARRANTIES: NONE

Publisher makes no representations or warranties with respect to the licensed material.

INDEMNITY

You hereby indemnify and agree to hold harmless publisher and CCC, and their respective officers, directors, employees and agents, from and against any and all claims arising out of your use of the licensed material other than as specifically authorized pursuant to this license.

NO TRANSFER OF LICENSE

This license is personal to you or your publisher and may not be sublicensed, assigned, or transferred by you to any other person without publisher's written permission.

NO AMENDMENT EXCEPT IN WRITING

This license may not be amended except in a writing signed by both parties (or, in the case of publisher, by CCC on publisher's behalf).

OBJECTION TO CONTRARY TERMS

Publisher hereby objects to any terms contained in any purchase order, acknowledgment, check endorsement or other writing prepared by you, which terms are inconsistent with these terms and conditions or CCC's Billing and Payment terms and conditions. These terms and conditions, together with CCC's Billing and Payment terms and conditions (which are incorporated herein), comprise the entire agreement between you and publisher (and CCC) concerning this licensing transaction. In the event of any conflict between your obligations established by these terms and conditions and those established by CCC's Billing and Payment terms and conditions, these terms and conditions shall control.

JURISDICTION

This license transaction shall be governed by and construed in accordance with the laws of the District of Columbia. You hereby agree to submit to the jurisdiction of the courts located in the District of Columbia for purposes of resolving any disputes that may arise in connection with this licensing transaction.

THESES/DISSERTATION TERMS

Publishing implications of electronic publication of theses and dissertation material

Students and their mentors should be aware that posting of theses and dissertation material on the Web prior to submission of material from that thesis or dissertation to an ACS journal may affect publication in that journal. Whether Web posting is considered prior publication may be evaluated on a case-by-case basis by the journal's editor. If an ACS journal editor considers Web posting to be "prior publication", the paper will not be accepted for publication in that journal. If you intend to submit your unpublished paper to ACS for publication, check with the appropriate editor prior to posting your manuscript electronically.

If your paper has already been published by ACS and you want to include the text or portions of the text in your thesis/dissertation in **print or microfilm formats**, please print the ACS copyright credit line on the first page of your article: "Reproduced (or 'Reproduced in part') with permission from [FULL REFERENCE CITATION.] Copyright [YEAR] American Chemical Society." Include appropriate information.

Submission to a Dissertation Distributor: If you plan to submit your thesis to UMI or to another dissertation distributor, you should not include the unpublished ACS paper in your thesis if the thesis will be disseminated electronically, until ACS has published your paper. After publication of the paper by ACS, you may release the entire thesis (**not the individual ACS article by itself**) for electronic dissemination through the distributor; ACS's copyright credit line should be printed on the first page of the ACS paper.

Use on an Intranet: The inclusion of your ACS unpublished or published manuscript is permitted in your thesis in print and microfilm formats. If ACS has published your paper you may include the manuscript in your thesis on an intranet that is not publicly available. Your ACS article cannot be posted electronically on a publicly available medium (i.e. one that is not password protected), such as but not limited to, electronic archives, Internet, library server, etc. The only material from your paper that can be posted on a public electronic medium is the article abstract, figures, and tables, and you may link to the article's DOI or post the article's author-directed URL link provided by ACS. This paragraph does not pertain to the dissertation distributor paragraph above.

Other conditions: v1.1

Nature Publishing

Licensee: Jade K Pettersen
License Date: Dec 01, 2009
License Number: 2320041169482
Publication: Nature
Title: Control of crystal nucleation by patterned self-assembled monolayers
Type Of Use: Thesis / Dissertation
Total: $0.00

Terms and Conditions for Permissions

Nature Publishing Group hereby grants you a non-exclusive license to reproduce this material for this purpose, and for no other use, subject to the conditions below:

NPG warrants that it has, to the best of its knowledge, the rights to license reuse of this material. However, you should ensure that the material you are requesting is original to Nature Publishing Group and does not carry the copyright of another entity (as credited in the published version). If the credit line on any part of the material you have requested indicates that it was reprinted or adapted by NPG with permission from another source, then you should also seek permission from that source to reuse the material.

Permission granted free of charge for material in print is also usually granted for any electronic version of that work, provided that the material is incidental to the work as a whole and that the electronic version is essentially equivalent to, or substitutes for, the print version. Where print permission has been granted for a fee, separate permission must be obtained for any additional, electronic re-use (unless, as in the case of a full paper, this has already been accounted for during your initial request in the calculation of a print run). NB: In all cases, web-based use of full-text articles must be authorized separately through the 'Use on a Web Site' option when requesting permission.

Permission granted for a first edition does not apply to second and subsequent editions and for editions in other languages (except for signatories to the STM Permissions Guidelines, or where the first edition permission was granted for free).

Nature Publishing Group's permission must be acknowledged next to the figure, table or abstract in print. In electronic form, this acknowledgement must be visible at the same time as the figure/table/abstract, and must be hyperlinked to the journal's homepage.
The credit line should read:

Reprinted by permission from Macmillan Publishers Ltd: [JOURNAL NAME] (reference citation), copyright (year of publication)

For AOP papers, the credit line should read:

Reprinted by permission from Macmillan Publishers Ltd: [JOURNAL NAME], advance online publication, day month year (doi: 10.1038/sj.[JOURNAL ACRONYM].XXXXX)

Adaptations of single figures do not require NPG approval. However, the adaptation should be credited as follows:

Adapted by permission from Macmillan Publishers Ltd: [JOURNAL NAME] (reference citation), copyright (year of publication)

Translations of 401 words up to a whole article require NPG approval. Please visit http://www.macmillanmedicalcommunications.com for more information. Translations of up to a 400 words do not require NPG approval. The translation should be credited as follows:
Translated by permission from Macmillan Publishers Ltd: [JOURNAL NAME] (reference citation), copyright (year of publication).

We are certain that all parties will benefit from this agreement and wish you the best in the use of this material. Thank you.
v1.1

Springer

Licensee: Jade K Pettersen
License Date: Dec 13, 2009
License Number: 2327130569955
Publication: Russian Chemical Bulletin
Title: Molecular recognition of organic guest vapor by solid adamantylcalix[4]arene
Type Of Use: Thesis/Dissertation
Total: 0.00 USD

Licensee: Jade K Pettersen
License Date: Dec 01, 2009
License Number: 2320080468591
Publication: Applied Physics A
Title: Scanning tunneling microscopy on self-assembled calix[4]resorcinarene monolayer adsorbates on Au(111)
Type Of Use: Thesis/Dissertation
Total: 0.00 USD

Introduction
The publisher for this copyrighted material is Springer Science + Business Media. By clicking "accept" in connection with completing this licensing transaction, you agree that the following terms and conditions apply to this transaction (along with the Billing and Payment terms and conditions established by Copyright Clearance Center, Inc. ("CCC"), at the time that you opened your Rightslink account and that are available at any time at http://myaccount.copyright.com).
Limited License

With reference to your request to reprint in your thesis material on which Springer Science and Business Media control the copyright, permission is granted, free of charge, for the use indicated in your enquiry. Licenses are for one-time use only with a maximum distribution equal to the number that you identified in the licensing process.

This License includes use in an electronic form, provided it is password protected or on the university's intranet, destined to microfilming by UMI and University repository. For any other electronic use, please contact Springer at (permissions.dordrecht@springer.com or permissions.heidelberg@springer.com)

The material can only be used for the purpose of defending your thesis, and with a maximum of 100 extra copies in paper.

Although Springer holds copyright to the material and is entitled to negotiate on rights, this license is only valid, provided permission is also obtained from the (co) author (address is given with the article/chapter) and provided it concerns original material which does not carry references to other sources (if material in question appears with credit to another source, authorization from that source is required as well). Permission free of charge on this occasion does not prejudice any rights we might have to charge for reproduction of our copyrighted material in the future.

Altering/Modifying Material: Not Permitted

However figures and illustrations may be altered minimally to serve your work. Any other abbreviations, additions, deletions and/or any other alterations shall be made only with prior written authorization of the author(s) and/or Springer Science + Business Media. (Please contact Springer at permissions.dordrecht@springer.com or permissions.heidelberg@springer.com)

Objection to Contrary Terms

Springer Science + Business Media hereby objects to any terms contained in any purchase order, acknowledgment, check endorsement or other writing prepared by you, which terms are inconsistent with these terms and conditions or CCC's Billing and Payment terms and conditions. These terms and conditions, together with CCC's Billing and Payment terms and conditions (which are incorporated herein), comprise the entire agreement between you and Springer Science + Business Media (and CCC) concerning this licensing transaction. In the event of any conflict between your obligations established by these terms and conditions and those established by CCC's Billing and Payment terms and conditions, these terms and conditions shall control.

Jurisdiction

All disputes that may arise in connection with this present License, or the breach thereof, shall be settled exclusively by the country's law in which the work was originally published.

v1.2

Wiley

– Obtained via email

(For Menozzi, Pinalli, Speets, Ravoo, Dalcanale, Reinhoudt (2004), *Surface-confined single molecules: Assembly and disassembly of nanosize coordination cages on gold (111)* , Chemistry – A European Journal, 10(9), 2199-2206 – Figure 2b)

From: Rights DE [mailto:RIGHTS-and-LICENCES@wiley-vch.de]
Sent: Wed 9/12/2009 10:52 PM
To: Jade Pettersen2

Subject: AW: Permission to use figure in a thesis.

Dear Customer,

Thank you for your email.

- We hereby grant permission for the requested use expected that due credit is given to the original source.
- For material published before 2007 additionally: Please note that the (co-)author's permission is also required.

If material appears within our work with credit to another source, authorisation from that source must be obtained.

Credit must include the following components:

- Books: Author(s)/ Editor(s) Name(s): Title of the Book. Page(s). Publication year. Copyright Wiley-VCH Verlag GmbH & Co. KGaA. Reproduced with permission.
- Journals: Author(s) Name(s): Title of the Article. Name of the Journal. Publication year. Volume. Page(s). Copyright Wiley-VCH Verlag GmbH & Co. KGaA. Reproduced with permission.

With kind regards

Bettina Loycke
****
Bettina Loycke
Senior Rights Manager
Wiley-VCH Verlag GmbH & Co. KGaA
Boschstr. 12
69469 Weinheim
Germany

Phone: +49 (0) 62 01- 606 - 280
Fax: +49 (0) 62 01 - 606 - 332
Email: rights@wiley-vch.de

_____

Wiley-VCH Verlag GmbH & Co. KGaA
Location of the Company: Weinheim
Chairman of the Supervisory Board: Stephen Michael Smith
Trade Register: Mannheim, HRB 432833
General Partner: John Wiley & Sons GmbH, Location: Weinheim
Trade Register Mannheim, HRB 432296
Managing Directors : Christopher J. Dicks, Bijan Ghawami, William Pesce